The impact of biogeochemical processes on the composition of dissolved organic matter in marine subsurface sediments

A Doctoral Dissertation

Shuchai Gan

MARUM (Zentrum für Marine Umweltwissenschaften)

Universität Bremen

The impact of biogeochemical processes on the composition of dissolved organic matter in marine subsurface sediments

Dissertation

zur Erlangung des Doktorgrades

der Naturwissenschaften

– Dr. rer. nat. –

Am Fachbereich Geowissenschaften

Der Universität Bremen

vorgelegt von

Shuchai Gan

Bremen, December 2017

The PhD thesis was prepared between October 2013 and December 2017 within the Organic Geochemistry Group of the MARUM – Center for Marine Environmental Sciences and Department of Geosciences, University of Bremen, Leobener Str., D-28359 Bremen, Germany.

1st Reviewer: Prof. Dr. Kai-Uwe Hinrichs

2nd Reviewer: Prof. Dr. Boris P. Koch

Date of the doctoral colloquium: 30.01.2018

Erklärung/ Affirmation

Ich versichere, dass / I affirm that

1. die Dissertation ohne unerlaubte fremde Hilfe angefertigt wurde /

I wrote the present thesis independently and without illicit assistance from third parties,

2. keine anderen als die von mir angegebenen Quellen und Hilfsmittel benutzt wurden und /

I used no sources other than those indicated nor aids other than those permissible,

3. die den benutzten Werken wörtlich oder inhaltlich entnommenen Stellen als solche kenntlich gemacht wurden. /

I appropriately referenced any text or content from other sources.

Bremen, den / on this day _____

_____

(Unterschrift / Signature).

Contents

Acknowledgements

Four years in Bremen are important experiences for my scientific carrier and life. I would like to thank my supervisor Prof. Kai-Uwe Hinrichs, who made the brave decision to accept me as a student in his group and brought me into the realm of geoscience. In the first year, I feel unsure about my project. Kai said: 'Let us have practices and start from a simple ideas', 'your project is like a tree, its location and trunk is there, there are uncertainty of the small branches and leafs now, you will make it grow'. After trying for almost one year without publishable work, we came up with some promising ideas. Starting from them, I finished three sub-projects in this dissertation, and two more exciting stories to be explored. I will keep my enthusiasm and those words in my mind for the future.

I am also deeply thankful to Dr. Verena B. Heuer and Dr. Frauke Schmidt, who contributed many suggestions to my PhD project, including the design of incubation, calculation of data set, revision of manuscripts. In my heart, I considered both of them as my co-supervisors. I would like to express my appreciation to the technicians – Xavier Prieto, Jenny Wendt, Evert Kramer, Jessica Arndt, our secretary – Birgit Schmincke, lab manager – Marcus Elvert for their excellent technical and administrative supports in the labs and offices. I would like to thank my colleagues, who shared the scientific experiences and happy moments during Kohltour/Spargeltour with me, assisted me in the project: Weichao Wu, Bernhard Viehweger, Susanne Alfken, Rishi Adhikari, Evert Kramer, Heidi Taubner, Travis Meador, Lars Wörmer, Julius Lipp, Florence Schubotz, Thomas Evans, Nadine Goldenstein, Xiaolei Liu, Guangchao Zhuang, Chun Zhu, Sitan Xie, Stanislav Jabinski, Jin-Xiang Wang, Qingzeng Zhu, Rong Zhu, Sarah Coffinet, Min Song, Kevin Becker, Felix Elling, Miriam Sollich, Gonzalo V. Gómez Sáez, Jan Schröder, Martin Könneke, Cengling Ma. I would also like to thank Prof. Patrick Hatcher for accepting me as guest student in Old Dominion University, USA and Dr. Isaiah Ruhl for introducing the NMR.

Four years in Germany is a long journey, the accompanying of my fiance, my Mr. Right – Lin Ming is the most important source of my energy, hope and persistence. Without Ming's supports, I won't come to another country for pursuing for the joy of science and experiencing the diverse cultures. I feel indebted to my parents, who hold dark in bay worrying me. I would like to thank the supports of Ming's parents, my younger sister Min, my bothers Zhong and Ling, Ming's sisters and brothers, I am so lucky to be one of this big and warm family. I will miss the time together with many unforgettable persons in Bremen, my former flat mates, Dahee, Alok, kind landlords – Mr. and Mrs. Knappert, my friends in Bremen Wei, Moling, Huixing, Ping.

None of this work would have been possible without financial supports from Chinese Scholarship Council, DFG through the Research Center/Excellence Cluster MARUM-Center for Marine Environmental Sciences, the Bremen International Graduate School for Marine Sciences (GLOMAR) and grants awarded to Kai-Uwe Hinrichs from DFG and ERC.

All of you – my supervisor, colleges, friends, fiance, and family members are the painters who make the last four years a colorful album of memory. As a closing remark, I would like to say: 'Life is like a box of chocolates, you never know what you are going to get'. *(Forrest Gump)*

Abstract

Organic matter in marine sediments is one of the largest pools of reduced carbon on Earth. It had been known as recalcitrant carbon pool with scarce living biomasses. The findings of microbes at several kilometers below seafloor suggest there is a substantial amount of living biomasses in the subsurface sediments under extreme conditions, for example, decreasing labile biomolecules as carbon sources, electron acceptors, and thermal conditions at deeper layers. Those microbes might drive a slow but extensive carbon flow and play an important role in the carbon cycle in deep Earth. It is not known how the microbes could survive on the recalcitrant organic matter (ROM) 'leftover'. The gap of knowledge is especially in the initial step of degradation process: how the ROM is degraded to assimilable substrates. Dissolved organic matter (DOM) encompasses the analytical window for the initial degradation of ROM. However, the DOM pool is complex and comprises tens of thousands of formulae. Therefore, this study focused on firstly the method of DOM characterization, secondly the DOM cycling and degradation process in subseafloor sediment. In further, this study aims to answer the questions: how the degradation patterns of organic matter change with environmental condition in the subsurface sediments, which are highly stratified by redox conditions and thermal gradients.

Characterization of DOM is the first step of this study. Fourier transform ion cyclotron resonance mass spectrometry (FT-ICR MS) is a powerful tool in characterizing DOM in molecular level but is a destructive tool and needs relatively large volume of sample (>10 mL). Whereas, the achievable volume of pore water in deep sediments is highly limited, an alternative method – Excitation Emission Matrix spectrum (EEMs) is promising in characterizing DOM due to its advantage of less volume, non-destructive and no pretreatments of solid phase extraction. The second chapter describes the method optimization of EEMs especially to understand matrix effects including the dilution effect, concentration of ions sensitive to redox conditions and storage conditions for samples from anoxic marine sediments.

Results were verified by FT-ICR MS. Pretreatments of pore water from anaerobic environment were suggested in this study and enable measurements with micro-liquid sampling (50 μL in this study). EEMs allows for observation of deep and stratified sediment at dense intervals in deep biosphere research.

In the third chapter, the impacts of redox conditions on the DOM and the degradation pathway were investigated by incubation experiments. Incubations were conducted under sulfate-reducing condition and methanogenic condition. Series with inhibitor aims to stop the terminal mineralization step and observe the accumulating substrates during degradation under sulfate reducing condition. DOM was characterized by EEMs and FT-ICR MS. Multiple lines of evidences, i.e., the quantification of DOC, production of ammonia and DIC ($\Delta NH_4^+/\Delta DIC$ ratio) were applied to verify the selectivity of degradation processes. The results showed that the DOM components differ under sulfate reducing and methanogenic conditions. The patterns of organic matter degradation are featured as follows: (1) under sulfate reducing condition, more oxidized DOM is accumulated and the formulae with 3 or 4 nitrogens are more depleted, a rapid turnover of protein-like compounds were observed; (2) under methanogenic condition, more reduced DOM with lower O/C ratio were detected; decreasing O/C ratio corresponds to a rapid blue-shift of humic-like compounds which suggests the contribution of humic-like compounds to microbial degradation, while the nitrogen-containing formulae is not preferred by microbes under methanogenic condition. In further, incubation experiment with the addition of yeast extracts confirmed that the biopolymer fragments emitting protein-like peaks are not favored under methanogenic condition but are mostly consumed in two days under sulfate-reducing condition. Results suggest that the organic matter degradation pathways vary with redox conditions, the degradation pathway are featured not only in the terminal step as is known, but also in the initial step of the degradation process.

At the greater depth, temperature might play an important role in organic matter degradation and preservation process. The fourth chapter compared DOM compositions at different temperatures (20-85°C) with Nankai Trough sediment retrieved during IODP Expedition 322. DOM was characterized by EEMs and FT-ICR MS. Concentration of dissolved Fe and Mn was monitored. Results showed that (1) at 85°C, there was a major contribution from abiotic process of acetate production and it contributes to terminal steps; (2) at 55°C, the abiotic decomposition

of humics could provide assimilable fragments that contribute to the monomer precursors for fermentation; (3) at 35°C, abiotic process could barely contribute to humics-decomposition but accelerate the release of organic molecules to mobile phase. By incubations of the Nankai Trough sediment, this study proposes mechanisms of heat-induced microbial metabolism via anaerobic degradation of organic matter in deep sediments, including release of the metal ions and organic matter, the exposure and decomposition of the aged macromolecules. A model for abiotic humic substances decomposition is proposed. In summary, results suggest the abiotic process might change the degradation pathways by offering precursors without energy cost from microbes, and therefore potentially affects the carbon cycle in deep earth and microbial community.

In summary, this dissertation addressed the interactions between microbes and DOM in stratified anaerobic sediments by combinations of EEMs and FT-ICR MS. It is indicated that the metabolism of microbes is sensitive and adaptive to environmental conditions, which ultimately influence the carbon and nitrogen flow in subsurface sediments due to the change of microbial metabolisms and abiotic processes.

Zusammenfassung

Organisches Material in Sedimentablagerungen auf dem Meeresboden ist das größte Kohlenstoffreservoir auf der Erde. Es gilt als schwer abbaubar. Die Entdeckung von mikrobiellem Leben selbst einige Kilometer tief unter dem Meeresboden beweist, dass es in marinen Sedimentablagerungen eine erhebliche Menge an Biomasse gibt, die unter extremen Bedingungen existieren kann, und wirft zahlreiche Fragen auf; zum Beispiel: welche Kohlenstoffquellen und Elektronenakzeptoren werden genutzt? Wie kann organisches Material abgebaut werden, obwohl ihr Gehalt an labilen Biomolekülen mit der Tiefe abnimmt? Welche Rolle spielt die zunehmende Erhitzung des organischen Materials in tieferen Schichten? Die in der tiefen Biosphäre lebenden Mikroorganismen könnten einen langsamen, aber extensiven Kohlenstoffffluss steuern und eine wichtige Rolle im Kohlenstoffkreislauf der tiefen Erde spielen. Es ist nicht bekannt, wie die Mikroben auf der Basis von schwer abbaubarem ‘Restmaterial‘ (ROM) der organischen Substanz überleben könnten. Eine große Wissenslücke besteht vor allem in Hinblick auf die ersten Schritte des Degradationsprozesses, in denen ROM zu assimilierbaren Substraten abgebaut wird. Die Analyse der Zusammensetzung des gelösten organischen Materials (DOM) erlaubt einen Einblick in die ersten Abbauschritte des ROMs. DOM besteht aus komplexen Molekülen mit Zehntausenden von Formeln. Daher konzentrierte sich diese Studie auf die Charakterisierung und den Abbauprozess von DOM im marinen Sediment. Diese Studie zielt außerdem darauf ab, die Fragen zu beantworten, wie sich die Muster des organischen Stoffumsatzes mit zunehmender Sedimenttiefe ändern, mit der sich auch Redox-Bedingungen und der Einfluss von thermischen Prozesse graduell ändern.

Die Charakterisierung von DOM ist der erste Schritt von dieser Forschung. Die Fourier-Transformations-Ionenzyklotronresonanz-Massenspektrometrie (FT-ICR MS) ist ein leistungsfähiges Werkzeug zur Charakterisierung von DOM auf molekularer Ebene. Für die Messung werden jedoch relativ große Probenvolumen (> 10 ml) benötigt und vollständig verbraucht. Das Porenwasservolumen, das aus tiefen Sedimenten gewonnen werden kann, ist jedoch nur sehr begrenzt. Für die Charakterisierung von DOM in Porenwässern sind Fluoreszenzspektroskopie und die Erstellung von Anregungs-Emissions-Matrix Spektren

(Excitation Emission Matrix Spectra, EEMs) eine vielversprechende alternative Methode, da für sie nur wenige Probenvolumen benötigt wird und die Messung zerstörungsfrei ist und ohne Vorbehandlung der Proben mit Festphasenextraktion durchgeführt werden kann. Das zweite Kapitel beschreibt die Methodenoptimierung. Dabei galt es insbesondere Matrixeffekte zu verstehen, einschließlich des Verdünnungseffekts, der Konzentration von Ionen, die gegenüber Redoxbedingungen empfindlich sind, und den Einfluss von Lagerungsbedingungen für Proben aus anoxischen Meeressedimenten zu untersuchen. Die auf EEMs basierenden Ergebnisse wurden mit FT-ICR MS Analysen verglichen. Aus dieser Methodenentwicklung resultieren Empfehlungen für die Vorbehandlungen von Porenwasser aus anaerober Umgebung, die DOM Analysen auch an sehr kleinen Porenwasserproben (~ µg C, 50 µL in dieser Studie) erlauben. Diese Methodenentwicklung bereitet den Weg für die Analyse von DOM in Porenwässern tief begrabener Sedimente und trägt damit zur Untersuchung des Kohlenstoffflusses in der tiefen marinen Biosphäre bei.

Im dritten Schritt wurden die Auswirkungen von Redoxbedingungen auf DOM und DOM-Abbauwege in Inkubationsexperimenten untersucht. Inkubationen wurden unter sulfatreduzierenden Bedingungen und methanogenen Bedingungen durchgeführt. Eine Serie mit Inhibitor-Zugabe zielte darauf ab, den terminalen Mineralisierungsschritt zu stoppen und die assimilierbaren Substrate während des Abbaus unter sulfatreduzierenden Bedingungen zu beobachten. DOM wurde durch EEMs und FT-ICR MS charakterisiert. Es wurden mehrere Beweislinien angewendet, z.B. die Quantifizierung von DOC, die Produktion von Ammoniak und DIC (ΔNH_4^+/ΔDIC-Verhältnis), um die Selektivität von Abbauprozessen zu verifizieren. Die Ergebnisse dieser Studie zeigen, dass sich die DOM-Komponenten unter sulfatreduzierenden und methanogenen Bedingungen unterscheiden. Die Muster des Abbaus organischer Substanz sind wie folgt gekennzeichnet: (1) unter sulfatreduzierenden Bedingungen wird mehr oxidiertes DOM akkumuliert, während Formeln mit 3 oder 4 Stickstoffatomen abnehmen; zusätzlich wurde ein schneller Umsatz von proteinartigen Verbindungen wurde beobachtet; (2) unter methanogenen Bedingungen wurde mehr reduziertes DOM mit einem niedrigeren O/C-Verhältnis nachgewiesen; ein abnehmendes O/C-Verhältnis entspricht einer schnellen Blauverschiebung von Huminstoff-ähnlichen

Verbindungen, was auf den Beitrag von Huminstoff ähnlichen Verbindungen zum mikrobiellen Abbau hindeutet, während die Stickstoff enthaltenden Formeln von Mikroorganismen unter methanogenen Bedingungen nicht bevorzugt werden. Ein Inkubationsexperiment mit der Zugabe von Hefeextrakten bewies darüber hinaus, dass die proteinähnlichen Peaks emittierenden Biopolymerfragmente unter methanogenen Bedingungen nicht bevorzugt werden, aber unter sulfatreduzierenden Bedingungen meistens schon in zwei Tagen verbraucht werden. Die Ergebnisse deuten darauf hin, dass die Abbauwege der organischen Substanz mit den Redoxbedingungen variieren, und zwar nicht nur wie bereits bekannt im Endschritt, sondern auch schon im Anfangsschritt des Abbauprozesses.

In größeren Sedimenttiefen könnte die Temperatur eine wichtige Rolle beim Abbau und Konservierungsprozess organischer Substanzen spielen. Das vierte Kapitel vergleicht DOM-Zusammensetzungen bei verschiedenen Temperaturen (20-85°C) in Inkubationsexperimenten mit tiefem Sediment, das während IODP-Expedition 322 aus dem Shikoku Becken am Rande des Nanaki Trogs vor Japan gewonnen wurde. DOM wurde durch EEMs und FT-ICR-MS charakterisiert. Die Konzentration von gelöstem Fe und Mn wurde überwacht. Die Ergebnisse zeigten, (1) bei 85°C einen wesentlichen Beitrag von abiotischen Prozessen zur Bildung von Acetat im terminalen Schritten; (2) dass bei 55°C die abiotische Zersetzung von Huminstoffen assimilierbare Fragmente liefert, die als Monomervorläufer zur Fermentation beitragen könnten; (3) dass bei 35°C abiotische Prozess kaum zur Zersetzung von Huminstoffen beitragen, aber die Freisetzung von organischen Fragmenten in die mobile Phase beschleunigt wird. Durch Inkubationen des Nankai-Trog-Sediments schlägt diese Studie Mechanismen des durch Hitze induzierten mikrobiellen Stoffwechsels durch anaeroben Abbau von organischem Material in tiefen Sedimenten vor, einschließlich der Freisetzung der Metallionen und organischen Substanzen, was zur Exposition und Zersetzung der gealterten Makromoleküle führt. Ein Modell für den Abbau von abiotischen Huminstoffen wird vorgeschlagen. Des Weiteren deuten die Ergebnisse darauf hin, dass der abiotische Prozess die Abbau-Selektivität und -Wege verändern könnte, indem er Vorläufer ohne Energiekosten von Mikroben anbietet und daher potenziell den Kohlenstoffkreislauf in der tiefen Biospähre beeinflusst.

Zusammenfassend lässt sich sagen, dass die Kombinationen von EEMs und FT-ICR MS zur Untersuchung der Wechselwirkungen zwischen Mikroorganismen und DOM in anaeroben Sedimenten zeigt, dass der Metabolismus von Mikroben sensitiv und adaptiv für Umweltbedingungen ist und auf diese Weise letztendlich der Kohlenstoff- und Stickstofffluss in tiefen marinen Sedimenten beeinflusst wird.

List of Figures

Figures in supplementary materials

List of Tables

Tables in supplementary materials

Chapter 1 Introduction

1.1. Marine sediments in the global carbon cycle

1.1.1 The significance of marine sediments as carbon reservoir

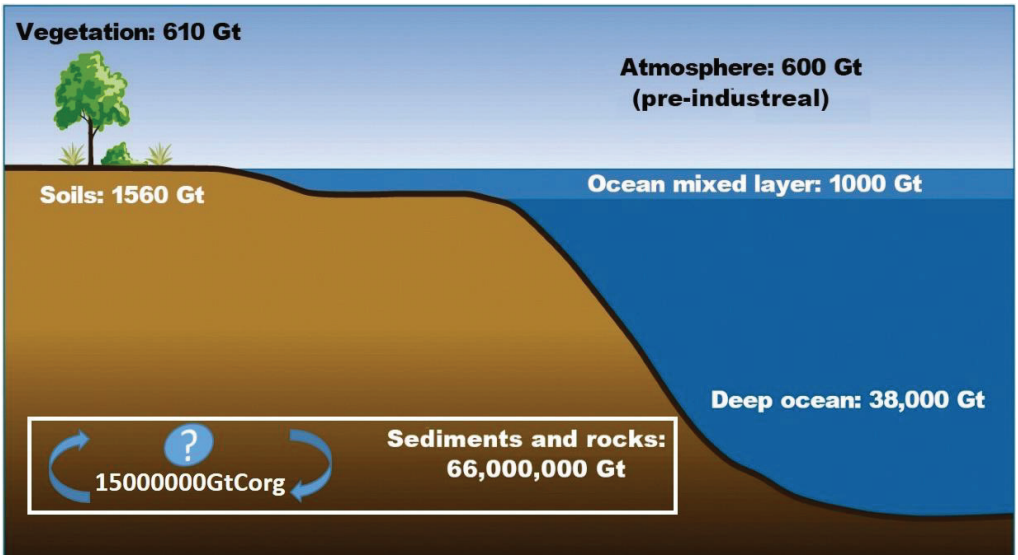

Fig. 1.1. The role of sedimentary organic carbon in the global carbon cycle. Figure has been adapted from Ruddiman (2014). Corg is an abbreviation for organic carbon. Data of Corg in sediments are from Hedges and Keil (1995).

Marine sediments play a key role in the global carbon cycle. They are the largest reservoir of organic carbon on Earth, containing 1.5×10^{17} g organic carbon in marine surface sediments and 1.5×10^{22} g organic carbon in sedimentary rocks, including kerogen (Emerson and Hedges, 1988; Berner, 1989; Hedges and Keil, 1995) (Fig. 1.1). The degradation and alteration of organic matter proceeds only slowly in subseafloor sediments, it hold reservoirs for methane (CH_4) (or gas hydrate) and higher hydrocarbons such as petroleum, which are of high societal relevance as greenhouse gases and energy resources.

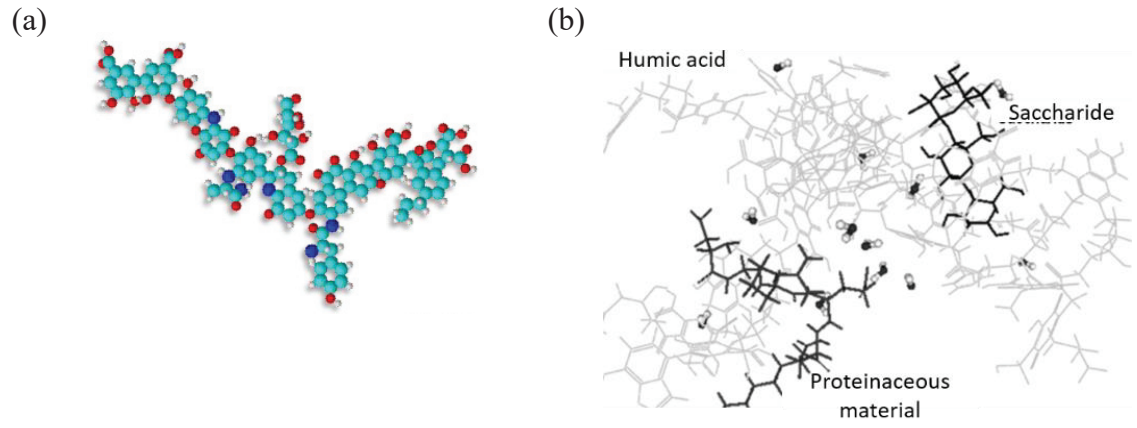

Fig. 1.2. The model of humic substances: (a) Structure of humic acid (Stevenson, 1994) and (b) Structure of soil organic matter (Schulten and Schnitzer, 1997; Saparpakorn et al., 2007). Blue, red and white balls represent carbon, oxygen and hydrogen atoms, respectively.

Subsurface sediments were considered as a huge pool for the preservation of organic matter. Intrinsically and biotically, the organic leftovers in subsurface sediments were reported to be compounds undergoing selective degradation and therefore were refractory (Henrichs, 1992; Wakeham and Canuel, 2006; Arndt et al., 2013). The preserved organic pool in sediments has been recognized as largely molecularly 'uncharacterized leftovers' (Wakeham et al., 1997; Hedges et al., 2000). Physically, the preservation of organic compounds can be sustained by a coating of organic compounds on minerals, which could protect the organics from degradation (Hedges et al., 2001). The accessibility of those labile molecules (e.g. amino acids, carbohydrates) can be reduced by the incorporation of organic compounds into refractory geomacromolecules or humic substances (Fig. 1.2) (Henrichs, 1992; Knicker and Hatcher, 1997; Schulten and Schnitzer, 1997; Zang et al., 2000). Moreover, chemically, polymerization and abiotic condensation of organics (polysaccharide and proteinaceous materials, phenol compounds) take place during diagenetic processes and produces geopolymers which are difficult to define structurally (Ertel and Hedges, 1985; Ishiwatari et al., 1986; Hedges and Keil, 1999; Wakeham and Canuel, 2006; Burdige, 2007). Without the availability of oxygen (O_2) as an electron acceptor, the rate of the mineralization process is slower in subsurface sediments (Henrichs and Reeburgh, 1987; Wakeham and Canuel, 2006).

Although the anaerobic mineralization processes are slow, they might drive a substantial microbial community in the subsurface (Schippers et al., 2005). Sedimentary organic matter provides carbon, energy and nutrients for microbial communities in the deep subseafloor biosphere, where intact microbial cells have been found down to 2.5 km below seafloor

(Inagaki et al., 2015). Life strategy of microbes is still obscure in the anoxic and energy-limited deep subsurface sediments. This would be informative for understanding the fate of the recalcitrant organic carbon pool. Are the marine sediments a pool for preservation or reactor? How could we observe the anaerobic degradation process of recalcitrant organic matter?

1.1.2 Continental margin sediments as an important reactor for organic matter

Continental margin sediments are a major sink of organic matter (Hedges and Keil, 1995). Although they account for only 20% of the surface area of the ocean, it contributes equally to carbon and nitrogen biogeochemical cycles in the sediments compared to deep sea sediments (Walsh, 1991). Due to river discharge of terrestrial organic matter and high productivity in coastal region, large amount of organic matter were exported to the surface sediments, however, organic preservation in the marine environment is less than 0.5% of the total exportation (Hedges and Keil, 1995).

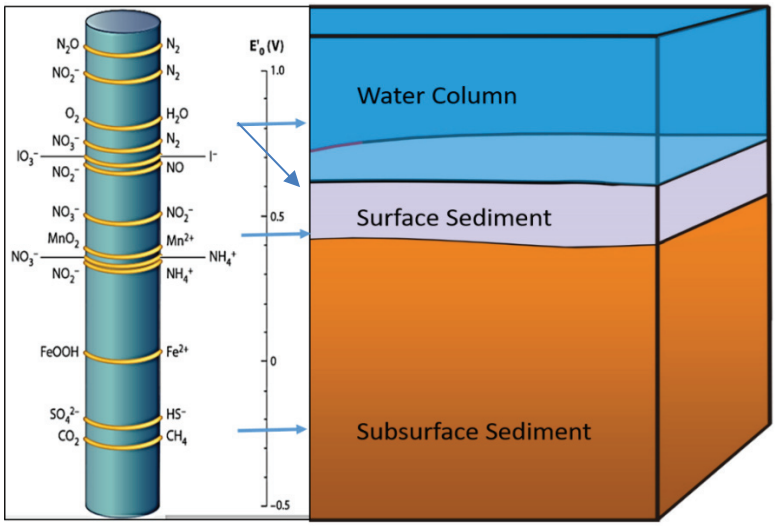

Fig. 1.3. Stratification of sediment and electron acceptors. Adapted from Lam and Kuypers (2011). E'_0 shows the electrode potentials of various redox couples at pH = 7.

The degradation of organic matter is an oxidation process, which is impacted by the oxidation-reduction potential (Fig. 1.3). The successive depletion of electron acceptors via denitrification, manganese (Mn) reduction, iron (Fe) reduction and sulfate (SO_4^{2-}) reduction is owed to a gradual decrease in the energy production per mole of organic carbon oxidized to carbon dioxide (Fig. 1.4) (Canfield et al., 1993; Chen et al., 2003; Parkes et al., 2014). Among those reactions, sulfate reduction has the highest contribution to the mineralization of organic

carbon in anoxic coastal sediment. Bowles et al. (2014) estimated that, 11.3 teramoles of sulfate is reduced yearly, globally accounting for the oxidation of 12 to 29% of the organic carbon fluxing to the seafloor. Sulfate reduction is the prevailing process in coastal sediments compared to pelagic sediments, where the reduction of oxygen and nitrate is dominant (Middelburg et al., 1993). In the deeper layer, the sulfate-methane-transition zone (SMTZ) is an important diagenetic redox boundary within marine sediments where the anaerobic oxidation of CH_4 (AOM) occurs (Hinrichs et al., 1999; Boetius et al., 2000; Lin et al., 2016). Below the sulfate-methane-transition zone (SMTZ), there is increasing production of CH_4 from CO_2 or volatile fatty acids (VFA, e.g., acetate). In the absence of sulfate, microbes largely depend on the generation of energy through reduction of CO_2 to CH_4.

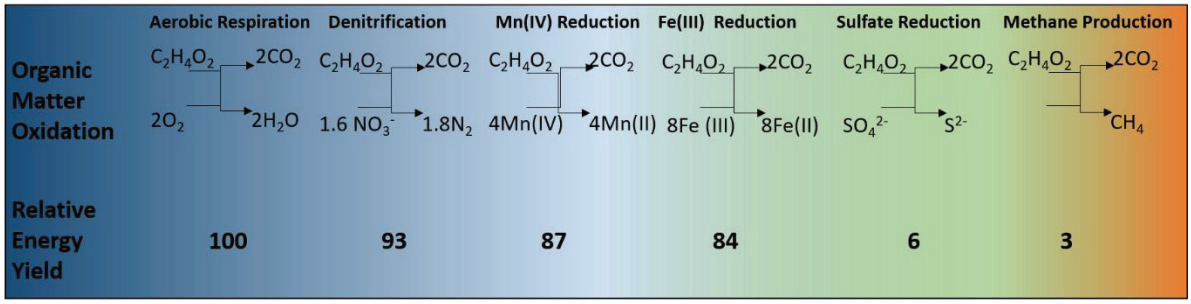

Fig. 1.4. Relative energy yield via different electron acceptors. Adapted from Lovley and Chapelle (1995). No units for the relative energy yield.

The *in situ* temperature in the sediments increases with depth. The continental subsurface sediments are featured by the deep thermal flow, especially in the deeply buried sediments near subduction zones in plate boundaries, ultimately leading to transformations of kerogen and release of hydrocarbons. Those extreme environments are supposed to be informative for the early life evolution and the origin of eukaryotes (Baross and Hoffman, 1985; Sogin, 1991; Martin and Müller, 1998). The gradual heating facilitates the abiogenic alteration of sedimentary organic matter and oil formation (Vandecasteele, 2008), it might potentially also stimulate the deep biosphere by producing acetate (Wellsbury et al., 1997), during these processes, the role played by the microbes is not clear.

1.1.3 DOM as a potential window to observe carbon cycling in the subseafloor

Plenty of studies have tried to observe the preservation and alteration of organic matter in the solid phase of sediments via bulk parameters (e.g., carbon content and isotope) or

biomarkers (e.g., lignin, sugar, amino acid) (Hedges et al., 1997; Dauwe and Middelburg, 1998; Dittmar and Lara, 2001; Schmidt et al., 2010; Arndt et al., 2013; Cathalot et al., 2013).

Most of the organic carbon in the sediments is in solid phase and slowly degraded. Mineralization fueled a small fraction of POC, which is not distinguishable by measurements of bulk parameters (Arnosti and Holmer, 2003). Investigations of the solid phase from *in situ* profiles result in information of long-term geologic carbon cycle in years to more than millions of years. Based on this information, however, it is difficult to understand the degradation processes and metabolism of microbes in subsurface sediments, where the biological cycle might take place relative rapidly (Arnosti and Holmer, 2003; Weston et al., 2006). In addition, variation in solid phase might result from biological, abiotic geological processes or varied organic matter sources during paleo-period. It is still unclear how the supposedly recalcitrant organic matter in marine sediments can serve as a food source as the degradation pathway is not known. Alternatively, the mobile organic matter in pore water is a potential window to observe the degradation processes and the carbon cycling during metabolism of microbes. The analysis of pore waters has become an important tool to elucidate the *in situ* metabolic activity of microbial communities (Heuer et al., 2009; Heuer et al., 2010; Rowe and Deming, 2011; Lin et al., 2012; Tong et al., 2013; Oni et al., 2015). Reactions of anaerobic organic matter degradation might be observable in the dissolved organic matter (DOM) pool as an intermediate pool during the remineralization of sedimentary organic matter. DOM receives the products of hydrolysis and fermentation processes, holding the substrates of terminal oxidation. It is differentiated from particulate organic matter by size limit below ~0.45 μm (Zsolnay, 2003).

A better mechanistic understanding of microbe-DOM-interactions is essential for the following aspects: (1) DOM could serve as electron donors and react with certain electron acceptors in a redox reaction, providing energy and nutrient for microbes. Via indoor-incubation, the transformation of DOM might be informative for the ongoing degradation process. The surviving strategy of microbes in subsurface sediment would be elucidated. (2) The investigation of DOM might provide new insights into the role of the deep subseafloor biosphere in the organic carbon preservation and global carbon cycle. However, so far little is known about the interaction between DOM and microbes and the impact of biogeochemical

processes on the composition of dissolved organic matter in marine subsurface sediments mainly due to the challenges of DOM characterization.

1.2 Interaction between microbes and DOM in marine subsurface sediment

1.2.1 Microbes in marine subsurface sediment

The study of the deep biosphere inferred that the mineralization and assimilation of organic carbon mainly exist in subsurface sediments. Although the diagenetic processes in the subseafloor are slow (Jørgensen and Marshall, 2016), there is a substantial amount of biomasses in the deep biosphere. The size of the deep biosphere is estimated to be huge: One of the first estimations by Whitman et al. (1998) suggested the global subseafloor sedimentary microbial abundance could be 3.5×10^{30} cells, comprising 55–86% of Earth's prokaryotic biomass and 27–33% of Earth's living biomass. The size of deep biosphere is remained under question: Other studies estimated that the microbial abundance in subseafloor sediments might be as high as 5×10^{30} cells (Lipp et al., 2008) or 2.9×10^{29} cells (corresponding to 4.1 petagram (Pg) C and ~0.6% of Earth's total living biomass (Kallmeyer et al., 2012)). An updated estimation results in 5.39×10^{29} cells and the depth integrated activity calculations demonstrate that subsurface sediments can be responsible for the majority of sediment activity (up to 90%) (Parkes et al., 2014). Considering this high amount of active biomass, a better knowledge of the diverse anaerobic metabolism would be important for the understanding of the carbon, nitrogen and sulfur cycling in sediments (Schulz and Zabel, 2006). Those cycles are closely connected to the chemistry of the ocean and the atmosphere on Earth and thus the global climate (Schippers et al., 2005).

Deep biosphere is characterized by microbial communities with slow metabolism. Jørgensen and Marshall (2016) suggested a cell community might go through only 10,000 generations from the time it is buried beneath the mixed surface layer until it reaches a depth of tens of meters several million years later. By adaptation of the radiotracer method, it has been possible to directly measure sulfate reduction rates that vary over more than 7 orders of magnitude, for example on the Peruvian shelf, from >1000 nmol $SO_4^{2-}cm^{-3}$ day^{-1} at the sediment surface to < 0.001 nmol SO_4^{2-} cm^{-3} day^{-1} at 100 m subsurface (Schulz and Zabel, 2006). The slow metabolism is accompanied with energy-limited conditions in deep sediments

(Jørgensen and Boetius, 2007). Nevertheless, sediments taken from depth more than one kmbsf have proved the existence of microbes (Roussel et al., 2008; Inagaki et al., 2015). It is not clear on which substrates the microbes are living. Up to 76% of total cells in the sediments incorporated heterotrophic substrates into their biomass carbon whereas 22% of total cells used CO_2 (Morono et al., 2011). The studies of archaea, which represent a major component of the deep marine subsurface biosphere, exhibit special autotrophic metabolism pathway (Berg et al., 2010). Autotrophy fixing CO_2 becomes more important in the hydrogen-producing deep layers with production of H_2 via radiolysis or heating (Sleep et al., 2004; Parkes et al., 2011). Impacts of deep biosphere on global biogeochemical cycles are not clear before we know which substrates the heterotrophic microbes could live on.

1.2.2 Anaerobic degradation of organic matter by microbes

1.2.2.1 DOM in the initial steps of anaerobic degradation

Organic matter in solid phase undergoes a series of steps during mineralization resulting in a complex organic pool in dissolved/mobile phase as DOM (Middelburg et al., 1993). The hydrolyzed organic matter in DOM pool is assimilable and passable for microbes via cell wall or remains in the pore water as leftover. During the degradation, the assimilable organic compounds provide the carbon, nutrients for microbes and electron donors for producing energy in subsurface sediment. Thus, as an intermediate pool in the degradation of organic matter, DOM in the pore water is a shuttle pool of organic matter reflecting the production and consumption during degradation (Weston et al., 2006).

Under oxic conditions, organic matter could be degraded directly to carbon dioxide via the tricarboxylic acid cycle by a single cell, while under anoxic conditions, a group of anaerobic microbes is participating in the food chain in sediments (Middelburg et al., 1993). The traditional well-known anaerobic degradation consists of three steps (Fig. 1.5). The initial step starts with breaking down the polymers via extracellular hydrolase, resulting in a soluble pool of high molecular weight (HMW) DOM. In the following, the HMW-DOM is further fermented into small volatile fatty acids or alcohols accompanying hydrogen production. These fermentation products are further metabolized by microorganisms that use oxidants (e.g., sulfate) to carbon dioxide and methane.

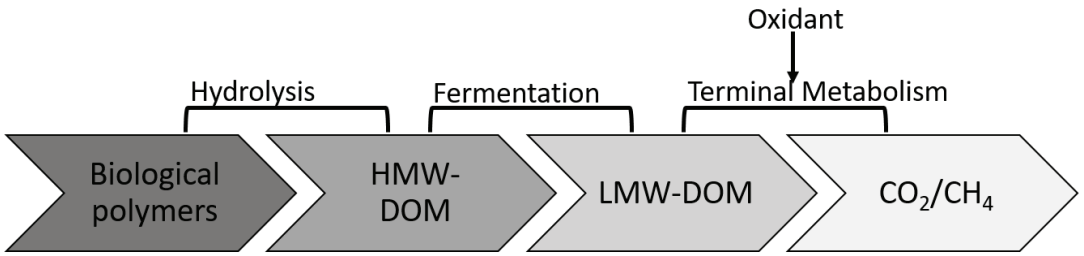

Fig. 1.5. Anaerobic degradation of organic matter, adapted from Middelburg et al. (1993). HMW-DOM and LMW-DOM stand for high and low molecular weight dissolved organic matter, respectively.

DOM is an intermediate pool sensitively revealing the production and consumption of organics. Microbial activities alter the molecular composition of DOM — potentially transform labile molecules into refractory dissolved organic matter (RDOM), which is assumed to be an important part of the microbial carbon pump in the ocean (Jiao et al., 2011). Different from the microorganisms in the water column with high primary production and freshly-produced bioavailable compounds, the 'dark life' in subsurface sediment survives from a complex and refractory organic residue. Prokaryotes dominate subsurface sediments and are featured by higher metabolic versatility than eukaryotes (Dworkin et al., 2006; Berg et al., 2010). To date little is known about the biogeochemical interactions between microbes and DOM in marine sediments.

Arnosti and Holmer (2003) reported that the dissolved organic carbon (DOC) in pore water was fast cycled, on average 8 - 31% of the sedimentary DOC pool must be turned over on a daily basis in Skagerrak; in the meantime, there is no distinguishable change in the bulk parameters of the solid phase. It suggested a close link between anaerobic degradation by microbes and DOM. Researches have investigated the turnover of DOM with molecular characterization in pore water by *in situ* profiles (Chen et al., 1993; Ohno, 2002; Schmidt et al., 2011; Tfaily et al., 2013; Seidel et al., 2015). However, it remains to be unclear as the DOM transformation deduced from *in situ* profiles might result from diverse environmental conditions, physical diffusions, and geological processes mixing with microbial processes.

1.2.2.2 Microbial degradation of biopolymers

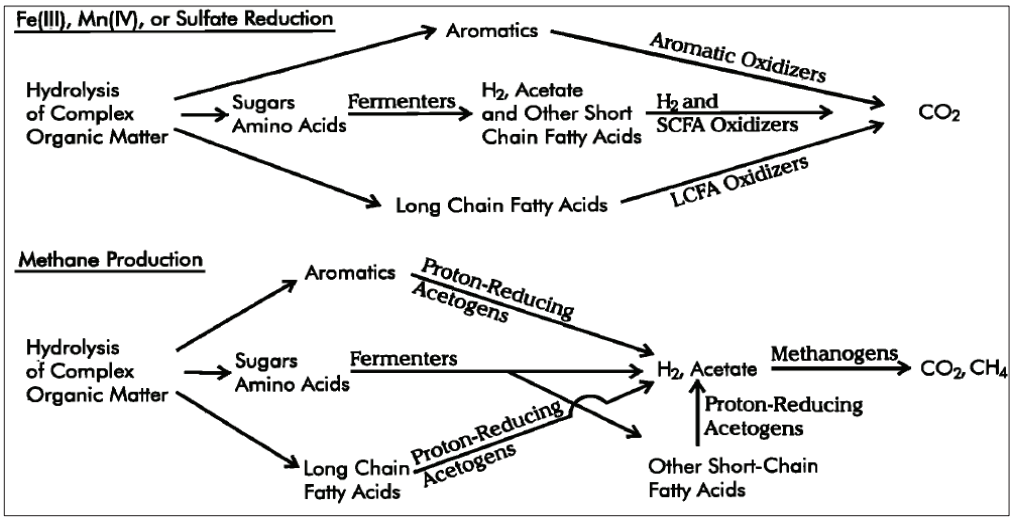

Fig. 1.6. Specific anaerobic degradation pathways of organic matter for aromatics, sugars, amino acids and long chain fatty acids, taken from Lovley and Chapelle (1995).

The anaerobic degradation processes of labile biopolymers were well investigated (Fig. 1.6). The organic matter is degraded via diverse metabolic pathways in anaerobic environments. Carbohydrates and proteins were conventionally considered as labile components for microbes. In an organic-rich coastal sediment, pore water carbohydrates constitute 85% of the DOC in near-surface intervals, while the fraction decrease to 24% at depths of 14–16 cm (Arnosti and Holmer, 1999), indicating that carbohydrates in pore water are likely turned over on short timescales in surface. Cellulose is the most abundant biopolymer in terrestrial environments and is normally associated with other natural compounds. It is decomposed by the anaerobic community through a complex microbial food chain: the first step is an enzymatic hydrolysis via celluloses, which mostly are large and multiprotein complexes produced by diverse anaerobes. Partial disassociation of the complexes might cause loss of activity of cellulase (Leschine, 1995). After hydrolysis, the hydrolysate is utilized by cellobiose-fermenters (Ljungdahl and Eriksson, 1985) or glucose-fermenters and terminally mineralized to CH_4, CO_2, and H_2O (Fig. 1.6). Fermentation is usually the rate-limiting step in the anaerobic decomposition of cellulose to methane (Wolin and Miller, 1987).

Proteins are also favorable food for microbes as they are a source for energy, carbon and nitrogen. It is estimated that the total hydrolysable amino acids make up 11 to 23% of the total carbon mineralized in a coastal sediments (Henrichs and Farrington, 1987). Proteins or peptides

are first hydrolyzed by proteinase. This process has not been well studied in natural anaerobic environments. Although there have been former studies of *in situ* profiles of amino acids, their turnover is hardly observed (Henrichs and Farrington, 1979; Alberic et al., 1996; Dauwe and Middelburg, 1998; Lomstein et al., 2006). Incubation experiments with sediments suggested that long peptide chains are fast degraded by a preferential cleavage of certain peptide bonds during hydrolysis (Pantoja et al., 1997). Afterwards, removal of amino group and acid oxidation commonly occurs in the anaerobic amino acid degradation before fermentation (Barker, 1981). It should be noticed that for the diverse types of amino acids microbes exhibit distinct preferences of degradation and metabolic pathways (Barker, 1981; Ramsay and Pullammanappallil, 2001; Leong et al., 2016).

Strong evidence of anaerobic degradation of aromatics has been found in 1934 (Tarvin and Buswell, 1934). Denitrification, sulfate reduction, fermentation or methanogenic fermentation could contribute to the degradation of aromatics (Evans and Fuchs, 1988). The pathways of aromatics degradation are diverse, and might happen in the side chains, aromatic rings or even both. The common step of cleavage of an aromatic ring is polarization of the stabilized conjugation structure resulting in a higher attainability of aromatic compounds during the transformation of aromatic rings to cyclohexane (Evans and Fuchs, 1988; Harwood et al., 1998). The attachment of hydroxyl or carboxyl groups to the aromatic nucleus facilitates biodegradation (Battersby and Wilson, 1989). Lignin is a representative of terrestrial organic matter with aromatic rings. Its relative inertness and massive production by land biomass makes it, or its derivatives, widespread compounds in coastal sediments and contributes to the formation of humic substances. Based on tests with aryl-^{14}C-labeled coniferyl alcohols, it was concluded that lignin is anaerobically not degraded (Hackett et al., 1977), but incubation of the solubilized lignin fractions with an inoculum from an anaerobic mesophilic sludge digester showed the cleavage of the intermonomer bonds during the degradation of lignin and a production of methane (Colberg and Young, 1982). Dittmar and Lara (2001) suggested the aromatic ring cleavage as a possible principal mechanism for lignin decay in sulfate-reducing sediments. Degradation of side chains, e.g., demethylation, was found under aerobic conditions (Dittmar and Lara, 2001; Frazier et al., 2005). The inconsistent results are a hint for that the anaerobic degradation of aromatic compounds, e.g. lignin in natural environment, might not be constrained to certain reported pathways and might change with experimental / environmental conditions (e.g., redox condition) or inoculum.

Long chain fatty acid (LCFA) are less labile for microbes compared to carbohydrates and proteins. Unsaturated fatty acids are easier degraded than the saturated LCFA and the degradability decreases with the length of saturated fatty acids (Novak and Carlson, 1970). The degradation could be fulfilled by α-oxidation or β-oxidation (Mackie et al., 1991). The former involves the sequential decrease in carbon number of fatty acids by oxidative decarboxylation; the latter starts with activation of fatty acids to acyl-CoA esters and involves a 2-carbon reduction in chain length with oxidation enzyme (Mackie et al., 1991; Sousa et al., 2009).

1.2.2.3 Microbial degradation of organic geopolymers

The definition of geopolymer proposed by Davidovits (1993) refers only to the inorganic geopolymers. Some geopolymeric materials can last for a long time due to their unique geopolymeric structure, so-called three-dimensional crosslink (Kim et al., 2006). Similarly, the humic substances in sediments are geopolymers polymerized from peptide, carbohydrate or phenols with crosslink to minerals (Ertel and Hedges, 1985; Ishiwatari et al., 1986; Schulten and Schnitzer, 1995; Schulten and Leinweber, 2000). Microbial degradation of the humic substances is not clear. This is especially an important topic for the subsurface sediments where the humic substances dominate in the organic carbon pool. Henrichs (1992) found that the specific compound classes that have been measured in sediments (e.g., hydrolyzable amino acids and carbohydrates, fatty acids and hydrocarbons) often decompose as slowly as total organic carbon (TOC) in the upper 1 m of coastal sediments. This study suggested that the compounds or fragments with higher bioavailability might not be selectively used in the sediments due to incorporation into the refractory macromolecules. As a potential explanation, Hedges et al. (2001) proposed that the physical coating of organic matter is correlated with the non-selective degradation in oxic environment. In summary, humic substances are supposed to be less efficiently degraded due to their irregular structures and coated compounds for enzyme attacks.

Nevertheless, humic substances could benefit the so-called humic-reducing microbes via electron transferring in quinone groups (Scott et al., 1998; Klüpfel et al., 2014). Immobilized humic substances and their analogues could even serve as effective redox mediators for the removal of recalcitrant pollutants (Costa et al., 2010; Martínez et al., 2013). It is not clear whether the humic substances could be carbon source or not. One interesting hint is that the methoxyl group of aromatics in coal could serve as carbon source for methanogen (Mayumi et

al., 2016), which is a common functional group in terrestrial humic compounds. Evidence is accumulating that Archaea with a heterotrophic life style play an important role in the deep biosphere (Biddle et al., 2006; Lipp et al., 2008; Berg et al., 2010) with their unique ability to cope with extreme energy starvation, and their presumed ability to degrade complex recalcitrant organic residues. It remains to be explored whether the humic substance might provide not only the electron donor but also the carbon or nutrient for microbes.

1.3 Methodologies for DOM characterization

1.3.1 EEMs

1.3.1.1 Principles of the method

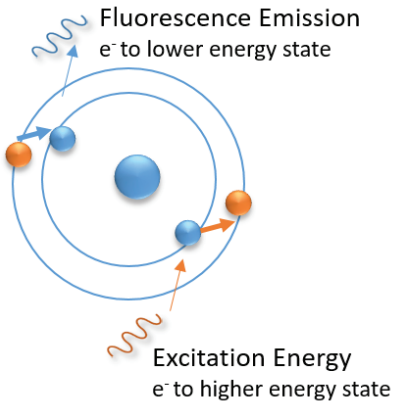

Fig. 1.7. Principle of fluorescence emission. Electrons from ground state orbitals to high energy levels, excited state (orange balls), afterwards relax to more stable ground state (small blue balls).

DOM is a potential window for observing the degradation processes of either geopolymers or biopolymers. In the pore water, DOM is a mixture of thousands of individual compounds (Schmidt et al., 2011; Oni et al., 2015; Schmidt et al., 2017; Valle et al., 2017), therefore molecular characterization is challenging. The analysis of such complex DOM compositions by Fluorescence Spectroscopy is an alternative approach since chromophores of DOM could absorb and emit light of specific wavelengths based on molecular structure of the compound. For example, conjugation structures of aromatic rings that contain π-electron can be excited by UV light effectively and emit fluorescence in the UV to visible light spectrum (Fig. 1.7). Excitation emission matrices spectra (EEMs) can be generated by exciting DOM containing

water samples with light over a range of wavelengths in the UV spectrum and simultaneously measuring wavelengths and intensity of light that is emitted from the excited samples. Typically, such EEMs contain thousands of wavelength-dependent data points of fluorescence intensity, which can be grouped into excitation-emission regions based on range of fluorescence peak (ex/em).

1.3.1.2 Indices derived from 2D fluorescence spectrum

FI, BIX and HIX derived from 2D-scan of emission spectrum resulting from excitation at 370 nm, 310 nm and 254 nm were interpreted as indexes of terrestrial source (FI), biological activity (BIX) and humification (HIX), respectively (Mcknight et al., 2001; Huguet et al., 2009).

The fluorescence index (FI) is the ratio of the fluorescence intensity at 450 and 500 nm emission resulting from the excitation at 370 nm (Mcknight et al., 2001). FI can be used to distinguish the origin of DOM. Generally, FI is less than 1.4 in terrestrial dominated DOM; FI of microbial-derived DOM is higher than 1.8 (Mcknight et al., 2001). The signal is based on humic-like peak C in long emission wavelength.

Biological activity index (BIX) is calculated from the ratio of fluorescence intensity emitted at 380 nm and 430 nm resulting from the excitation at 310 nm. BIX provides an information about fresh autochthonous DOM (BIX > 1) (Huguet et al., 2009). The signal is derived mainly from humic-like peak M, which is less conjugated than humic-like peak C.

Humification index (HIX) is calculated from the ratio of integrated fluorescence emission in 435–480 nm to that in 300–345 nm at excitation of 254 nm (Ohno, 2002; Huguet et al., 2009). HIX more than 10 and HIX less than 4 indicates humified DOM and autochthonous DOM, respectively (Huguet et al., 2009). Higher HIX values correspond to maximal fluorescence intensity at long wavelength and thus the presence of complex molecules like high molecular weight aromatics (Senesi and Miano, 1991; Huguet et al., 2009).

1.3.1.3 Peaks and index derived from 3D fluorescence spectrum

Application of EEMs in water column is firstly proposed in 1990s (Coble et al., 1990; 1996). The EEMs of samples varies with organic matter composition and is hard to be quantified and categorized by direct observation (examples in Fig. 1.8).

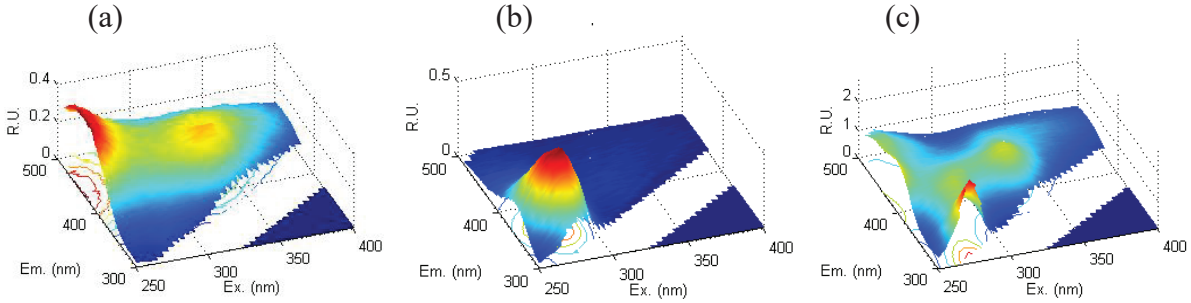

Fig. 1.8. Typical EEMs Spectrum and chromophore regions. (a) Pore water sample dominated by humic-like peaks; (b) Yeast extract dominated by protein-like peak; (c) Pore water sample from heated sediment with both high protein-like peaks and humic-like peaks.

Parallel factor analysis (PARAFAC) is a generalization of Principal Components Analysis (PCA) to higher order arrays. Decomposition of multi-dimensional arrays leads to the mathematical identification and quantification of independently varying fluorophores, e.g., a simple and robust result for easier interpretation (Bro, 1997; Stedmon and Bro, 2008; Murphy et al., 2013). PARAFAC analysis was developed in recent years and enables the classification of compounds (Stedmon and Bro, 2008; Murphy et al., 2010; Murphy et al., 2013; Cuss and Guéguen, 2016). Combined with PARAFAC analysis (Stedmon et al., 2007; Stedmon and Bro, 2008), the Excitation-Emission-Matrix Spectra (EEMs) (Coble, 1996; 2007) can be used to identify different fluorescent DOM components such as protein-like and humic-like compounds. An example of PARAFAC analysis was shown in Fig. 1.9.

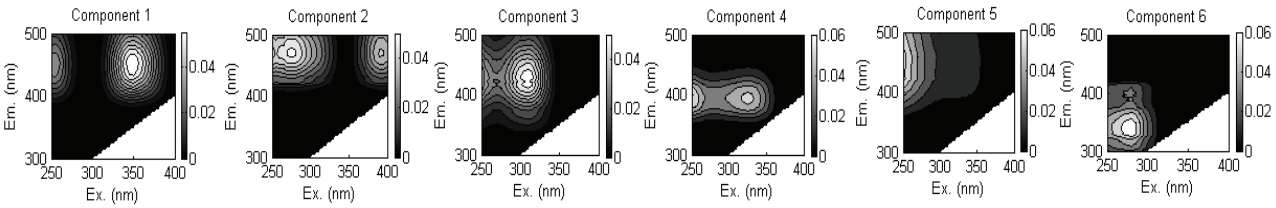

Fig. 1.9. An example of peaks identified by PARAFAC analysis. Six peaks (from component 1 to 6: C1, C2, M1, M2, A and T, respectively).

Protein-like peaks are mainly classified into tyrosine-like peak B (ex/em 270-280 nm/300-310 nm) and tryptophan-like peak T (ex/em 270-280 nm/340-370 nm) (Coble, 1996; Yamashita and Tanoue, 2003; Yamashita and Tanoue, 2004; Fu et al., 2006; Martínez-Pérez et al., 2017). Protein-like peaks are induced by aromatic amino acids, e.g., tryptophan, tyrosine and phenylalanine, and represent a relatively labile DOM pool in some water column studies (Stedmon and Markager, 2005b; Fellman et al., 2010; Lønborg et al., 2010). Proteins containing aromatic amino acid residues, generally emit fluorescence due to tryptophan, and tyrosine fluorescence is only observed in the absence of tryptophan (Creighton, 1983; Yamashita and Tanoue, 2003). Tryptophan-like DOM was reported to be consumed preferentially compared to tyrosine-like materials (Jaffé et al., 2014). Accordingly, in the surface water of Sagami Bay, amino acid-containing DOM in the high molecular mass fractions was comprised of protein molecules or least degraded proteins (polypeptides) exhibiting protein-like peak T, while in the deep water (1000 m) other forms of amino acids were dominant and exhibited peak T and B (Yamashita and Tanoue, 2004). The other compounds, e.g., gallic acid and tannins were reported to emit protein-like peaks (Maie et al., 2007) as phenol compounds with auxochrome could be fluorescent at the region of protein-like peaks. This is not surprising due to the diverse possibility of compounds for certain fluorescent peak. It should be noticed that the protein-like peak do not necessarily correspond to the high bioavailability (Cory and Kaplan, 2012). One thing for certain is that protein-like peaks should imply less conjugated structure mainly with two or less aromatic rings for natural DOM samples (Zsolnay, 2003).

Humic-like peaks represent irregular geopolymers – humic substances, which emit fluorescence at > 400 nm with mainly four to seven aromatic rings (Zsolnay, 2003). Those peaks imply different sources of organic matter in the studies of water column, e.g., terrestrial and marine humic-like components (Coble, 1996; Fellman et al., 2010). They were classified as peaks C, M and A according to Coble (1996). Peak C (ex/em 350/450 nm), with longest emission wavelength at UVA range represents large molecules with aromatic functional groups and conjugations. Such components are commonly referred as terrestrial origin (Coble, 1996; Fellman et al., 2010). Peak M (ex/em: 300-320/395-410 nm) represents compounds that are less aromatic than peak C, and is commonly referred to as autochthonous, microbial or marine components with relatively lower molecular weight (Coble, 1996; Fellman et al., 2010; Ishii and Boyer, 2012). Peak A shows the shortest excitation wavelength at UVC range and emission

wavelength at UVA range. It represents common components in natural aquatic systems and resembles aromatic fulvic acids from terrestrial sources (Stedmon and Markager, 2005a; Coble, 2007).

Humic-like peaks and protein-like peaks identified in 3D spectra were conventionally considered as the labile and refractory components in many studies (Hudson et al., 2007; Lønborg et al., 2009; Fellman et al., 2010; Lønborg et al., 2010; Lønborg and Álvarez-Salgado, 2012; Jaffé et al., 2014). Recent studies based on the incubation of sludge implied a preferential utilization of carbohydrate and protein-like DOM in anaerobic degradation processes, while humic-like compounds were most resistant to biodegradation (Li et al., 2014; Li et al., 2015).

Humic substances dominate in sedimentary organic matter and are considered to be refractory. The preservation of this material might be attributed to its complexity and irregularity that inhibits the efficiency of microbial degradation. On the one hand, the humic fraction of high-molecular-weight (HMW) DOM accumulated in sediments as abiotic condensation products of low-molecular-weight (LMW) DOM during humification (Krom and Sholkovitz, 1977). One the other hand, the observation of blue-shift of fluorescence spectra suggests an opposite process: less conjugation of humic substances during diagenesis (Sierra et al., 2001). Other studies suggest the humic substances are contributing to the energy achieving process for microbes for transferring the electrons (Scott et al., 1998; Martínez et al., 2013; Klüpfel et al., 2014). It is not clear whether the humic substances is refractory and what is the role of microorganisms in the transformation processes.

The ratio of peaks A and C to peak M (AC/M) or C/M ratio can be used to identify a blue-shift of the fluorescent signal of organic compounds. Such a shift is produced by the loss of conjugation structures. The AC/M ratio represents the proportion of compounds with longer emission wavelength, i.e., large terrestrial molecules with aromatic functional groups and conjugations. The blue-shift is indicated by the decrease of AC/M ratio and indicates a loss of aromaticity, e.g., loss of aromatic ring or auxochrome. In further, it indicates the ratio of terrestrial DOM and autochthonous DOM in water column.

1.3.1.4 Advantages and disadvantages

This method enables the sensitive observation of the complex DOM in small sample volume, which makes high-frequency observations possible especially for the samples limited

by volumes. Unlike many other methods, pretreatments including desalting and concentrating are not necessary before measurements. Low instrument and maintenance costs made it possible to use this method extensively in recent years in marine and environmental sciences.

Care needs to be taken due to the ambiguity of EEMs in molecular-level information and multi-possibility for non-natural DOM fluorescent compounds. Identification of the chromophores is a major challenge. Interpretation limitations is especially a problem for small data sets with little spectral variability, the results of PARAFAC analysis might be over-simplified and show models with few (≤ 3) components (Rosario-Ortiz and Korak, 2017). Moreover, the implication of protein-like and humic-like peak is not consistently accepted in former studies. For example, protein-like peak has been found to be closely related with the the content of labile amino acid, whereas, this peak might also consist of labile fluorescent compounds encapsulated in the non-fluorescent recalcitrant fractions or other biopolymers (Yamashita and Tanoue, 2004; Cory and Kaplan, 2012). Therefore, verification of the information characterized by this method is important. For example, in this thesis, yeast extracts were used to confirm the turnover of protein-like biopolymer fragments.

Besides, the fluorescent signal is affected by several factors. Quenching might happen due to the complexation between DOM and ions or particles (Manciulea et al., 2009). Change in pH may have large effect in the shape of humic-like compounds with phenol groups (Mobed et al., 1996). In addition, the matrix effect and the effect of oxygen/redox conditions are not fully understood. For samples and wavelengths where DOM absorption coefficients are above approximately 10 m^{-1} or 0.1 cm^{-1}, inner filter effect might impact the spectra (Stedmon and Bro, 2008), which could be corrected by mathematical methods (Mobed et al., 1996).

1.3.1.5 Applications in environmental researches

The methods have been successfully applied in water column studies of ocean, estuary water, and rivers (Coble, 2008; Murphy et al., 2008; Yamashita and Tanoue, 2008; Murphy et al., 2010; Lønborg et al., 2010; Guo et al., 2010; Yang et al., 2011; Jaffé et al., 2014; Gan et al., 2016). It has been also applied in the surface sediment pore water or underground water (Komada et al., 2002; Chen and Hur, 2015; Huang et al., 2015). Without identifying exact molecular composition, water column studies showed EEMs provided information about aromaticity (Ishii and Boyer, 2012), size (Her et al., 2003; Cuss and Guéguen, 2015), quinone-

like compounds (Cory and McKnight, 2005), transformations and turnover (Yamashita and Tanoue, 2003; Coble, 2008; Catalá et al., 2015) as well as the potential bioavailability of DOM (Stedmon and Markager, 2005b; Lønborg et al., 2009; Lønborg et al., 2010). Its application is not limited to natural DOM, pollutions due to fluorescent compounds in natural water could be determined by EEMs with PARAFAC analysis (Zhou et al., 2013; Ferretto et al., 2014; Peleato et al., 2017).

1.3.2 FT-ICR MS

1.3.2.1 Principles of the method

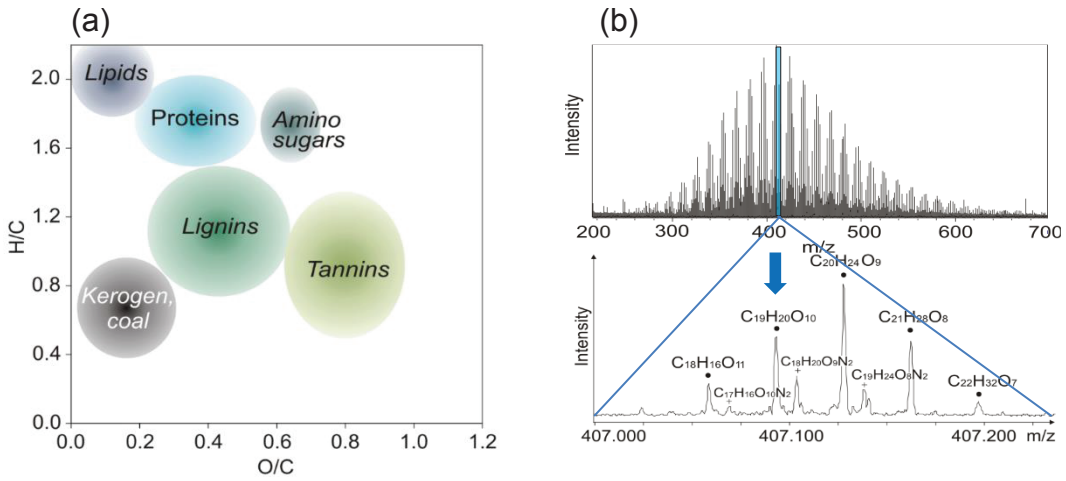

Fig. 1.10. Grouping of formulae by elemental ratio and original spectrum of FT-ICR MS sample, adapted after (Kim et al., 2003; Sleighter and Hatcher, 2008; Schmidt, 2009). (a) Potential regional plots of some major biomolecular components in the van Krevelen diagram; (b) Original spectrum of ESI-negative FT-ICR MS and expanded sections of mass spectra at nominal mass 407 of sediment pore water from mud belt.

The molecular formula for DOM could be achieved by Fourier transform ion cyclotron resonance mass spectrometry (FT-ICR MS). The molecular characterization of DOM could be informative for examining the role and dynamics of sedimentary organic matter pool. Its high resolution is realized by ions bent into a circular path by the magnetic field excited (excited at their resonant cyclotron frequencies) and cycling by passing near detection plates; continuous injections of one samples enable the accumulation of signals and resolution of peaks. The technique was invented in 1974 (Comisarow and Marshall, 1974a; Comisarow and Marshall, 1974b). The high resolution is especially an advantage for the complex mixtures, e.g., natural DOM with resolving power of 8×10^5 at m/z 300 (Kujawinski et al., 2001).

Base on the H/C ratio and O/C ratio, a van Krevelen Diagram could be generated for the visualization of compositional variations (Fig. 1.10) (Kim et al., 2003; Kujawinski et al., 2004). It should be noticed that in the natural DOM pool compounds over longtime diagenesis process might not necessarily correspond to the regions shown in Fig. 1.10a.

1.3.2.2 Application in environmental researches

With the development of statistical approach (Kujawinski and Behn, 2006; Koch et al., 2007; Sleighter et al., 2010; Herzsprung et al., 2014), time-consuming manual formula assignment could be avoid. It has been successfully applied to characterize seawater DOM (Koch et al., 2005; Hertkorn et al., 2006; Hertkorn et al., 2013), river water DOM to evaluate land usage (Wagner et al., 2015), investigate organic matter degradation (Gonsior et al., 2009; Koch et al., 2014; Lechtenfeld et al., 2014) and thermal transformation of OM (Hawkes et al., 2015; Gomez-Saez et al., 2016; Hawkes et al., 2016; Lin et al., 2017). Characterization of DOM in marine pore water is reported in several recent studies (Schmidt et al., 2009; Schmidt et al., 2011; Schmidt et al., 2014; Seidel et al., 2014; Schmidt et al., 2017; Valle et al., 2017): DOM in marine pore water is characterized by abundant nitrogen-containing formulae (CHNO). CHNO compounds are transformed via: (a) hydrolysis and deamination with reducing molecular size and nitrogen content; (b) oxidation and hydration; and (c) methylation and dehydration (Schmidt et al., 2011; Abdulla et al., 2017).

1.3.3 Other techniques in characterizing DOM

Nuclear magnetic resonance spectroscopy (NMR) is a conventional analytical method in characterizing organic matter, especially for pure compounds. It is first described and measured by Rabi et al. (1938). Based on the type of nuclei and its chemical environment (electron), signals of absorbed electromagnetic radiation differ. ^{1}H-NMR (Fig. 1.11) and ^{13}C-NMR is most commonly used nuclei, which determine the chemical environment of hydrogen and carbon, respectively. Multi-dimension of NMR is proposed and developed in 1980s-1990s (Ernst et al., 1987; Brüschweiler et al., 1991; Wüthrich, 1994) and it has been applied in the DOM characterization in recent seawater investigations (Hertkorn et al., 2006; Hertkorn et al., 2013; Abdulla and Hatcher, 2014). It is a powerful tool in resolving the functional group and chemical structure, for example, carboxylic acids, aromatic rings, and aliphatic chains etc., which could not be directly identified by FT-ICR MS or EEMs. The data analysis of NMR is usually done

by manual processes; automation of data processing is not popularized. The natural DOM often shows overlapping signals in the spectra.

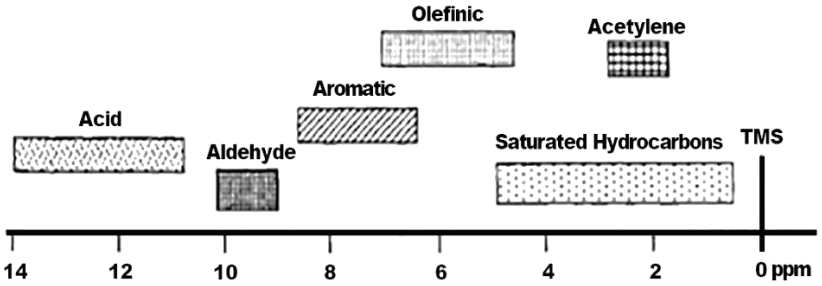

Fig. 1.11. Identification of the functional group by chemical shift in ^{1}H-NMR. Figure has been redrawn from Balci, 2005. TMS is abbreviation for tetramethylsilane.

Other methods, e.g., infrared spectroscopy, are also commonly applied in the characterization of pure compounds and occasionally in the studies of natural organic matter combined with NMR or EEMs (Guo et al., 2012; Abdulla and Hatcher, 2014). Vibration of certain atom/bond show vibrational frequency close to infrared light. Functional groups or carbon bonds absorbing light at specific wavelength show characteristic peaks and vary with surrounding chemical environments. It is a qualitative method for characterization of the chemical groups. The three methods (EEMs, FT-IR and NMR) are summarized in Fig. 1.12.

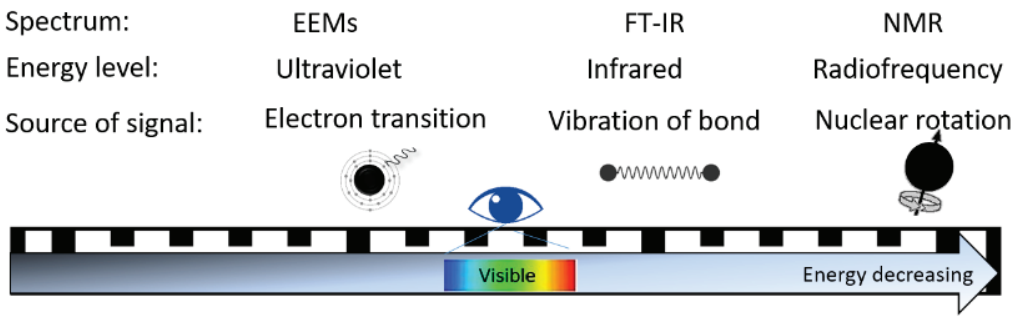

Fig. 1.12. Comparisons of the principles of the three methods (EEMs, FT-IR, and NMR).

1.4 Environmental conditions modulating the terminal steps of organic matter degradation

1.4.1 Terminal steps of degradation

There are plenty of intermediates in an anaerobic organic matter degradation chain, e.g., short-chain fatty acid, alcohol etc., of which acetate and hydrogen are two of the most common products or substrates in anoxic sediment.

Acetate is produced from diverse substrates: chemolithoautotrophic substrates (e.g., H_2-CO_2), sugar and O-demethylate methoxylated aromatic compounds (Ljungdahl, 1986; Drake et al., 2013). Acetogens coexist and cooperate with terminal mineralizer (e.g., sulfate reducers and methanogens) due to a better life strategy and energetic cost of biosynthesis, of which energy yields per substrate is not necessarily the only variable controlling microbial metabolism in energy-depleted environment (Lever, 2012). Acetate could be oxidized in anoxic conditions via citric acid cycle, carbon monoxide dehydrogenase pathway and disproportionation to carbon dioxide and methane (Thauer et al., 1989). The energy yields vary with the metabolic pathway. For example, in standard condition (0°C, 101 kPa, 1 mol/L), the denitrifying bacteria produce energy of 802 kJ/mol (Payne, 1981). Whereas, the sulfate reducers-Desulfotomaculum acetoxidans produce energy of 63 kJ/mol via carbon monoxide dehydrogenase pathway (Widdel and Pfennig, 1977), the energy production is 36 kJ/mol for methanogens, which is sufficient for driving the synthesis of only 0.5 mol ATP (Thauer et al., 1989).

Metabolism of acetate could produce H_2 and the metabolism is endergonic (ΔG^0 = +95 kJ/mol) when the pressure of H_2 was kept below $10^{-4.2}$ atm (Zinder and Koch, 1984). The bacteria that degrade acetate into CO_2 and H_2 could grow syntrophically with H_2-consuming microbes. Hydrogen is also produced during fermentation process, which is ultimately consumed by terminal mineralizer – sulfate reducers or methanogens etc. via interspecies hydrogen transfer (Stams and Plugge, 2009). Theoretically, concentration of H_2 in a steady state is associated with the redox conditions. Independent to the organic matter composition, Lovley and Goodwin (1988) determined typical range of H_2 concentration of 7-10 nM for methanogenesis; l-l.5 nM for sulfate reduction; 0.2 nM for Fe reduction; less than 0.05 nM for

Mn(IV) or nitrate reduction. Metabolism of H_2 in subsurface sediment attracted attention lately due to its contribution to the survival of microorganisms in the deep biosphere, especially the thermophilic bacteria and archaea that obtain H_2 from abiotic processes instead of biological processes (Szatmari, 1989; Freund et al., 2002; Sokolova et al., 2004; Hellevang, 2008; Verhaart et al., 2010).

1.4.2 Impact of redox conditions on terminal steps of anaerobic degradation

The terminal processes are modulated by the availability and type of electron acceptors. They are fulfilled by denitrifying bacteria, iron/sulfate reducing bacteria and methanogenic archaea. Consistently, the intermediates (volatile fatty acid, alcohol) could be metabolized in different ways. For example, denitrifying bacteria degrade acetate via the citric acid cycle (TCA) cycle, which is a common metabolism in aerobic microorganisms, sulfate reducers degrade acetate via carbon monoxide dehydrogenase pathway. Difference of degradation between sulfate–reducing and methanogenic condition is summarized in Fig. 1.13. Methanogens disproportionate acetate to CH_4 and CO_2. It was reported that acetate is the only organic compound with a carbon-carbon bond that methanogens can degrade (Zellner and Winter, 1987; Thauer et al., 1989). Methanogens also rely on the so-called 'secondary fermenters', which produce mainly C1/C2 intermediates or methylated compounds (Oremland and Polcin, 1982; Demirel and Scherer, 2008). The compounds for methanogenic processes were listed in Table 1.1. In addition, the recent findings suggest that methanogens are capable of several other metabolisms: reduction of Fe(III) oxides and extracellular quinones (Bond and Lovley, 2002); a single methanogen has been proven to produce methane from coal by methoxy group in complex compounds (Mayumi et al., 2016).

As a comparison, the sulfate reducers are more versatile in degrading the small intermediates: the secondary fermenters are not necessary; a monomer or intermediates fermented from monomers could be utilized by sulfate reducers (Muyzer and Stams, 2008). The anaerobic degradation chain consists of the terminal mineralization and initial steps, e.g., hydrolysis or fermentation. It is not clear whether the initial steps of anaerobic degradation would change with the redox conditions. Kristensen et al. (1995) suggested that soluble and labile substrates were metabolized in a similar rate with or without oxygen. However, the particulate and complex macromolecule were degraded far more slowly under anaerobic

conditions compare to aerobic conditions, due to the limiting step in initial phase (hydrolytic and fermentative enzymatic attack) under anaerobic conditions (Kristensen et al., 1995).

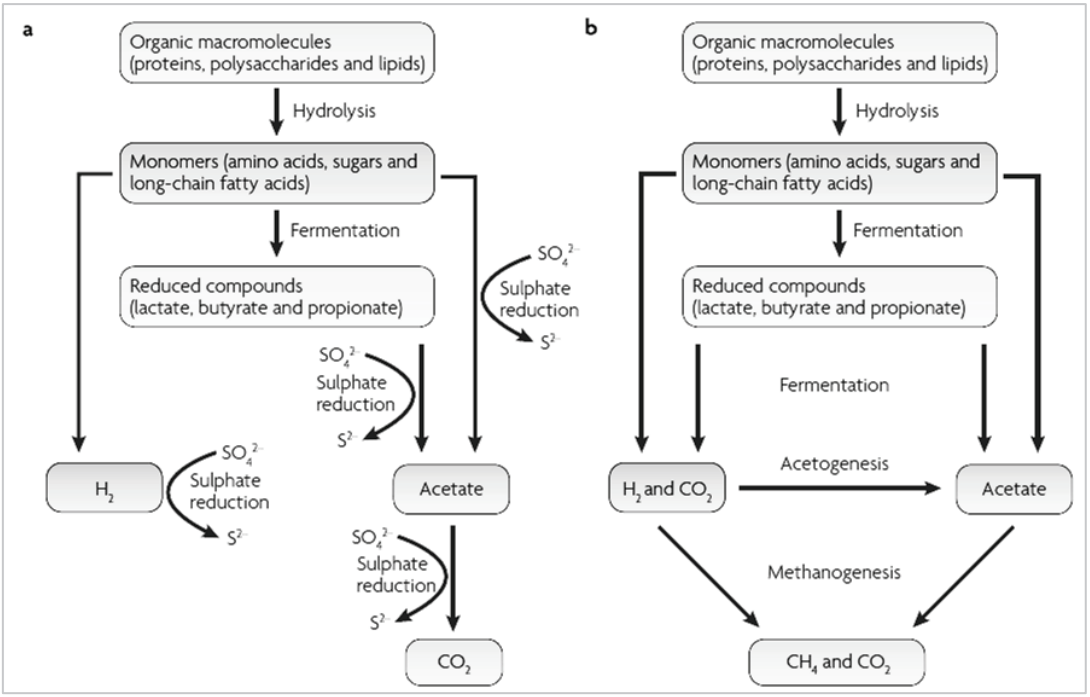

Fig. 1.13. Anaerobic degradation of organic matter under (a) sulfate-reducing condition and (b) methanogenic condition, figure was adapted from Muyzer and Stams, 2008.

Although the major parts of sediments were uniformly defined as anoxic zone, the immobility of solid phase results in stratification of redox conditions in sediments. It is enigmatic whether the different anaerobic conditions are related to the specific pathways of organic matter degradation, especially the initial steps.

Table 1.1. Typical reactions during methanogenesis

Reaction carried out by methanogenes	
Hydrogen:	$4\ H_2 + CO_2 \rightarrow CH_4 + 2\ H_2O$
Acetate :	$CH_3COOH \rightarrow CH_4 + CO_2$
Formate:	$4HCOOH \rightarrow CH_4 + CO_2 + 2\ H_2O$
Methanol	$4\ CH_3OH \rightarrow 3\ CH_4 + CO_2 + 2\ H_2O$
Carbon monoxide:	$4\ CO + 2\ H_2O \rightarrow CH_4 + 3\ H_2CO_3$
Trimethylamine:	$4(CH_3)_3N + 6\ H_2O \rightarrow 9\ CH_4 + 3\ CO_2 + 4\ NH_3$
Dimethylamine:	$2(CH_3)_2NH + 2\ H_2O \rightarrow 3\ CH_4 + CO_2 + 2\ NH_3$
Methylamine:	$4(CH_3)NH_2 + 2\ H_2O \rightarrow 3\ CH_4 + CO_2 + 4\ NH_3$
Methylmercaptans:	$2(CH_3)_2S + 3\ H_2O \rightarrow 3\ CH_4 + CO_2 + H_2S$
Metals:	$4Me^0 + 8\ H^+ + CO_2 \rightarrow 4\ Me^{++} + CH_4 + 2\ H_2O$

Source from Chynoweth (1996) and Demirel and Scherer (2008)

1.4.3 Impact of temperature on terminal steps of anaerobic degradation

Temperature increases with depth due to geothermal heating in subsurface environments and has important role in chemical reactions and kinetics. Chemically, temperature may affect the Gibbs free energy yield from a redox reaction, accordingly, temperature is modulating microbial energy production, which drives the survival of microbes and maintenance requirements (Tijhuis et al., 1993). Microbial community composition and cell membrane adapt to the surrounding temperature (Cossins and Prosser, 1978; Schouten et al., 2002; Gagliano et al., 2014; Schmidt et al., 2015; Pollo et al., 2016). Microbial habitat is distinguished in wide range of temperature. There are psychrophiles (≤ 20°C), mesophiles (20-42°C), thermophiles (42-70°C) and hyperthermophiles (> 70°C). Some prokaryotes can grow at temperatures as high as +120°C (Kashefi and Lovley, 2003). At temperature higher or lower than optimum growth temperature, the growth rate decreases sharply due to the thermal inactivation of enzymes and disruption of the membrane structure (Dworkin et al., 2006). With the increase of temperature, cell membrane contains more saturated bond or cyclization instead of olefinic bond (De Rosa et al., 1980; Elling et al., 2015). In addition, temperature affects the optimum pathway of terminal mineralization. Roussel et al. (2015) examined the impact of temperature on terminal mineralization processes at the range of 0-80°C with sediments from tidal flat, Woodhill Bay, UK (non-thermal sediments): acetate oxidation has maximum activity at up to ~34°C for metal oxide reduction with metal oxide as electron acceptor and up to ~50°C for sulfate reduction with sulfate as electron acceptor. Below 50°C, sulfate reduction by utilizing acetate is increasing with temperature, but H_2 is more preferred substrate (Roussel et al., 2015). Methanogens also show similar change of substrates to preferentially use H_2 at high temperature, meanwhile methanogenesis from methylamine ceased at high temperature (> 43°C) (Schulz and Conrad, 1996; Roussel et al., 2015).

It is noteworthy that optimum temperature of microbes is not limited to the above ranges. It depends on the *in situ* temperature of sediments and on microbial communities. Furthermore, as for the initial steps, enzymatic hydrolysis and fermentation is reported to be impacted by temperature: the maximum hydrolysis rate were found at 10-20°C for Arctic sediment and > 30°C for intertidal sediment of North Sea (Arnosti, 1998; Arnosti and Jørgensen, 2003; Hao and Wang, 2015). The biological hydrolysis is limited by the enzyme thermostability and denaturation of enzymes (protein) is generally rapid at high temperature (Colussi et al., 2012).

Protein degradative reactions at high temperatures (> 80°C) occur only slowly in conformationally intact proteins (Koch et al., 1990; Daniel, 1996). In some specialized cases, some bonds or ions are helpful to increase thermostability of certain enzyme, e.g., disulfide bridges (Matsumurat et al., 1989), hydrogen bonding (Vogt et al., 1997). The extremely thermostable amylolytic enzyme found in archaea has half-life of 2 h at 120°C (Koch et al., 1990). Considering the short half-life of the enzyme at high temperature, it would be expensive to renew the extracellular enzyme and repair thermal damage. The upper limit of life is as high as 121°C (Blöchl et al., 1997; Kashefi and Lovley, 2003). It is interesting whether the biotic hydrolysis is efficiently supporting the survival of microbes at high temperature and whether there is 'rough and ready' foods for microbes from abiotic processes. Lin et al. (2017) suggested that hydrothermal heating of young rift sediments released massive bioavailable DOM at 90°C. It is not clear to what extent the abiotic process has contributed to the release of carbohydrate and peptides in dissolved phase and ultimately to microbial metabolism. Moreover, in the aged and oligotrophic sediment, this process might play a less important role due to the limitation of bioavailable organic matter.

1.5 Objectives and outline of thesis

One key question in deep biosphere research is microbial carbon metabolism in the extreme conditions with recalcitrant organic residue and limited electron acceptors, i.e., the mechanisms of anaerobic degradation in different extreme environmental conditions. Stratification of sediments lead to variation in redox conditions and temperature, which leads to the change of microbial community and terminal mineralization (Clark et al., 1998; Biddle et al., 2005; Briggs et al., 2013; Roussel et al., 2015). The terminal step of degradation reviewed above suggested varied patterns due to the change of environmental conditions. It raises questions of initial steps of degradation: Could the refractory organic matter be degraded to assimilable substrates and how is the degradation pathway under varied environmental conditions (summarized in Fig. 1.14).

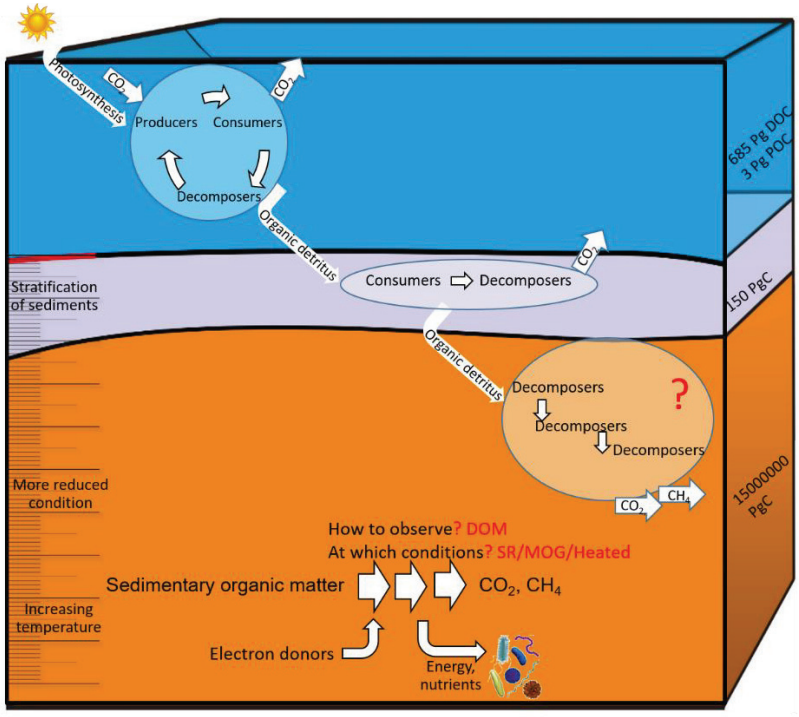

Fig. 1.14. Carbon cycle in the ocean and questions remained in subseafloor sediments. SR and MOG refer to the sulfate reducing condition and methanogenic condition, respectively.

The initial steps of anaerobic degradation are largely unknown especially due to the complexity of dissolved organic matter (DOM). To investigate the impact of biogeochemical processes on the composition of DOM in marine subsurface sediments, this thesis aims to answer following questions in a generalized way:

1. Can fluorescence spectroscopy be applied for the analysis of DOM in subsurface sedimentary pore water, especially for the geopolymers?
2. Could the geopolymers be degraded and consumed by microbes? Which substrates were preferentially degraded or assimilated by microbes in energy-limited environments?
3. How do redox conditions and temperature influence the DOM cycling?

To address these questions, three sub-projects were designed:

1.5.1 Sub-project 1: method establishment

Aim: (1) impacts of matrix effects and sample storage; (2) pretreatments of EEMs samples from anoxic marine sediments.

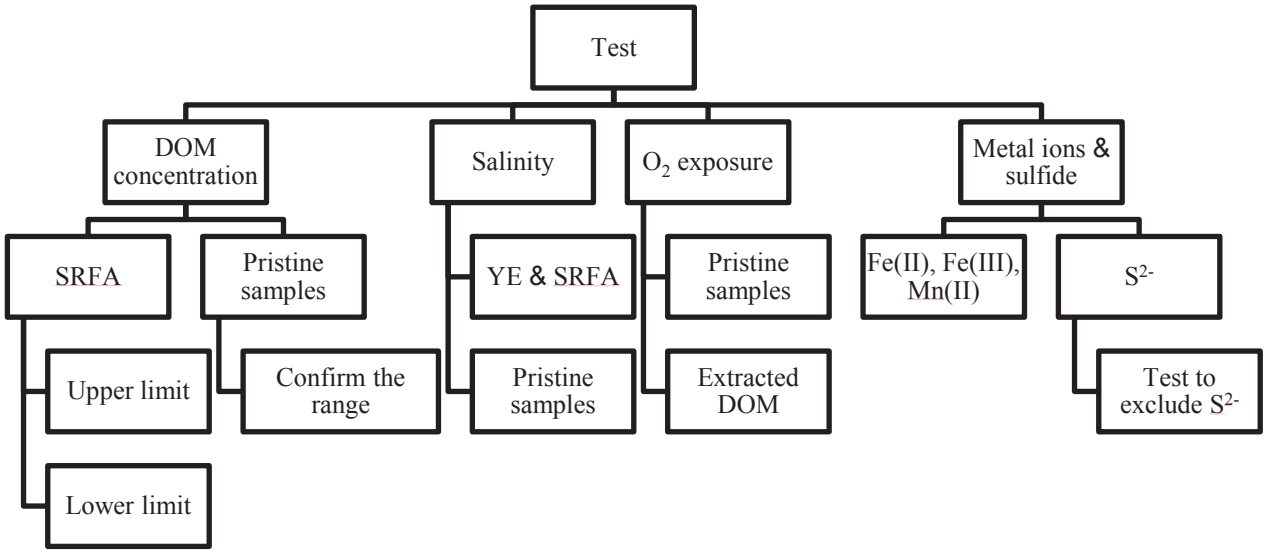

Fig. 1.15. Scheme of first experimental design. SRFA and YE are abbreviation of Suwannee River Fulvic Acid and yeast extracts, respectively. For pristine samples, the liquid was filtered by filter (pore size 0.2 μm) from sediment slurries.

Compared to these oxic environments, pore water in deep sediment is unique with highly concentrated DOC, high concentrations of redox-sensitive inorganic ions. It is unclear how to pretreat the samples and to what extent the matrix effects affect the indexes. This study aims to investigate the impacts of pretreatments on the fluorescence spectra. Impact of DOM concentration, NaCl, Fe(II), Fe(III), Mn(II), S^{2-} and O_2 exposure were investigated (Scheme flow in Fig. 1.15). Tests were made on humic-like DOM represented by Suwannee River Fulvic Acid and protein-like DOM represented by yeast extract. For confirmation, natural pristine samples from anoxic incubations of sediments were used; sediments samples from North Sea and Rhône Delta represent for metal-ion-rich terrestrial DOM and sulfide-rich DOM, respectively. For the validity of the results, we used FT-ICR MS as a complementary method. EEMs could be used to continuously monitor changes of DOM in incubations or in-situ profiles at high sampling frequency in a small amount of liquid (50 μL in this study, the magnitude of order at μg C). This is especially an advantage for the study of deep biosphere as sampling of pore water is a demanding task for the deep compacted sediments. A manuscript of method establishment was written and will be submitted soon.

1.5.2 Sub-project 2: impacts of redox conditions on DOM cycling

Aim: (1) DOM cycling under sulfate reducing *vs.* methanogenic conditions; (2) selectivity of the initial steps before fermentation and terminal mineralization; (3) carbon cycle and preservation modulated by redox-conditions.

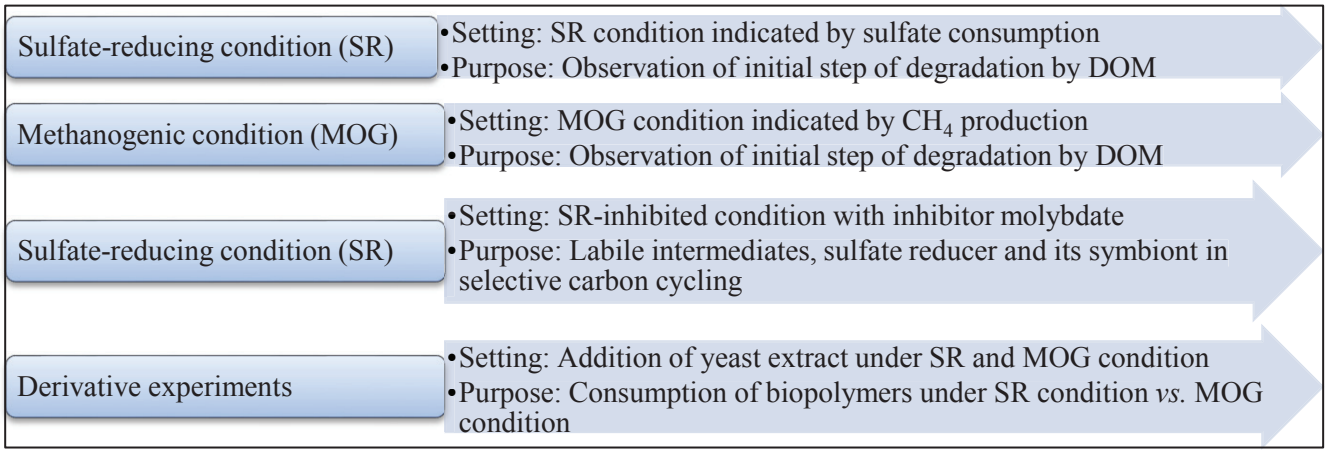

Fig. 1.16. Scheme of second experimental design.

The microbes are surviving under the limitation of electron acceptors in the deep reduced sediments. The coastal anoxic sediments are typically stratified into sulfate-reducing and methanogenic conditions. Incubations with different sulfate addition were conducted to evaluate the impact of redox conditions on DOM cycling and thereafter the anaerobic degradation path (Fig. 1.16). Inhibitors were added to one batch to allow the accumulation of metabolites and observation of fermentation and terminal steps. By EEMs and ultrahigh resolution FT-ICR MS, we found typical mechanism of anaerobic degradation in different redox conditions in subsurface sediment (sulfate-reducing zone and methanogenic zone). Based on incubation of sediment from the Mediterranean Sea, it was elucidated how the selectivity of anaerobic degradation and pathways of organic matter degradation prior to the terminal step shifts in response to the stratification of redox conditions. A manuscript based on the experiment was written and is ready for submission.

1.5.3 Sub-project 3: impacts of thermal conditions on DOM cycling

Aim: (1) impact of temperature of DOM and acetate production in heated deep sediments; (2) define the contribution of biotic and abiotic process in the initial step on the degradation of organic matter.

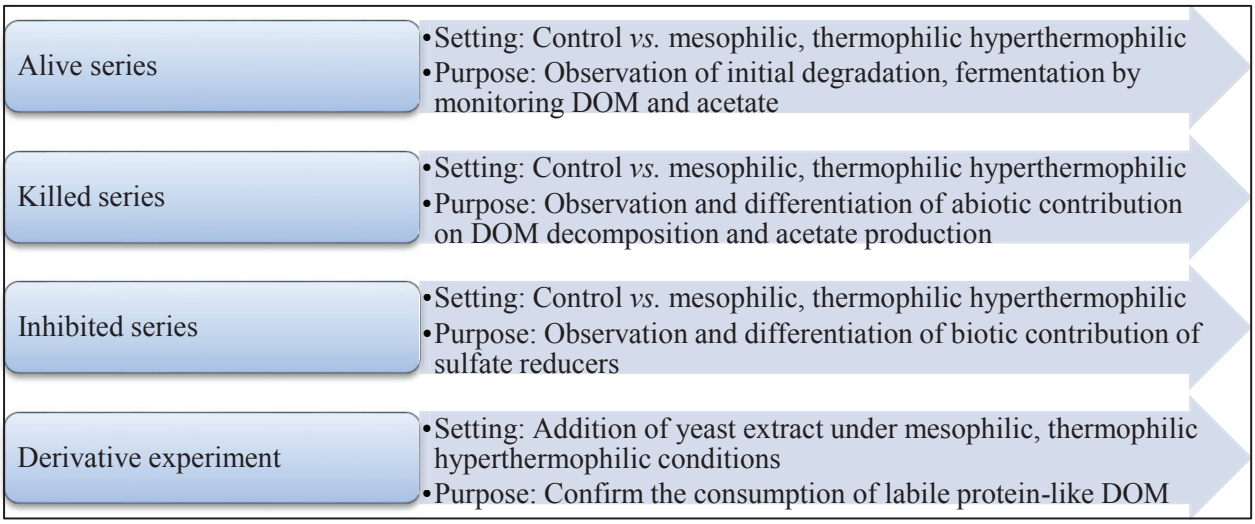

Fig. 1.17. Scheme of third experimental design.

In the deep subseafloor, geothermal heating is an important environmental factor and associated with alteration of organic matter and minerals. It is not clear whether and how heterotrophic organisms in deep sediments are stimulated by heating. This study investigated the microbial carbon cycling at mesophillic, thermophilic and hyperthermophilic conditions in subseafloor sediments recovered from a high heat-flow area in the Nankai Trough (IODP Site C0012). Experiments were conducted in the temperature range of 20°C to 85°C and consisted of alive, killed and partly inhibited series for differentiation of biotic/abiotic and intermediate/terminal processes (Fig. 1.17). Microbial activity, transformation of organics and metabolic intermediates were monitored via analysis of hydrogen gas, hydrogenase enzyme activity, dissolved organic matter (DOM), Mn & Fe, and volatile fatty acids. DOM was characterized by EEM spectroscopy and FT-ICR MS. Results showed temperature modulated the contribution of abiotic process on the anaerobic degradation of humic substances. The aged (7.8 Ma old) macromolecular – humic substances are split into labile and refractory units during heating. This study provided the basis for a new conceptual model for the initiation of humic substance degradation. The model suggests that the combination of abiotic and biotic processes in DOM degradation is crucial for the sustenance of the deep life in moderately heated sediments. A manuscript based on the experiment was written and is under revision by coauthors.

Chapter 2 Application of Excitation Emission Matrix Spectroscopy (EEMs) for the characterization of dissolved organic matter (DOM) in anoxic marine sediments

Shuchai Gan*, Verena B. Heuer, Frauke Schmidt, Lars P. Wörmer, Kai-Uwe Hinrichs

MARUM – Center for Marine Environmental Sciences, University of Bremen, Leobener Straße, D-28359 Bremen, Germany

*correspondence: sgan@uni-bremen.de

Abstract

Marine sediment is the major carbon reservoir on Earth and a possible pool of substantial carbon cycling stimulated by the deep biosphere. Dissolved organic matter (DOM), a feedstock linked to carbon cycling in these sediments, is difficult to be characterized. Moreover, recovery of pore water from anoxic deep sediments is a demanding task. This study aims to apply excitation-emission-matrix spectroscopy (EEMs) for DOM characterization in small amounts of liquid. We investigated the impacts of DOM concentration, ionic strength, the presence of typical redox sensitive ions and oxygen exposure on the fluorescence spectra. Parameters determined by fluorescence spectra include 3D-indices after PARAFAC analysis including P/H, AC/M (or C/M) ratio and common 2D-indices including FI (contribution of terrigenous DOM), BIX (autochthonous DOM and biological activity), HIX (humification index). Tests were made with Suwannee River Fulvic Acid (SRFA) representing humic-like DOM and yeast extract (YE) representing protein-like DOM, and results were confirmed with sedimentary DOM samples from anaerobic incubations. (a) For high humics concentration (20 mg/L), quantitative information is lost while qualitative information (peak ratio, FI and BIX) remains reliable; over-dilution (< 0.6 mg/L) makes analysis more susceptible to noise. Humics concentrations in the range of 0.9 mg/L-6 mg/L (absorption coefficient < 0.06 cm^{-1}) result in both consistent quantitative and qualitative results; for natural water in this study, ~ 1 μg of dissolved organic carbon is enough. (b) O_2 exposure significantly impacts the fluorescence of sedimentary Fe(II)-

rich DOM samples from the Rhône Delta due to changes of the matrix instead of intrinsic change of DOM, which remained relatively constant according to Fourier transform ion cyclotron resonance mass spectrometry. (c) The major redox-sensitive elements including Fe(II), Mn(II) in anoxic sedimentary pore water resulted in a loss of fluorescence even without oxidation. This effect is negligible if the concentration of Fe(II), Mn (II) is below 0.06 mM in the final diluted samples. Sulfide induces a red-shift of the fluorescence spectra, therefore, we recommend to flush sulfide-rich samples with N_2 before storage. (d) EEMs is a complementary method for DOM characterization to FT-ICR MS, as for the latter the protein-like DOM is selectively lost during solid phase extraction. Based on these observations we propose a sample preparation pipeline for pore water from anaerobic environments that enables measurements with micro-liquid sampling (50 μL in this study) and thereby the time-efficient, high-resolution observation of DOM composition in deep biosphere research.

Key words: deep subsurface sediment, EEMs, PARAFAC, pore water

2.1 Introduction

Marine sediments and sedimentary rocks play a key role in the global carbon cycle as the largest carbon pool on Earth (Berner, 1982; Berner, 1989; Hedges and Keil, 1995). The anoxic subsurface sediments were commonly considered as the pool for preservation of recalcitrant organic matter (Henrichs and Reeburgh, 1987). During the past two decades, however, abundant microbial communities have been found to exist in deeply buried sediments, even down to 2.5 km below seafloor (Parkes et al., 1994; Roussel et al., 2008; Inagaki et al., 2015), and the widespread occurrence of biogenic methane and gas hydrate in subseafloor environments testifies to their biological activity (Kvenvolden, 1995; Inagaki et al., 2006; Sherwood Lollar et al., 2006). The discovery of the deep subseafloor biosphere challenges our understanding of the carbon cycle and raises new questions about the nature of sedimentary organic matter, its degradation, and preservation.

Sediments contain both particulate organic matter (POM) attached to sediment grains and dissolved organic matter (DOM) in their interstitial waters. Since turnover rates are slow, alterations in the large POM pool are difficult to observe, but reactions of organic matter degradation might be observable in the much smaller, more short-lived DOM pool. As an intermediate pool during the remineralization of sedimentary organic matter, DOM receives

the products of hydrolysis and fermentation processes, thus holding the pool substrates accessible to terminal remineralization (Middelburg et al., 1993). Detailed analyses of sedimentary DOM can potentially open a window to examine carbon cycling in sediments (Krom and Sholkovitz, 1977; Chin et al., 1998; Weston, Porubsky, V. a. Samarkin, et al., 2006; Tfaily et al., 2013; Valle et al., 2017).

Marine sedimentary DOM is a complex mixture of thousands of different compounds (Schmidt et al., 2009; Schmidt et al., 2011). The analysis of DOM in marine sediments is typically complicated by small sample volumes, for which pore-water samples need to be extracted from sediment cores by a rhyzon sampler or squeezer. So far, concentrations of bulk dissolved organic carbon (DOC) have been determined routinely, for example in the context of scientific ocean drilling programs, e.g., IODP, ODP (Simoneit and Sparrow, 2002; Heuer et al., 2009; Lin et al., 2012; Lin et al., 2015), and analyses of individual compound classes, such as volatile fatty acids (VFAs) and alcohols, have been carried out occasionally (Heuer et al., 2009; Zhuang et al., 2014), but an overall characterization of the complex DOM pool in the deep biosphere has rarely been achieved. Methods such as Fourier Transform Ion Cyclotron Resonance Mass Spectrometry (FT-ICR MS) for formulae assignments, Nuclear Magnetic Resonance Spectroscopy (NMR) for functional groups (Hertkorn et al., 2006; Hertkorn et al., 2013), and Infrared Spectroscopy (IR) for chemical bonds (Artham and Doble, 2012; Guo et al., 2012), have been successfully applied in environmental studies. Especially, FT-ICR MS resolves thousands of individual molecular formulae in highly complex mixtures, and can be used for unraveling the composition of hitherto ‘uncharacterizable’ DOM (Koch et al., 2005; Dittmar et al., 2007; D’Andrilli et al., 2010; Hertkorn et al., 2013; Schmidt et al., 2014; Schmidt et al., 2017). All three methods require relatively large sample volumes (tens of milliliter or more) for pore water DOM samples. The retrieval of samples in excess of a few milliliters pore water, however, is a demanding task. This is especially true for deep biosphere studies, as pore water yields decrease with increasing depth and consolidation of sediments.

Fluorescence Spectroscopy is an alternative approach to the direct molecular characterization of DOM by FT-ICR MS, NMR and IR. Compared to the latter, Fluorescence Spectroscopy can be carried out on smaller sample volumes (2-3 mL for seawater) without pretreatment by solid phase extraction (SPE), is non-destructive and lower-cost. It takes advantage of the presence of chromophores in DOM that absorb and emit light of specific

wavelengths, which are related to the molecular structure of the compounds. 3D fluorescence spectra, also known as Excitation Emission Matrix Spectra (EEMs), contain thousands of excitation and emission wavelength-dependent data points of fluorescence intensity that can be grouped into different DOM components by Parallel Factor Analysis (PARAFAC) as statistical tool (Stedmon and Bro, 2008; Murphy et al., 2010; Murphy et al., 2013; Cuss and Guéguen, 2016).

EEMs can be used to identify and quantify different fluorescent DOM components such as protein-like peaks related to labile compounds (Yamashita and Tanoue, 2003; Stedmon and Markager, 2005a; Fellman et al., 2010; Lønborg et al., 2010), and humic-like peaks indicating highly aromatic terrestrial DOM, microbial or marine DOM (Coble et al., 1990; Coble, 1996; Coble, 2007; Fellman et al., 2010; Ishii and Boyer, 2012). Based on the individual fluorescent peaks in 3D-scans, peak ratios can be used to infer the aromaticity, sources, and bioavailability of DOM without determination of the exact molecular composition and regardless of unambiguous identification of fluorescent component pools. In addition, 2D-scans of emission spectra resulting from excitation at 370 nm, 310 nm, and 254 nm serve as indices for terrestrial source (FI), biological activity (BIX) and humification (HIX), respectively (Mcknight et al., 2001; Ohno, 2002; Huguet et al., 2009). More indices can be derived from 3D-scans and 2D-scans, e.g., A/T, C/A, C/T ratio (Baker et al., 2008; Hansen et al., 2016), redox index (Cory and McKnight, 2005), molecular weight by E4/E6 ratio (Chen et al., 1977), Freshness index (β:α) (Parlanti et al., 2000), etc.

EEMs have been successfully applied to investigate DOM in the water column of oceans, estuaries and rivers (Coble, 2008; Murphy et al., 2008; Yamashita and Tanoue, 2008; Murphy et al., 2010; Lønborg et al., 2010; Guo et al., 2010; Yang et al., 2011; Jaffé et al., 2014; Gan et al., 2016; Martínez-Pérez et al., 2017), shallow sediments and underground water (Burdige, 2001; Komada et al., 2002; Burdige et al., 2004; Chen and Hur, 2015; Huang et al., 2015). The applicability of EEMs for deep anoxic sedimentary DOM is rarely explored. In particular, the following matrix and sample handling effects require attention compared to the aquatic systems or surface sediments. (a) Concentrations of chromophoric DOM are one to two orders higher in pore-waters, and this might cause inner filter effects (i.e., chromophore optical absorption in the excitation or emission region) and need to be corrected (Tucker et al., 1992; Kubista et al., 1994; Mobed et al., 1996; Ohno, 2002; Gu and Kenny, 2009; Luciani et al., 2009). By

separating peaks by PARAFAC analysis, the upper limit of DOM concentration for the quantitative and qualitative analysis would be clearer. More importantly, given the small volumes available for the deep pore-water from compacted sediments, it is valuable to consider dilution of samples and therefore to verify the lower limit of DOM concentration. (b) High concentrations of metal ions in anoxic sediments might lead to complexation of DOM and precipitation, thus affecting chromophore properties and identification of EEMs peaks; iron has shown effect of quenching (Poulin et al., 2014), it is not clear at which concentration range the ions interfere with the EEMs or could be negligible. (c) Anaerobic redox conditions prevail in marine sediments, and the contact of sedimentary DOM samples with ambient air during sample handling might trigger oxidation, complexation, and precipitation that can affect optical signals. (d) Dilution of high concentration samples leads to decrease of ionic strength, the effect of which has been tested for humic acids (Mobed et al., 1996), while its impact on individual peaks after PARAFAC analysis and indices of natural pore water samples is not known.

Therefore, we investigated the potential matrix effects in sediment pore-waters in a series of experiments, including impacts of DOM concentration, ionic strength, major redox-sensitive metal ions, and S^{2-}. We tested the Suwanee River Fulvic Acid Standard (SRFA) and yeast extract (YE) as representatives for humic-like and protein-like DOM, respectively, as well as two mixtures of natural sedimentary DOM prepared from slurries of coastal marine sediments (North Sea and Rhône Delta). The anoxic natural samples also served to test the effect of oxygen exposure during sample handling for EEMs and FT-ICR MS analyses.

2.2 Materials and methods

2.2.1 Experiments

The experiments were summarized in the flow chart in Fig. 2.S1.

2.2.1.1 Test of matrix effects in DOM samples prepared from SRFA and YE

Potential matrix effects that might occur in marine sedimentary DOM due to high concentrations of DOM, salts, metals and sulfide in pore water were tested with two reference samples. Humic-like DOM was investigated using a 1 g/L stock solution prepared from SRFA (standard reference material of the International Humic Substances Society) and N_2-flushed,

O_2-free Milli-Q water. Protein-like DOM was investigated using a 10 g/L stock solution, which had been prepared from yeast extract (YE) (Alfa Aesar, H26769) in O_2-free Milli-Q water. Both solutions were kept under N_2 atmosphere in 100-mL serum bottles that were closed with grey butyl rubber stoppers and crimp caps.

Four sets of tests were performed to evaluate the influence of DOM concentration, salts, metals and sulfide: (a) In order to test the effect of DOM concentration, secondary stock solutions (SRFA: 400 mg/L) were diluted with Milli-Q water in nine dilution steps, yielding a concentration range of 0.18-20 mg/L SRFA. (b) NaCl or KCl was commonly used in the test of ionic strength in physio-chemical experiment (Mobed et al., 1996; Snowden et al., 1996; Icenhower and Dove, 2000). In order to investigate the impact of ionic strength, secondary stock solutions (SRFA: 400 mg/L; YE: 1000 mg/L) were mixed with NaCl solution, yielding a DOM concentration of 4 mg/L for SRFA and 10 mg/L for YE and NaCl concentrations ranging from 0 to 327 g/L. (c) The impact of major redox-sensitive metal ions was tested by addition of $FeCl_3$, $FeCl_2$, $MnCl_2$, yielding a concentration range of 0-0.9 mM for the metals ions and a DOM concentration of 4 mg/L for SRFA and 10 mg/L for YE. (d) The potential interference of sulfide was tested over a concentration range of 0-10 mM in 4 mg/L SRFA and 10 mg/L YE respectively. Stock solutions of Na_2S were prepared at concentration of 200 mM and kept under N_2. All dilution series were prepared on the same day and analyzed immediately by fluorescence spectrometry.

2.2.1.2 Preparation of slurries for in-house standards of marine sedimentary DOM

In order to confirm the matrix and sampling effects in natural anoxic pore-water samples, two in-house standards of marine sedimentary DOM were prepared using large sediment samples from two contrasting environments – North Sea tidal flat and surface sediment from the Rhône Delta. While the former has low TOC and high sulfide concentrations, the latter is characterized by high concentrations of TOC and metals. The first in-house standard was prepared from surface sediment (~2-7 cm) of the North Sea tidal flat Janssand off Spiekeroog Island, North Sea (53° 44.18′ N, 7° 41.97′ E), that was accessed by foot during ebb tide in October, 2013. The coastal sediment was sandy, black, and odorous due to a high abundance of dissolved sulfide. The total organic carbon (TOC) content was low (0.2 wt.%). The sediment was representative of natural sulfide-enriched autochthonous DOM samples. The second in-house standard (Rhône Delta) was prepared from surface sediments (mixtures of sediments

from depth 0-18 cm) from the Rhône Delta in the Gulf of Lions, Western Mediterranean Sea, sampled at site GeoB17306 (43° 18.95' N, 4° 52.18' E, 30 m water depth) during *RV Poseidon* Cruise POS450 in April 2013. This coastal site is characterized by high riverine input, high TOC contents (1.3 wt.%), anoxic conditions, and high concentrations of dissolved metal ions. This sample represents a typical terrestrial DOM end member dominated by humic-like compounds with slight admixture of protein-like compounds. The surface sediment was retrieved by multi corer (GeoB17306-1). Immediately after core recovery, the upper 0-18 cm of sediment were transferred into three Schott glass bottles, which were flushed with N_2, closed with butyl rubber stoppers and stored at +4°C until further processing on shore. Details on coring operations and sample handling onboard are given in the cruise report (Heuer et al., 2014).

For the generation of large-volume aqueous samples for DOM analyses, the sediment samples were homogenized and further processed in the following way: 100 mL of wet sediment were slurried 1:1 with oxygen-free autoclaved artificial seawater, which was prepared from 0.682 g KCl, 1.5 g $CaCl_2*2H_2O$, 5.7 g $MgCl_2*6H_2O$, 26.4 g NaCl, 6.8 g $MgSO_4*7H_2O$, 0.099 g KBr in 1 L Milli-Q water, to which finally 10 mL of 1 M $NaHCO_3$ solution were added. The slurries were kept under N_2 atmosphere in 250-mL Schott glass bottles closed with butyl rubber stoppers, and incubated in the dark at room temperature for one year for samples from the Rhône Delta and two years for samples from the North Sea. For the slurry of the latter, 20-mL liquid was taken and filtered through N_2-flushed acetate cellulose filter (Sartorius, 0.2 µm), samples were used for test of precipitation, oxidation and removal of sulfide; the rest of the slurry was incubated at 85°C for 15 days for being representative of natural DOM samples containing both protein-like and humic-like compounds. After incubation, the liquid phase was sampled by syringe and filtered through N_2-flushed acetate cellulose filter (Sartorius, 0.2 µm) prior to further processing, storage, or analysis. For FT-ICR MS analysis, 20-mL samples of the filtered liquid phase were stored in glass serum vials under N_2 atmosphere at +4°C.

2.2.1.3 Test of matrix effects of natural marine sedimentary DOM

In order to confirm potential matrix effects in natural samples, dilution series were prepared from our in-house marine sedimentary DOM standards in the following way: (a) The effect of DOM concentration was confirmed by diluting filtered liquid phase samples with O_2-free Milli-Q water (NaCl, 35 wt.‰) in dilution steps of 1:1, 1:11 (v:v, natural sample/total) yielding

concentration of dissolved organic carbon of 36 mg C/L, 3.3 mg C/L for samples from the Rhône Delta, 60 mg C/L, 5.5 mg C/L for samples from the North Sea. (b) The effect of ionic strength was tested with additional NaCl concentrations of 0, 32.7 g/L and 327 g/L, each sample containing 3500 µL NaCl solution and 350 µL natural sample. For natural samples from the North Sea and the Rhône Delta, there are no amendments of redox-sensitive ions (Fe(III), Fe(II), Mn(II), sulfide) because their concentration was already high in the DOM samples. The samples for testing DOM concentration and ionic strength series were analyzed within one day by EEMs and each EEMs was performed immediately after sample preparation.

2.2.1.4 Effects of sample storage on DOM samples from anoxic slurries

While EEMs can be conducted at the time of sampling without further sample treatment, FT-ICR MS requires sample preparation by solid phase extraction (SPE, Dittmar et al., 2008), and usually the limited access to the analytical infrastructure requires sample storage. Here, we tested (a) the effect of long-term O_2 exposure on DOM samples after SPE on the results of FT-ICR MS and, for comparison, on the results of EEMs, and (b) the effect of short-term O_2 exposure of pristine liquid phase of the in-house-prepared DOM samples on the results of EEMs. The reported change of FT-ICR MS data and EEMs of DOM after SPE refers to only the variation of DOM without matrix effects.

Solid phase extraction of DOM was performed on 20-mL liquid phase samples using pre-cleaned Bond Elut-PPL cartridges (200 mg sorbent, Agilent Inc.) according to Dittmar et al. (2008) and Schmidt et al. (2014). Extraction was carried out in a glove bag under N_2 atmosphere. DOM was eluted from the cartridge with 1.5 mL methanol (LiChrosolv, Merck). The residue after solid phase extraction was sampled to check the loss of fluorescence signal during extraction. The DOM extracts of both in-house standards for FT-ICR MS and EEMs analysis were further split into two parts and stored for two months at -20°C, one under ambient air and the other one under N_2 atmosphere. For storage, we used 2-mL glass vials closed with Teflon coated septa. DOM extracts after SPE were analyzed by EEMs and FT-ICR MS. In order to ensure O_2-free storage conditions, the 2-mL sample vials were kept in N_2 flushed 50-mL Schott bottles. For EEMs measurements, 20 µL DOM extracts in methanol were taken, dried, and dissolved in O_2-free Milli-Q water.

In addition, the original liquid phase of the in-house-prepared samples from the Rhône Delta and North Sea sediments was measured by fluorescence spectrometer prior to O_2 exposure, after two-hours and after 24-hours O_2 exposure.

2.2.2 Analytical Methods

2.2.2.1 EEMs – Measurements

Spectra were recorded by a fluorescence spectrophotometer (Agilent Cary Eclipse, USA). The integral area of the Raman peak at excitation 350 nm was determined using Milli-Q water as a reference. Excitation wavelengths were increased in 5 nm steps from 230 nm to 410 nm, and emission spectra were recorded in 2 nm intervals from 300 nm to 530 nm. More than 100 samples were analyzed by PARAFAC analysis (Stedmon and Bro, 2008). The spectra with significant loss of signal or uncommon peaks resulting from the addition of metal ions were deleted during the PARAFAC processing. The relative standard deviation of the Raman peak excited at 350 nm was below 0.5% from a routine measurement tested with fresh Milli-Q water. Reproducibility test of 4 mg/L SRFA suggests that the relative standard deviation of peaks modeled by PARAFAC was better than 2%.

The undiluted samples were tested by absorption spectrum to quantify the chromophoric dissolved organic matter (CDOM) which might absorb the fluorescence. Absorption spectra were measured on a Shimadzu UV-1280 UV-vis absorption spectrophotometer with 1 cm cuvette. Absorption at wavelength 350 nm (a_{350}) was recorded. Absorption measured in the machine (abs) could be transformed to absorption coefficient (m^{-1} or cm^{-1}) by the equation:

$$a_{(\lambda)} = 2.303 \cdot A_{(\lambda)}/L \quad \text{Eq. 2.1}$$

L is the cell path-length in meters or centimeters. λ is the wavelength. Absorption spectra were measured to quantify the concentration of chromophoric DOM when inner filter effects occur and therefore, confirm upper and lower limit of DOM concentration.

2.2.2.2 EEMs – Peaks and Indices

Based on EEMs and PARAFAC, the following peaks were identified in 3D-scan spectra and named based on the maxima of excitation and emission intensities (ex/em) (Fig. 2.S2): peaks B, T, M, A', C. Peak P represent the total protein-like DOM (B and T, B: ex/em 275/305

nm; T: ex/em 280/350 nm); peaks M (ex/em: 315(250)/400 nm), A' and C (ex/em: 2/450-460 nm) represent humic-like DOM and together named as peak H. Value in parenthesis (250) is secondary peak. A' represents peak A together with peak C in the PARAFAC analysis results. 'AC' represents the sum of peak A' and peak C. The intensity of fluorescence is normalized by the Raman peak and the unit is R.U.

The indices FI, BIX and HIX derived from 2D-scans of emission spectra were interpreted as proxies of terrestrial organic matter source (FI), biological activity (BIX) and humification (HIX), respectively (Mcknight et al., 2001; Huguet et al., 2009). The fluorescence index (FI) was determined as ratio of the fluorescence intensity at 450 nm to 500 nm emission excited at 370 nm, indicating terrestrial-derived DOM (higher plant originated) with FI less than 1.4 and microbial-derived DOM with FI more than 1.8 (Mcknight et al., 2001). BIX is the ratio of fluorescence intensity emitted at 380 nm and the maximum of intensity at 430 nm excited at 310 nm, indicating fresh autochthonous DOM production (BIX > 1). Humification index (HIX) is calculated from the ratio of integrated fluorescence emission in the range 435–480 nm to that in the range 300-345 nm, indicating humified DOM with HIX higher than 10 and autochthonous DOM with HIX less than 4 (Huguet et al., 2009). High HIX values correspond to maximal fluorescence intensity at long wavelength and thus to the presence of complex molecules like high-molecular-weight aromatics (Senesi and Miano, 1991; Huguet et al., 2009).

2.2.2.3 FT-ICR MS

Samples were analyzed in methanol/water 1:1 (volume ratio) with negative-ion electrospray ionization (ESI, Apollo II electrospray source, Bruker Daltonik GmbH, Bremen, Germany) with a flow rate of 5 µL/min on a Bruker SolariX XR FT-ICR MS (Bruker Daltonik GmbH, Bremen, Germany) equipped with a 7 T refrigerated actively shielded superconducting magnet (Bruker Biospin, Wissembourg, France). Sodium trifluoroacetate was used as a calibration compound (Moini et al., 1998). DOM extracts were injected at the concentration of ~20 mg/L. 200 scans were added to one mass spectrum with an accumulation time of 0.02 s. Molecular formulae were calculated in the mass range of 200-650 Da with a formula tolerance of ±0.5 ppm. Peak intensity was calibrated by the base peak of the mass spectrum and named relative intensity (rInt). Formulae were deleted if they had no corresponding isotopic formulae. Formulae containing N_4P_2, N_2P_2, S_2P_2, O_1, O_0 were not considered in the final data set. All peaks that matched contaminant formulae (anthropogenic surfactants listed on

http://www.terrabase-Inc.com) or detected in the blank sample (rInt > 0.1) were deleted. More details were described in Schmidt et al. (2014). The formulae were classified as groups of CHO, CHNO and CHOS compounds, which contain exclusively C, H, O atoms, C, H, N, O atoms, or C, H, O, S atoms, respectively. The peak magnitudes reported in this manuscript are relative intensity normalized to the sum of all peaks, i.e., $rIntn = Int_{Peak}/\sum Int_{allPeaks}$.

2.3 Results and discussion

2.3.1 Investigated peaks and indices

Apart from the five peaks identified after PARAFAC analysis and the indices FI, BIX and HIX derived from the 2D-scan of the emission spectrum, there are more parameters that can be derived from individual peaks. The ratio of peak A and C to peak M or peak C to M can be used to identify a blue-shift of the fluorescent signal of organic compounds. Decrease of AC/M ratio is attributed to the loss of conjugation structures, for example, less aromatic rings, double bonds etc. In the aquatic systems, the peak C represents the more conjugated terrestrial DOM compared to peak M, which in studies of seawater has been recognized to comprise marine/autochthonous compounds (Coble, 2007; Ishii and Boyer, 2012). Another interesting index is P/H, e.g., the ratio of protein-like peaks to humic-like peaks.

2.3.2 Experimental evaluation of potential matrix effects on EEMs

2.3.2.1 Humic-like DOM

(a) Impact of DOM concentration on fluorescence of humic-like DOM

The effects of DOM concentration on the widely used parameters derived from EEMs were firstly investigated using SRFA. The humic components AC and M showed a linear response of the fluorescence signal to DOM concentration over a concentration range of 0.18 mg/L-6.0 mg/L ($a_{350} < 0.06$ cm^{-1}) (Fig. 2.1a). High concentrations lead to an underestimation of the peak intensity of the humic-like peak; for example, at 20 mg/L the fluorescence peak was 21% lower than expected based on the linear regression of fluorescence and concentration at lower concentrations. This is confirmed by natural samples of in-house-prepared sedimentary marine DOM from the North Sea and the Rhône Delta: high concentrations of DOM without dilution

resulted in a substantial loss (> 50%) of the fluorescent signal due to the inner filter effect (Fig. 2.1b). Thus, fluorescence intensity of peaks AC and M, and consequently total humic-like peaks, are underestimated if DOM concentration is too high. The AC/M ratio is less sensitive to high concentration, and increases by 6% at a concentration of 20 mg/L SRFA compared to the average values for SRFA concentrations between 0.18 mg/L and 6 mg/L (Fig. 2.1c).

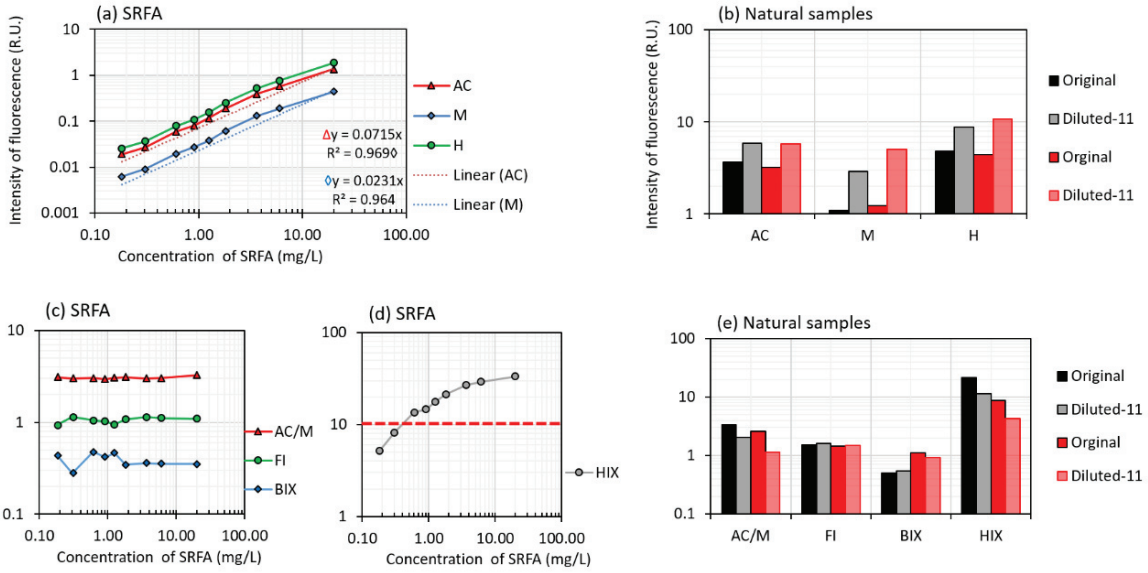

Fig. 2.1. Impacts of concentration of SRFA and in-house-prepared natural DOM samples on indices derived from humic-like peaks. (a) Effect of dilution on 3D indices tested by SRFA; (b) impact of over-concentrated sample without dilution on 3D indices tested by natural samples, black column for Rhône Delta and red column for North Sea; sample after appropriate dilution (11-fold) was compared, data have been corrected to original concentration by dilution factor; (c) impact of SRFA concentration on 3D and 2D indices; (d) impact of SRFA concentration on HIX; (e) effect of 11-fold dilution on 3D and 2D indices, tested by natural samples, black column for Rhône Delta and red column for North Sea. HIX above 10 indicates humified DOM; the red dash line in figure (d) shows HIX at 10.

The HIX index derived from 2D spectra is likewise affected by SRFA concentration and particularly sensitive to changes in the low concentration range (SRFA < 0.6 mg/L, a_{350} < 0.006 cm^{-1}, H peaks <0.08 R.U.) (Fig. 2.1d). HIX higher than 10 and HIX less than 4 indicate humified DOM and autochthonous DOM, respectively (Huguet et al., 2009). The implication of the index is therefore lost at low concentrations range (SRFA < 0.6 mg/L) as HIX is below 10 for the humic substances (Fig. 2.1d). Ohno (2002) introduced a method to correct HIX by defining the humification index as the fluorescence intensity in the 300-345 nm region divided by the sum of intensity in the 300-345 nm and 435-480 nm regions. In this study, the corrected

HIX (HIX-c) becomes constant with concentrations above 0.6 mg/L SRFA (Fig. 2.S3). Therefore, for samples varying in DOM concentration, HIX must be corrected. Care should be taken in interpreting HIX, even if it is corrected to HIX-c, as it might not correctly reflect humification processes if the concentration of fluorescent DOM is low (intensity of humic-like peaks < 0.08 R.U., SRFA < 0.6 mg/L). Stepwise dilution from 0.18 mg/L to 20 mg/L resulted in relatively constant FI, BIX values of SRFA.

Concentration of pristine in-house prepared DOM samples from the North Sea (60 mg/L DOC) and the Rhône Delta (36 mg/L DOC) is far beyond the highest concentration of SRFA (20 mg/L SRFA, 10 mg/L DOC) tested in this study. The analysis of these two natural DOM samples confirmed that high DOM concentration in pristine samples result in an underestimation of humic-like DOM and slight bias of AC/M, BIX, and HIX compared to the diluted sample.

(b) Impact of salinity on fluorescence of humic-like DOM

The humic-like peaks from the SRFA standard and the related indices change only slightly with salinity (Fig. 2.2a, c). A previous study has shown that in the range of 0 to 1 M KCl, ionic strength has no significant impact on EEMs spectra (Mobed et al., 1996). However, these authors compared overall spectra instead of indices and individual peaks. In our study, we confirm that ionic strength has minor impacts on AC/M ratio, BIX and FI of SRFA spectra (Fig. 2.2a, c), while the humic-like peak increased slightly by 6% and HIX increased by 5% with addition of 32.7 g/L NaCl (Table 2.1). Similarly, spectra of the samples from the Rhône Delta and North Sea responded only slightly and inconsistently to changing NaCl concentration (Fig. 2.2b, e). Reasons for that might be extensive, for example, salt induced probably a change in complexation between organic matter and ions, e.g., ionic strength affects the complexation of Cu-natural organics (Cao et al., 2004); the inorganic ions in pristine natural samples is not clear and the impact of NaCl on the organic complexes is not predictable in this study due to the diversity of organics and ions.

Table 2.1. Original dataset and derived parameters after PARAFAC analysis. P and H is the abbreviation of protein-like peaks and humic-like peaks (AC and M).YE is the abbreviation of yeast extract. Conc. (mM) is the final concentration of added ions; in the series of O_2 exposure, concentration of O_2 is not recorded and '/' stands for no data available. Addition of high concentration of ions resulted in significant change of the spectra shape or noise, these spectra were deleted during PARAFAC analysis due to unsuccessful split-half validation procedure, 'N.P.' is abbreviation of 'No results from PARAFAC analysis. 'S.F.' stands for taking supernatant without precipitates due to oxidation.

Experiment	Series	Subseries	Treatments	Conc.(mM)	AC (R.U.)	M (R.U.)	T (R.U.)	B (R.U.)	P (R.U.)	H (R.U.)	AC/M	P/H	FI	BIX	HIX
1 Impact of oxygen	1-1 Representative of H-dominated natural DOM	Rhône Delta	O_2, 0h	/	3.70	1.09	0.18	0.02	0.20	4.79	3.40	0.04	1.51	0.50	21.67
			O_2, 2h, S.F.	/	4.07	1.50	0.54	0.03	0.57	5.57	2.71	0.10	1.57	0.60	15.15
			O_2, 24h	/	N.P.	N.P.	N.P.	N.P.	N.P.	N.P.	N.P.	N.P.	1.53	0.63	15.93
			O_2, 24h, S.F.	/	6.19	2.99	0.87	0.10	0.98	9.18	2.07	0.11	1.56	0.62	17.38
	1-2 Representative of P and H-dominated natural DOM	North Sea N_2-flushed	O_2, 0h	/	5.77	5.00	3.25	2.23	5.48	10.77	1.15	0.51	1.47	0.91	4.30
			O_2, 2h	/	5.58	5.15	3.28	2.27	5.55	10.73	1.09	0.52	1.47	0.90	4.06
			O_2, 24h	/	5.27	5.11	3.05	2.19	5.24	10.38	1.03	0.51	1.52	0.93	4.14
		North Sea extracts	N_2,	/	0.15	0.10	0.04	0.02	0.05	0.24	1.54	0.22	1.55	0.62	8.06
			O_2, 2month	/	0.17	0.11	0.05	0.02	0.06	0.28	1.59	0.22	1.44	0.63	8.58
2 Impact of metal ions sensitive to redox conditions	2-1 Impact of FeIII	Test of H-SRFA 4mg/L	$FeCl_3$	0	0.32	0.11	0.02	N.P.	0.02	0.43	3.03	0.05	1.11	0.33	26.72
			$FeCl_3$	0.007	0.29	0.10	0.02	N.P.	0.02	0.39	2.93	0.05	1.15	0.37	24.15
			$FeCl_3$	0.03	0.19	0.07	0.01	0.00	0.02	0.26	2.72	0.06	1.23	0.39	15.29
			$FeCl_3$	0.2	N.P.	N.P.	N.P.	N.P.	N.P.	N.P.	N.P.	N.P.	2.04	1.79	2.50
			$FeCl_3$	0.9	N.P.	N.P.	N.P.	N.P.	N.P.	N.P.	N.P.	N.P.	1.25	1.99	/
		Test of P - YE 10mg/L	$FeCl_3$	0	0.04	0.02	0.78	0.37	1.15	0.06	1.79	18.19	1.53	0.89	0.25
			$FeCl_3$	0.06	0.03	0.01	0.62	0.29	0.92	0.05	2.17	19.52	1.33	1.02	0.27
			$FeCl_3$	0.2	0.02	0.01	0.21	0.04	0.25	0.03	1.69	9.37	1.55	1.19	0.41
			$FeCl_3$	0.9	N.P.	N.P.	N.P.	N.P.	N.P.	N.P.	N.P.	N.P.	1.76	N.P.	8.88
	2-2 Impact of MnII	Test of H - SRFA 4mg/L	$MnCl_2$	0.00	0.32	0.11	0.02	N.P.	0.02	0.42	3.01	0.06	1.09	0.36	27.97
			$MnCl_2$	0.007	0.29	0.10	0.02	N.P.	0.02	0.39	2.88	0.06	1.13	0.38	25.26
			$MnCl_2$	0.06	0.29	0.10	0.02	N.P.	0.02	0.39	2.85	0.06	1.13	0.35	24.74
			$MnCl_2$	0.6	0.18	0.07	0.02	0.00	0.02	0.24	2.55	0.07	1.14	0.40	19.32
		Test of P - YE 10mg/L	$MnCl_2$	0.00	0.04	0.02	0.78	0.37	1.15	0.06	1.79	18.19	1.53	0.89	0.25
			$MnCl_2$	0.06	0.04	0.02	0.77	0.38	1.15	0.06	1.71	18.14	2.13	1.06	0.26
			$MnCl_2$	0.6	0.04	0.03	0.71	0.35	1.07	0.07	1.34	15.77	1.55	0.89	0.31
	2-3 Impact of FeII	Test of H - SRFA 4mg/L	$FeCl_2$	0.00	0.32	0.11	0.02	N.P.	0.02	0.42	3.01	0.06	1.09	0.36	27.97
			$FeCl_2$	0.007	0.31	0.11	0.02	N.P.	0.02	0.42	2.94	0.06	1.11	0.35	26.62
			$FeCl_2$	0.06	0.29	0.10	0.02	N.P.	0.02	0.39	2.86	0.06	1.09	0.41	24.98
			$FeCl_2$	0.2	0.27	0.10	0.02	N.P.	0.02	0.37	2.76	0.06	1.16	0.35	24.00
			$FeCl_2$	0.6	N.P.	N.P.	N.P.	N.P.	N.P.	N.P.	N.P.	N.P.	1.54	0.72	4.92
			$FeCl_2$	0.9	N.P.	N.P.	N.P.	N.P.	N.P.	N.P.	N.P.	N.P.	1.51	0.89	4.37
3 Impact of sulfide	3-1 Representative of H	SRFA 4mg/L	Na_2S	0	0.32	0.11	0.02	N.P.	0.02	0.42	3.01	0.06	1.09	0.36	27.97
			Na_2S	0.3	0.33	0.09	0.02	N.P.	0.02	0.42	3.83	0.05	1.05	0.33	31.30
			Na_2S	1	0.33	0.09	0.02	N.P.	0.02	0.42	3.88	0.06	1.12	0.39	30.91
			Na_2S	4	N.P.	N.P.	N.P.	N.P.	N.P.	N.P.	N.P.	N.P.	1.12	0.61	4.23
			Na_2S	10	N.P.	N.P.	N.P.	N.P.	N.P.	N.P.	N.P.	N.P.	1.17	0.58	4.14
	3-2 Representative of P	Test of P - YE 10mg/L	Na_2S	0	0.04	0.02	0.78	0.37	1.15	0.06	1.79	18.19	1.53	0.89	0.25
			Na_2S	1	0.04	0.03	1.05	0.27	1.32	0.07	1.55	17.91	1.49	1.50	0.31
			Na_2S	4	N.P.	N.P.	N.P.	N.P.	N.P.	N.P.	N.P.	N.P.	1.36	1.75	0.43
			Na_2S	10	N.P.	N.P.	N.P.	N.P.	N.P.	N.P.	N.P.	N.P.	1.54	1.57	0.49

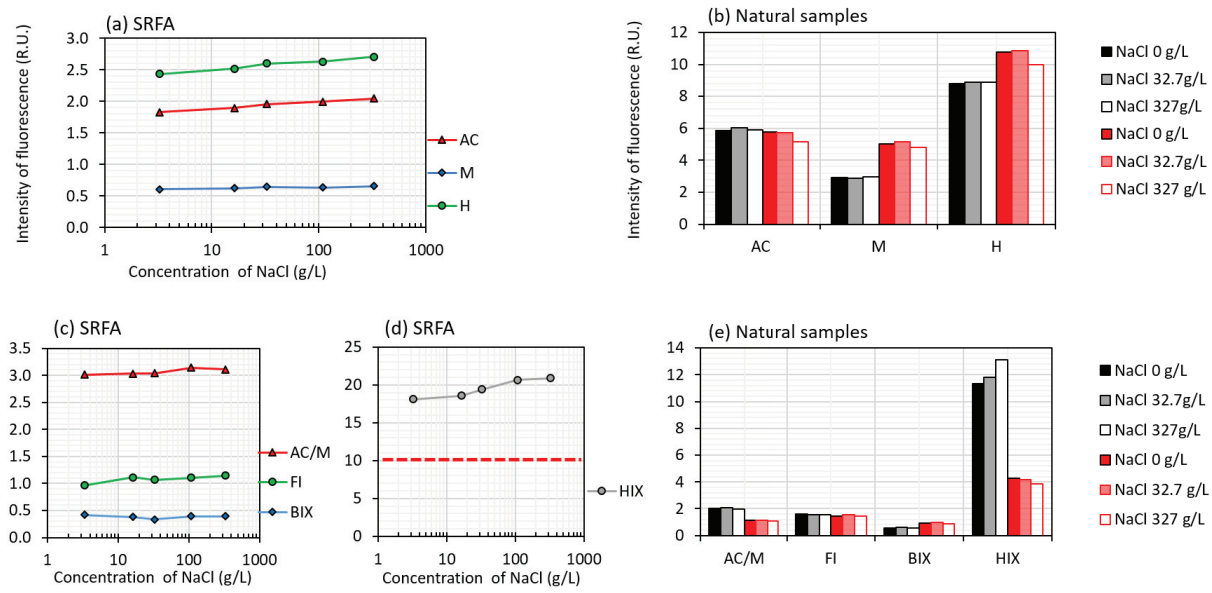

Fig. 2.2. Impacts of NaCl concentration on the indices derived from humic-like peaks. (a) Effect of ionic strength on 3D indices tested by SRFA; (b) effect of ionic strength on 3D indices tested by natural samples, black column for Rhône Delta and red column for North Sea; (c) effect of ionic strength on 3D and 2D indices tested by SRFA; (d) effect of ionic strength on 2D index – HIX tested by SRFA; (e) effect of ionic strength on 3D and 2D indices, tested by natural samples, black column for Rhône Delta and red column for North Sea, samples were 11-fold diluted. SRFA at concentration of 4 mg/L was used for tests. HIX above 10 indicates humified DOM; the red dash line in figure (d) shows HIX at 10.

Attention should be paid to the potential effect of salts (NaCl), because they might impact the intensity of Raman peak, which leads to a worse calibration (Fig. 2.S5). Therefore, a consistent salinity for one dataset is easier for calibration process.

(c) Impact of transition metal ions and sulfide on EEMs of humic-like DOM

Fe(III), Mn(IV) and sulfate are the main electron acceptors during organic degradation in marine anoxic sediment. Their reduction produces oxygen-sensitive ions such as Fe(II), Fe(III), Mn(II), S^{2-}, which may affect the fluorescence spectra because they may lead to the formation of metal-organic complexes and/or precipitation. Moreover, their concentration might vary largely due to the stratification and diagenesis process in sediments (Canfield et al., 1993; Schulz et al., 1994). For example, as a consequence of iron reduction, high concentrations of Fe(II) may accumulate: as much as 0.5 mM dissolved iron were detected in the subsurface of the Rhône Delta in this study. Our results suggest that the EEMs of DOM sample is most sensitive to Fe(III) even at 0.03 mM, high concentrations of both Fe(II) (0.2 mM) and Mn(II)

(0.6 mM) also affect the fluorescence spectra and the derived parameters (H, AC/M, FI, HIX and BIX) (Table 2.1, Fig. 2.3); this is possibly due to the complexation between transition metal ions and organic matter (Poulin et al., 2014) and formation of small particles of metal oxides, which might induce quenching of fluorescence (Manciulea et al., 2009). Especially, one reason for the decrease of AC/M, i.e., blue-shift of fluorescence, might be that long-emission regions of the fluorescence spectra associated with greater DOM conjugation were more susceptible to iron quenching (Poulin et al., 2014). Addition of Fe(II) and Mn(II) in concentrations < 0.06 mM did neither affect the DOM spectra nor the indices (< 5% for Fe(II), < 3% for Mn(II) compared to the sample without ions addition) (Table 2.1, Fig. 2.3). Addition of Na_2S in SRFA resulted in a red shift of the spectra, i.e. longer excitation and emission wavelength and accordingly bias of index AC/M, FI, BIX, HIX (Table 2.1, Fig. 2.3)

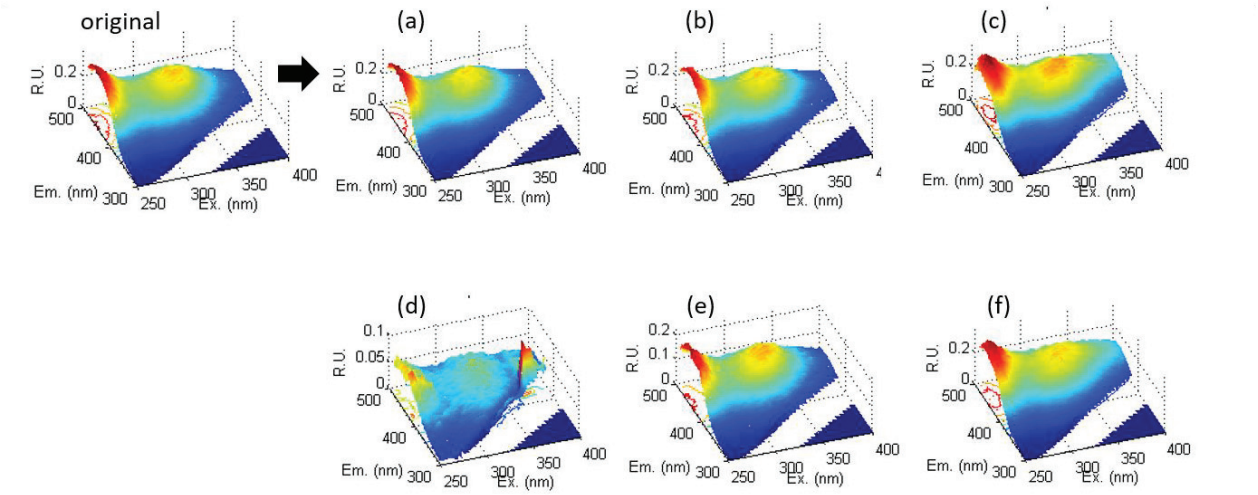

Fig. 2.3. Effect of redox conditions-sensitive ions on humic-like peaks. (a)-(f) show the EEMs spectra of SRFA samples with addition of Fe(II), Mn(II), S^{2-}. (a)-(c): Fe(II), Mn(II), S^{2-} at concentrations of 0.06 mM, 0.06 mM, 0.3 mM, respectively. (d)-(f) show the EEMs spectra of SRFA samples with addition of Fe(II), Mn(II), S^{2-} at concentrations of 0.6 mM, 0.6 mM, 1 mM, respectively. SRFA used for test was at concentration of 4 mg/L

2.3.2.2 Protein-like DOM

In general, humic-like compounds are thought to dominate the marine sedimentary DOM pool while protein-like DOM likely comprises only a minor fraction, as amino acid-C contributes < 10% of DOC in sediment pore waters (Alberic et al., 1996; Lomstein et al., 1998). Protein-like peaks comprise roughly 5% of the fluorescence intensity of humic-like peaks in

SRFA and (< 15%) in natural sample from the Rhône Delta. In the sample from the North Sea, fluorescence intensity of protein-like peaks is half of the humic-like peaks. For comparison, protein-like peaks in YE are 18 times higher than humic-like peaks (Fig. 2.4).

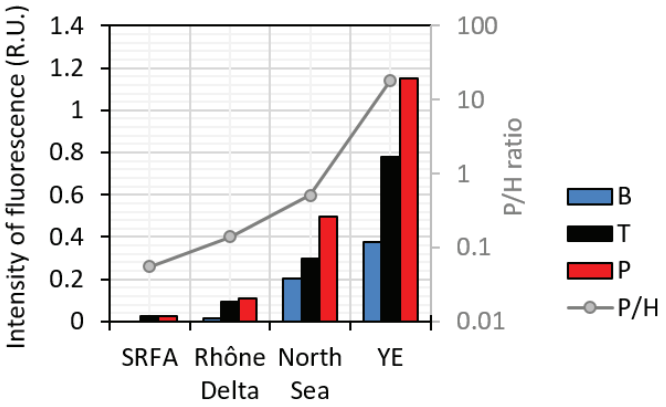

Fig. 2.4. Comparisons of samples with different proportions of protein-like compounds. SRFA is representative of DOM with rare protein-like peaks; natural samples from Rhône Delta and North Sea represent for DOM with slight visible protein-like peaks and significant protein-like peaks, respectively; YE is representative of DOM constitute of protein-like peaks. SRFA at concentration of 4 mg/L and YE at concentration of 10 mg/L were used for tests.

Impact of dilution on protein-like peaks was investigated in the natural samples containing mixtures of protein-like and humic-like peaks. The threshold of over-concentrated and over-dilution is investigated. Similar to what was observed for humics, the intensity of protein-like peaks increased from 0.3 R.U. to 5.5 R.U. after 11-fold dilution for natural North Sea samples and increased from 0.2 R.U. to 1.3 R.U. after 11-fold dilution of Rhône Delta samples (Fig. 2.5b) (corrected by dilution factor). This effect is attributed to the quenching of protein-related fluorescence by concentrated humics (Wang et al., 2015). This study showed that it can be reduced by dilution. On the other hand, the test using SRFA showed that over-dilution induced another problem (SRFA < 0.9 mg/L) as all the fluorescent peaks are small and the noise peak near peak B and Raman peak might be recognized as a real protein-like peak during PARAFAC analysis (Fig. 2.5a), accordingly the P/H ratio is strongly overestimated at low concentration of SRFA (Fig. 2.S4). Thus, both over-concentration and over-dilution led to bias of intensity and proportion of protein-like peaks.

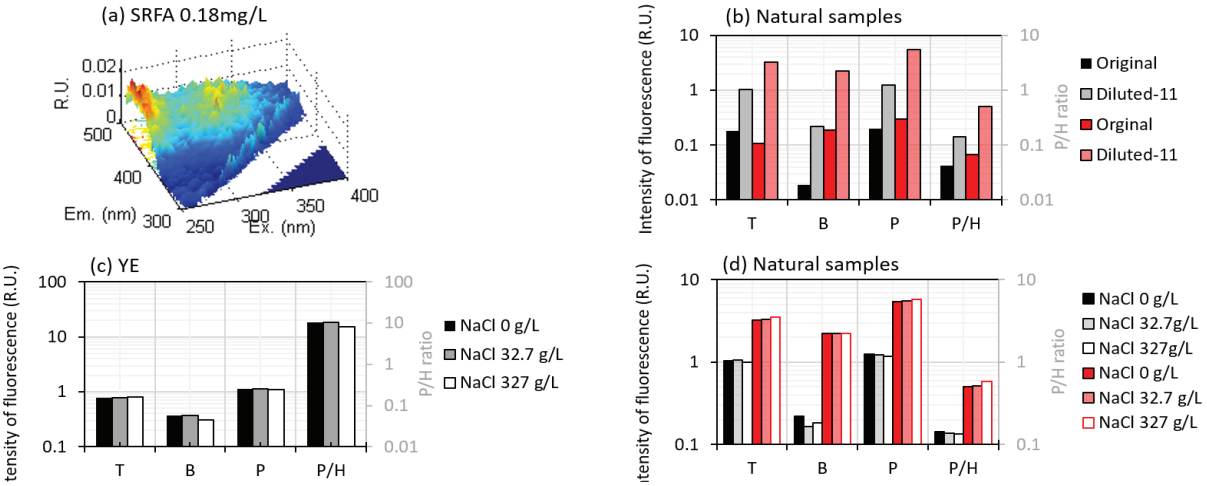

Fig. 2.5. Impacts of dilution and NaCl on the indices derived from protein-like peaks and the ratio of protein-like peaks and humic-like peaks (P/H). (a) Example of over-dilution sample tested by SRFA; (b) results of over-concentrated sample without dilution on on protein-like peaks-related parameters tested by natural samples, black column for Rhône Delta and red column for North Sea; sample after appropriate dilution (11-fold) was compared, data have been corrected to original concentration by dilution factor; (c) effect of different salt concentrations on protein-like peaks-related parameters tested by YE; (d) impacts of different salt concentrations on protein-like peaks-related tested by natural samples, black column for Rhône Delta and red column for North Sea. SRFA at concentration of 4 mg/L and YE at concentration of 10 mg/L were used for tests.

We found slight increases (< 4% in yeast extract) in the intensity of protein-like peaks with increasing NaCl concentration (Fig. 2.5c). Changes in the protein-like peaks with ionic strength may result from slight variations of the quaternary structure of proteins due to changes in the non-covalent bond with ionic strength (Lakemond et al., 2000), slight structural reorganization changes the chemical environment of fluorescent groups and consequently their fluorescence behavior.

Impact of transition metal ions and sulfide on EEMs of protein-like DOM is shown in Table 2.1 and in Fig. 2.6: EEMs spectra of YE samples were slightly affected by addition of Fe(III), Mn(II) at concentrations of 0.2 mM and 0.6 mM respectively. Compared to humic-like DOM, protein-like DOM is less sensitive to these ions. Addition of 1 mM Na_2S results in loss of fluorescence intensity in protein-like peaks at low excitation wavelength (250 nm) and a sharp increase at higher excitation wavelength, e.g., red-shift of the spectra (B/T ratio in Table 2.1, Fig. 2.3c).

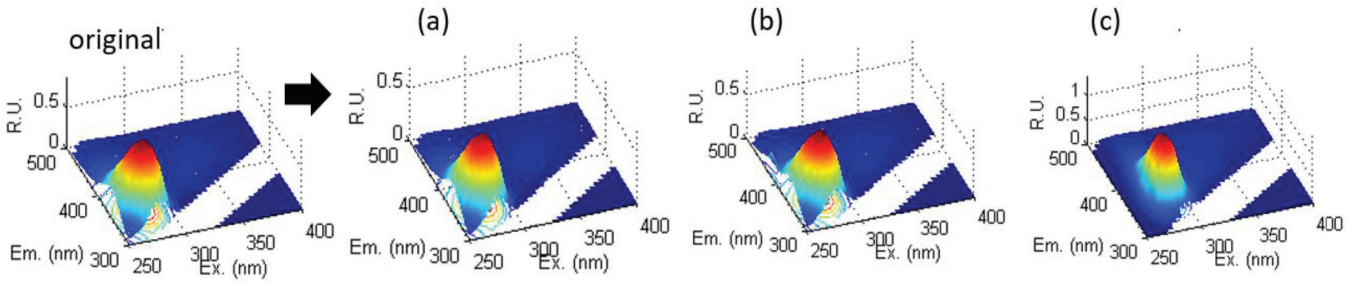

Fig. 2.6. Effect of redox conditions-sensitive ions on protein-like peaks. (a)-(c) shows the EEMs spectra of YE samples with addition of Fe(III), Mn(II), S^{2-} at concentrations of 0.2 mM, 0.6 mM, 1 mM. Protein-like DOM is less sensitive than humic-like DOM to addition of Fe(III), Mn(II). YE solution at concentration of 10 mg/L was used for the experiments. Y-axis in figure (c) is different from the other three figures.

2.3.3 Experimental evaluation of O_2 exposure effects during sample storage

The effect of O_2 exposure on EEMs spectra was tested with extracted DOM and with in-house prepared natural sedimentary DOM.

As for the SPE-extracted sample from the North Sea, FT-ICR MS characterization showed a slight change of DOM after 2 months O_2 exposure compared to storage under N_2 (Fig. 2.7). The few formulae in the blue circle suggest compounds with low O/C and m/z were most significantly transformed (Fig. 2.7a, c, d): there are in total 109 formulae decreasing by more than 0.02 in relative intensity (i.e., rIntn > 0.00004), which account for only 1.2% of all the formulae. EEMs showed consistent results: the AC/M ratio increased by 0.05 (3%) after O_2 exposure and P/H ratio before and after O_2 exposure remained the same (0.22) for the extracted DOM (Table 2.1). For the extracted DOM, quantitative change of fluorescence peaks after O_2 exposure was not compared.

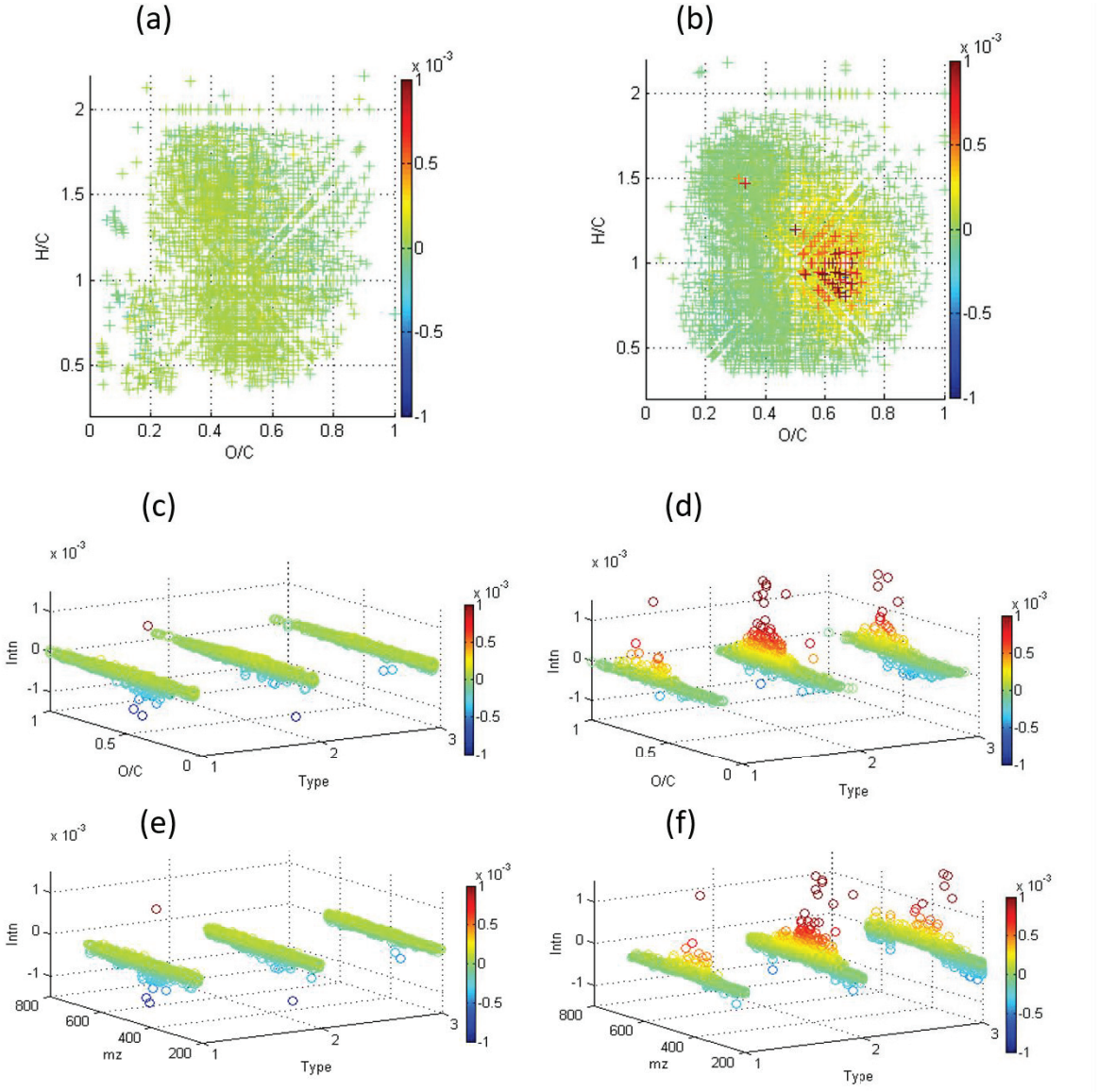

Fig. 2.7. Effect of O_2 exposure on pore water DOM characterized by FT-ICR MS. (a) change of DOM sample from North Sea in Van Krevelen diagram; (b) change of DOM sample from Rhône Delta in Van Krevelen diagram; (c) change of O/C ratio in DOM sample from North Sea, formulae were classified by aromaticity; (d) change of O/C ratio in DOM sample from Rhône Delta, formulae were classified by aromaticity; (e) change of molecular weight in DOM sample from North Sea, formulae were classified by aromaticity; (f) change of molecular weight in DOM sample from Rhône Delta, , formulae were classified by aromaticity. Type 1: aliphatic compounds, AI $<$ 0; type 2: highly unsaturated compounds, 0.55 $\geq$ AI $\geq$ 0; type 3: aromatic compounds (including condense aromatic compounds), AI $>$ 0.5. The peak magnitude shown in figures is relative intensity normalized to the sum of all peaks. rIntn $>$ 0: increase after air exposure; rIntn $<$ 0: decrease after air exposure. $AI = \frac{1+C-\frac{1}{2}O-S-\frac{1}{2}(N+P+H)}{C-\frac{1}{2}O-N-S-P}$

As for the sample from the Rhône Delta Site GeoB17306 as representative of terrestrial DOM, there is more loss of smaller aromatic compounds (mz < 400) and production of larger O-rich highly unsaturated or aromatic compounds (mz > 400) when stored in the presence of O_2 (Fig. 2.7b, d, f). According to the O/C and H/C ratio in van Krevelen diagram, these formulae could be tannin-like polyphenol compounds (Fig. 2.7b). Possible mechanism is the formation of C-O-C bond between phenol aromatic rings in oxygen-sensitive organic compounds resulting in longer linear macromolecules after oxygen exposure (Poncet-Legrand et al., 2010). To be more specific, the larger O-rich formulae increased by more than 0.02 (rIntn > 0.00004) in relative intensity and accounted for 1.2% of all assigned CHO formulae and 0.05% of all CHNO formulae (data not shown in figures). CHOS formulae were more sensitive to O_2 exposure, 8.9% of all CHOS formulae increased in rInt by more than 0.02 (rIntn > 0.00004); this is possibly due to oxidation of sulfur-containing functional groups, e.g., thiol groups (Barnard et al., 1961; De Filippis and Scarsella, 2003).

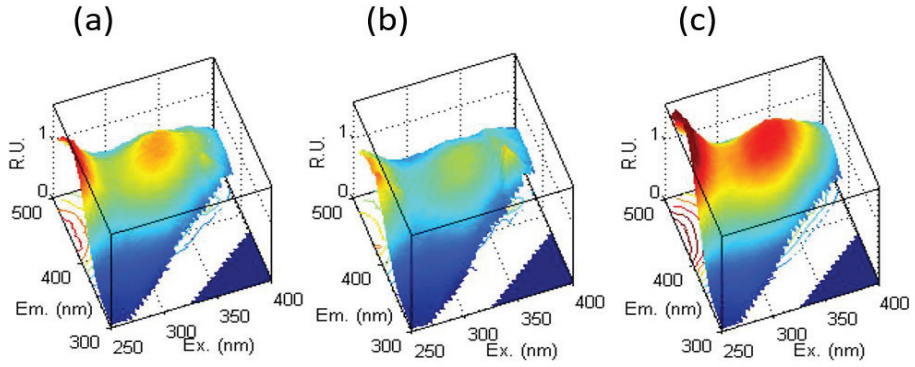

Fig. 2.8. Effect of O_2 exposure on EEMs spectra of sample from Rhône Delta. (a) EEMs spectra of fresh sample without exposure to O_2; (b) EEMs spectra of fresh pore water exposed to O_2 for 2 hours, fluorescence peak reduced and noise peak appeared; (c) EEMs spectra of sample without precipitation, of which the fluorescence intensity is higher.

Without SPE, the original DOM sample from the Rhône Delta showed a recognizable change of EEM spectra (Fig. 2.8b) after only 2 hours exposure to O_2; at the same time, the pellucid liquid became turbid. Fig. 2.8c showed that after O_2 exposure for 24 hours the EEMs of supernatant of DOM sample emitted more intense fluorescence than that of the original fresh air-free pore water. As extracted DOM remained similar after O_2 exposure, the change of spectra might be caused by the oxidation of redox-sensitive metal ions in the original sample. As a comparison, for the sulfide-enriched sample from North Sea without high concentrations

of the redox-sensitive metal ions, EEMs were similar before and after O_2 exposure for 24 hours (Table 2.1).

2.3.4 Recommendations for the analysis of anoxic interstitial water DOM by EEMs

The impacts of dilution, ionic strength, metal ions, sulfide, and oxygen are summarized in Table 2.2.

Table 2.2. Change of fluorescent signal due to concentration, NaCl concentration, metal ions, sulfide, O_2 exposure. 'NS represents no significant impact. The relative changes below 3% were defined as 'NS'. '↑' and '↓' represent increase and decrease of the parameters with higher concentration of DOM, added ions or O_2 exposure.

	Index	Concentration (SRFA)	NaCl concentration	Fe(III)	Fe(II)	Mn(II)	Na_2S	DOM after O_2 exposure
Acceptable range	All indices in this study	0.9-6 mg/L (~1 µg C)	0-32.7 g/L	0-0.007 mM	0-0.06 mM	0-0.06 mM	<0.03 mM	2 months
2D indices	FI	NS	NS	↑	NS	NS	↑	↓
	HIX	↑	↑	↓	↓	↓	↓	↑
	BIX	NS	NS	↑	NS	NS	↑	NS
3D indices	Protein-like peaks	NS if>0.9 mg/L	↓ or ↑	↓	↓	↓	↑	/
	Humic-like peaks	NS	NS	↓	↓	↓	NS (sum)	/
	AC/M	NS	↑	↓	↓	↓	↑	NS

The inner filter effect in concentrated DOM samples can be compensated either via complex calculation with absorption spectra (Tucker et al., 1992; Kubista et al., 1994; Mobed et al., 1996) or by dilution (Burdige et al., 2004). Due to the usually limited volume of pore water in deep sediments, dilution using smaller volumes of the original sample was chosen as an approach to avoid the inner filter effects. In former studies of shallow pore water, the upper limit of absorption coefficient is inconsistent: e.g., below 0.02 cm^{-1} (Tfaily et al., 2013), 0.05 cm^{-1} (Burdige et al., 2004), 0.1 cm^{-1} (Stedmon and Bro, 2008). We suggest further that the upper limit of concentration depends on the target parameters of EEMs. For quantitative information, concentration range of SRFA from 0.18 mg/L to 6 mg/L ($a_{350} < 0.06$ cm^{-1}) shows linear response of the fluorescence signal of humic-like peaks; for qualitative information, concentration range of SRFA from 0.9 mg/L to 20 mg/L ($a_{350} > 0.009$ cm^{-1}, > 0.11 R.U. of humic-like peaks) shows reliable data of peak ratios and indices. The highest dilution factor depends on the fluorescence quantum efficiency and concentration of fluorescent DOM instead of DOC, and it might vary largely in different samples. Estimates of the contribution of chromophoric DOM to total dissolved organic carbon (DOC) in the ocean ranged from 20% to

70% (Coble, 2007). In this study, 80-fold dilution is also possible for both the samples from North Sea and Rhône Delta, sample volumes could be reduced to 50 µL (~ µg carbon) (> 0.11 R.U., > 0.5 mg C/L). The highest concentration depends on the absorption coefficient, which should not exceed 0.06 cm^{-1} in the diluted sample.

For dilution, Milli-Q is an acceptable choice since the individual peaks and indices of fluorescence spectra are slightly changed with NaCl (mostly < 4%). To maintain the same Raman peak induced by NaCl and the same concentration of NaCl after dilution, we suggest that water at similar salinity of seawater (35‰ NaCl) instead of Milli Q water could be used for the dilution and easier for the calibration of Raman peak.

O_2 exposure led to slight transformation of DOM (AC/M increased by 3%) in two-months. For long-term storage to years, it could be possible that storage might lead to more bias of spectra especially for DOM enriched in polyphenols sensitive to O_2. A consistent way of storage including duration and headspace is necessary. Attention needs to be paid on major redox-sensitive ions in natural sedimentary DOM samples (metal-ion-rich or sulfide-rich). (1) For an original sample with Fe(II) and Mn(II) in concentrations < 0.6 mM, impacts of both ions are negligible at a dilution factor of 11-fold, and sample should be stored under N_2 and diluted with O_2-fee water. In the case of inevitable O_2 exposure or storage under air atmosphere, precipitation is likely to occur in the metal-ion-rich pore water samples, and it should be avoided during measurements. (2) The sulfide-rich sample is recommended to be purged with N_2. In the original in-house-prepared DOM sample from North Sea, the concentration of sulfide is 3.95 mM, after purging with N_2 for 2 minutes, it decreased to 0.01 mM (Table 2.S1). Alternatively, after inevitable oxidation of sulfide happened, within one week there was 2.06 mM sulfide oxidized to sulfate and the residue sulfide is only 0.24 mM (Table 2.S1), i.e., ca. 1 mM sulfide precipitated as sulfur. The precipitation of elemental sulfur is observed over longtime storage. Unlike the metal oxides, the sulfur precipitates remained in suspension and should be excluded via filtration.

At last, it is worthwhile to notice that the signal of protein-like DOM is found to be significantly lost after solid phase extraction, accordingly the P/H ratio decreased by 60% (Table 2.S2), indicating the signal of labile DOM might be selectively lost during the extraction process. If the pore water samples contain a significant fraction of protein-like DOM, combination of FT-ICR MS with EEMs is especially recommended. By the latter information

on both protein-like and humic-like DOM are included and a dataset of hundreds of samples is easily realizable; based on the overview of EEMs, by FT-ICR MS the molecular-level characterization on selected samples is feasible and provide complementary information.

2.4 Conclusions

Based on tests of SRFA representing humic-like peaks, YE representing protein-like peaks and in-house-prepared natural samples, impacts of different pretreatments were examined: (1) over-dilution results in bias of qualitative information including P/H and HIX, while BIX and FI is constant over a broad range of DOM concentrations and insensitive to inner filter effects; (2) concentrations of Fe(II) and Mn(II) above 0.09 mM in the diluted sample result in noise peak interfering PARAFAC analysis and loss of fluorescence signal especially for humic-like peaks; sulfide can cause observable red-shift of both humic-like peaks and protein-like peaks; (3) O_2 exposure led only to slight changes of EEMs for extracted in-house-prepared natural DOM in two month, while for the same original water, the EEMs were highly sensitive to oxygen, possibly due to reactions of redox-sensitive metal ions.

Therefore, we recommend the following measures to reduce the matrix effect on EEMs: (1) Storage without headspace of air or uniform exposure to O_2 if inevitable; sulfide-rich samples should be flushed with N_2 for 2 min to exclude sulfide; (2) dilution with O_2-free NaCl solution (35‰ wt) before measurements; (3) measurements of supernatant if sample is exposed to O_2 and precipitation is formed. For sedimentary DOM samples examined in this study, micro-liquid sampling (50 µL, ~ 1 µg C) is sufficient without necessity of solid phase extraction.

With appropriate pretreatments, EEMs make high-frequency observations possible for anoxic and volume-limited pore water samples.

Acknowledgements

We thank the captain and crew of RV POSEIDON for their excellent support during cruise POS450. The open discussions with Prof. Weidong Guo and Prof. Michael Gonsior during poster session of XMASIII conference (2017) were appreciated. Many thanks to the technical assistances of Jenny Wendt and Xavier Prieto Mollar. The FT-ICR-MS facility at the University of Bremen was funded by the ERC under the European Union's Horizon 2020

research and innovation programme (grant agreement No. 670115 ZOOMECULAR; PI K.-U.H.). This research was accomplished with samples from the project of European Research Council under the European Union's Seventh Framework Programme–"Ideas" Specific Programme, ERC grant agreement No. 247153 (Advanced Grant DARCLIFE; PI: Kai.-Uwe Hinrichs). The study was supported by the DFG through the Research Center/Excellence Cluster MARUM-Center for Marine Environmental Sciences, Project GB2. I am thankful to the jointly support from Chinese Scholarship Council (CSC) for the accomplishment of this project.

2.5 Supplementary materials

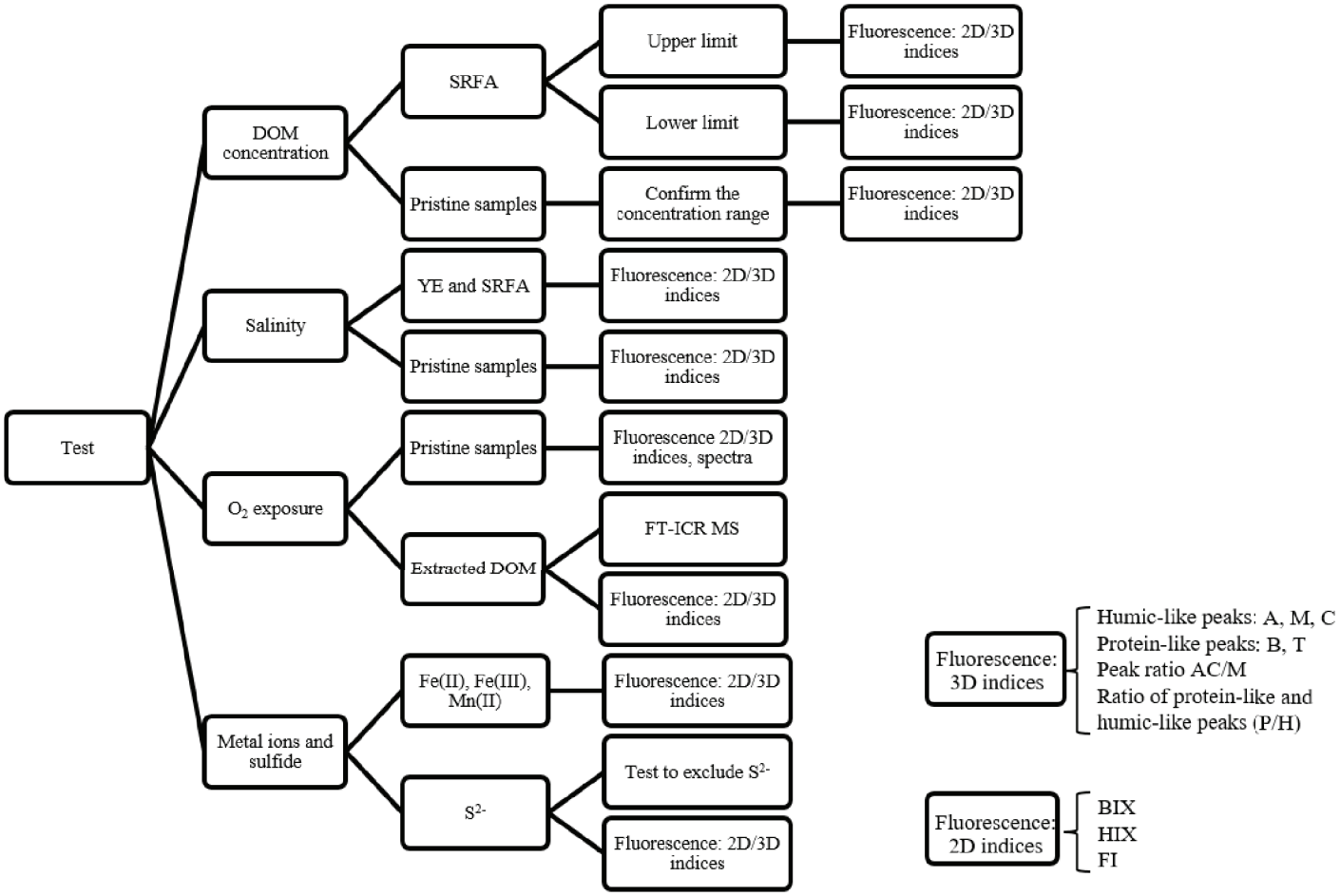

Fig. 2.S1. Flow scheme of the tests. 'YE' and 'SRFA' represent the yeast extract and Suwannee River Fulvic Acid. 'Pristine samples' are the in-house prepared natural sedimentary DOM samples from North Sea and Rhône Delta. The 'Extracted DOM 'is DOM from the pristine sample after solid phase extraction.

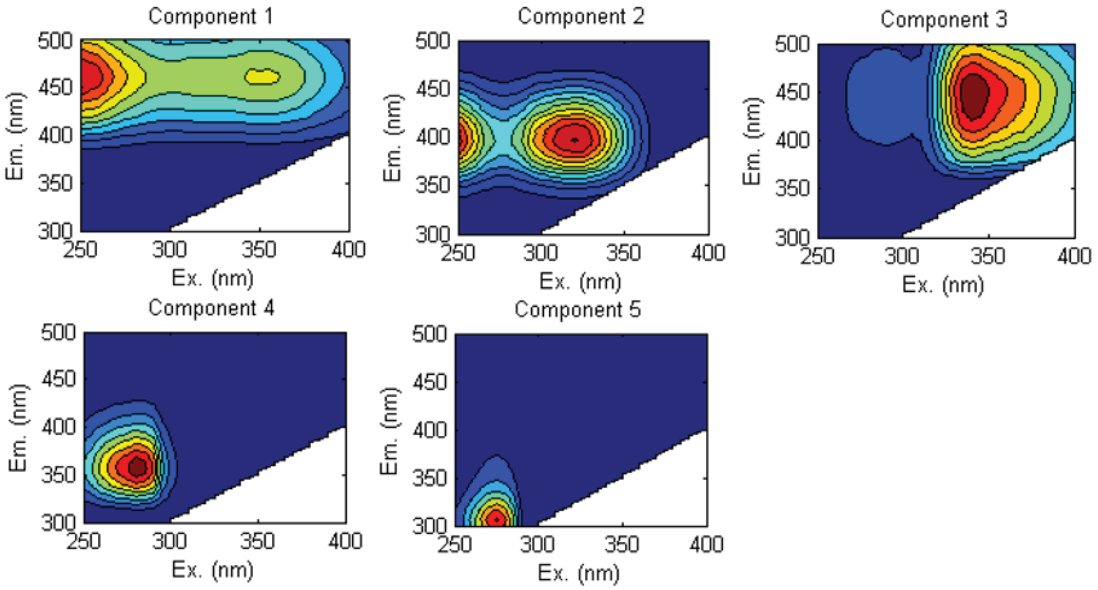

Fig. 2.S2. EEMs components identified by PARAFAC analysis. Components 1, 2, 3, 4, 5 represents peak A(C), M, C, T and B, respectively.

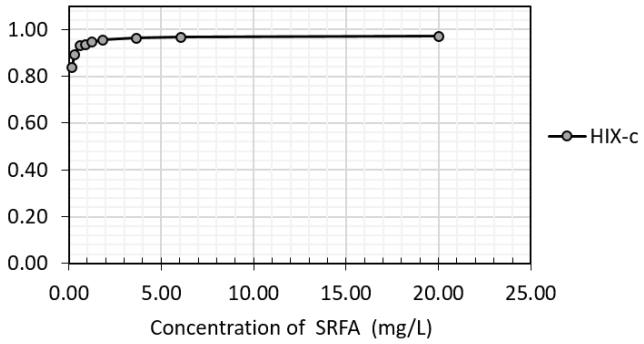

Fig. 2.S3. Variation of HIX-c with concentration of SRFA. HIX-c is corrected HIX based on the equation $HIX\text{-}c = \sum I_{435\text{-}480} / (\sum I_{300\text{-}345} + \sum I_{435\text{-}480})$ (Ohno, 2002). I is the fluorescence intensity at each wavelength.

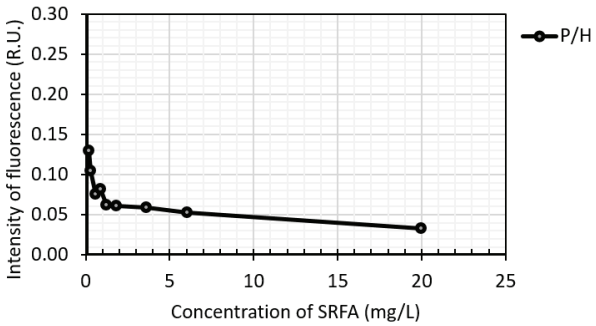

Fig. 2.S4. Variation of the ratio of protein-like and humic-like peak (P/H) with increasing concentration of SRFA.

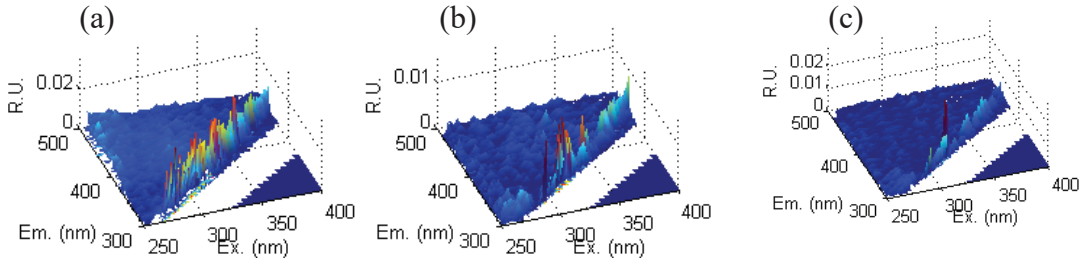

Fig. 2.S5. Impact of salt on the Raman peak: (a) The EEMs spectra of the Milli-Q water in NaCl concentrations of 327, (b) 32.7 g/L and (c) 0 g/L.

Table 2.S1. Variation of sulfide and sulfate after treatments of N_2 flushing and O_2 exposure. In-house-prepared samples from North Sea sediments were tested.

	Concentration of sulfide (mM)		Sulfate accumulation (mM)	
Samples	Original	After pretreatments	After one day	After one week
Flush with N_2 for 2 min	3.95	0.01	/	/
O_2 exposure	3.95	0.24 (one week)	0.92	2.06

Table 2.S2. Comparisons of DOM fluorescence spectra before and after solid phase extraction (SPE) by PPL cartridge. 20-mL liquid sample was used for solid phase extraction. In-house-prepared samples from North Sea sediments after incubation were tested as the pristine sample contains both substantial protein-like and humic-like compounds.

Sample	P/H	AC/M	FI	BIX	HIX
Before SPE	0.5	1.2	1.5	0.9	4.3
After SPE - DOM extract	0.2	1.5	1.6	0.6	8.1
After SPE - residue liquid	1.5	0.6	1.8	1.2	0.5

Chapter 3 Impacts of redox conditions on dissolved organic matter (DOM) quality in marine sediments off the River Rhône, Western Mediterranean Sea

Shuchai Gan[a], Frauke Schmidt[a], Verena Heuer[a,*], Tobias Goldhammer[a,b], Matthias Witt[c], Kai-Uwe Hinrichs[a]

[a]MARUM – Center for Marine Environmental Sciences, University of Bremen, Leobener Straße, D-28359 Bremen, Germany

[b]Leibniz Institute for Freshwater Ecology and Inland Fisheries, Department of Chemical Analytics and Biogeochemistry, Mueggelseedamm 301, 12587 Berlin, Germany

[c]Bruker Daltonik GmbH, Fahrenheitstraße 4, 28359 Bremen, Germany

Abstract

Sedimentary dissolved organic matter (DOM) is an important pool of intermediates produced during carbon cycling in the subseafloor. Rapid degradation of organic matter in the Rhône delta sediment results in significant stratification of redox zones. However, to date little is known about the quality of largely unknown DOM and anaerobic degradation path adapted to redox conditions in sediment. In order to study the effect of redox conditions (sulfate reducing *vs*. methanogenic) on DOM quality and transformation, sediments (0-18 cm) from the Rhône River Delta were incubated under anaerobic condition, with redox conditions being controlled by sulfate amendment. The progress of incubation was monitored by H_2, CH_4, sulfate, DIC, DOC, acetate production and changes in the DOM composition were determined by 3D Fluorescence Spectroscopy, i.e., Excitation Emission Matrix Spectroscopy (EEMs), and ultra-high-resolution Fourier Transform Ion Cyclotron Resonance Mass Spectrometry (FT-ICR-MS). Parallel Factor analysis (PARAFAC) of EEMs was used to distinguish different groups of DOM (humic-like and protein-like compounds) to evaluate composition, conjugation and size of DOM. Prior to incubation humic-like sedimentary DOM predominated and nearly half were CHO and one third were CHNO compounds of the molecular formulae (> 5000) identified by FT-ICR-MS. During incubation, protein-like DOM and CHNO formulae with 3 and 4 N atoms formulae were rare under both sulfate reducing and methanogenic conditions. (1) Incubation under sulfate reducing conditions resulted in a fast release and net accumulation

of dissolved organic carbon (DOC). Protein-like DOM was rapidly cycled while humic-like DOM accumulated. Consistently, CHNO formulae with 3 and 4 N atoms decreased and accumulated faster, whereas formulae with one N and oxygen-rich unsaturated compounds (AI: 0-0.5) became more enriched. (2) In contrast, during incubation under methanogenic conditions, there was no net accumulation of DOC; Blue-shift of the fluorescence spectra indicated that humic-like DOM was transformed possibly associated with loss of oxygen-bearing functional groups. This interpretation is consistent with the relative decrease of oxygenation and carbon number in the pool of aromatic and highly unsaturated compounds in the FT-ICR-MS. Approximately 90% of molecular formulae that were lost under methanogenic conditions were accumulated under sulfate reducing conditions. Our results suggest that under sulfate reducing conditions organic matter degradation results in the accumulation of highly oxidized DOM, while protein-like compounds are selectively consumed; when the redox regime changes to methanogenic conditions, microbes apparently utilize the humic-like and oxygen-rich compounds of the oxidized DOM pool that accumulated under sulfate reducing conditions. Consequently, redox regimes and the associated biogeochemical processes influence rate and fractions of DOM released by and consumed in the deep biosphere, which could ultimately shape the composition of the preserved sedimentary organic matter and the DOM released to the ocean.

Key words**:** DOM characterization, sulfate reduction, methanogenesis, Excitation Emission Matrix Spectroscopy (EEMs), Fourier Transform Ion Cyclotron Resonance Mass Spectrometer (FT-ICR-MS)

3.1 Introduction

Marine sediments are a major reservoir of organic carbon (Hedges and Keil, 1995; Burdige, 2007). Sedimentary organic matter plays an important role as substrate for benthic organisms, which contribute to its degradation during low-temperature diagenesis. Degradation is rapid in surface sediments and decreases with increasing sediment depth concomitantly with the depletion of oxygen and other terminal electron acceptors in subsurface layer (Middelburg, 1989; Hartnett et al., 1998; Dauwe et al., 2001; Rysgaard et al., 2001; Mincks et al., 2005; Arndt et al., 2013). Nevertheless, up to 90% of sediment prokaryotic activity takes place in

subsurface layers (Parkes et al., 2014). This subsurface activity fueled by recalcitrant organic matter and limited supply of electron acceptors raises questions about survival mechanisms in the subseafloor biosphere (Jørgensen and Boetius, 2007; Rowe and Deming, 2011; Lever et al., 2015). While the control imposed by electron acceptors has been studied intensively (D'Hondt et al., 2004; Biddle et al., 2005; Jorgensen et al., 2012; Briggs et al., 2013), little is known about electron donors, e.g., organic matter. Sedimentary pore water DOM is produced during organic matter degradation; its molecular composition is controlled by the source of organic matter as well as biogeochemical processes such as hydrolysis, fermentation, and terminal mineralization (Middelburg et al., 1993; Burdige and Zheng, 1998; Billerbeck et al., 2006; Rowe and Deming, 2011; Arndt et al., 2013; Koho et al., 2013; Schmidt et al., 2017).

Terminal step differ according to the redox conditions. In sulfate-rich subsurface sediments, sulfate reducing microbes, mainly bacteria, are responsible for much of the terminal organic matter mineralization in coastal region (Capone and Kiene, 1988; Chen et al., 2003). Sulfate reducers gain energy from intermediates produced during organic matter degradation (Muyzer and Stams, 2008), such as short-chain fatty acids and alcohols (Oremland and Polcin, 1982; Hansen, 1994; Liu and Whitman, 2008) and a few polymers (Labes and Schönheit, 2001). After sulfate is depleted, the importance of methanogenesis (MOG) increases; methanogenic archaea mainly utilize C1 and C2 compounds or hydrogen (Oremland and Taylor, 1978; Zinder, 1993; Liu and Whitman, 2008).

As the anaerobic degradation of organic matter involves multiple steps and substrate types, from particulate organic matter, over complex DOM, and monomeric intermediates, to the terminal products CO_2 and CH_4 (Middelburg et al., 1993; Muyzer and Stams, 2008; Rowe and Deming, 2011; Arndt et al., 2013), we hypothesize that pathways of organic matter degradation prior to the terminal step differ according to the redox condition and are thus reflected in the molecular composition of pore water DOM. The aim of this study is to examine how the composition of pore water DOM is modulated by the prevailing redox conditions, specifically under sulfate reducing vs. methanogenic conditions, and whether there are predominant mechanisms of organic matter degradation.

The complexity (Mopper et al., 2007) of pore water DOM and rapid turnover of substrates (Henrichs, 1992; Weston, Porubsky, Samarkin, et al., 2006) necessitate complementary analytical methods for DOM characterization. Combined with Parallel Factor analysis

(PARAFAC) as statistical tool (Stedmon et al., 2007; Stedmon and Bro, 2008), the Excitation-Emission-Matrix Spectra (EEMs, also known as 3-D fluorescence spectra) can be used to measure peaks representing either a group of labile autochthonous protein-like compounds or a group of refractory humic-like compounds (Coble, 1996; Yamashita and Tanoue, 2003; Coble, 2007; Ishii and Boyer, 2012). Applications of this approach provided information about the degree of aromaticity in soil DOM (Zsolnay, 2003), DOM size in water column studies (Her et al., 2003; Cuss and Guéguen, 2015), and transformations and turnover (Coble, 2008; Catalá et al., 2015) as well as the potential bioavailability of DOM (Stedmon and Markager, 2005b; Lønborg et al., 2009; Lønborg et al., 2010; Gan et al., 2015), without determination of the exact molecular composition. It is a non-destructive method and requires small sample volumes (e.g., 0.3 mL in this study), which enables a high sample throughput and application to studies in which sample volume is limited. Molecular-level characterization of DOM can be achieved with Fourier-transform ion-cyclotron resonance mass spectrometry (FT-ICR MS) (Koch and Dittmar, 2006; Hertkorn et al., 2006; Schmidt et al., 2011; Hertkorn et al., 2013; Lechtenfeld et al., 2014; Schmidt et al., 2014) although losses during sample extraction and selectivity of electrospray ionization preclude representation of the entire DOM pool (Dittmar et al., 2008; Green et al., 2014; Perminova et al., 2014). FT-ICR MS has been applied to studies investigating the microbial processes in water column and pore water (D'Andrilli et al., 2010; Schmidt et al., 2011; Lechtenfeld et al., 2014; Koch et al., 2014), photochemical alteration of DOM (Kujawinski et al., 2004; Dittmar et al., 2007; Gonsior et al., 2009) and degradation state of DOM (Flerus et al., 2012; Lechtenfeld et al., 2014), thereby showing its power in high-resolution detection of thousands of individual constituents. The combination of the bulk-level information of the fluorescent DOM pool and the molecular information accessible by FT-ICR MS has provided complementary insights into the properties of lake water DOM (Stubbins et al., 2014; Kellerman et al., 2014; Tfaily et al., 2015; Kellerman et al., 2015). Thus, the EEMs and FT-ICR MS could be combined for an overview of DOM (especially, geopolymers) in intensive time/geological scale by former and more detail information by latter for selected samples.

We incubated sediments from Rhône River pro-delta in the Mediterranean Sea in laboratory experiments mimicking in-situ diagenesis over a period of 75 days. Sediments from the Rhône River pro-delta are particularly suited for such experiments as they are characterized by rapid remineralization, predominance of terrestrial organic matter and a shallow depth of the

transition zone from sulfate-reducing to methanogenic conditions. This study investigates the composition of pore-water DOM in marine sediments of the Rhône River Delta by EEMs to obtain an overview of *in situ* DOM profile in the redox-condition-stratified sediment. Additionally, sediment slurries were incubated in laboratory experiments to study how redox conditions and associated biogeochemical processes influence the composition of DOM during early diagenesis. The complementary application of EEMs (repeated sampling throughout the experiment) and FT-ICR MS (sampling at start and end when the redox conditions were achieved) for DOM characterization provides new insights into the transformation of DOM during the initial stages of degradation. Moreover, in order to monitor transformation during fermentation and terminal processes, analyses of low molecular weight organic compounds (volatile fatty acids, e.g., acetate) and inorganic products (DIC, NH_4^+) were conducted to establish a comprehensive view of the biotic degradation pathways under different redox conditions in marine sediments.

3.2 Methods and Sampling Sites

3.2.1 Study site and sampling

The Rhône River delta is characterized by rapid turnover of organic matter and high sedimentation rates (Ludwig et al., 2003; Miralles et al., 2005), high remineralization rates and significant stratification of redox conditions. Therefore, site GeoB 17306 was selected; it is located in the prodelta of the River Rhône (43° 18.96' N, 4° 52.17' E, 30 m water depth), Gulf of Lions, Western Mediterranean Sea. Samples were obtained during *RV Poseidon* cruise POS450 in March 2013 (Fig. 3.S1 in supplementary materials). The Rhône River is the largest freshwater source in the modern Mediterranean Sea with an average sediment flux of 14.2 Mio t/year, corresponding to a sediment deposition yield of 324 t/km^2/year (Ludwig et al. 2003). Sediments in the Rhône River delta contain high total organic carbon content (TOC) > 1.36%, with TOC being derived from marine and terrestrial sources with a predominance of terrestrial organic matter (Cathalot et al., 2013). There is rapid oxygen uptake in the sediment (Lansard et al., 2009) resulting in anoxic conditions below the upper mm of sediment and high rates of sulfate reduction, resulting in a shallow sulfate-methane transition zone (Zhuang et al., in preparation; Zhuang, 2014). Sediment cores GeoB 17306-1 and GeoB 17306-2 were retrieved by multi-corer and gravity corer, respectively.

For in-situ profiles, pristine pore-waters were extracted from the gravity core immediately after recovery onboard *RV Poseidon*. The pore-water samples were filtered via Rhizon suction samplers (0.1 μm porous polymer, Rhizosphere Research, Wageningen, the Netherlands) and stored at -20°C.

For incubation experiments with sediment slurries in the laboratory, sediment was sampled from three depth layers of the multi-corer (0-6 cm, 6-12 cm, 12-18 cm), each representing sulfate-reducing conditions. Sediment was transferred into Schott bottles and sealed under N_2 atmosphere immediately after core recovery. Sediments have been stored at 4°C for two years in lab before incubation.

3.2.2 Incubation experiments

3.2.2.1 Preparation of slurries

The recipe of artificial seawater includes major elements (Na, Mg, K, Ca, Cl) (artificial seawater with sulfate: 0.682 g KCl, 1.5 g $CaCl_2 \cdot 2H_2O$, 5.7 g $MgCl_2 \cdot 6H_2O$, 26.4 g NaCl, 6.8 g $MgSO_4 \cdot 7H_2O$, 0.099 g KBr; artificial seawater without sulfate: 0.682 g KCl, 1.5 g $CaCl_2 \cdot 2H_2O$, 11.3 g $MgCl_2 \cdot 6H_2O$, 26.4 g NaCl, 0.682 g $MgSO_4 \cdot 7H_2O$, 0.099 g KBr). The artificial seawater was autoclaved at 120℃ and flushed with N_2 for 2 hours. 1 M $NaHCO_3$ (aq) was sterilized by filtration with 0.1 μm filter (PES, Sartorius). The sediment slurry was prepared in a glovebox under N_2 atmosphere (2% H_2). Before being mixed with sediment, 10 mL $NaHCO_3$ (aq) and 0.5 mL of thiosulfate (30 g/L) was added to each liter of artificial seawater. To test whether the artificial seawater is oxygen-free, an aliquot of 10 mL artificial seawater was transferred to a tube and tested by resazurin; lack of color change to pink indicated the absence of oxygen in artificial seawater. In this study, no resazurin was added to the artificial seawater used for slurries since it would interfere with optical parameters measured by fluorescence spectroscopy. Sulfide was added to a final concentration of 200 μM. Nutrients were added to a final concentration of 1.5 mM ammonia and 0.5 mM phosphate.

The temperature of sediment was slowly increased from 4℃ to room temperature in an insulation can one day before preparing a slurry. For the incubation experiments, the three sediment samples from upper 18 cm of the multi core GeoB 17306-1 were combined, homogenized, and subsequently split into 8 subsamples each containing 100 g sediment and

100 artificial seawater under N_2 atmosphere. In detail, firstly 800 mL sediment is mixed with 20 mL sulfate-free artificial seawater in a sealed sterile plastic bag and homogenized for 2 hours by continually malaxating the bag. The mixture was then separated into ten 200-mL Schott bottles (280 mL total volume) and six Hungate tubes (16 mL total volume), which contained 100 mL and 5 mL sediment, respectively.

The pre-incubation lasted for 3 days at room temperature. The headspace is filled with N_2 atmosphere containing 2% H_2. The bottles and Hungate tubes were sealed with butyl rubber stoppers at a pressure of two bar in headspace to avoid intrusion of air. The concentration of iron is ~ 0.4 mM, which is close to the value (0.5 mM) in the in-situ pore water profile under sulfate reducing condition (data not shown).

3.2.2.2 Incubation settings with control subseries

Table 3.1. Design of incubation experiments. There are three series (I, II, III) and for the main incubation and three series for the additional experiments (IV, V, VI) after the main incubation. There are two duplicates for each series. SR: sulfate reduction; MOG: methanogenesis. YE: Yeast extracts

No.	Series name	Addition	Purpose	Parameters	Duration
I	'SR' series	Continuous sulfate addition	SR condition	CH_4, H_2, SO_4^{2-}, acetate, DIC, DOC, EEMs, FT-ICR-MS	75 days
II	'SR→MOG' series	No addition (sulfate residue 4.5 mM on day 0)	MOG condition (37^{th}-75^{th} day)	CH_4, H_2, SO_4^{2-}, acetate, DIC, DOC, EEMs, FT-ICR-MS	75 days
III	'SR-inhibited' series	Molybdate 20 mM	To achieve intermediates	CH_4, H_2, SO_4^{2-}, acetate, DIC, DOC, EEMs	75 days
IV	'YE-SR' series	YE 0.1 g/L	Degradation of biopolymer (SR condition)	EEMs	40 days
V	'YE-MOG' series	YE 0.1 g/L	Degradation of biopolymer (MOG condition)	EEMs	40 days
VI	'YE-SR-inhibited' series	YE 0.1 g/L molybdate 20 mM	Impacts of sulfate reduction on initial steps	EEMs	40 days

In order to study the impact of redox conditions, we incubated the sediment under sulfate-reducing and methanogenic conditions by controlling the concentration of sulfate. The slurries were made from sediment and artificial seawater according to a volume ratio of gas: liquid: solid phase 0.8:1:1. All the six series (in duplicates) are listed in Table 3.1. The details are described as follows:

Three major series: In order to ensure sulfate-reducing conditions, sulfate was supplied. Artificial seawater containing 30 mM sulfate was added to four Schott bottles, resulting in the final concentration of sulfate at ca. 25 mM. Sulfate-reducing condition was maintained during the incubation by addition of Na_2SO_4 solution when the sulfate concentration was lower than 18 mM. In contrast, methanogenic conditions were established through addition of sulfate-free artificial seawater in another two Schott bottles, for which the final slurries contained residual sulfate from original sediment at 5 mM. This series was named 'SR→MOG' series. To observe the intermediates formed under sulfate reducing condition, two Schott bottles added with sulfate-containing artificial seawater were amended with 20 mM molybdate as inhibitor of the terminal step of sulfate-reduction (Banat et al. 1983); this series is named 'SR inhibited'. A dead control was not feasible, as methods commonly used for sterilization will slightly affect the DOM pool or DOM analyses, e.g., addition of zinc chloride would quench the fluorescence signal, heating during autoclaving would induce changes in the DOM pool.

Three subseries with added protein-like compounds: The three additional series amended with yeast extract aimed to confirm the degradation of bioavailable biopolymers, which represents DOM emitting protein-like peaks, in this case proteinaceous compounds. The subseries with substrate addition were incubated in Hungate tubes. The redox condition was controlled in the same way as the main series. After 75 days pre-incubation, the three series in Hungate tubes including duplicates were incubated for 40 days with addition of yeast extract to the final concentration ca. 0.5 g/L in pore water and named as 'YE-SR' series, 'YE-MOG' series, and 'YE-SR-inhibited' series (Table 3.1), respectively.

All bottles were placed in an incubator at 28°C. Before sampling at the first time point, the headspace was flushed again with N_2 for 5 min and afterwards kept under two bar N_2 for 75 days. The solid and liquid phases were equilibrated overnight for the first time point of sampling.

3.2.2.3 Time series of sampling and sample preparation

In addition to EEMs and FT-ICR MS analyses for monitoring changes in DOM, we measured H_2, CH_4, sulfate for monitoring the redox condition, and quantified DOC and DIC and acetate. For the major series, samples for EEMs, CH_4 and H_2 were taken twice per week to monitor the progress of incubation. For FT-ICR MS, samples were taken at start and end due to the high

sample requirement (>10 mL); one more sample on 37th day was taken when the methanogens thrived. For acetate, sulfate, DIC and DOC, samples were collected after 0, 4, 12, 20, 37, and 75 days. Liquid was firstly transferred to a glass vial and then split into subsamples, and further processed in a glovebox (anaerobic chamber). The samples for sulfate measurements were amended with $ZnCl_2$ before storage to avoid interference from sulfide oxidation after precipitation of ZnS. After sampling of each time-point, gas pressure was recorded by digital pressure probe and each bottle was supplemented with N_2 to maintain a constant pressure at two bars after sampling. For additional series with yeast extract, samples for EEMs were taken on day 0, 2, 5, 10, 40.

Subsamples for acetate analysis were filtered using nylon filters (0.2 μM, Omni lab). Subsamples for or all other analyses were filtered using cellulose filter (0.2 μM, Sartorius AG). Vials were sealed in glovebox and covered with Parafilm afterwards. FT-ICR MS samples were stored at +4°C, while all other liquid samples were stored at -20°C.

As for FT-ICR MS sample, DOM was concentrated by solid-phase extraction (SPE) using PPL cartridges (Agilent, 3mL, 200mg) according to the protocol by Dittmar et al. (2008). 10-20 mL liquid was taken for extraction. SPE was carried out in a glove box under N_2 atmosphere to avoid possible oxidation of samples. Prior to extraction, samples were acidified with hydrochloric acid (Supra pure, Merck) to pH 2. Cartridges were rinsed with diluted hydrochloric acid (pH = 2) to remove salts and dried before elution. DOM was eluted with 1.5 mL methanol (Lichrosove quality, Merck). One blank sample was extracted and analyzed to check for possible contamination during extraction. Samples after SPE were stored under N_2 at -20°C in the dark.

3.2.3 Analytical techniques

3.2.3.1 EEMs

Samples were measured by a fluorescence spectrophotometer (Agilent Cary Eclipse, USA) at room temperature in a 1-cm (path length) quartz fluorescence cell. Samples were diluted with N_2-flushed Milli-Q water (NaCl, 35 g/L) in a ratio of 1:10. The absorption coefficient was checked by UV detector at 280 nm and 350 nm to assure it did not exceed 0.05 cm^{-1} (Tucker et al., 1992; Burdige et al., 2004). The integral area of the Raman peak (excitation 350 nm) was

calculated using Milli-Q water as a reference. Emission spectra ranging from 300 nm to 530 nm were recorded every 2 nm while exciting at wavelengths in the range of 230-410 nm in 5-nm increments. Fluorescence spectra of each sample were combined to create excitation emission matrices (EEMs). Inner filter effects were not taken into consideration after dilution. EEMs of more than 100 samples (including *in situ* samples from the cruise) were modeled by parallel factor analysis (PARAFAC) in MATLAB software (Stedmon and Bro, 2008). Without samples with molybdate addition, the appropriate number of components was validated by split-half analysis. The relative standard deviation of the Raman peak excited at 350 nm was 0.47% from a daily routine measurement of fresh Milli-Q water. The relative standard deviation for peaks modeled by PARAFAC analysis was better than 2% from the reproducibility test of samples in this study. EEMs are used as basic means for DOM characterization. Names of the peaks were assigned according to Coble (2007) including three humic-like peaks (M, A, C) and one protein-like peak (T). Molybdate affected humic-like peaks in excitation wavelength close to 250 nm, samples with molybdate addition is not included in the final data set for humic-like peaks.

Peak C represents large molecules with aromatic functional groups and conjugations, which is commonly referred to as terrestrial DOM; Peak M commonly represents autochthonous, microbial or marine material with relatively lower molecular weight; Peak A represents common components in natural aquatic systems and resembles aromatic fulvic acid (Coble, 1996; Stedmon and Markager, 2005a; Coble, 2007; Fellman et al., 2010; Ishii and Boyer, 2012)

3.2.3.2 FT-ICR-MS

DOM extracts were analyzed on a Bruker SolariX XR FT-ICR mass spectrometer (Bruker Daltonik GmbH, Bremen, Germany) equipped with a 12 T refrigerated actively shielded superconducting magnet (Bruker Biospin, Wissembourg, France), a dual ionization source (ESI and MALDI, Apollo II electrospray source, Bruker Daltonik GmbH, Bremen, Germany) and a dynamically harmonized analyzer cell (ParaCell^{TM}, Bruker Daltonik GmbH, Bremen, Germany). All samples were analyzed in sequence on one day using identical instrument settings. Initially, mass spectra were calibrated externally with arginine clusters in negative ion mode using a linear calibration. Samples were diluted to similar concentrations of ~20 mg C/L and ionized by electrospray ionization in negative ion mode. 200 scans were added to one mass spectrum ranging from m/z 150 to 4000 with syringe flow rate at 5.0 uL/min and ion

accumulation time of 0.08 s. Molecular formulae were assigned to peaks with signal-to-noise ratios > 4. Spectra were internally calibrated with compounds that were repeatedly identified in marine interstitial water DOM samples (Schmidt et al., 2014). The mean square errors of internal calibration were below 0.1 ppm. Molecular formulae were calculated in the range of m/z 200-650 within a mass error window of ±0.5 ppm. The oxygen-to-carbon ratio (O/C) and hydrogen-to-carbon ratio (H/C) were set in the range of 0.01 > O/C > 1.2 and H/C > 0.35. Molecular formulae were calculated by considering the following elements ^{1}H, ^{12}C, $^{13}C_{0–1}$, ^{16}O, $^{14}N_{0–4}$, $^{32}S_{0–2}$, $^{34}S_{0–1}$, $^{31}P_{0–2}$. Mass peaks that are consistent with anthropogenic surfactants (http://www.terrabase-Inc.com) or in the list of peaks identified in the blank sample with a relative intensity (rInt) > 0.3 were deleted. rInt is calculated by normalization to the base peak of each sample. Multiple formulae were filtered with the homologous series approach and isotope check (Koch et al., 2007). Double bond equivalents (DBE) represent the numbers of double bonds and rings in a molecule (Eq. 3.3), including the double bonds of carboxyl groups. Formulae with rInt > 0.02 and signal-to-noise ratios >10 were used in the final data analysis and included < 10 double assignments. The formulae with peak intensities varying by more than 0.02 in parallel samples were not included in the final dataset (< 0.1%). Formulae with ^{13}C were not considered in the data interpretation. rInt was used in the first step of data analysis and Van Krevelen Diagram.

$$\mathrm{rInt} = \mathrm{Int}_{\mathrm{Peak}} / \sum \mathrm{Int}_{\mathrm{base\ peak}} \quad \text{Eq. 3.1}$$

Sum-normalized intensity (rIntn) used for further data interpretation was the relative intensity normalized to the sum of all peaks intensities to investigate the loss of different types of compounds (aliphatic, highly unsaturated and aromatic compounds):

$$\mathrm{rIntn} = \mathrm{Int}_{\mathrm{Peak}} / \sum \mathrm{Int}_{\mathrm{allPeaks}} \quad \text{Eq. 3.2}$$

DBE-O (Eq. 3.4) is the approximation of DBE in a molecule without consideration of double bonds associated with oxygen. Aromaticity index (AI) refers to the density of carbon-carbon double bonds in a molecule and can be calculated after Eq. (3.5) (Koch and Dittmar, 2006; Koch and Dittmar, 2016). Formulae with AI > 0.67, 0.67 ≥ AI > 0.5, 0.5 ≥ AI ≥ 0, AI < 0 are characterized by condensed aromatic, aromatic, highly unsaturated and aliphatic compounds, respectively.

$$\mathrm{DBE} = \mathrm{C} - \frac{1}{2}\mathrm{H} + \frac{1}{2}\mathrm{N} + \frac{1}{2}\mathrm{p} + 1 \quad \text{Eq. 3.3}$$

$$\mathrm{DBE-O} = \mathrm{C} - \frac{1}{2}\mathrm{H} + \frac{1}{2}\mathrm{N} + \frac{1}{2}\mathrm{p} + 1 - \mathrm{O} \quad \text{Eq. 3.4}$$

$$\mathrm{AI} = \frac{1+\mathrm{C}-\frac{1}{2}\mathrm{O}-\mathrm{S}-\frac{1}{2}(\mathrm{N}+\mathrm{P}+\mathrm{H})}{\mathrm{C}-\frac{1}{2}\mathrm{O}-\mathrm{N}-\mathrm{S}-\mathrm{P}} \quad \text{Eq. 3.5}$$

3.2.3.3 Analytical methods for other geochemical parameters

The concentration of H_2 in headspace was measured instantly by Peak Performer 1 gas chromatograph (Peak Laboratories, USA). A 3-mL gas-lock syringe was used to take 0.8 mL gas from the Schott bottle. The gas in syringe was balanced to around 1.6 mL under atmospheric pressure. Precise volume of 1 mL gas is needed for each injection. Calculation of H_2 in solution (Lin et al. 2012): χH_2 expressed as ppb, obtained from chromatographic analysis to molar concentrations $[H_2]g = \chi H_2 \times P \times R^{-1} \times T^{-1}$ (where P is the total gas pressure in the headspace, R is the universal gas constant, and T is the temperature in Kelvin). β is the solubility coefficient of H_2 for calculation of H_2 in liquid phase based on data in gas phase, 1/β is 67 by calculation according to Crozier and Yamamoto (1974). $[H_2]aq = \beta \times [H_2]g$

The concentration of methane was analyzed instantly by GC (ThermoFinnigan GmbH, Bremen, Germany) equipped with a CPPoraBOND Q column (Agilent Technologies Deutschland GmbH, Böblingen, Germany) and flame ionization detector. The column temperature program was set at 60°C. 200-µL gas was injected for each sample. Chromatographic responses were calibrated using hydrocarbon standards (Scott Specialty Gas Co., 100 ppm). The concentration is described as µmol/L (µM) in slurry according to Henry's law. The detection limit for methane is 0.078 µM.

Samples for sulfate determination were centrifuged and the supernatant was taken for further analysis. Measurements of sulfate were conducted by photometric determination (Tabatabai 1974). The precipitation reagent (barium ions and gelatin) were added to the acidified sample and the turbidity was measured by spectrophotometer (UVmini-1240, Shimazu) at wavelength of 420nm. A quantitative 6-point calibration ranged from 0.1 mM to 1 mM was carried out prior to the analysis of samples. Samples at concentration above 1 mM were diluted before adding precipitation reagent. Each sample was separated into two subsamples, each of which was measured three times. This method permits determination of sulfate at concentration as low as 0.05 mM.

DOC and DIC were measured by Carbon analyzer MultiN/C 2100s (Analytic Jena, Germany). For DOC analysis 2 mL sample was acidified (pH < 2) by adding 30 µL 30% hydrochloric acid (Supra pure, Merck) before analysis. DOC was measured as non-purgeable organic carbon in acidified samples purged with CO_2-free synthetic air. The measurements were carried out by high-temperature catalytic oxidation at 750°C and product CO_2 was detected with an infrared detector. Final DOC concentrations were average values of triplicate measurements. The detection limit was 20 µmol C/L. For DIC measurements, CO_2 was liberated from the original sample in a 10% phosphoric acid trap. The detection limit was 10 µmol C/L.

Concentration of acetate were analyzed by liquid chromatography-isotope ratio monitoring mass spectrometer (irm-LC-MS) as reported previously (Heuer et al., 2006; Heuer et al., 2010). Sample is firstly seperated with high performance liquid chromatography (ThermoFinnigan Surveyor HPLC) and oxidized in an LC IsoLink interface (ThermoFinnigan, Germany). The oxidized product CO_2 was measured on a DELTA Plus XP mass spectrometer (ThermoFinnigan). The quantitative analysis of acetate is based on the linear correlation between signal area recorded by irm-LC-MS and injected amount of carbon (Heuer et al., 2006). The detection limit for quantitative analysis of acetate was 5 µM.

3.3 Results

3.3.1 Confirmation of redox conditions and ongoing initial/ intermediate/ terminal processes

The redox conditions of three major series were achieved and confirmed by hydrogen, methane and sulfate. The concentration of methane in the ‘SR’ series with sufficient sulfate addition remained low during incubation (< 5 µM) (Fig. 3.1a). The ‘SR→MOG’ series without sulfate addition showed two phases: during the first phase (day 0 to day 37), sulfate decreased by 4.2 mM to 0.3 mM. Concentration of methane was low, ranging from 2.9 µM to 12.9 µM; in the second phase from day 37 to day 75, sulfate was mostly depleted (0.3 mM at day 37) and the methane concentrations increased from 12.9 µM to 671.3 µM with concurrent accumulation of hydrogen (Fig. 3.1a, b). In ‘SR-inhibited’ series with SR inhibited by 20 mM molybdate, methane concentrations reached the highest value of 1.9±0.3 mM (> 2% in the headspace). It showed the lowest sulfate reduction rate and concentration of hydrogen decrease at a lower

rate, compared to 'SR' series. In both 'SR' and 'SR-inhibited' series, hydrogen reached similar concentration at the end of incubation (Fig. 3.1b).

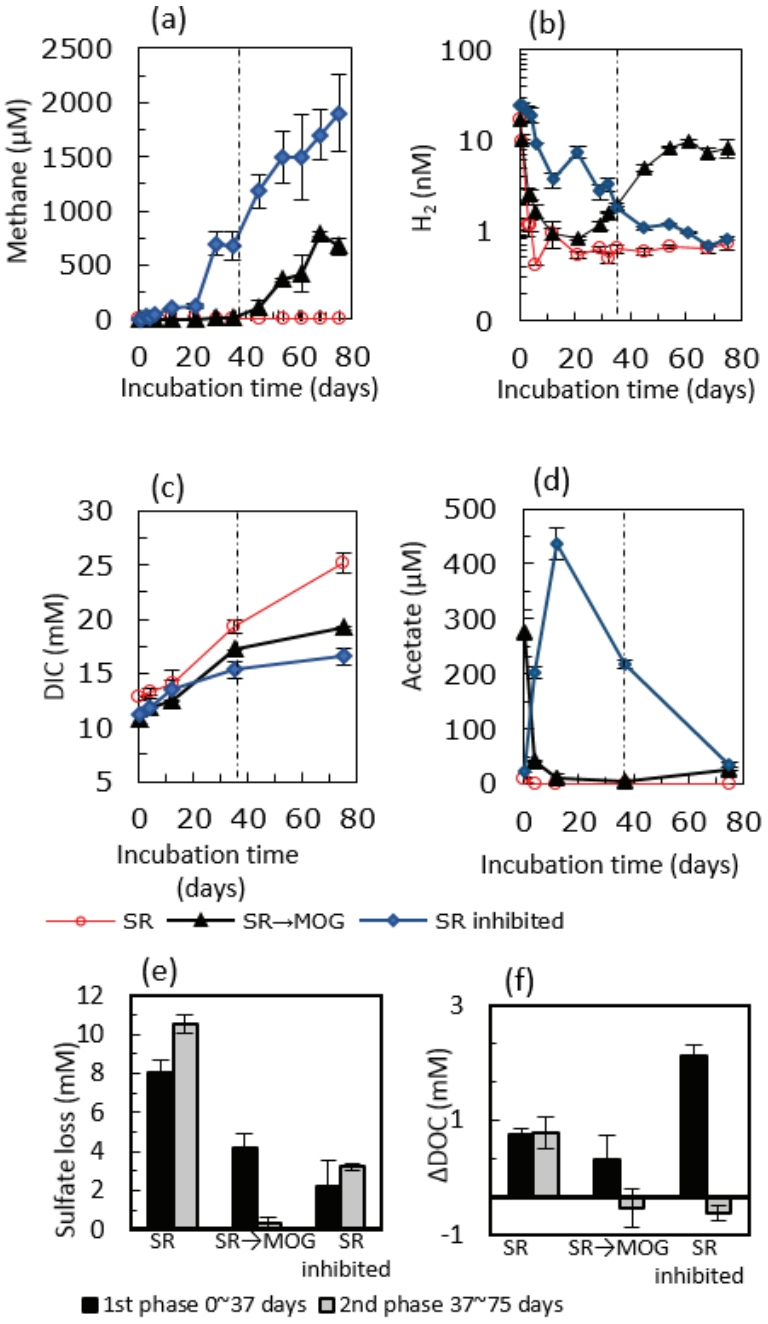

Fig. 3.1.Background information during incubation for confirmation of the redox conditions and ongoing initial/ intermediate/ terminal processes: (a) concentration of methane, (b) hydrogen, (c) DIC, (d) acetate, (e) loss of sulfate, and (f) accumulation of DOC expressed as ΔDOC in two phases (0-37 days and 37-75 days); concentration of acetate during incubation (f). Series I: SR-alive; series II: SR→MOG; series III: SR-inhibited. Incubations were conducted at 28°C using slurries with a solid/liquid ratio of 1 (v/v).

DIC concentrations increased in all series during incubation (Fig. 3.1c). The most significant accumulation of DIC and DOC (ΔDOC) was observed in the 'SR' series coinciding with the fastest sulfate loss (Fig. 3.1e, f). The 'SR→MOG' series showed a clear turning point after 37 days when methanogenic conditions were established (Fig. 3.1c). After sulfate was depleted, DIC increased slowly and the DOC concentration remained constant (Fig. 3.1c, f). In the 'SR-inhibited' series, DIC accumulation was significantly lower than the 'SR' series (Fig. 3.1c). DOC rose sharply from day 0 to day 12, and remained relatively constant afterwards (Fig. 3.S5 in supplementary material).

Acetate, as an important intermediate in anaerobic metabolism, was below detection in the 'SR' series. In the 'SR→MOG' series, acetate dropped from day 0 to day 37 and afterwards increased from 5.4 µM to 24.4 µM after day 37 (methanogenic conditions) (Fig. 3.1d). In the 'SR-inhibited' series, acetate reached the maximum concentration of 438 µM on day 12, which is equivalent to 876 µM dissolved organic carbon. Afterwards acetate decreased gradually to concentrations of 34.3 µM at the end of the incubation. The fasted accumulation of acetate occurred concurrently with the sharpest DOC increase between days 0 and 12.

3.3.2 Monitoring DOM by EEMs during incubation

3.3.2.1 Peaks identification by PARAFAC analysis and derived indices

The peaks are named according to Coble (1996) and listed in supplementary materials (Fig. 3.S2). Peaks C1, C2, M1, M2 and A are humic-like peaks. Peak T is a protein-like peak. Peaks C1 and C2 are derived from peak C with peak A (C1: ex/em 350/450 nm; C2: ex/em 270(380)/480 nm), with longest emission wavelength. Humic-like Peak M1 and M2 were both in the range of M peak (ex/em: 300-320/395-410 nm). The emission wavelength of peak M2 is 20 nm shorter than M1. Peak M represents compounds that are less aromatic than peak C. Humic-like peak A shows the shortest excitation wavelength and same emission wavelength as peak C. Since the peak A and peak C is inseparable after PARAFAC analysis, sum of them (AC) were presented in the results. Two indices derived from peak ratios, i.e., AC/M ratio and M1/M2.ratio were used to describe the red-shift or blue-shift of fluorescence signal and therefore the variation of conjugation in humic-like compounds.

3.3.2.2 In-situ profile of EEMs

In the core GeoB 17306-2, the SMTZ is assigned on the basis of data of sulfate and methane (Zhuang, 2014). The sum of fluorescent peaks (∑Fluo) increased at depth until ~200 cmbsf and remained constant below this depth (Fig. 3.2). The ratio of two humic-like peaks M1/M2 increased from 14 cm to 75 cm. The AC/M ratio decreased in the upper 175 cm, indicating a selective loss of terrestrial humic-like compounds (C and A) at longer wavelength of fluorescence emission.

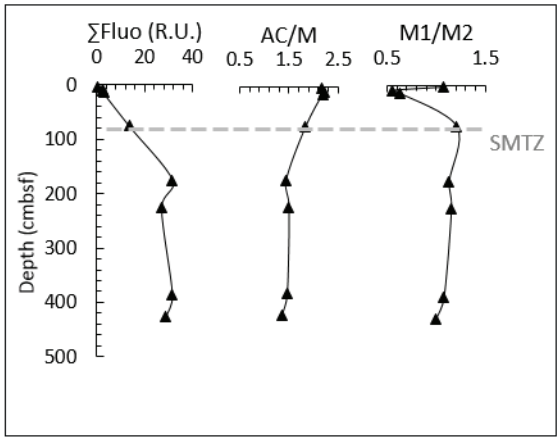

Fig. 3.2. In-situ profiles of DOM characterized by EEMs including sum of fluorescent peaks (∑Fluo), AC/M and M1/M2 at station GeoB17306, Rhône Delta. Unit of fluorescence intensity is Raman Unit (R.U.). AC/M ratio indicates the blue-shift of the bulk humic-like compound pool. M1/M2 ratio indicates the blue-shift of autochthonous DOM. Sulfate-methane transition zone (SMTZ) is indicated by grey dash line.

3.3.2.3 EEMs during incubations of three major series

For the incubation series in which the sulfate reducer were not inhibited by molybdate, the protein-like peak T was small (Fig. 3.3a, b) and contributed approximately 5% of the overall fluorescence (∑Fluo) in the pore water at the start of incubation; 95% of ∑Fluo derived from humic-like signals (EEMs of original sample in Fig. 3.3b). In 'SR-inhibited' series, the intensity of the protein-like peak (peak T) (Fig. 3.3a) increased sharply from 0.7 R.U. on day 0 to 1.8 R.U. on day 4, it reached up to 2.6 R.U. within 21 days, and afterwards remained relatively constant, thus showing a similar trend as DOC (Fig. 3.S5).

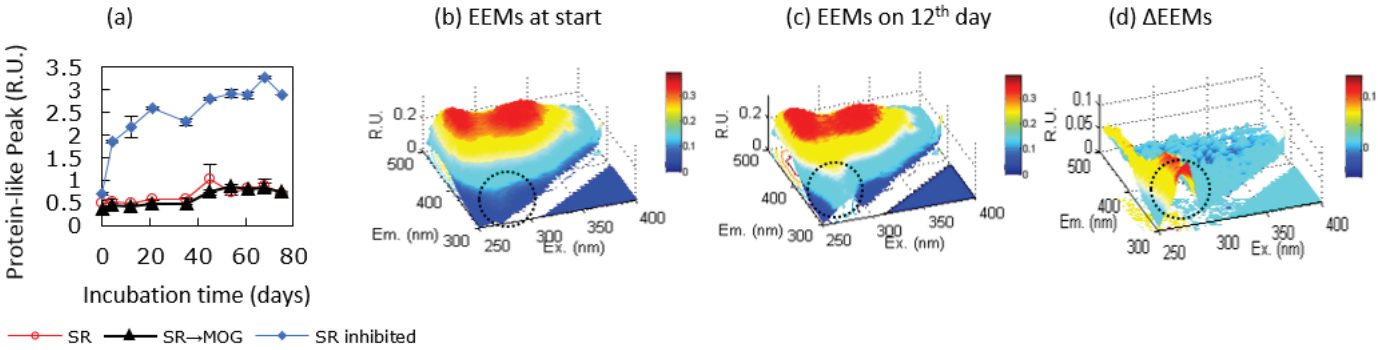

Fig. 3.3. Variation of protein-like DOM during incubations characterized by EEMs: (a) variation of protein-like peak during incubation in three series; (b) EEMs of series III 'SR-inhibited' on day 0; (c) EEMs of series III 'SR-inhibited' on day 12; (d) the difference of EEMs: ΔEEMs = $EEMs_{day\ 12}$ - $EEMs_{day\ 0}$ showing accumulation of protein-like peak. The protein-like peak was emphasized by dashed circles in the EEMs.

Humic-like compounds increased in both 'SR' and 'SR→MOG' series during incubation (Fig. 3.4a). The ratio of sum of peak A and C and peak M (AC/M) represents the proportion of compounds with longer emission wavelengths, i.e., large terrestrial molecules with aromatic functional groups and conjugations. Ratio M1/M2 (Fig. 3.4c) indicates the change of the DOM pool represented by M peak, i.e., in-situ autochthonous or marine DOM. The blue-shift is shown by the decrease of AC/M and M1/M2 and both ratios indicate loss of aromaticity, e.g., loss of aromatic ring or auxochrome. AC/M in 'SR' series showed a slight blue-shift of fluorescence spectra resulting from an increased fluorescence of peaks M with short excitation and emission wavelengths (Fig. 3.4b). The decrease of AC/M and M1/M2 is particularly strong in 'SR→MOG' series after 37 days when sulfate was depleted and methanogenic conditions were established (Fig. 3.4b, c).

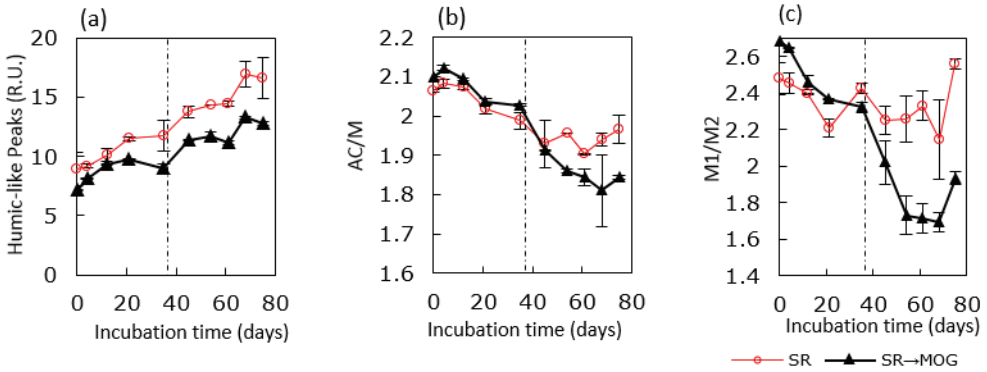

Fig. 3.4 Changes of humic-like DOM during incubations as indicated by EEMs: (a) quantitative change of all humic-like peaks; (b) AC/M representing the blue-shift of the bulk humic-like compound pool; (c) ratio of peak M1 and M2 (M1/M2) during incubation representing the blue-shift in autochthonous DOM.

3.3.2.4 EEMs in additional series with substrates additions

The additional experiments with yeast extract addition compared the consumption of protein-like DOM under different redox condition. After 2 days, the protein-like peak has been substantially reduced (80%) in the 'YE-SR' series under sulfate reducing conditions (Fig. 3.5a, c), meanwhile no significant loss of peak T was observed in 'YE-SR-inhibited' (figure not shown in figure) or 'YE-MOG' series, even on the 10th day (Fig. 3.5b, d). The extended incubation of 40 days under methanogenic condition finally resulted in loss of 89% of the protein-like peak (data not shown in figure).

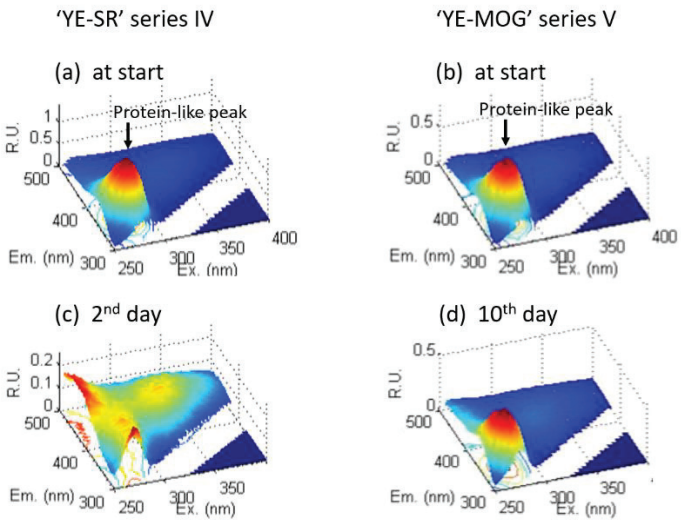

Fig. 3.5. Changes in yeast-derived proteinaceous DOM during incubations under sulfate-reducing (YE-SR) and methanogenic (YE-MOG) conditions: (a) EEMs at start with yeast extraction added under sulfate reducing condition; (b) EEMs at start with yeast extraction added under methanogenic condition; (c) EEMs on 2nd day with yeast extract added under sulfate reducing condition; (d) EEMs on 10th day with yeast extraction added under methanogenic condition. The black arrows show the position of protein-like peak in the EEMs (ex/em 280/350). Scale of the color is based on fluorescence intensity of z-axis.

3.3.3 Molecular composition of DOM characterized by FT-ICR MS during incubations

3.3.3.1 Changes of intensity-weighted averages of characteristic parameters during incubation

FT-ICR MS data of DOM from 'SR' and 'SR→MOG' series were compared. The DOM sample at start is from slurry of homogenized sediment and sulfate-free artificial seawater before incubation. 6386 discrete formulae were identified in the m/z range of 200-650 Da.

48.1% of the peaks were CHO compounds (weighted-average value by accounting for peak intensity: 66.8%), 38.7% (weighted-average: 21.0%) were CHNO compounds (dominated by formulae with one N atom, i.e., CHNO-N1) and 12.5% of the peaks were CHOS compounds (dominated by formulae with one S atom) (Fig. 3.S3). In 'SR' series, the formulae were on average more oxygen-rich and had a more aromatic character as indicated by an increased weighted-average (wa) O/C_{wa} ratio, DBE/C_{wa} ratio, $DBE\text{-}O_{wa}$ and decreased H/C_{wa} ratio at the end of incubation (Table 3.2). The formulae 'SR→MOG' series showed decreased O/C_{wa} ratio, DBE/C_{wa}, m/z_{wa} and increased H/C_{wa} ratio and $DBE\text{-}O_{wa}$ at the end of incubation (Table 3.2).

Table 3.2. Intensity-weighted averages of characteristic parameters derived from FT-ICR MS analysis. SD: average of standard deviation of the duplicates (* formulae with ^{13}C or ^{34}S were not included).

Series, phase	C_{wa}	m/z_{wa}	O/C_{wa}	H/C_{wa}	DBE/C_{wa}	N/C_{wa}	S/C_{wa}	$DBE\text{-}O_{wa}$
All series, day 0,	19.4	414.1	0.50	1.17	0.48	0.013	0.0051	-0.21
SR series, day 75	19.5	422.8	0.53	1.06	0.53	0.016	0.0029	0.18
SR→MOG series, day 37	18.0	394.7	0.54	1.08	0.53	0.016	0.0037	-0.13
SR→MOG series, day 75	17.6	381.4	0.52	1.11	0.51	0.015	0.0036	0.02
SD	0.23	5.7	0.005	0.008	0.004	0.0002	0.0001	0.05

At the end of the incubation on day 75, 75% and 86% of the originally present formulae were still detected in the 'SR' and 'SR→MOG' series, respectively. The differential mass spectra in Fig. 3.6, nevertheless, show that the relative abundance of formulae changed substantially over the course of the experiments. Peaks with a decreased relative abundance in the 'SR' series were distributed across a larger m/z window from m/z 250 to 650 (Fig. 3.6a). Although the m/z_{wa} in 'SR' series was higher at the end, the average molecular carbon number was similar (C_{wa}: 19.4 at start *vs.* 19.5 at end); the slightly increased molecular weight was attributed to the increased contribution of oxygen and nitrogen. Peaks with the strongest increase in the relative abundance within the 'SR' series had low to intermediate molecular weight (m/z 250 to 380) (Fig. 3.6a). Unlike the 'SR' series, the 'SR→MOG' series showed a small relative increase of formulae in lower m/z range and a strong decrease in relative peak intensity of formulae within the low to intermediate m/z range (Fig. 3.6b).

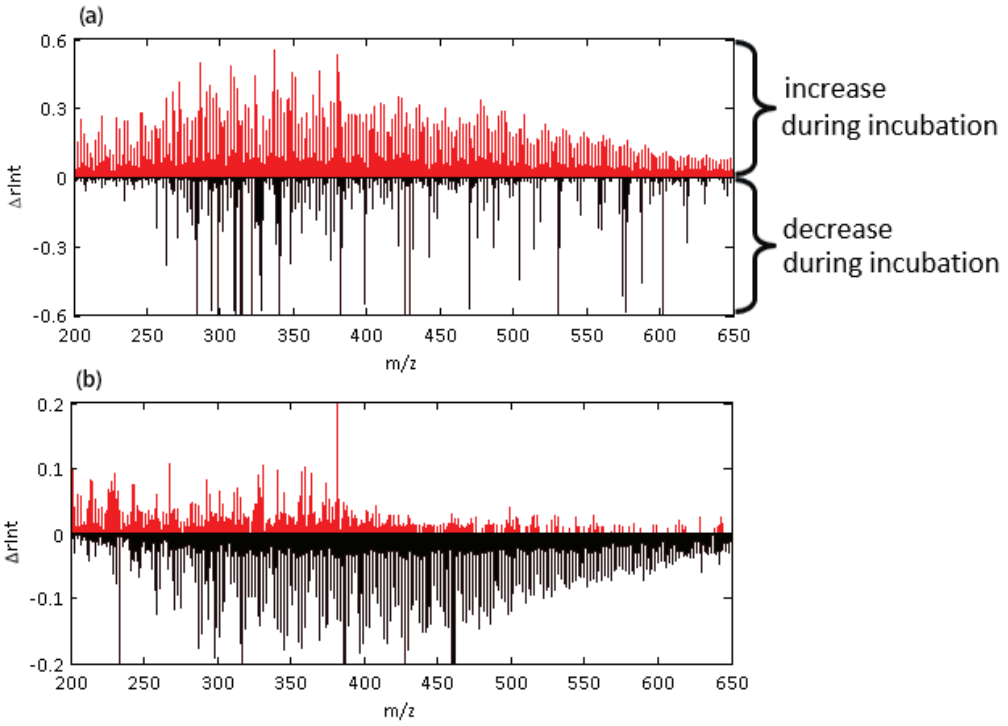

Fig. 3.6. Differential mass spectra showing changes in the relative peak intensity of formulae during incubations (a) from day 0 to day 75 of series I 'SR', (b) from day 37 to day 75 of series II 'SR→MOG' when methanogenic conditions was achieved. ΔrInt = rInt(end)- rInt(start). ΔrInt > 0, relative intensities of formulae increased; ΔrInt < 0, relative intensities of formulae decreased during incubation. rInt is the peak intensity normalized to base peak.

3.3.3.2 Variation of CHO, CHNO and CHOS compounds during incubation

In 'SR' series, the number of CHNO compounds increased slightly by 3.6% (average-weighted, no increase), while the number of CHOS compounds increased by 0.6% (average-weighted, no increase) (Fig. 3.S3); In 'SR→MOG' series, percentages of CHNO compounds remained constant during incubation and CHOS relatively decreased by 1.3% when the sulfate was depleted.

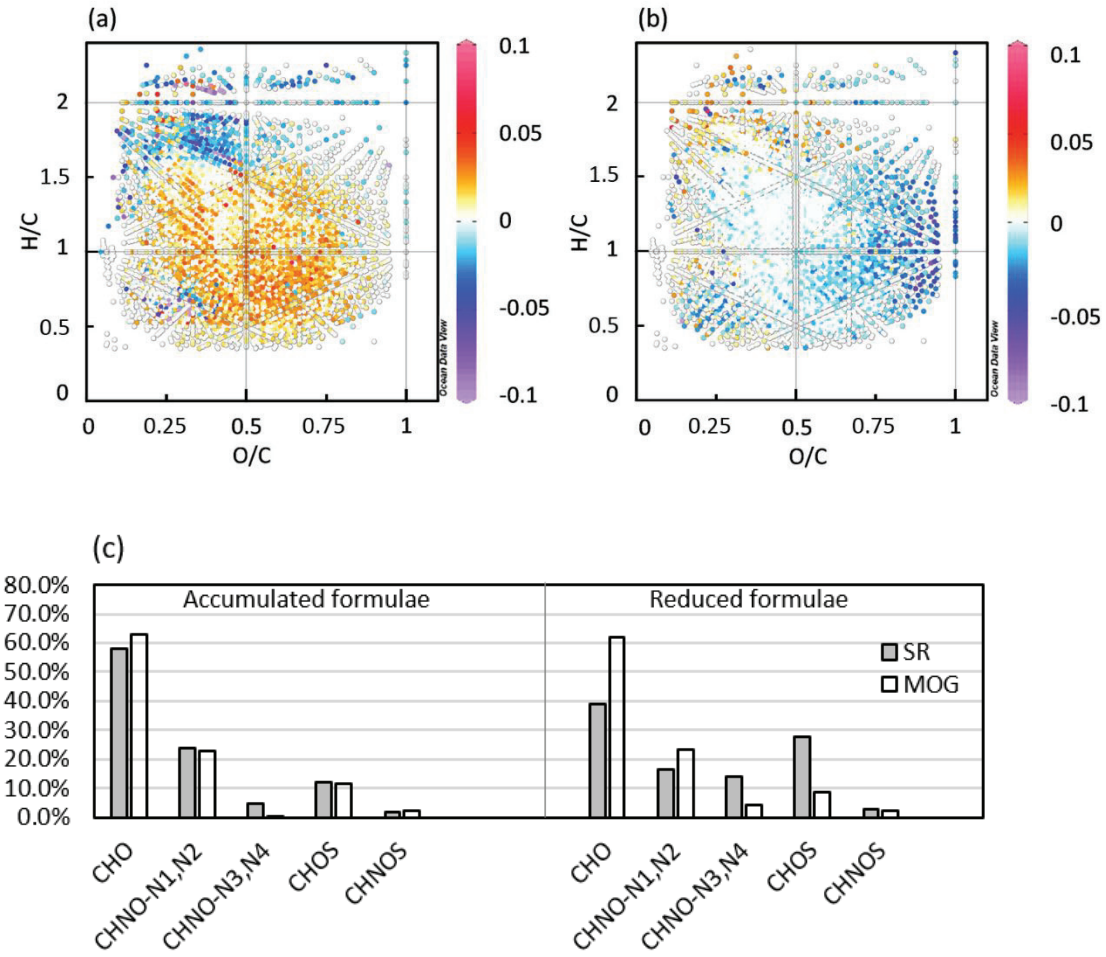

Fig. 3.7. Differential van Krevelen diagram showing changes in the relative peak intensity of formulae during incubations (a) from day 0 to day 75 of series I 'SR', (b) from day 37 to 75 of series II 'SR→MOG'. Color bar shows the change of relative intensity (ΔrInt = rInt(end)- rInt(start)); ΔrInt > 0, relative intensities of formulae increased, ΔrInt < 0, relative intensities of formulae decreased during incubation; data points ranged from ΔrInt > 0.1 and ΔrInt < -0.1were shown in the same color as ΔrInt = 0.1 and ΔrInt = -0.1, respectively. (c) Percentage of different groups of accumulated and reduced formulae during incubation under sulfate reducing (SR) and methanogenic conditions (MOG). ΔrInt > 0: accumulated during incubation; ΔrInt < 0: lost during incubation. rInt is the peak intensity normalized to base peak (rInt = $Int_{Peak}/Int_{Base\ peak}$).

Under sulfate reducing condition, oxygen-poor compounds were lost and oxygen-rich compounds were enriched (Fig. 3.7a). For example, CHNO-N3/N4 compounds were preferentially lost (14% of the lost formulae) compared to its original percentage in all formulae (3%), while CHNO-N1/N2 compounds slightly accumulated (24% of the accumulated formulae at the end compared to 21% of all formulae originally) (Fig. 3.7c). Under methanogenic conditions, highly oxygen-rich CHO compounds with relatively low H/C ratio

were lost (Fig. 3.7b); CHNO-N1/N2 compounds were more depleted than that under sulfate reducing condition (Fig. 3.7c). There is no preferential utilization of CHNO-N3/N4 under methanogenic conditions**.** It is noteworthy that for the formulae (rInt > 0.1, i.e., rIntn > 0.0002) lost under methanogenic condition, more than 90% of them were enriched under sulfate reducing condition while not vice versa.

3.3.3.3 Variation of compounds according to aromaticity during incubation

The EEMs mainly comprise fluorescent compounds with aromatic moieties. For a better comparison of EEMs and FT-ICR MS data, molecular formulae were classified into four groups based on AI, including aliphatic, highly unsaturated, aromatic and condensed aromatic compounds (condensed aromatic compounds are included among the aromatic compounds in the following description) (Fig. 3.8).

Compounds with varied aromaticity showed partly different trends in 'SR' series and 'SR→MOG' series. Under sulfate reducing conditions, the highly unsaturated formulae (compounds possessing 7-15 oxygen atoms, with O/C ratio 0.2-0.4) were more oxygen-rich at the end (Fig. 3.8a). Aliphatic compounds mainly decreased in abundance; in comparison, highly unsaturated and aromatic compounds mainly increased (Fig. 3.8a). There is no preference of molecular size (evaluated by carbon number) under sulfate reducing condition (Fig. 3.8b). Regardless of the aromaticity, mainly compounds in the intermediate size range (C number 15-20) with elevated O/C ratio (0.4-0.6) accumulated during incubation (Fig. 3.8b).

Under methanogenic conditions, relatively smaller compounds (carbon number 10-20) accumulated (Fig. 3.8d). Compared to aliphatic compounds, the abundance of highly saturated and aromatic compounds was more reduced during the incubation (Fig. 3.8c, d) and the molecular assemblage shifted to lower carbon numbers (Fig. 3.8d). The oxygen content was reduced within the group of highly unsaturated and aromatic compounds (Fig. 3.8c). This loss of oxygen and carbon coincided with the blue-shift observed in EEMs during incubation, which was stronger under methanogenic condition.

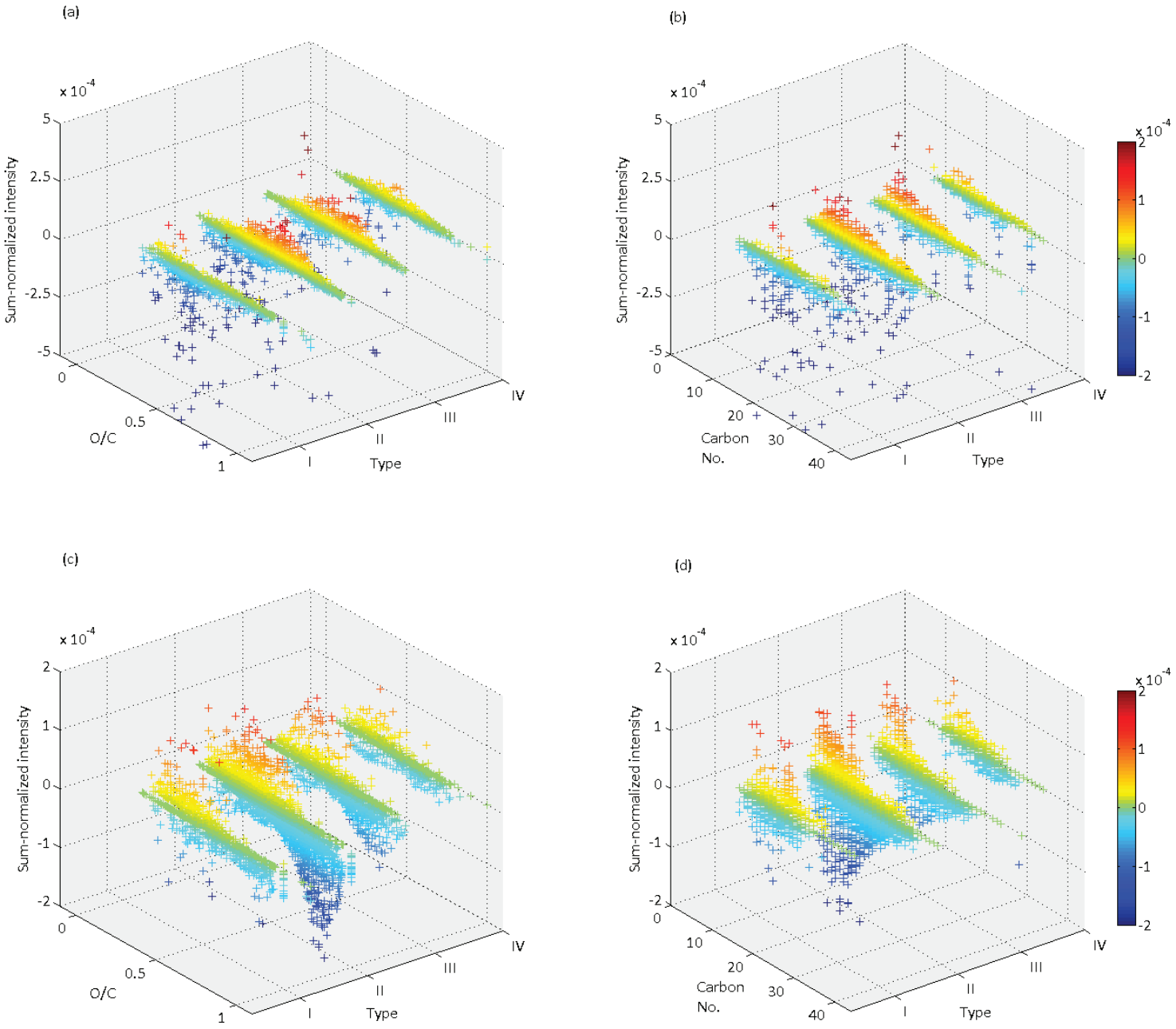

Fig. 3.8. O/C ratio and carbon number distribution of formulae during incubations for aliphatic, highly unsaturated and aromatic compounds under sulfate reducing condition (a, b) and methanogenic condition (c, d). Z-axis shows the change of sum-normalized intensities (ΔrIntn) during incubation, i.e., ΔrIntn = rIntn(end)- rIntn(start)). ΔrIntn > 0: accumulated during incubation. ΔrIntn < 0: lost during incubation. Formulae with AI > 0.67, 0.67 ≥ AI > 0.5, 0.5 ≥ AI ≥ 0, AI < 0 are characterized as condensed aromatic (Type IV), aromatic (Type III), highly unsaturated (Type II) and aliphatic compounds (Type I), respectively. rIntn represents the sum-normalized intensities ($rIntn = Int_{Peak}/\sum Int_{allPeaks}$).

3.4 Discussion

3.4.1 DOM transformation under sulfate reducing conditions

3.4.1.1 Quantitative change of DOM

Sulfate reducers are among the main microbial players in anaerobic carbon cycling in marine sediments (Jørgensen, 1982) and sulfate reduction is the predominant terminal step in organic carbon mineralization in coastal marine sediments (Capone and Kiene, 1988; Canfield et al., 1993; Chen et al., 2003; Muyzer and Stams, 2008). Consistent with this, we observed highest DIC production under sulfate reducing conditions (Fig. 3.1). At the same time, DOC increased concurrently with sulfate consumption and remained constant after sulfate was depleted. Sulfate reduction apparently stimulates DOM release from the solid phase resulting in a net accumulation in the pore waters. Observations based on a wide range of coastal and continental margin sediments pore water also suggested a positive relationship between pore water DOC concentrations and carbon mineralization rate (Burdige and Zheng, 1998).

When sulfate reducers were inhibited, both DOC and DIC remained constant at concentrations of 3.5-3.8 mM and 15.4-16.5 mM, respectively, which suggests that the observed DOC release during sulfate reduction was a biotic process. There is no evidence for sulfate reducers directly taking part in DOC production by hydrolysis of particulate organic carbon (POC) in the sediment; however, the biotic factor appears to be central for the release and subsequent mineralization of DOC. Since most of the sulfate reducers cannot degrade polymers (Hansen, 1993) and sulfate reducers depend on other microbes providing fermentation and degradation products (Schink, 1997; Plugge et al., 2011), syntrophic partners of sulfate reducers are potential candidates for the transformation of POC to DOC. This is supported by the fact that on day 12, inhibition of sulfate reduction resulted in maximum concentration of intermediates and stable DOC concentrations (Fig. 3.1, S6). Accordingly, we suggest that inhibition of the terminal step of sulfate reduction resulted in accumulation of intermediates, which in turn resulted in a slowing down of the initial hydrolytic steps associated with DOC release.

The three major experiments showed that the activity of sulfate reduction influences the final concentration of DOC in pore water by indirectly affecting the upstream processes (POC to DOC) and directly controlling the downstream processes (DOC to DIC).

3.4.1.2 Qualitative change of DOM

(a) Cycling of protein-like compounds

The fluorescence signal of protein-like peak T represents a relatively labile pool of DOM in lake and ocean water (Yamashita and Tanoue, 2003; Stedmon and Markager, 2005b; Fellman et al., 2010; Lønborg et al., 2010). In the *in situ* pore water sample peak T was small (< 5%), which was expected as amino acid-C contributes 4-9% of DOC in sediment pore waters (Alberic et al., 1996; Lomstein et al., 1998) and 1–13% of the pore water DON (Landén and Hall, 2000). The rapid release and degradation of intermediates resulted in a low abundance of protein-like peak and acetate in 'SR' series, which is important because the pool of intermediates needs to remain small to allow efficient carbon flow between fermenters and sulfate reducers (Schink, 1997). The inhibited experiment supports this reasoning: the inhibition of terminal step – sulfate reduction resulted in a sharp increase of protein-like peak during incubation (Fig. 3.3), suggesting that protein-like compounds were rapidly released from a particulate precursor pool and subsequently utilized if without inhibition. This is not surprising as the solid phase has a great potential of releasing labile DOM intermediates due to the considerably high concentrations of bound amino acids compared to dissolved free amino acid in liquid phase (e.g., 16,632 mg C/m^2 *vs.* 43 mg C/m^2 in bound amino acids *vs.* dissolved free amino acid in Southern Hatteras Abyssal plain at depth 0-10 cmbsf (Rowe and Deming, 2011)). By inference, the accumulation of protein-like compounds in 'SR-inhibited' series suggests rapid consumption of labile protein-like DOM when sulfate reduction is active, because comparable accumulation of protein-like compounds was not observed in 'SR' series. Although protein-like peak T and acetate were both actively cycled, they showed different trends in the 'SR inhibited' series after the 12th day: acetate was consumed after the maximum concentration of 438 μM on day 12 (Fig. 3.1), whereas, the protein-like peak T remained constant afterwards. This suggests that acetate is consumed without active sulfate reduction, e.g., via methanogenic processes, while degradation of protein-like peak appears to be inhibited without active sulfate reduction.

A few studies linked EEMs with molecular formulae and found significant correlations. For example, Stubbins et al. (2014) reported that a significant proportion of the protein-like peak is linked to N-containing aromatic compounds and correlates with concentrations of hydrolysable amino acids in natural water. In terrestrial pore waters the protein-like peak appears to be associated with more saturated compounds (Tfaily et al., 2015). We found a consistent pattern of CHNO-N3/N4 compounds and the protein-like peak T: firstly, the abundance of both was low (former: 2-5%; latter: 5%); secondly, they varied slightly during incubation and showed rapid cycling. CHNO-N3/N4 compounds were more preferentially produced and consumed under sulfate reducing conditions compared to methanogenic conditions (Fig. 3.7c). Preferential hydrolysis of PON relative to POC was also suggested in a former study at shallow layers (Weston et al., 2006). Moreover, based on a 14-days incubation of pore water with inoculates from shallow layers, 54% of the DON (dominated by combined/free amino acid, urea) was rapidly utilized by bacteria (Guldberg et al., 2002). Thus, CHNO-N3/N4 compounds appear to include a readily bioavailable fraction, possibly consisting of labile proteinaceous molecules or derivatives derived from peptides. It should be noted that CHNO-N1/N2 show different trends compared to CHNO-N3/N4 compounds: the former compounds rather accumulated under sulfate reducing conditions (Fig. 3.7c). This suggests a different bioavailability of CHNO-N1/N2 compounds, which are either more recalcitrant or have an elevated production during incubation. These compounds could be produced during early diagenetic reactions by incorporation of ammonia (Amrani et al., 2007; McKee and Hatcher, 2010) or deamination during degradation of proteinaceous molecules/ CHNO-N3/N4 compounds (Schmidt et al., 2011; Abdulla et al., 2017).

(b) Transformation of humic-like peaks and aromatic, highly unsaturated compounds *vs.* aliphatic compounds

Humic-like DOM accumulated rapidly during the ‘SR’ incubation (Fig. 3.4a). This suggests that the accumulation of aromatic or highly unsaturated fraction under sulfate reducing condition. The relative constant composition ratio of humic-like DOM (Fig. 3.4b,c) implied it was not strongly transformed or degraded during incubation. It is consistent with studies of oxic environments, which suggested that humic-like DOM is refractory against microbial attack (Yamashita and Tanoue, 2008; Fellman et al., 2010; Lønborg et al., 2010).

Congruently, FT-ICR MS showed that the aromatic compounds did not decrease during incubation; they were mainly produced under sulfate reducing conditions as inferred by an increased rIntn (Fig. 3.8a, b). The pool of aromatic and highly unsaturated formulae generally became enriched in compounds with greater number of O atoms during the incubation. An increase in O-rich compounds with depth has been reported for shallow marine sediments (Oni et al., 2015; Seidel et al., 2014) and for the sulfate reduction zone in the Rhône Delta and Gulf of Lions shelf (Schmidt et al., 2017) and is probably a result of diagenetic processes during oxidation, e.g., by sulfate reduction. The formulae accumulated during incubation were mainly in the range of $0.6 > O/C > 0.8$ and $0.67 > AI > 0$ producing the observed shift in O/C_{wa} ratio at the end; the respective compounds fall in the range of hydrolysable tannins in a van Krevelen diagram (Mopper et al., 2007) or degraded/modified lignin (Liu et al., 2011; Waggoner et al., 2015).

In contrast to aromatic compounds, compounds of lower aromaticity were depleted, especially aliphatic compounds (Fig. 3.8a, b). In general, the relative intensity of aliphatic compounds decreased during the incubation regardless of O/C ratio or carbon numbers (Fig. 3.8a, b) suggesting non-selectivity of oxidation state or molecular size for aliphatic compounds. These lost aliphatic formulae were dominated by CHNO compounds.

In sum, under sulfate reducing condition, microbes prefer compounds accessible for initial hydrolytic and enzymatic attack on organic matter.

3.4.2 DOM transformation under methanogenic conditions

3.4.2.1 Quantitative change of DOM

After sulfate was depleted, the accumulation of DOC stopped and DIC production slowed down, which suggests that the fresh DOM production during organic matter degradation was limited under methanogenic conditions. A stop in the accumulation of DOC after the depletion of sulfate was also observed in estuary sediments by Weston et al. (2006) and in the *in situ* DOC profiles of Rhône Delta sediments (Schmidt et al., 2017). A potential reason for the decreased hydrolysis could be that a greater fraction of the organic matter becomes associated with mineral surfaces with increasing burial in sediments and thus less accessible for enzymatic hydrolysis (Wakeham and Canuel, 2006). By contrast, sediments and length of incubation in

our experimental study are identical in all three series, so that the different rates of DOC production are probably related to the redox conditions rather than interactions with mineral surfaces. Cease of DOC accumulation with depleted sulfate imply that the decreasing electron acceptors are limiting factor for initial steps and therefore result in decreasing substrates in the dissolved phase. Accordingly, it is assumed that limited substrates influence the microbial community at deep sediments. Consistently, in former studies of in-situ profiles, change in the microbial community structures and energy turnover between different layers have been observed (Biddle et al., 2005; Durbin and Teske, 2011; Jorgensen et al., 2012; Miyatake et al., 2013) and cell density below the sulfate-methane transition zone (SMTZ) layer dropped in the deeper sediment layers (Leloup et al., 2009; Briggs et al., 2013).

3.4.2.2 Qualitative change of DOM

(a) Protein-like peaks and CHNO compounds under methanogenic conditions

After sulfate was depleted in the 'SR → MOG' experiment, the protein-like peak remained constant. This constancy signals balanced between production and consumption of protein-like DOM, it does not provide information on the kinetics the underlying processes. A rather slow kinetics is supported by evidence from the additional experiments in which yeast extract was added for investigation of biopolymer fragments (Fig. 3.5b,d). Under methanogenic conditions, the degradation of protein-like DOM was far slower than that under sulfate reducing conditions (Fig. 3.5). Second evidence is that, without yeast extract addition, release and degradation of CHNO-N3/N4 were both less under methanogenic conditions (Fig. 3.7c). The slow cycling of CHNO and protein-like DOM under methanogenic conditions is further corroborated by slightly decreasing ammonium concentrations during the experiment (Fig. 3.S4 in supplementary materials). Thus, we conclude that the continuously small percentage of protein-like peak resulted from slow production and consumption of protein-like DOM under methanogenic conditions. Accordingly, we suggest that redox conditions not only influence the terminal step but also the initial step regarding to hydrolysis of biopolymers. Notably, despite protein being considered a labile compound pool, its degradation appears to be retarded in methanogenic sediment.

(b) Transformation of humic-like compounds and aromatic, highly unsaturated compounds *vs.* aliphatic compounds

The *in situ* data from the Rhone prodelta (Fig. 3.2) showed that the accumulation of humic-like DOM ceased when sulfate was depleted. Data from incubation experiments are consistent with this observation: humic-like DOM accumulated more slowly under methanogenic conditions (Fig. 3.4). Humic-like DOM, which is generally considered to be a refractory organic matter pool (Stedmon and Markager, 2005b; Yamashita et al., 2010) showed the most pronounced changes in composition under methanogenic conditions. We observed a blue-shift in form of decreased AC/M and M1/M2 ratio after sulfate was depleted and methanogenesis was most active. The decrease of AC/M and M1/M2 ratio could be caused by the loss of aromatic moieties (Zsolnay, 2003), auxochrome/chromophore (e.g. -OH,-OCH_3, –COOH, -CO-) attached to aromatics (Gauglitz and Vo-Dinh, 2003; Mistry, 2009), which is accompanied by a decreasing molecular weight. The obvious blue-shift under methanogenic conditions is probably a result of the transformation of DOM and low inputs of freshly released DOM from the POM pool (see DOC and DIC in Fig. 3.1). The decreasing AC/M ratio and M1/M2 ratio of humic-like peaks suggests that there is preferable utilization of peak A, C and M1, which suggests the loss of conjugation structures in larger terrestrial and autochthonous humic substances. Thus, microbes metabolize the humic-like DOM pools under methanogenic conditions when the release of fresh DOM from POM is limited.

FT-ICR MS data show that the relative abundance of O-rich and larger aromatic/highly unsaturated compounds decreased under methanogenic conditions (Fig. 3.8c, d) indicating a reduction of DOM. The van Krevelen diagram (Fig. 3.7b) suggests that the compounds with decreased abundance are in the range of lignin-like compounds. Oxidized aromatic compounds are chemically more susceptible to nucleophilic attack by electron donors. Accordingly, smaller and more reduced aromatic or highly unsaturated compounds accumulated. The compositional data from FT-ICR MS are consistent with the observations from EEMs that indicate a loss of functional groups (-OH, -OR, -COOH) and aromatic rings under methanogenic conditions. Both aromatic formulae and most significantly highly unsaturated oxygen-rich formulae were lost under methanogenic conditions. Moreover, these degraded oxygen-rich compounds were mostly smaller molecules with lower carbon number and higher O/C ratio. This is in line with a former study by Guo et al. (2012) who suggests a loss of

functional group -CH_3 and -COOH during anaerobic fermentation using Fourier-transform infrared spectroscopy.

Our results suggest that humics serve not only as reversible electron donor (Scott et al., 1998; Martínez et al., 2013; Klüpfel et al., 2014) for sedimentary microbes but also as carbon and energy sources. It is interesting to know that the humic substances, which are conventionally known as recalcitrant substrates for aerobic microbes, are favorable methanogenic condition.

For methanogenic conditions, FT-ICR MS suggests a lower loss of aliphatic compounds, which is in contrast to the trend observed under sulfate reducing condition. Formulae that plot in the van Krevelen diagram in the range of lipids, carbohydrates, and amino acids were less efficiently degraded under methanogenic conditions.

3.4.3 Different substrates selectivity under sulfate-reducing vs. methanogenic condition due to changing electron acceptors

The preferential cycling of CHNO- and protein-like compounds under sulfate reducing relative to methanogenic conditions implies a different substrate selectivity of microbial organic matter degradation. It implies an intriguing figure in deep biosphere of syntrophic mechanism fulfilling a degradation chain from high-molecular-weight organic matter to terminal products adapted to starvation of inorganic electron acceptor. This is summarized in Fig. 3.9.

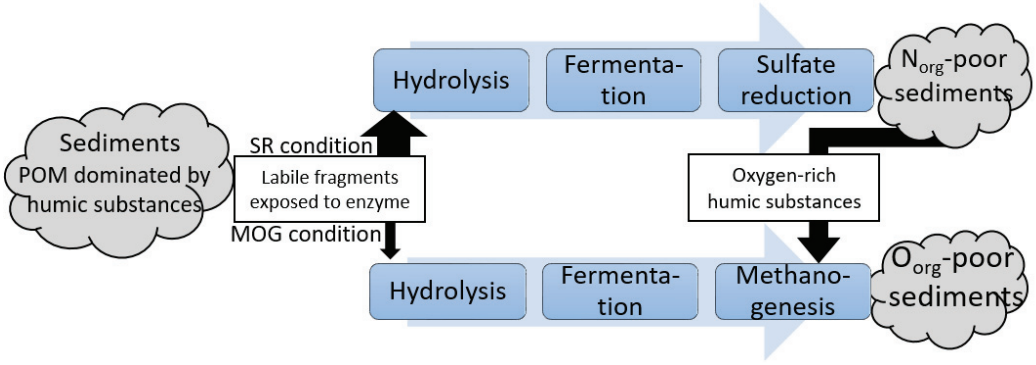

Fig. 3.9 Proposed scheme of DOM cycling and energy flow in anoxic marine sediments. Black arrows show the flow of organic matter. The width of arrows represents relative rate of flow. N_{org} and O_{org} are abbreviation of N and O in organic compounds, respectively.

Several plausible factors may be responsible. (1) This phenomenon might result from a higher efficiency of hydrolysis under sulfate reducing conditions, as supported by the higher DOC production in our experiments. (2) Schink (1997) suggested that a syntrophic community of terminal mineralizers and fermenters is energetically favored compared to a corresponding methanogenic community, e.g., $\Delta G^{0'} = -48.1$ kJ/mol acetate via sulfate reduction (Glombitza et al., 2015), $\Delta G^{0'} = -31$ kJ/mol acetate via methanogenesis (Hattori, 2008). Under environmental conditions, less than one ATP can be synthesized under methanogenic condition (Deppenmeier and Müller, 2008). Under *in situ* conditions in marine sediments, Gibbs free energies of reaction for sulfate reduction are about twice as high as under methanogenic conditions (e.g., Wang et al., 2010). Considering the high cost in synthesizing enzymes for hydrolyzing biopolymers, proteins and carbohydrates would be more effectively degraded under sulfate-reducing conditions. (3) Under methanogenic conditions, degradation of fermentation products such as fatty acids with more than two carbon atoms, the so-called secondary fermenters are needed for methanogenesis (Schink, 1997), while sulfate reducing bacteria as terminal mineralizer are metabolically more versatile (Hansen, 1994) and can utilize products of primary fermentations. Thus, under methanogenic conditions the microbial activity, including that of methanogen, is more limited by supply of adequate substrates derived from hydrolysis and fermentation. They prefer smaller 'processed' compounds.

When the inorganic electron acceptors are depleted, humic substances may serve as electron acceptors (Lovley et al., 1996). Redox potential ranges for sulfate reduction are -150 to 0 mV and for methanogenesis via CO_2 reduction in natural environment are -250 mV, respectively (Schuring et al., 1999). Humics as natural compounds in anaerobic environment with redox potential ranges of -230 to +180 mV (Yang et al., 2016). Turning point of the direction of electron flow to/from humics is controlled by redox potential and reached when the system turns to methanogenic conditions. FT-ICR MS and EEMs suggested that oxygen-bearing functional group were lost during the reduction of humics under methanogenic condition. Consistent with our observations, a recent study demonstrated that methoxylated aromatic compounds could serve as substrate for methanogenesis in subsurface sediments via the loss the methoxy group (Mayumi et al., 2016), which is a typical functional group of lignin and terrestrial humics (Malcolm, 1990).

3.5 Conclusions

(1) EEMs and FT-ICR MS complement each other in DOM characterization and provide an in-depth view of the compositional changes in initial step of anaerobic degradation. They enabled the elucidation of the different patterns of DOM cycling under sulfate reducing *vs.* methanogenic conditions.

(2) Under sulfate reducing conditions, sufficient sulfate drives a fast upstream process (production of DOC from POC) as well as the terminal mineralization. In the pool of newly released organic matter from POC, there was a rapid turnover of protein-like compounds and consistently aliphatics and CHNO-N3,4-formulae were readily lost. In the meantime, refractory compounds accumulated in the DOM pool, which are dominated by oxygen-rich humic-like compounds.

(3) Under methanogenic conditions, hydrolysis process was less efficient and there was no accumulation of DOC with inability of releasing organic carbon from solid phase. Microbes tend to utilize refractory DOM, and congruently rapid transformation of 'refractory' humic-like peaks occurred. As a result, smaller aromatic and highly unsaturated compounds with low O/C accumulated, suggesting the utilization of aromatic humic substances via losing oxygen-containing functional groups and side chains as fluorochromes. Different from the situation under sulfate reducing conditions that the selectivity depends more on the type and diagenesis degree of compounds (aliphatic, biopolymers), DOM is preferentially degraded along a gradient from a high to low nominal oxidation state of carbon under methanogenic conditions.

(4) Electron acceptor (sulfate) not only modulates directly the terminal step of mineralization as is known, but also indirectly shapes the initial steps of degradation chain. The varied preference of type, element (O, N) of molecules along with redox conditions suggests different selectivity modulated by sulfate availability. The life strategy of anaerobic microbes responds to availability of terminal electron acceptor at initial steps. Considering the important role of delta sediments in the carbon cycle, the redox regimes and the associated biogeochemical processes would influence the regional carbon and nitrogen cycle via preferential DOM released, consumed, and ultimately shape the composition of organic carbon preserved.

Acknowledgements

We thank the ship staff and the scientific party during Poseidon Cruise 450 of DARCSEAS II. We are grateful for the sampling during incubation by Stanislav Jabinski, Jenny Wendt, and Xavier Prieto for the acetate measurements. This study is funded by the European Research Council under the European Union's Seventh Framework Programme–"Ideas" Specific Programme, ERC grant agreement No. 247153 (Advanced Grant DARCLIFE; PI: Kai.-Uwe Hinrichs), DFG through the Research Center/Excellence Cluster MARUM-Center for Marine Environmental Sciences (Project GB2) and China Scholarship Council.

3.6 Supplementary materials

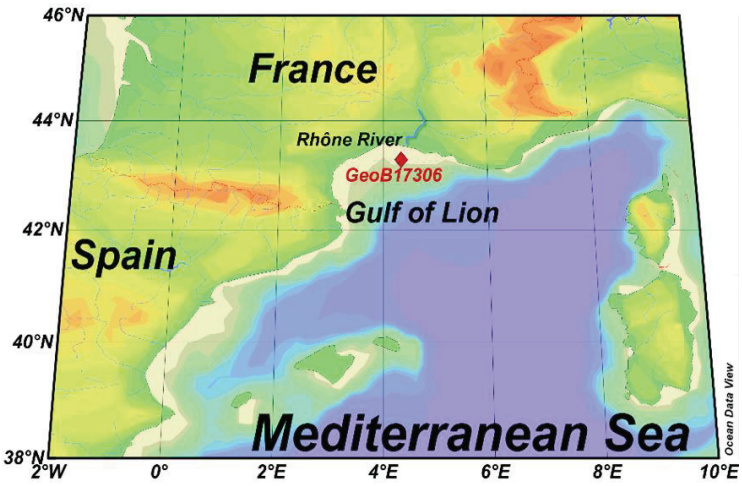

Fig. 3.S1. Location of Site GeoB17306 in the Rhône River Delta, West Mediterranean.

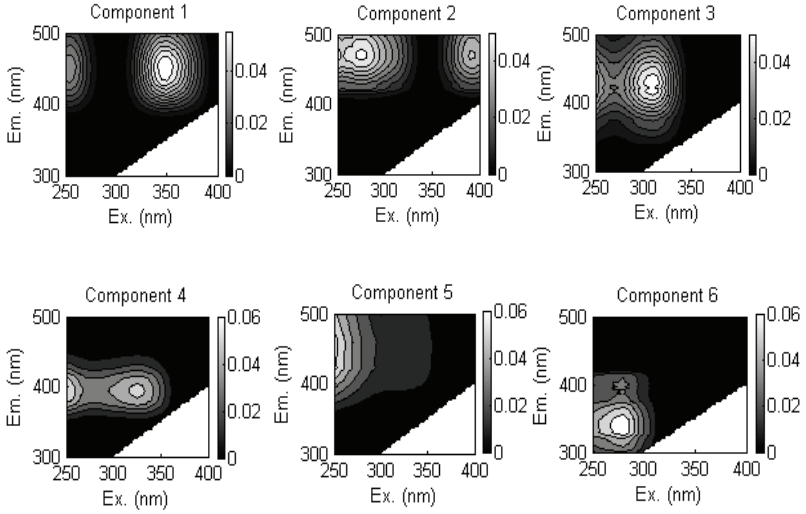

Fig. 3.S2. Six peaks (Component 1 to 6: C1, C2, M1, M2, A, T, respectively) identified by PARAFAC analysis.

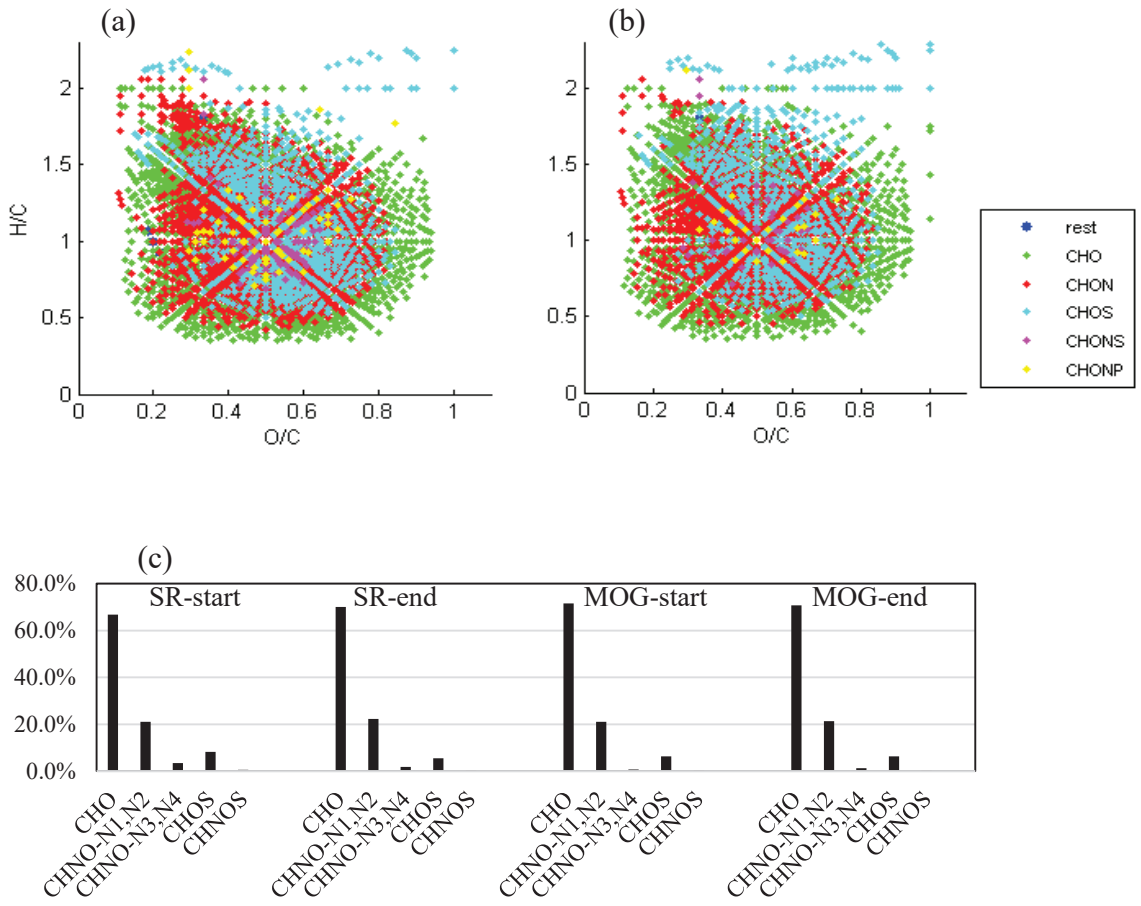

Fig. 3.S3. Composition of DOM characterized by FT-ICR-MS. (a): van Krevelen plot of 'SR' series with sulfate addition at end on 75th day; (b) van Krevelen plot of 'SR→MOG' series at end on 75th day (c) CHO, CHNO, CHOS, CHNOS compounds 'SR' series and SR→MOG' series after methanogens thrived. The percentages were average-weighted. SR: abbreviation for sulfate reducing condition, MOG: abbreviation for methanogenic condition.

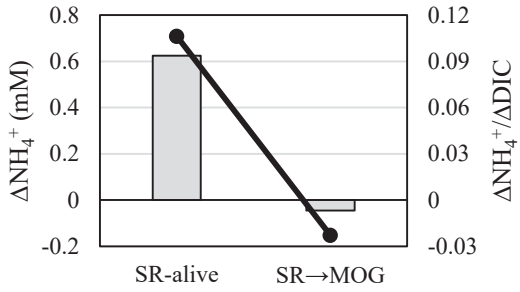

Fig. 3.S4. Variation of ammonia (column) and $\Delta DIC/\Delta NH_4^+$ (dot) during incubation of 'SR' series I and 'SR→MOG' series II from 37-75 days when the system turned into methanogenic condition. ΔDIC = DIC(end)-DIC(start), ΔNH_4^+ = NH_4^+(end)- NH_4^+(start).

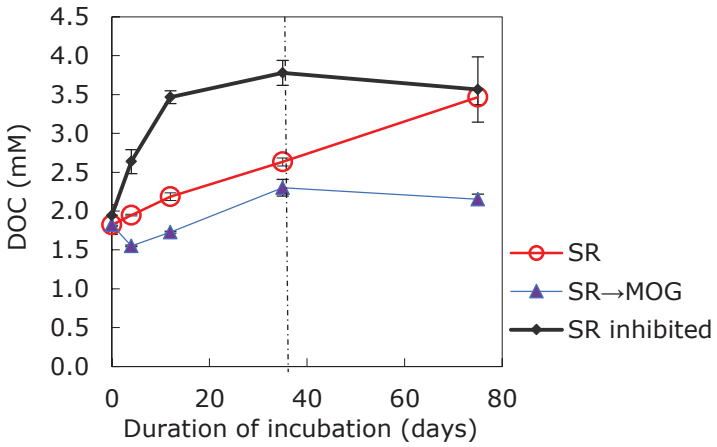

Fig. 3.S5. Variation of DOC during incubation of all the three major series.

Chapter 4 Biotic and abiotic carbon cycling in geothermally heated sediments from the Nankai Trough

Shuchai Gan*, Verena B. Heuer, Frauke Schmidt, Lars P. Wörmer, Rishi R. Adhikari, Kai-Uwe Hinrichs

MARUM – Center for Marine Environmental Sciences & Department of Geosciences, University of Bremen. Leobener Straße, D-28359 Bremen, Germany (*correspondence: sgan@uni-bremen.de)

Abstract

Life strategies in Earth's deep biosphere are largely unknown and possibly informative for understanding early life and the deep carbon cycle. In the deep subseafloor, geothermal heating is an important environmental factor and is associated with the alteration of organic matter and minerals. While autotrophic organisms are thought to benefit from hydrogen producing reactions, it is not clear whether and how heterotrophic organisms in deep sediments are stimulated by heating. This study investigated microbial carbon cycling at mesophillic, thermophilic and hyperthermophilic conditions in the sediments recovered from a high heat-flow area in the Nankai Trough (IODP Site C0012). Experiments were conducted in the temperature range of 20°C to 85°C and consisted of alive, killed and partly inhibited series of incubations for the differentiation of biotic/abiotic and intermediate/terminal processes. Microbial activity, transformation of organics, solid phase and metabolic intermediates were monitored via analysis of hydrogenase enzyme, dissolved organic matter (DOM), Mn and Fe, and volatile fatty acids. DOM was characterized by Excitation Emission Matrix Spectroscopy and Fourier Transform Ion Cyclotron Resonance Mass Spectrometry. With increasing temperature the following changes occurred compared to the control series at 20°C: (a) At mesophilic conditions (35°C), DOM is released due to heating via abiotic process; hydrolysis of biopolymer fragments and fermentation are accelerated and attributed to biotic processes. (b) At thermophilic conditions (55°C), abiotic reactions became more important and humics

are decomposed in both alive and killed controls; hydrolysis of biopolymer fragments is inhibited and accelerated fermentation is attributed to abioticcally-produced precursors. (c) At hyperthermophilic conditions (85°C), breakdown of humics (mainly CHNO with one or two nitrogen atoms) coincided with the limitation of microbial hydrolysis; rapid accumulation of acetate from abiotic decomposition outcompeted microbial fermentation. Our data suggest that aged (7.8 Ma old), macromolecular humic substances are split into both labile and refractory units during heating, and provide the basis for a new conceptual model for humics cracking. The model suggests that the combination of abiotic and biotic processes in DOM degradation is crucial for sustaining the deep biosphere in moderately heated sediments.

Key words: deep biosphere, DOM, humics-decomposition, thermal environment, hydrogenase

4.1 Introduction

Marine sediments are the largest reservoirs of organic Carbon on Earth (Hedges and Keil, 1995). In the anoxic subsurface layer, sediments were long considered as a pool of preserved refractory Carbon (Henrichs and Reeburgh, 1987). In recent decades, however, researchers of the Integrated Ocean Drilling Program (IODP) have revealed that subseafloor sediments harbor over half of all prokaryotic cells on Earth. This community, inhabiting what is known as the marine deep biosphere, has a size of > 10^{29} living cells (Schippers et al., 2005; Kallmeyer et al., 2012; Parkes et al., 2014) and extends to > 2 kmbsf (Roussel et al., 2008; Ciobanu et al., 2014; Inagaki et al., 2015; Inagaki et al., 2016). Studying the survival strategy of the deep biosphere is crucial for understanding the deep carbon cycle.

Biotically, anaerobic degradation of organic matter consists of three steps: hydrolysis by extracellular enzymes, intracellular fermentation and terminal mineralization (e.g., sulfate reduction, methanogenesis) (Middelburg et al., 1993; Muyzer and Stams, 2008). The deep sediment intrinsically faces aged material, leftover after long diagenesis and largely consisting of molecularly-uncharacterized humic substances (Hedges et al., 2000), which is less degradable via the conventional microbial pathway. Moreover, the physical environment in the deep subsurface controls the availability of habitats for life due to decreasing porosity (Parnell and Mcmahon, 2016) and mineral-encapsulated organic matter (Schulten and Schnitzer,

1997)s, which results in steric hindrance for extracellular enzymes. These difficulties suggest the recalcitrant organic matter is hardly utilized via the conventional microbial degradation pathway and point to an unknown mechanism providing available substrates.

Heat-induced stimulation of chemoautotrophic microbes via abiotic hydrogen production has been reported as one of the survival strategies in the deep biosphere (Sleep et al., 2004; Parkes et al., 2011). As for heterotrophic microbes, it is assumed that during heating recalcitrant organic matter might be degraded to feedstock for microbes (Horsfield et al., 2006; Riedinger et al., 2015), e.g., by production of acetate (Wellsbury et al., 1997). However, it is not clear how the heated refractory organic matter in sediments degrades and supplies the carbon needed for deep life. Indirect evidence arises from the well-known 'oil window', i.e. the transformation of organic matter above 50°C due to the thermal transformation of kerogen during millions of years (Vandecasteele, 2008), which suggests that, at the microbial-tolerable range (as high as 120°C, Kashefi and Lovley, 2003), the abiotic decomposition might happen at the same time with biological degradation. It is not known how the abiotic and biotic processes are coupled to each other. This research aims to better understand this coupling, identify the role of abiotic process, and define at which temperature and at which step they trigger or stimulate the biological degradation process.

Sediments in the Nankai Trough, located Southeast of Japan, are exposed to high heat flow at deep layers (Yamano et al., 1984) and are thus an ideal environment for investigating the microbial degradation processes of deep life under different thermal conditions. In a laboratory experiment, four sub-series were incubated at 20°C, 35°C (mesophiles), 55°C (thermophiles) and 85°C (hyperthermophiles). Aiming at the complete degradation path from polymer to end products – hydrolysis, fermentation, and terminal mineralization were investigated. Excitation Emission Matrix Spectroscopy (EEMs) and Fourier Transform Ion Cyclotron Resonance Mass Spectrometry (FT-ICR MS) were used to characterize DOM compounds released during heating and their subsequent transformation. For the turnover of low-molecular-weight compounds, production and consumption of labile intermediates (acetate) was monitored in alive and sulfate-reducer-inhibited series. The abiotic processes were evaluated by dead controls. Based on above, a degradation model under changing thermal conditions is proposed.

4.2 Methods and sampling site

4.2.1 Study sites

Core C0012A-13R2 was collected during cruise IODP 322 in the Nankai Trough (Fig. 4.1). The site (32°45'N / 136°55'E) is located in Shikoku Basin on the subducting Philippine Sea plate. Temperature increased in the deep sediments, the temperature at 530 mbsf is ~62°C. The temperature at the seafloor was estimated to be 2.85°C, with an average thermal gradient of 135°C/km. The sulfate-reduction zone at Site C0012 is at ~250 mbsf (Strasser et al., 2014). A sample from a depth of 159 mbsf was selected for the incubation experiments. The sample originates from a layer of hemipelagic mudstone, with an age of 7.8 Ma, an in-situ concentration of sulfate of ca. 10 mM and a temperature at ~22°C calculated from in-situ profiles (Marcaillou et al., 2012; Torres et al., 2015).

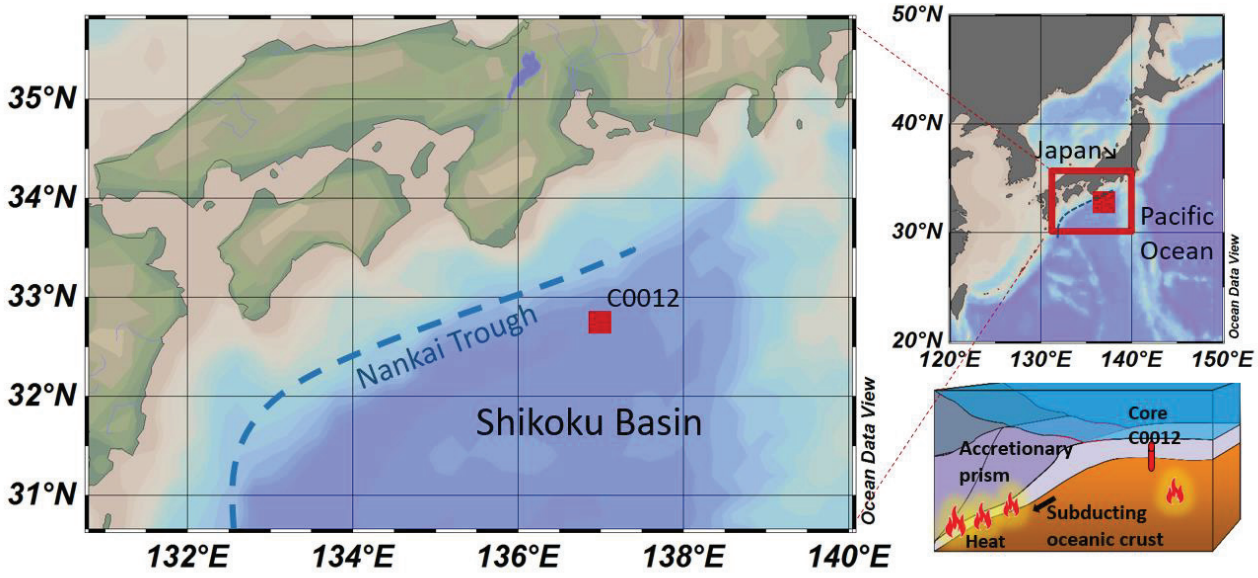

Fig. 4.1. Location of sampling site and tectonic structure in Nankai Trough.

4.2.2 Incubation

For the preparation of sediment slurries, artificial seawater was prepared. The recipe of 1 L artificial seawater with 30 mM sulfate included 0.682 g KCl, 1.5 g $CaCl_2 \cdot 2H_2O$, 5.7 g $MgCl_2 \cdot 6H_2O$, 26.4 g NaCl, 6.8 g $MgSO_4 \cdot 7H_2O$ and 0.099 g KBr. For 1 L artificial seawater without 30 mM sulfate, recipe remains the same except that amount of $MgCl_2 \cdot 6H_2O$ was increased to 11.3 g and $MgSO_4 \cdot 7H_2O$ reduced to 0.682 g. 500 mL of each were mixed to obtain 1 L artificial seawater containing 15 mM sulfate. The artificial seawater was autoclaved at 120°C and flushed with N_2 for 2 hours. Trace elements solution, thiamin solution, vitamin B12 solution and vitamins mixture solution (0.3 mL for each) were added to 1 L artificial seawater. The trace element solution was acidified and contained 0.5 mM H_3BO_3, 0.5 mM $MnCl_2 \cdot 4H_2O$, 0.8 mM $CoCl_2 \cdot 6H_2O$, 0.1 mM $NiCl_2 \cdot 6H_2O$, 0.01 mM $CuCl_2 \cdot 2H_2O$, 0.5 mM $ZnSO_4 \cdot 7H_2O$, 0.15 mM $Na_2MoO_4 \cdot 2H_2O$. The vitamins mixture solution was made according to Widdel and Bak (1992). 1 M $NaHCO_3$ (aq) was sterilized by filtration with 0.1 μm filter (PES, Sartorius) and kept under CO_2. 1 mL $NaHCO_3$ (aq) was added to 1 L artificial seawater. The sediment slurry was prepared in a glovebox under N_2 atmosphere (2% H_2). 0.5 mL of thiosulfate (30 g/L) was added. Sulfide was added to the final concentration of 500 μM. Nutrients were added to final concentration in the slurry of 1 mM ammonium and 0.3 mM phosphate.

Sediment was first mixed with artificial seawater in a sealed sterile plastic bag in a ratio of 4:5 (v:v) and homogenized for 2 hours by continually malaxating the bag. The mixture was then incubated in a 1 L-Schott bottle for the first week under N_2 atmosphere with 2% H_2. The headspace was replaced by pure N_2 after a week and incubated for another week. Two weeks later, after the sediment mudstone was softened, the slurry was homogenized again. Then the slurry was separated into subsamples with a final ratio of 3:1:1 (v:v:v, headspace:medium:sediment) in a glove box. The bottles were sealed with butyl rubber stoppers and the slurry was kept under N_2 at a pressure of two bar for another two weeks at room temperature.

After pre-incubation, slurries were incubated at 20°C, 35°C, 55°C and 85°C. For the heated series, the temperature was gradually increased at an interval of 10°C/hour. The killed series were autoclaved at 120°C twice. Long-time killed controls are not feasible due to the recovery of spores after autoclaving (Tuominen et al., 1994; Berns et al., 2008). Therefore, the trustable data set was shortened to 3 weeks although the incubation of killed controls lasted for 55 days.

In another series ('inhibited'), sulfate reduction was inhibited by the addition of 20 mM molybdate on the 15th day. Before sampling of the first time point, the headspace was flushed again with N_2 for 5 min and kept under two bar N_2. All the series (all in duplicates except the killed series at 20°C and 85°C) and the incubation conditions are listed in Table 4.1. Additional yeast extract (YE) series were incubated under similar conditions as a comparison for biopolymer fragments and monomers as yeast extract shows protein-like peak in EEMs. Two duplicates were added with yeast extract, the other two were added with hydrolyzed yeast extract, for which the YE were hydrolyzed in oxygen-free 4 M NaOH at 85 °C for 16 h under pure N_2.

Table 4.1. Incubation settings. There are two duplicate incubations for each series except the killed series at 20°C and 85°C.

Series No.	Series naming	Temperature of Subseries	Duration (days)
I	Controlled series	20°C	55
II	Alive series	35°C, 55°C, 85°C	55
III	Inhibited series	20°C, 35°C, 55°C, 85°C	55 (molybdate addition on 15th day)
IV	Killed series	20°C, 35°C, 55°C, 85°C	55 (data after 21 days were not interpreted)
V	YE series	35°C, 55°C and 85°C	10

Hydrogen gas concentrations were measured two times a week to monitor incubation. Samples for EEMs were collected at time point 0, 1, 3, 15, 30 and 55 days. The liquid phase was sampled by first transferring it to a glass vial and then separating it into subsamples in a glovebox: a) subsamples for acetate analysis were filtered using nylon filters (0.2 µM, Omni lab); b) subsamples for other analyses (DOM, inorganic ions) were filtered using cellulose acetate filter (0.2 µM, Sartorius AG). Vials were sealed in the glovebox and covered with Parafilm afterwards. Due to the volume limitation of incubated slurry, subsamples for FT-ICR MS analysis were taken only at day 0 and at the end of incubation for alive series at 20-55°C; for alive series at 85°C, samples were taken on day 0, 1, and at the end of incubation. FT-ICR MS samples were stored at +4°C. Before measurements, samples were acidified to pH 2. DOM were extracted with PPL cartridges (Agilent, 3 mL, 200 mg) under N_2 atmosphere (Dittmar et al., 2008) to remove salts. The cartridges were eluted with 1.5 mL methanol (Lichrosove quality, Merck) and the eluents were stored at -20°C for further DOM analysis. Samples for

EEMs and inorganic ions were stored at -20°C. Sediment samples for hydrogenases analysis were stored at -80°C under N_2. For series with YE addition, EEMs samples were taken on day 0 and day 10.

4.2.3 Analytical techniques

4.2.3.1 DOM characterization by EEMs

Samples were measured on a fluorescence spectrophotometer (Agilent Cary Eclipse, USA) after dilution with O_2-free Milli-Q water (NaCl 35g/L). More than 300 samples were modeled by parallel factor analysis (PARAFAC). Five components were identified (Fig. 4.S1) including two protein-like peaks (ex/em: 275 nm/310 nm; 275 nm/350 nm); two humic-like peaks (ex/em in 325(250) nm/400 nm as peak M; ex/em in 360(250) nm/460 nm as peak AC) and one peak also presents in the blank of artificial seawater with addition of vitamin (ex/em: 250(280)/350 nm). We attribute the peak to the fluorescence emitted by the vitamin solution overlapping with a protein-like peak. In the final dataset, the fluorescence signal was corrected by subtracting signal shown in artificial seawater. Wavelength number in parenthesis of ex/em data refers to the peak shown together with the other one. In the figures, humic-like and protein-like peaks were abbreviated as peaks H and peaks P.

4.2.3.2 DOM characterization by FT-ICR MS

Samples were diluted to a DOM concentration of 20 mg C/L in solvent of methanol: water (1:1, v/v). Samples were ionized with electrospray ionization (ESI, Apollo II electrospray source, Bruker Daltonik GmbH, Bremen, Germany) and characterized in negative ion mode on a Bruker SolariX XR FT-ICR MS (Bruker Daltonik GmbH, Bremen, Germany) equipped with a 7 T refrigerated actively shielded superconducting magnet (Bruker Biospin, Wissembourg, France). The mass spectrometer was calibrated with sodium trifluoroacetate (Moini et al., 1998). Samples were injected at rate of 5 µL/min. 200 scans were added for each measurement. Internal calibration resulted in mass accuracy better than 0.1 ppm. Formulae were calculated in the m/z range of 200-650 considering the following elements: ^{1}H, ^{12}C, $^{13}C_{0–1}$, ^{16}O, $^{14}N_{0–4}$, $^{32}S_{0–2}$, $^{34}S_{0–1}$, $^{31}P_{0–2}$. Only formulae in the range of O/C ratio of 0.01-1.2 and H/C ratio of 0.35-2.3 were considered in the calculation process and unrealistic formulae in the DOM samples with N4P2, N2P2, S2P2, O1, O0 were removed from the dataset. During initial processing,

peak magnitude is presented as relative intensity (rInt), which was calculated by normalization to the base peak. Multiple formulae were filtered as described by Koch et al. (2007). Less than five multiple assignments were observed in the final data set. Peaks found in the list of contamination formulae (anthropogenic surfactants listed on http://www.terrabase-Inc.com) or blank sample (rInt > 0.1) were deleted. In the figures, formulae are shown in relative intensity of individual formulae normalized to all the assigned formulae.

CHO formulae contain only C, H, O atoms and CHNO formulae contain C, H, N, O atoms, those formulae with sulfur or phosphorus are included in the group of CHNO in this study. CHNO-N1, N2 and CHNO-N3,N4 represent compounds with one or two nitrogen atoms and three or for nitrogen atoms, respectively.

4.2.3.3 Hydrogen concentration

0.5 mL headspace was taken for H_2 measurement by Peak Performer 1 gas chromatograph (Peak Laboratories, USA) according the method described by Lin et al. (2012). Concentration of H_2 in slurry was calculated according to Crozier and Yamamoto (1974).

4.2.3.4 Acetate concentration

Samples were measured by liquid chromatography-isotope ratio monitoring mass spectrometer (irm- LC/MS) as described by Heuer et al. (2006, 2010). The high performance liquid chromatography (ThermoFinnigan Surveyor HPLC) is combined with an LC IsoLink interface (Therm Finnigan) for chemical oxidation of the effluents and subsequently a DELTA Plus XP mass spectrometer (ThermoFinnigan) for detection of oxidized product – CO_2. The detection limit for quantitative analysis of acetate is 5 μM.

For series at 55°C and 85°C, biotic and abiotic productions of acetate were calculated from alive, inhibited and killed series. (1) Abiotic production of acetate was calculated from killed series:

$$A_{\text{abiotic production}} = A_{15\text{days}} - A_{0\text{day}} \quad \text{Eq. 4.1}$$

For the abiotic production of acetate after 15 day, data were calculated from incubation from 0 to 15 days. (2) Total production of acetate:

$$A_{\text{total production}} = A_{\text{net production}} + A_{\text{biotic consumption}} \quad \text{Eq. 4.2}$$

$A_{\text{net production}}$ calculated from the accumulation of acetate in alive series. (3) Biotic production of acetate:

$$A_{\text{biotic production}} = A_{\text{Total production}} - A_{\text{abiotic production}}. \quad \text{Eq. 4.3}$$

A in the equation is abbreviation of acetate. (4) Biotic consumption (minimum) is calculated from the difference between sulfate reducer inhibited and alive series; the biotic consumption (minimum) refers to only the consumption by sulfate reducer.

4.2.3.5 Ammonium, sulfate, manganese, iron concentration

Concentration of NH_4^+ and sulfate was determined by photometry (Quick Chem 8500, Lachat) and ion chromatography (882 Compact IC plus, Metrohm), respectively. Since no zinc is added to fixing the S^{2-}, the concentration of sulfate included the reduced sulfur oxidized to sulfate during storage and refer to the total dissolved sulfur. Fe and Mn ions were detected by Inductively Coupled Plasma Optical Emission Spectrometer (ICP-OES) (Vista Pro CCD-simultaneous, Agilent).

4.2.3.6 Hydrogen oxidation potential

After the incubation experiment ended, the incubation vials were stored at -80°C. The sediment slurry was later incubated with radiolabeled hydrogen gas to investigate the potential activity of hydrogenase enzymes. Hydrogenase enzymes are ubiquitous in subsurface microorganism, exclusively intracellular and catalyze hydrogen metabolism. Duplicate sediment samples were incubated under tritium gas. Over time, hydrogenase enzyme catalyzed isotope reaction between tritium gas and water molecule, which produced tritiated water. The radioactivity of tritiated water was measured by liquid scintillation counter (PerkinElmer Tricarb 2810TR®). The more details of the method is described elsewhere (Soffientino et al., 2009; Adhikari et al., 2016).

4.3 Results

4.3.1 Background information of microbial activity: ongoing terminal process and inhibition of terminal step

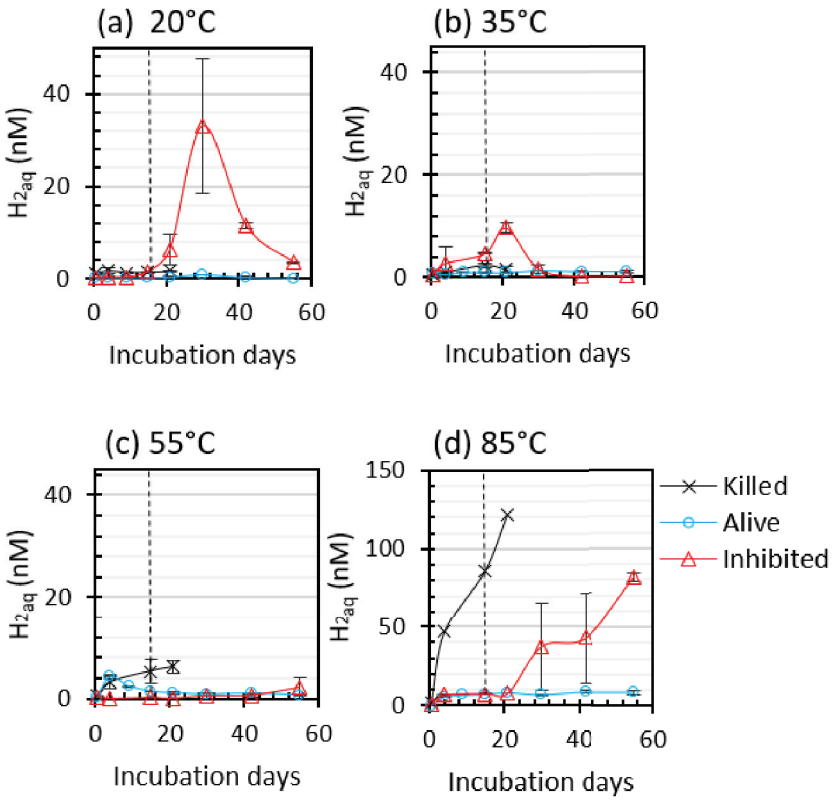

Fig. 4.2. Concentration of H_2 during incubations: (a) series at 20°C; (b) series at 35°C; (c) series at 55°C; (d) series at 85°C. In the inhibited series sulfate reducers were inhibited by molybdate addition at day 15. The killed series was monitored for 55 days, data after 21 days were not shown here as microbes recovered in the final phase of incubation. Vertical dashed line shows the timepoint of molybdate addition. Note that the scale of y-axis in figure (d) differs from the others.

Radiotracer based hydrogenase enzyme assay showed H_2 turnover (> 10^{-7} mol $g^{-1}day^{-1}$) in all alive series (Fig. 4.S2). At 20°C, the concentration of H_2 was low and remains constant in the alive series. Inhibition of sulfate reducers led to a dramatic decrease of hydrogenase activity and an accumulation of H_2 that peaked shortly after molybdate addition clearly pointing to the relevance of sulfate reduction on H_2 metabolism (Fig. 4.2a, S2). Series at 35°C were featured by high hydrogenase activity, low and balanced concentration of H_2 and a weaker effect of sulfate reducer inhibition on H_2 metabolism compared to the series at 20°C (Fig. 4.2b, S2). At

55°C, heat induces instant H_2 accumulation, which was quickly consumed after 3 days in the alive series; the inhibited series showed a decrease of hydrogenase and an increase of H_2 concentration at the end (Fig. 4.2c, S2). At 85°C, H_2 concentration was high in all subseries; the killed control showed a contribution of H_2 from abiotic process (>10 times higher than that in the series at 20-55°C), which was consumed and balanced by microbes in the alive series. Compared to alive series, the inhibited series showed higher accumulation of H_2 after 15 days after molybdate addition due to the lagged inhibition of sulfate reducer (Fig. 4.2d, S2). Interestingly, H_2 concentration in the inhibited series at 20°C and 35°C decreased after their maxima; at 55°C and 85°C it kept increasing.

4.3.2 Initial step of thermal alteration of organic matter characterized by DOM

4.3.2.1 Quantitative changes of DOM

Peak C results from large molecules with aromatic functional groups and conjugated systems typically found in terrestrial DOM (Coble, 1996; Fellman et al., 2010; Ishii and Boyer, 2012); peak M is related to compounds that are less aromatic, and is commonly referred to as autochthonous, microbial or marine material with relatively lower molecular weight (Coble, 1996; Fellman et al., 2010; Ishii and Boyer, 2012). Peak A is thought to result from aromatic fulvic acids that are common in natural aquatic systems (Stedmon and Markager, 2005a).

Heating resulted in immediate accumulation of humic-like peaks (CA and M) after overnight balance on the first day, which is linearly correlated with temperature ($R^2 = 0.97$) in alive series (Fig. 4.3a). Killed controls similarly confirm the linear response of humic-like peaks with temperature (Fig. 4.3b). Thus, the release of humic-like DOM seems to be modulated by abiotic process and increased by temperature instead of hydrolysis via hydrolase.

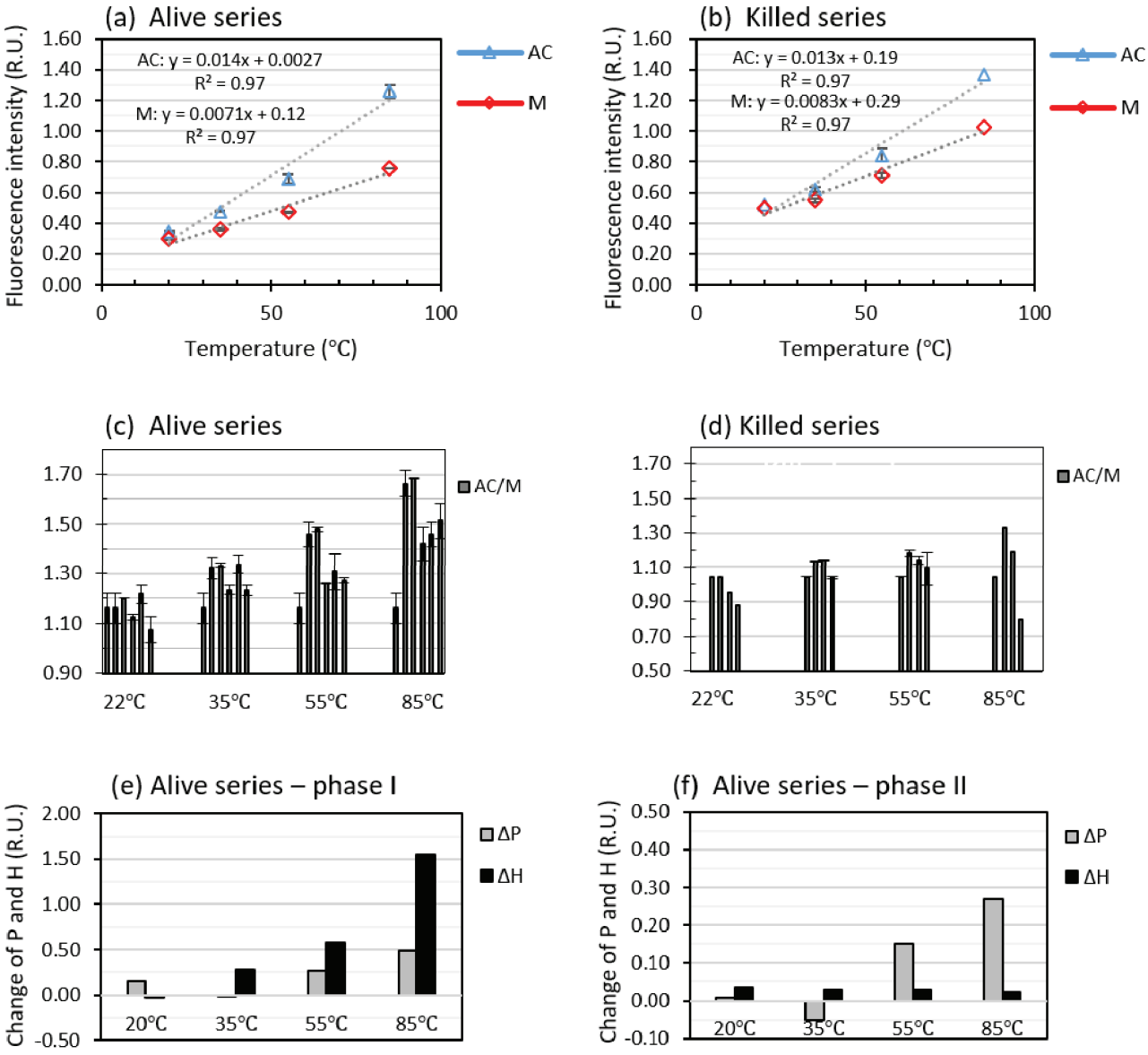

Fig. 4.3. Quantification and qualification of DOM by EEMs during incubations. (a) Concentration of humic-like DOM increases linearly with temperature after overnight incubation in the alive series; (b) Concentration of humic-like DOM increases linearly with temperature after overnight incubation in the killed series; (c) Composition change of humic-like DOM during incubation in the alive series; for each series, the individual bars correspond to day 0,1,3,15,30,55 from left to right; (d) Composition change of humic-like DOM during incubation in the killed series; for each series, the individual bars correspond to day 0,1,3,15 from left to right; (e) Change of humic-like DOM and protein-like DOM during incubation phase I (0-3 days) of the alive series; (f) Change of humic-like DOM and protein-like DOM during incubation phase II (3-15 days) of the alive series. $\Delta P = P_{end}-P_{start,}$ and $\Delta H = H_{end}-H_{start.}$. P and H are abbreviation of protein-like and humic-like peaks, respectively.

4.3.2.2 Qualitative changes of DOM

(a) Characterization of DOM by EEMs

Humic-like peak M, which implies smaller molecule, is less effectively retained in the extracted DOM compared to humic-like peak AC, thus AC/M ratio can be used to identify a blue-shift of the fluorescent signal of organic compounds. Such a shift is produced by the loss of conjugation structures, which might be auxochrome or aromatic ring. AC/M increased slightly in the alive series at 35°C compared to 20°C; The AC peak was relatively enriched compared to M peak during the initial stages of incubation in the alive series at 55°C and 85°C, resulting in an increased AC/M ratio (Fig. 4.3c). This effect was more pronounced at higher incubation temperatures. After 3 days, this trend was inverted, and a relative depletion of the AC *vs.* the M peak was observed (Fig. 4.3c). Simultaneously, the protein-like peaks increased more than humic-like peaks at 55°C and 85°C (Fig. 4.3). Besides, it is noticed that AC/M is lower in the killed series from the starting time point and decreased faster afterwards probably due to being heated during autoclaving at 120°C before incubation. Based on these observations we divided the incubations into two phases: Phase I includes 0-1 days and Phase II includes 3-55 days (1-55 days for FT-ICR MS). Phase I was dominated by the process of quantitative accumulation of mainly humic-like DOM. Phase II was characterized by breakdown of humic substances and production of humic fragments and protein-like DOM.

The protein-like peaks (P) were balanced and lowest at 35°C without accumulation in phase I and II (Fig. 4.3e, f). At 55°C and 85°C, protein-like peaks increased strongly during phase II (Fig. 4.3e, f). For further confirmation of the turnover of protein-like compounds, the YE series amended with yeast extract and hydrolyzed yeast extract showed similar consumption of protein-like peaks during incubations in 10 days at 35°C. As a comparison, consumption of protein-like DOM in YE hydrolyzed series is higher than that in YE series at 55°C and 85°C (Fig. 4.S5).

(b) Characterization of DOM by FT-ICR MS

Data from FT-ICR MS analysis revealed that the DOM before incubation is featured by a high H/C_{wa} ratio (1.5) and a low O/C_{wa} ratio (0.38) (Table 4.2), as well as 40% nitrogen-containing formulae (dominated by CHNO-N1, N2), which result in an N/C_{wa} ratio of 0.026

(Table 4.2). There are scarce formulae in the region of high O/C in the Van Krevelen diagram (Fig. 4.4). Our data also show that after 55 days of incubation samples from alive series at 20°C-55°C show a relatively similar profile, without major differences in molecular formula composition (Table 4.2).

Table 4.2. Intensity-weighted averages ('wa' in subscript) of characteristic parameters derived from FT-ICR-MS analysis. Formulae with ^{13}C or ^{34}S were not included.

Sample	mz_{wa}	C_{wa}	H_{wa}	O_{wa}	N_{wa}	S_{wa}	P_{wa}	DBE-O_{wa}	H/C_{wa}	O/C_{wa}
20°C, start	378.2	18.7	27.6	6.79	0.43	0.36	0.03	-0.69	1.51	0.38
20°C, start	388.4	19.2	28.5	6.79	0.56	0.36	0.07	-0.46	1.51	0.38
35°C, end	404.3	20.2	28.7	7.36	0.54	0.26	0.03	-0.23	1.44	0.38
55°C, end	397.4	19.9	28.3	7.03	0.57	0.28	0.06	0.02	1.44	0.37
85°C, 1 day	444.3	22.3	37.5	6.96	1.21	0.30	0.06	-1.75	1.68	0.33
85°C, end	413.1	20.8	31.2	6.92	0.89	0.27	0.06	-0.26	1.50	0.35

The alive series at 85°C was investigated with more details by FT-ICR MS, adding data points on 1 day. In phase I (1 day), there was release of larger DOM resulting in the increase of carbon number from 19.0 to 22.3 and m/z_{wa} from 383 to 444 (Table 4.2). The freshly released DOM was more saturated and less oxygenated (Fig. 4.4c). The increased N/C_{wa} ratio was attributed to accumulation of CHNO-N1, N2 in higher molecular weight (Fig. 4.4a). Most of the formulae with increased signal intensity were located in the peptide-like region in the van Krevelen diagram according to their H/C_{wa} and O/C_{wa} ratios. At phase II, CHNO-N1, N2 formulae decreased and CHO compounds in the lower molecular weight range accumulated (Fig. 4.4b).

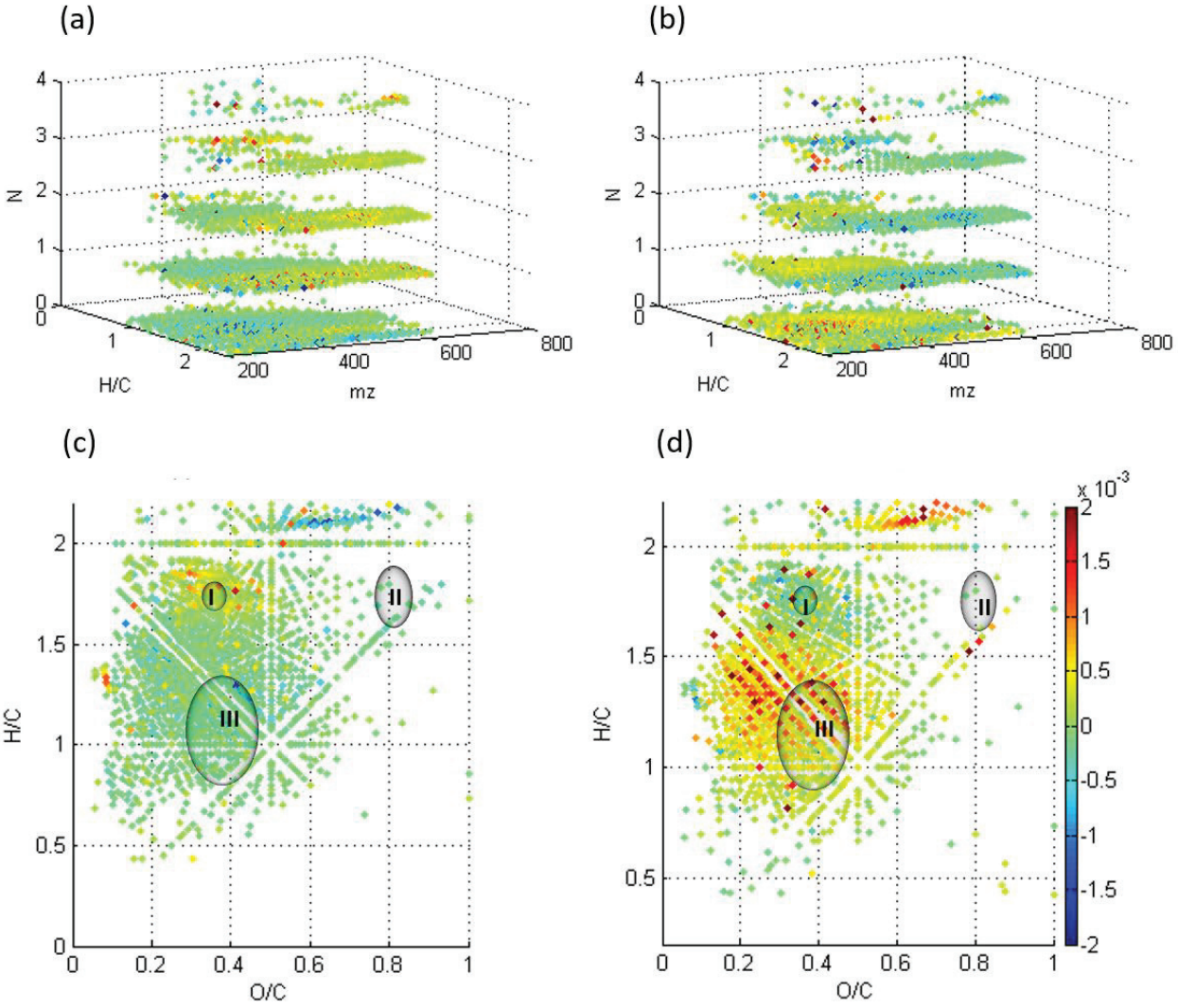

Fig. 4.4. DOM characterized by FT-ICR MS during incubations of alive series at 85°C. (a) Change of formulae during phase I, z-axis shows the number of nitrogen atoms in formulae; (b) Change of formulae during phase II, z axis shows the number of nitrogen atoms in formulae; (c) Change of formulae shown in a Van Krevelen Diagram during phase I; (d) Change of formulae shown in a Van Krevelen Diagram during phase II. Color scale shows changes in normalized intensity of individual formulae during incubation. Positive values and negative values represent increased and decreased normalized intensity of formulae, respectively. The three circles in the Van Krevelen Diagram represent for the potential range of biomolecular components: protein (I), lignin (II) and cellulose (III) (Kim et al., 2003), which are only based on elemental compositions, geopolymer mixtures of biomolecular fragments might locate in these regions

4.3.3 Intermediate and terminal step: turnover of labile intermediates

Acetate consumed by terminal mineralizer (sulfate reducers) was calculated from the loss of acetate in the alive series and accumulation of acetate in the inhibited series (method of

calculation: see also 2.3.4). Abiotic production rate of acetate is based on data from 0-15 days and assumed to be constant during incubation. Biotic consumption by sulfate reducer was determined using the data from 30-55 days when sulfate reducers were inhibited because hydrogen concentration in the inhibited series suggested the inhibition effect worked after 30 days at 55°C and 85°C, which is 15 days later than series at 20°C and 35°C. The apparent biotic consumption by sulfate reducer is assumed to be constant during incubation with enough acetate at 55°C and 85°C.

At 20°C and 35°C, acetate decreased continuously in the alive series due to faster consumption than production; biotic consumption (15-55 days) by sulfate reducer corresponds to 583 μM and 257 μM, respectively (Fig. 4.S3). For series at 20°C and 35°C, there were no comparisons of abiotic and biotic production in Fig. 4.6 as the abiotic decomposition process is negligible.

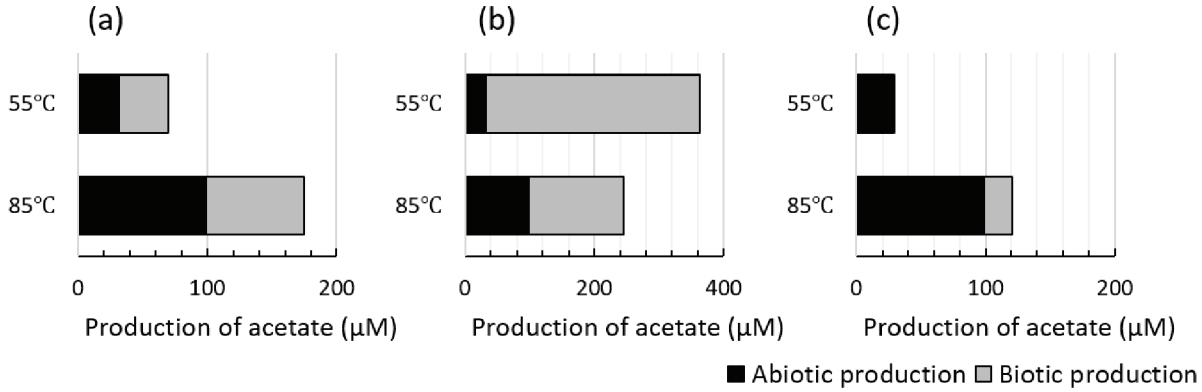

Fig. 4.5. Production and consumption and acetate during incubation: (a) biotic and abiotic production of acetate calculated from alive series, killed series, and inhibited series during 0-15 days; (b) biotic and abiotic production of acetate calculated from alive series, killed series, and inhibited series during 15-30 days; (c) biotic and abiotic production of acetate calculated from alive series, killed series, and inhibited series during 30-55 days. Total production (minimum) = accumulation + biotic consumption(minimum); Abiotic production: production in killed series; Biotic production = Total production - abiotic production; biotic consumption(minimum) is calculated from the difference between sulfate reducers inhibited and alive series.

At 55°C, alive series showed a fast net accumulation of acetate (258 μM) from 15 days to 30 days, and afterward a fast decrease of 113 μM due to biotic consumption (Fig. 4.S3). A portion of the acetate derived from abiotic process (Fig. 4.5), however, it was not enough to support the biotic consumption proved by the decrease of acetate after 30 days. Biotic production contributed most to total acetate production, especially during 15-30 days.

At 85°C, there was continuous net accumulation of acetate from the start in the alive series, which became slower after 30 days; the biotic consumption by sulfate reducer was 237 µM during 30-55 days; the killed series showed a fast production of acetate from abiotic process within 15 days at 85°C, which contributed apparently more than half of the total acetate production during 0-15 days and 30-55 days (Fig. 4.5).

4.3.4 Inorganic ions released from solid phase to dissolved phase

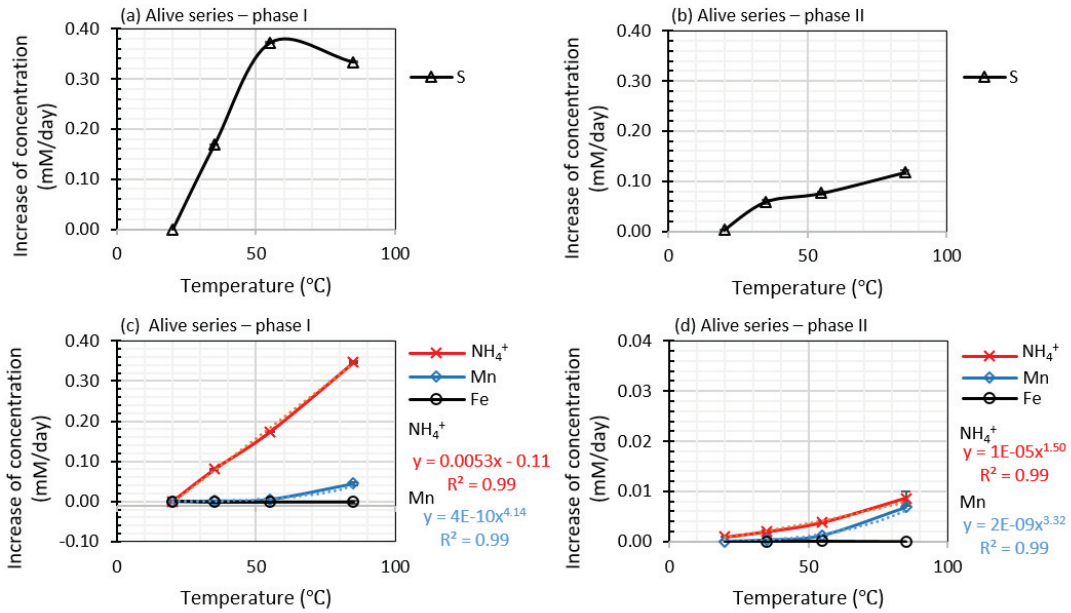

Fig. 4.6. Release of inorganic ions from solid phase during incubation: (a) total dissolved S production in pore water in phase I; (b) total dissolved S production in pore water in phase II; (c) ammonia Fe, Mn, production in pore water in phase I; (d) ammonia, Fe, Mn, production in pore water in phase II. Y-axis in (d) is ten times smaller than the others. The error bars are invisible due to their smaller size than the symbols.

During incubation, the concentration and production of iron remained low (Fig. 4.6c,d). The increase of ammonia, total dissolved sulfur and Mn started already at low temperature (Fig. 4.6). At 35°C, the overnight (phase I) increase in humic-like peaks described above takes place simultaneously with increasing concentrations of total sulfur (170 µM), ammonia (83 µM) and Mn (1 µM) (Fig. 4.6a,c). Similar to humic-like compounds, the ammonia production is linearly correlated with temperature (R^2 = 0.99), while production of total dissolved Mn shows an exponential increase with temperature (R^2 = 0.99). In phase II, concurrent with humics-

decomposition, there was slower release of ammonia, sulfur and Mn. Both the ammonia and Mn increase correlates exponentially with temperature ($R^2 = 0.99$) (Fig. 4.6b,d).

4.4 Discussion

4.4.1 Proposed degradation path of humic substances

4.4.1.1 Variations in degradation with increasing temperature

As the conventional anaerobic degradation is considered to consist of mainly three steps, the mechanisms involved at each temperature will be discussed in this same order: from the initial step of hydrolysis, to the intermediate step of fermentation and the terminal step of mineralization (e.g. sulfate reduction).

(a) Series at 35°C

At mesophilic conditions (35°C), in the initial step, the increased humic-like pool could not contribute to the labile substrates via self-decomposition: slightly varied AC/M ratio in alive series (Fig. 4.3) suggested the released humic substances were not transformed, and there is no observable breakdown of humics due to abiotic heating confirmed by the killed series. This implies that humic substances as geopolymers tend to be refractory at 35°C. Both FT-ICR MS and EEMs suggest only small changes in the dissolved organic pool during incubation (Fig. 4.3, Fig. 4.4). Considering the fast mineralization in series incubated at 35°C indicated by acetate (Fig. 4.S3), the consistent composition of the dissolved phase might result from an equilibrated balance between production and consumption of labile substrates. The killed series indicated geopolymers represented by humics were not abiotically transformed. Instead of abiotic thermal decomposition, hydrolysis by extracellular enzyme would produce monomers that could be accessible for fermenters at 35°C. Protein-like compounds were released together with humic-like DOM and thereafter protein fraction, which is encapsulated and protected in refractory compounds (Knicker and Hatcher, 1997; Zang et al., 2000), were exposed to enzyme. Thus, the release of humics to the liquid phase facilitates enzymatic cleavage of co-released biopolymers. As there is no evidence of abiotic production of acetate and H_2 due to heating at 35°C, both intermediates should be biotically produced via fermentation.

(b) Series at 55°C

At thermophilic conditions (55°C), in the initial step, humic-like compounds were rapidly released and afterwards decomposed abiotically from day 3 to day 15 (Fig. 4.3). After the decomposition of humic-like compounds during 3-15 days, the high production of acetate in the alive series and low abiotic production implies that acetate is mainly produced by fermentation (Fig. 4.5, S3). At this point, it is not clear what the precursors of acetate or H_2 are, nevertheless, monomers should be available for fermentation. In sum, although the contribution of abiotic process to acetate production is low under thermophilic condition (Fig. 4.5), we suggest that the abiotic process has contributed largely in the initial steps and facilitated the presence of assimilable DOM as precursor for fermentation.

A further question is to which extent the biological hydrolysis contributes to the initial step at 55°C, to be more specific, whether biological hydrolysis is efficiently supporting fermentation at 55°C or not. For this question, there is no direct evidence in this study. Former studies suggested production of acetate benefits from increasing hydrolysis at 55/50°C. Glucosidase and protease were suggested to be active at 55°C (Hao and Wang, 2015). Consistently, an additional incubation with young surface sediment (North Sea) showed ratio of protein-like peaks to humic-like peaks increase most sharply before day 3 at 55°C (Fig. 4.S4). This trend did not continue after three days. This can however be explained by the lagged denaturation of enzyme, its half-life period might take 16.7-44.9 hours at 55°C (Abdel-Naby et al., 2017), which means the hydrolase might work in the first few hours or days resulting the increase of protein-like peaks. Whereas, opposite phenomenon was observed in this study of Nankai Trough. There was more production of humic-like peaks resulting in lower ratio of protein-like peaks to humic-like peaks before day 3 (Fig. 4.S4). Assumed that the biological hydrolysis is ongoing and a main contributor of producing precursors for fermentation, the highest acetate accumulation would be expected during the first hours or days, before denaturation of enzymes as shown in former incubations (Hubert et al., 2009; Hubert et al., 2010; Hao and Wang, 2015). However, acetate increased only after 15 days after the decomposition of humic-like compounds happened. Since the hydrolyzed monomers is more favorable suggested by the comparison of YE and YE hydrolyzed series (Fig. 4.S5), the monomers (e.g. amino acid) tend to be from decomposition of humic-like compounds via abiotic process rather than the biotic hydrolysis. In summary, the delayed accumulation of

acetate (during days 15-30 instead of at start) after the decomposition of humic-like compounds suggests that, the biological hydrolysis is not efficiently supporting fermentation at 55°C.

(c) Series at 85°C

At hyperthermophilic conditions (85°C), in the initial steps, enzymatic hydrolysis producing monomers is considered to be less important due to the following reasons: (1) this process is already inhibited when temperature increase from 35°C to 55°C; consequently, the inhibition of hydrolase due to heating should be more at 85°C; (2) although the optimum hydrolysis rate might be shifted according to the different type of organic matter (Arnosti and Jørgensen, 2003) or source of microbes (Arnosti, 1998), the enzyme is expected to be very quickly denatured above 55-65°C (Colussi et al., 2012); (3) there the protein-like peak in the YE series did not decrease indicating protein-like DOM was not consumed.

The next question is whether the low molecular intermediates were mainly originated from abiotic or biotic processes (fermentation). Our results, shown in Fig. 4.5, suggested that acetate is mainly produced from abiotic processes (Fig. 4.5). Since the abiotic production of acetate is larger than the acetate consumed by sulfate reducers, within 15 days, the acetate from thermal decomposition would be sufficient to fuel sulfate reduction in this sediment. Therefore, biotic hydrolysis and fermentation were less important, as electron donors were generated during abiotic decomposition of macromolecular humics; acetate in terminal mineralization was mainly produced from abiotic processes and afterwards utilized biotically.

Based on above, variations of the degradation mechanisms with increasing temperature are summarized in Fig. 4.7.

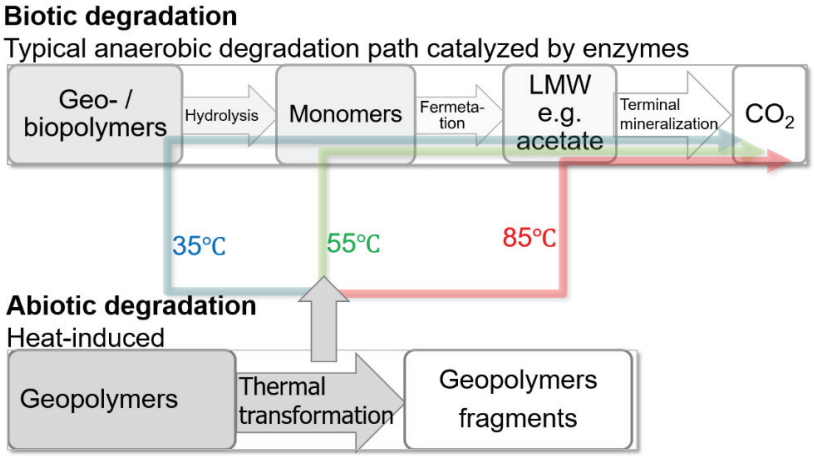

Fig. 4.7. Degradation path of organic matter at 35°C, 55°C and 85°C including biotic and abiotic processes. At 85°C, abiotic process contribute to the pool of acetate and thereby to terminal steps; at 55°C, the abiotic decomposition of humics could provide assimilable fragments that could contribute to the monomer precursors for fermentation; at 35°C, abiotic process barely contributed to humics decomposition but accelerate the release of organic fragments to the liquid phase.

4.4.1.2 Intrinsic mechanism of humics-decomposition

Humic substances are geopolymers in dynamic association with recognizable biomolecular fragments of low molecular mass components including aliphatic and aromatic fractions (Stevenson, 1994; Leenheer and Rostad, 2004; Sutton and Sposito, 2005); the associations being stabilized by hydrogen bonds or through attachment to the solid phase (Schulten and Schnitzer, 1995; Schulten and Leinweber, 2000).

Release of humics fragments and further decomposition of these fragments can be attributed to different chemical bond cracking processes. In phase I, the breakdown of weak bonds, e.g., ionic bonds and hydrogen bonds, result in the exposure and stretch of capsuled sedimentary organic matter and the release of ammonia and metal ions from metallic oxides and sulfides. Consistently, total dissolved Mn and sulfur increased by 0.044 mM and 0.33 mM overnight after incubation at 85°C (Fig. 4.6). Even after a small temperature increase from 20°C to 35°C, concentrations of dissolved metal ions increased. Similarly, ammonia increased after overnight incubation and was linear correlated with temperature, pointing to an abiotic process (Fig. 4.6). Chemically, the major limit of deep life is attributed to scarce labile substrates, especially for the deep and aged sediments having underwent long-term diagenesis with abundant molecularly uncharacterized geopolymers (Wakeham et al., 1997). Moreover, the labile

monomers are encapsulated in the solid phase (Knicker and Hatcher, 1997). Thus, chemically the cracking of ionic bonds or hydrogen bonds contributes to the exposure of substrates to further degradation.

In phase II, especially at temperatures of 55°C and 85°C, the production rate of dissolved Mn and ammonia is slower than in phase I (Fig. 4.6), suggesting the breakdown of weak bond breakdown was less important than in phase I. AC/M ratio was decreased. This suggests that the conjugation structure of humic-like compounds was reduced and humic substances were decomposed at increased temperature. The consistent pattern of AC and M peak in killed series after heating, i.e. increase during the initial stage followed by decrease from day 3 on, suggests that the decomposition of humics was a result of abiotic processes instead of hydrolase. The decomposition of humics in this phase is mainly attributed to the loss of conjugation structures and the chemical bonds in the organic matter (covalent bond). Although humic substances are considered as complex molecules, they are composed of mainly C-H, C-C, C = C, C-O, C = O, C-N bonds (Stevenson, 1994; Schulten and Schnitzer, 1995; Chefetz et al., 2002). In phase II, the decrease of larger aliphatic CHNO-N1,N2 compounds suggested formation of small aliphatic compounds in series at 85°C (Fig. 4.4). The decomposition of CHNO should not be attributed to peptide bond as C-N in peptides is thermally stable and only cleavable by strong acid, base or proteolytic enzymes. Moreover, CHNO-N1,N2 at m/z 200-650 in this study, which is located in the region of aliphatics, should not be identified as peptides, but rather as semi-degraded peptides attached to other refractory CHO fractions (Schmidt et al., 2011; Schmidt et al., 2014), via deamination (Abdulla et al., 2017) or incorporation of N (Amrani et al., 2007). The bond energy of C-N is lower than C-O and followed by C-C (Gray, 1965). The former more tends to be cracked, although the adjacent functional group and the reaction product might affect the tendency of cracking.

Based on above, variations of the decomposition mechanisms of humics are summarized in Fig. 4.8.

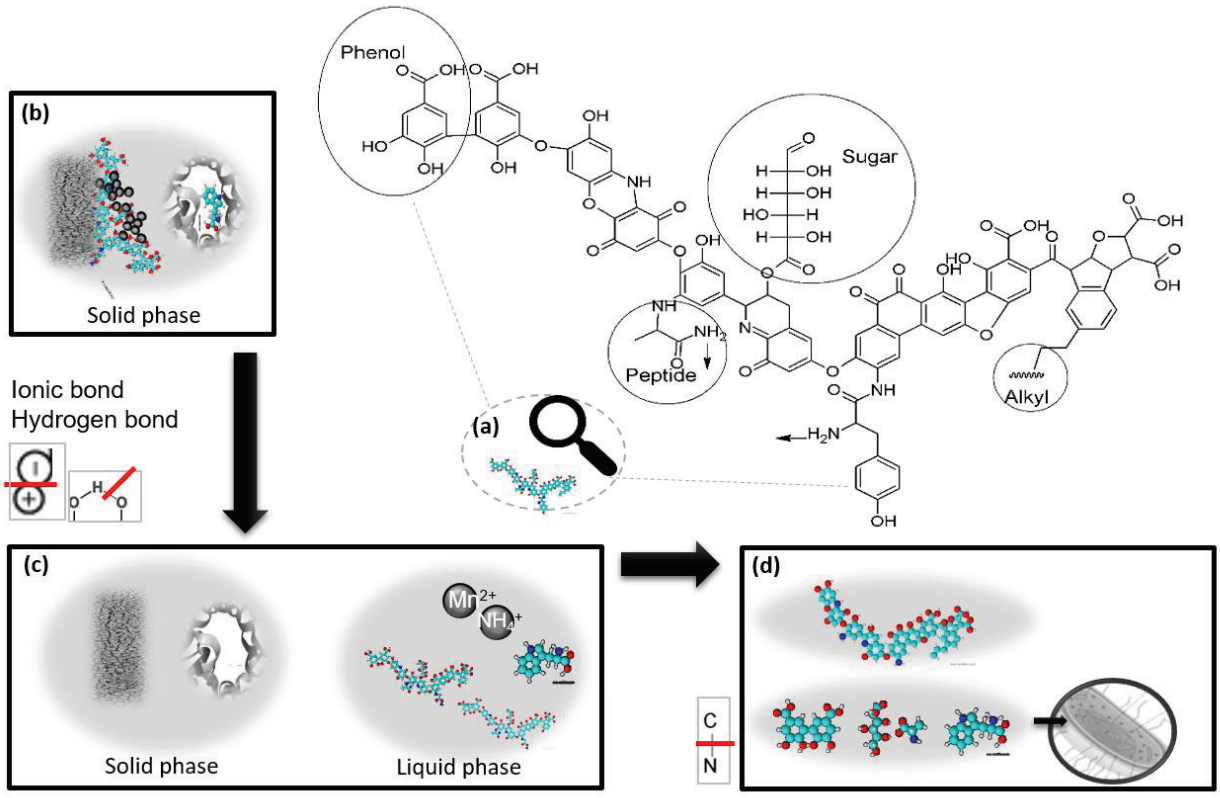

Fig. 4.8. A proposed model for abiotic decomposition of humic substances due to heating. (a) Model of humic substance, adapted from Stevenson's model and new insights from Leenheer and Rostad (2004); (b) humic substances attached to minerals and labile compounds trapped in humic substances in solid phase; Humic substances adsorbed on solid phase minerals contribute to the formation of hydrogen bonds between clay minerals and ammonia (Zhang et al., 2013); (c) humic substances were detached from solid phase and labile compounds trapped in humic substances were released; (d) large humic substances were decomposed due to heating, during the decomposition the small monomers were produced and assimilated by microbes.

4.4.2 Implication for carbon flow and microbial survival in thermal deep earth

Although the percentage of abiotic acetate production within 15 days is small (0.06 wt.% of TOC), it could represent a huge carbon flow and 'feast' for deep life considering the huge pool of 15000000 Gt sedimentary organic carbon (Hedges and Keil, 1995). This mechanism is of less importance at the surface, where the biotic fermentation of fresh materials more efficiently produces the substrates. Wellsbury et al. (1997) showed that acetate production in alive series from deep sediment at 690 mbsf is substantially lower than in surface sediment at either 30°C or 55°C. This study suggests that heat induced an accelerated shunt of carbon into two pools:

one is favorable for microbes, while the other one is a more refractory reservoir for long preservation of carbon. FT-ICR MS analyses suggested that the residual refractory DOM consisted of smaller and aromatic compounds (Fig. 4.4), whereas the labile compounds consisted of aliphatic fragments of CHNO-N1,N2 compounds. The higher the temperature is, the more assimilable and smaller substrates are produced from abiotic processes.

According to our data, the abiotic decomposition at temperatures below the upper limit of life might play a crucial role in sustaining life in deep biosphere. Our study showed that the biotic degradation chain becomes shorter at higher temperatures. This suggests that due to the assistance of heating in abiotic hydrolysis and intermediate production, some microbial communities including hydrolyzers and fermenters are not as necessary as initially expected or might play a lesser role in the deep biosphere. Terminal mineralizers, e.g., acetate and hydrogen utilizers would benefit from the thermal environment. Accordingly, microbial community structures should change. Consistently, the shift of microbial community and metabolic preference with temperature has been reported in former studies of terminal mineralization processes (Roussel et al., 2015).

4.5 Conclusions and outlook

Organic matter in sediments is stabilized by intrinsic recalcitrance of organic compounds, spatial inaccessibility and interaction with minerals (Lützow et al., 2006). According to our study, heating processes released the metal ions and organic matter leading to increased accessibility of polymers or free monomers; in further, the aged macromolecules can be decomposed and produce labile substrates available for microbial life.

We identified the contribution of biotic and abiotic processes in three steps. With increasing temperature, the humic-like DOM became more decomposed and smaller labile substrates were produced, whereas biotic degradation became less important. (1) At 35°C, abiotic processes could barely produce acetate or other assimilable fragments from heat-induced decomposition. Heating resulted in the fast release of weakly bonded macromolecules from the solid phase, including detachments of biopolymer fragments, which are most efficiently used and balanced by microbes. (2) At 55°C, biological hydrolysis could not efficiently support fermentation, while the abiotic decomposition of humics provided assimilable fragments as precursors for

fermentation; afterwards, biotic processes continued via fast fermentation; (3) At 85°C, abiotic processes contributed to microbial life by providing macromolecules (mainly CHNO-N1,N2) which were decomposed to smaller molecules, while the biotic fermentation was minor. The excess abiotic production of acetate suggests that a simpler primitive life with a lower energy cost and simpler carbon metabolism is possible in thermal environments with less necessity of fermentation and hydrolysis by hydrolase.

Acknowledgements

We appreciate the assistance from Jenny Wendt, Xavier Prieto during measurements of acetate. We are grateful to Silvana Pape and Matthias Zabel for measuring ammonia, iron, and manganese in pore water samples. We thank the captains, crew, and the scientific shipboard party for taking sediment during IODP Expedition 322. Funding was provided by the Deutsche Forschungsgemeinschaft (DFG) and China Scholarship Council (CSC).

4.6 Supplementary materials

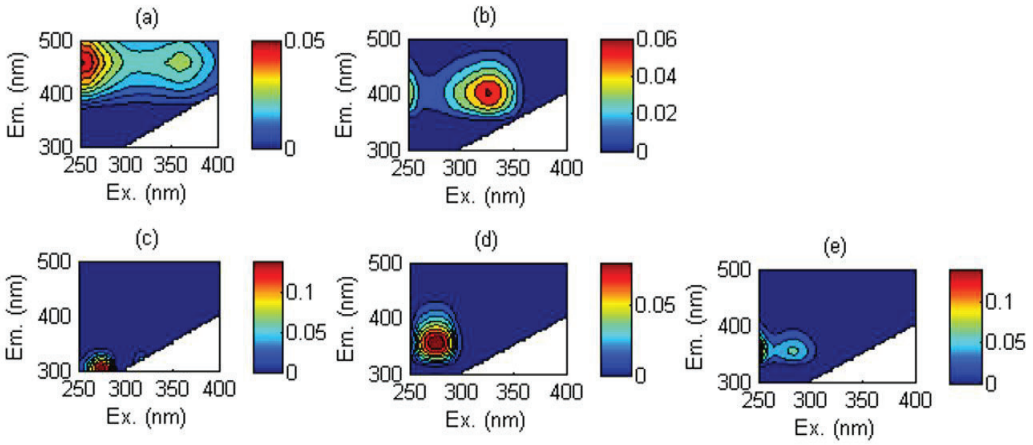

Fig. 4.S1. Five peaks identified by PARAFAC analysis, including two protein-like peaks (ex/em: 275 nm/310 nm; 275 nm/350 nm; two humic-like peaks (ex/em: 325(250) nm/400 nm; 360(250) nm/460 nm) and one peak of mixture of protein-like peak and vitamin shown in the blank of artificial seawater with addition of vitamin (ex/em: 250(280)/350 nm).

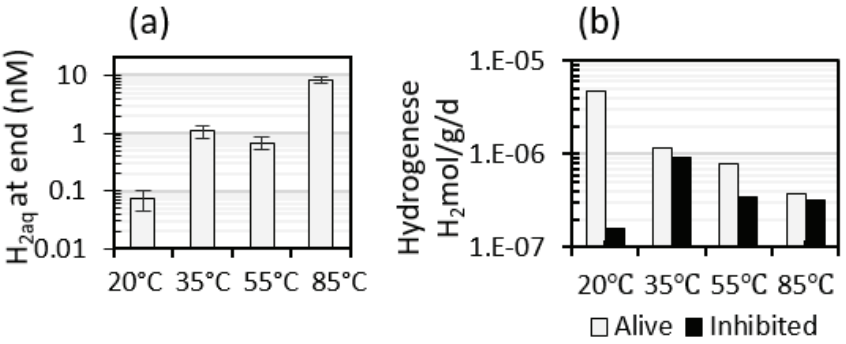

Fig. 4.S2. Background information of microbial activities: (a) hydrogen concentration measured at the end of the incubation experiment;(b) Hydrogenase enzyme based hydrogen utilization potential.

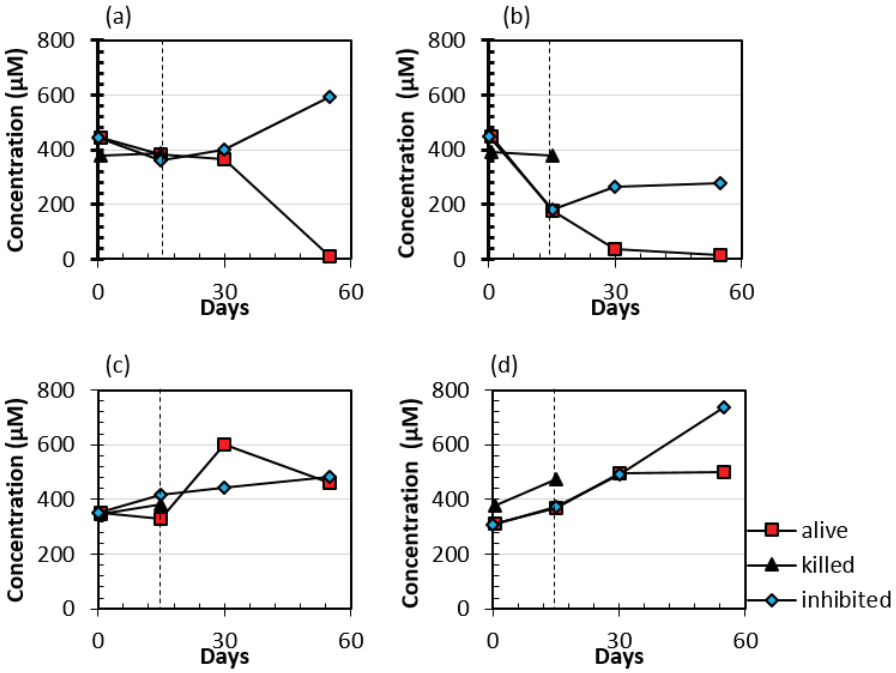

Fig. 4.S3. Acetate concentration in various series during incubation: (a) series at 20°C; (b) series at 35°C; (c) series at 55°C; (d) series at 85°C. The dashed line shows the timepoint of molybdate addition.

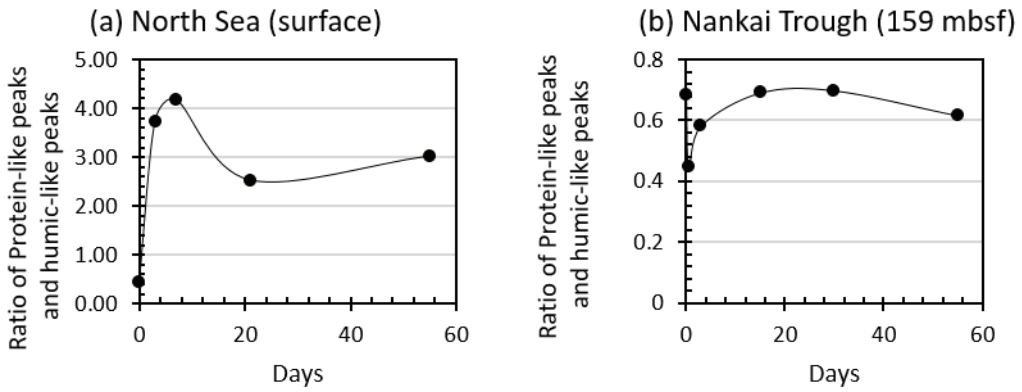

Fig. 4.S4. Comparison of the ratio of protein-like peaks and humic-like peaks during incubations. (a) Incubation at 55°C of sediments from North Sea as representative young sediment, (b) Incubation at 55°C of sediment from Nankai Trough.

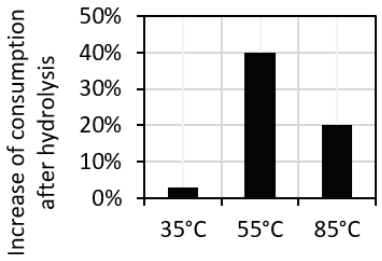

Fig. 4.S5. Increase consumption of protein-like DOM in YE (hydrolyzed) series compared to YE series, YE series is for testing biopolymer fragments consumption and YE (hydrolyzed) series is for testing monomers consumption. The increase of consumption after YE has been hydrolyzed showed faster consumption of monomers. YE = yeast extract.

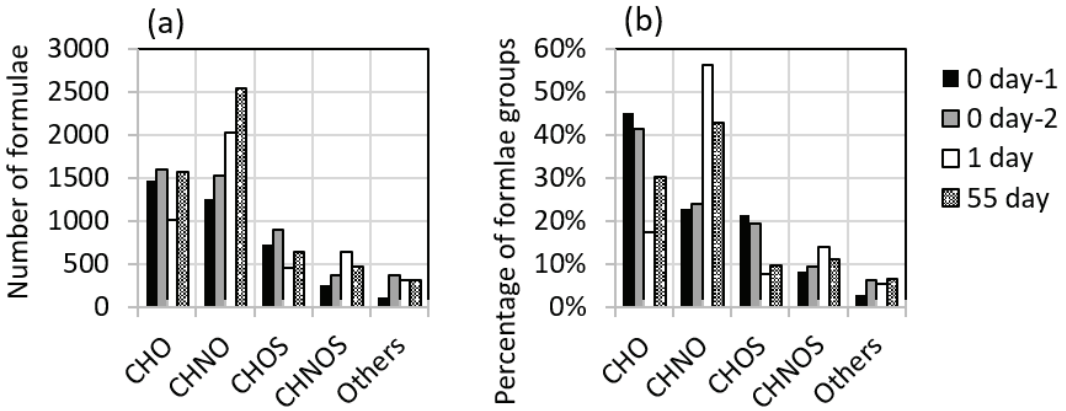

Fig. 4.S6. Distribution of different formulae groups (grouped by elemental composition: CHO, CHNO, CHOS, CHNOS, and the others): (a) number and (b) percentage of each type of formulae. The percentage of formulae is calculated by $rIntn = \sum rIntn_{each\ group} / \sum rIntn_{all\ formulae}$

Chapter 5 Conclusions and outlooks

5.1 Conclusions

This thesis investigated the interaction between DOM and geomicrobial processes in subseafloor sediments. Firstly, we evaluated the application of EEMs in analysis of DOM in subsurface sediment pore water. By focusing on DOM, the initial steps of the degradation of particulate organic matter to smaller, soluble compounds were observed. The products of fermentation and terminal degradation steps were monitored by measurements of volatile fatty acids (e.g. acetate) and end products (DIC or NH_4^+). Based on these data, we concluded that redox conditions and temperature affect the DOM composition and cycling. Results suggested that the preference of substrates and degradation pathways varied with environmental conditions in the subsurface sediments.

5.1.1 Analytical window sensitive to microbial metabolism in subsurface sediments

The combination of EEMs and FT-ICR MS was successfully applied in the incubations aiming at the impacts of redox conditions (sulfate reducing *vs.* methanogenic conditions) and heating. With overview of DOM via EEMs at high-frequency sampling intervals, quantitative and qualitative information of DOM transformation was obtained. Based on this information, FT-ICR MS analysis at selected time point enabled a precise observation of DOM and explained the transformation for protein-like and humic-like compounds.

Cares should be taken for EEMs pore water samples. Concentration, salts, redox-sensitive inorganic ions, and O_2 exposure affect the EEMs. Accordingly, an appropriate method for DOM characterization is validated for anaerobic pore water samples. (1) To avoid impacts of O_2 on redox-sensitive inorganic ions, samples should be stored without headspace of air for the metal ions-rich samples and purged with N_2 for sulfide-rich samples. O_2 exposure has a negligible impact on the composition of most organic compounds detected by FT-ICR MS in two months. (2) The final concentration of Fe(II) or Mn(II) should below 0.06 mM to avoid their impacts on humic-like peaks. (3) Samples should be diluted with O_2-free NaCl solution (35‰ wt.) (a_{350} after dilution: 0.009-0.06 cm^{-1}) in appropriate concentrations to avoid inner

filter effect at high concentration and noise peaks at low concentration. (4) If inevitably exposed to O_2 for Fe(II) or Mn(II)-rich samples, precipitation should be avoided during measurements. Micro-liquid sampling (50-300 μL) is sufficient. Without loss of protein-like compounds caused by solid phase extraction, EEMs enables a promising application in quantitative and qualitative analysis of the DOM for deep biosphere research.

5.1.2 Microbial metabolism in subsurface sediments implied from DOM

In this study, we focus on the impacts of environmental conditions (redox conditions, temperature) on the composition of electron donors and the microbial metabolism. In the stratified subsurface sediments, there are different ongoing degradation processes and microbial metabolism.

(1) Cooperation of microbes by multi-stage degradation

Under sulfate reducing conditions, the production of DOM from the particulate organic matter pool was stimulated. Qualitatively, there was a rapid turnover of protein-like peaks and accumulation of humic-like DOM leading to a more concentrated refractory DOC pool due to selective degradation inferred by EEMs. FT-ICR MS analysis confirmed that CHNO-N3,4 formulae were readily lost while CHNO-N1 compounds accumulated. Compared to series under methanogenic conditions, the microbes under sulfate reducing conditions preferentially utilized biopolymers fragments rapidly. With inhibition of sulfate reducer, turnover of acetate was not inhibited while the turnover of labile biopolymers fragments was continuously inhibited. It suggests the preferential degradation of labile biopolymers and the initial step of hydrolysis is closely linked to the terminal process (sulfate reduction). Different selectivity in initial step was modulated by sulfate availability and, more specifically, sulfate reducer.

It is known that the availability of sulfate modulates the terminal step of mineralization; in further, this study suggests it shapes the upper steps of degradation chain as inferred by high molecular weight-DOM. The initial degradation steps are sensitive to the availability of electron acceptor, which is utilized in terminal step. It implies an intriguing figure in the deep biosphere of syntrophic degradation chain from HMW organic matter adapted to starvation of electron acceptor.

(2) It’s better not be a ‘picky’ eater.

Under methanogenic conditions, potential metabolic energy through respiratory processes is severely limited. During incubation, release of DOC slowed down and net accumulation ceased with depleted sulfate, suggesting that the release of fresh DOM from sediment slowed down. Microbes tend to shift to assimilate former refractory DOM with inability of releasing organic carbon from solid phase. The 'refractory' humic-like compounds were rapidly transformed: the blue-shift of fluorescence spectra occurred. Consistently, FT-ICR MS analysis showed the production aromatics with less carbon and oxygen suggesting the mechanism of blue-shift of humic-like peaks by losing oxygen-containing functional groups and side chains as fluorochromes. Consequently, the microbial communities inhabiting the methanogenic layer benefit from the residues of microbial metabolism within the sulfate-reducing layer. Processed humic-like compounds in dissolved phase were more degraded. Although the microbes in methanogenic layer exhibit less capability in hydrolysis processes, they are not 'picky' and utilize the residue of humic-like compounds.

(3) Adapt to environmental conditions, e.g., heating

The incubation under heated condition provided insight into the mechanism of heat-induced microbial metabolisms with contribution of abiotic processes in deep sediment including three steps (35-85°C): (1) fast abiotic release of the weakly-bound macromolecules from the solid phase; this process started at 35°C and increased with temperature; (2) slow abiotic decomposition of humic substances (mainly CHNO-N1,N2) to smaller molecules, it occurs at 55°C and 85°C; (3) abiotic production of substrates for terminal mineralization, it plays a major role at 85°C. The higher temperature led to more production of molecule in low-molecular weight from abiotic processes and less dependency of metabolites produced after hydrolysis and fermentation. Thus, the higher the temperature is, the shorter the biotic degradation chain could be. It implied a life with a simpler carbon metabolism in achieving 'food' in thermal environment with less dependence on fermentation and hydrolysis by hydrolase.

5.1.3 Implication for the carbon cycle in subsurface sediments

Redox conditions and temperature affect the selectivity of degradation. As for the former, considering the important role of delta sediments in the carbon cycle, the redox regimes and the associated biogeochemical processes would influence the regional carbon and nitrogen cycle via preferential DOM released, consumed, and ultimately shape the composition of

carbon preserved in the coastal sediments. In the deeply buried, heated sediments, the abiotic decomposition produces acetate for terminal mineralization from organic matter. The compounds sensitive to heating could be preferentially utilized and escape the preserved carbon pool. The recalcitrant organic matter – humic substances are mobilized and become accessible to microbial carbon cycling. Thus, heat induced an accelerated shunt of preserved carbon into two pools: one is favorable for microbes, while the other one is a more refractory reservoir for long preservation of carbon. In sum, the interactions of DOM and microbes indicate a varying microbial-drived carbon cycling and close interactions between biosphere and geosphere in the subsurface sediments.

5.2 Outlook and limitations

There are several open questions remaining after completion of this thesis. It is not clear what the intrinsic reason is for varied selectivity of organic compounds under different redox conditions. The first possibility might be the shift in the microbial community. For example, under sulfate reducing conditions, the terminal mineralizer are sulfate-reducing bacteria, while under methanogenic condition it is methanogenic archaea. These microbes along with their syntrophic community partners might exhibit different affinity to various types of organic matter. A second possibility might come from the energy limitation: different energy yields depending on electron acceptors might be one of the driving factors for the change of pathways. As for the terminal process, the energy produced from methanogen is less than that from sulfate reduction with same amount of acetate. The initial steps – hydrolysis of the biopolymers necessitate high amount of energy. The Gibbs free energy for all the steps is required to be calculated to verify the second possibility.

Besides, particular monomers or functional groups for abiotic acetate production are not clear and remain to be examined in the future studies. It is interesting and remains to be quantified that the potential contribution of acetate or H_2 production under geothermal condition in formation of methane in subsurface sediments under more reduced environments.

More work is needed before the principal findings of this PhD thesis can be transferred to other marine sedimentary settings. For the impact of heating, this study should be less implicative for environments with many fresh biopolymer fragments, the substrates produced

from biotic process might be enough for the luxious production and turnover of hydrolase at high temperature and the contribution of abiotic processes might have less impacts on the degradation of organic matter in these environments.

References

Abdel-Naby M. A., Ahmed S. A., Wehaidy H. R. and El-Mahdy S. A. (2017) Catalytic, kinetic and thermodynamic properties of stabilized Bacillus stearothermophilus alkaline protease. *Int. J. Biol. Macromol.* **96**, 265–271.

Abdulla H. A., Burdige D. J. and Komada T. (2017) Accumulation of deaminated peptides in anoxic sediments of Santa Barbara Basin. *Geochim. Cosmochim. Acta*.

Abdulla H. A. N. and Hatcher P. G. (2014) Dynamics of dissolved organic matter: A view from two dimensional correlation spectroscopy techniques. *J. Mol. Struct.* **1069**, 313–317.

Adhikari R. R., Glombitza C., Nickel J. C., Anderson C. H., Dunlea A. G., Spivack A. J., Murray R. W., D'Hondt S. and Kallmeyer J. (2016) Hydrogen utilization potential in subsurface sediments. *Front. Microbiol.* **7**, 1–16.

Alberic P., Sarazin G. and Michard G. (1996) Combined amino acid speciation in lake sediment and porewater (Aydat Lake, France). *Aquat. Geochemistry* **2**, 29–49.

Amrani A., Turner J. W., Ma Q., Tang Y. and Hatcher P. G. (2007) Formation of sulfur and nitrogen cross-linked macromolecules under aqueous conditions. *Geochim. Cosmochim. Acta* **71**, 4141–4160.

Arndt S., Jørgensen B. B., LaRowe D. E., Middelburg J. J., Pancost R. D. and Regnier P. (2013) Quantifying the degradation of organic matter in marine sediments: A review and synthesis. *Earth-Sci. Rev.* **123**, 53–86.

Arnosti C. (1998) Temperature dependence of microbial degradation of organic matter in marine sediments: polysaccharide hydrolysis, oxygen consumption, and sulfate reduction. *Mar. Ecol. Prog. Ser.* **165**, 59–70.

Arnosti C. and Holmer M. (1999) Carbohydrate dynamics and contributions to the carbon budget of an organic-rich coastal sediment. *Geochim. Cosmochim. Acta* **63**, 393–403.

Arnosti C. and Holmer M. (2003) Carbon cycling in a continental margin sediment: contrasts between organic matter characteristics and remineralization rates and pathways. *Estuar. Coast. Shelf Sci.* **58**, 197–208.

Arnosti C. and Jørgensen B. B. (2003) High activity and low temperature optima of extracellular enzymes in Arctic sediments: implications for carbon cycling by heterotrophic microbial communities. *Mar. Ecol. Prog. Ser.* **249**, 15–24.

Artham T. and Doble M. (2012) Bisphenol A and metabolites released by biodegradation of polycarbonate in seawater. *Environ. Chem. Lett.* **10**, 29–34.

Baker A., Bolton L., Newson M. and Spencer R. G. M. (2008) Spectrophotometric properties of surface water dissolved organic matter in an afforested upland peat catchment. *Hydrol. Process.* **22**, 2325–2336.

Balci M. (2005) *Basic 1H-and 13C-NMR Spectroscopy*. Elsevier B.V., Amsterdam.

Banat I. M., Nedwell D. B. and Balba M. T. (1983) Stimulation of Methanogenesis by Slurries of Saltmarsh Sediment after the Addition of Molybdate to Inhibit Sulphate-reducing Bacteria. *J. Gen. Microbiol.* **129**, 123–129.

Barker H. A. (1981) Amino acid degradation by anaerobic bacteria. *Annu. Rev. Biochem.* **50**, 23–40.

Baross J. A. and Hoffman S. E. (1985) Submarine hydrothermal vents and associated gradient environments as sites for the origin and evolution of life. *Orig. Life Evol. Biosph.* **15**, 327–345.

Battersby N. S. and Wilson V. (1989) Survey of the Anaerobic Biodegradation Sludge Survey of the Anaerobic Biodegradation Potential of Organic Chemicals in Digesting Sludge. *Appl. Environ. Microbiol.* **55**, 433–439.

Berg I. A, Kockelkorn D., Ramos-Vera W. H., Say R. F., Zarzycki J., Hügler M., Alber B. E. and Fuchs G. (2010) Autotrophic carbon fixation in archaea. *Nat. Rev. Microbiol.* **8**, 447–60.

Berner R. A. (1989) Biogeochemical cycles of carbon and sulfur and their efect on atmospheric oxygen over Phanerozoic time. *Palaeogeogr. Palaeoclimatol. Palaeoecol.* **75**, 97–122.

Berner R. A. (1982) Burial of organic carbon and pyrite sulfur in the modern ocean: Its geochemical and environmental significance. *Am. J. Sci.* **282**, 451–473.

Berns A. E., Philipp H., Narres H.-D., Burauel P., Vereecken H. and Tappe W. (2008) Effect of gamma-sterilization and autoclaving on soil organic matter structure as studied by solid state NMR, UV and fluorescence spectroscopy. *Eur. J. Soil Sci.* **59**, 540–550.

Biddle J. F., House C. H. and Brenchley J. E. (2005) Microbial stratification in deeply buried marine sediment reflects changes in sulfate/methane profiles. *Geobiology* **3**, 287–295.

Biddle J. F., Lipp J. S., Lever M. A., Lloyd K. G., Sørensen K. B., Anderson R., Fredricks H. F., Elvert M., Kelly T. J., Schrag D. P., Sogin M. L., Brenchley J. E., Teske A., House C. H. and Hinrichs K. -U. (2006) Heterotrophic Archaea dominate sedimentary subsurface ecosystems off Peru. *Proc. Natl. Acad. Sci.* **103**, 3846–3851.

Billerbeck M., Werner U., Polerecky L., Walpersdorf E., deBeer D. and Huettel M. (2006) Surficial and deep pore water circulation governs spatial and temporal scales of nutrient

recycling in intertidal sand flat sediment. *Mar. Ecol. Prog. Ser.* **326**, 61–76.

Blöchl E., Rachel R., Burggraf S., Hafenbradl D., Jannasch H. W. and Stetter K. O. (1997) Pyrolobus fumarii , gen . and sp . nov ., represents a novel group of archaea , extending the upper temperature limit for life to 113 ° C. *Extremophiles* **1**, 14–21.

Boetius A., Ravenschlag K., Schubert C. J., Rickert D., Widdel F., Gieseke A., Amann R., Jørgensen B. B., Witte U. and Pfannkuche O. (2000) A marine microbial consortium apparently mediating anaerobic oxidation of methane. *Nature* **407**, 623–626.

Bond D. R. and Lovley D. R. (2002) Reduction of Fe(III) oxide by methanogens in the presence and absence of extracellular quinones. *Environ. Microbiol.* **4**, 115–124.

Bowles M. W., Mogollón J. M., Kasten S., Zabel M. and Hinrichs K.-U. (2014) Global rates of marine sulfate reduction and implications for sub-sea-floor metabolic activities. *Science* **344**, 889–91.

Briggs B. R., Graw M., Brodie E. L., Bahk J. J., Kim S. H., Hyun J. H., Kim J. H., Torres M. and Colwell F. S. (2013) Microbial distributions detected by an oligonucleotide microarray across geochemical zones associated with methane in marine sediments from the Ulleung Basin. *Mar. Pet. Geol.* **47**, 147–154.

Bro R. (1997) PARAFAC. Tutorial and applications. *Chemom. Intell. Lab. Syst.* **38**, 149–171.

Brüschweiler R., Blackledge M. and Ernst R. R. (1991) Multi-conformational peptide dynamics derived from NMR data: A new search algorithm and its application to antamanide. *J. Biomol. NMR* **1**, 3–11.

Burdige D. J. (2001) Dissolved organic matter in Chesapeake Bay sediment pore waters. *Org. Geochem.* **32**, 487–505.

Burdige D. J. (2007) Preservation of organic matter in marine sediments: Controls, mechanisms, and an imbalance in sediment organic carbon budgets? *Chem. Rev.* **107**, 467–485.

Burdige D. J., Kline S. W. and Chen W. (2004) Fluorescent dissolved organic matter in marine sediment pore waters. *Mar. Chem.* **89**, 289–311.

Burdige D. J. and Zheng S. L. (1998) The biogeochemical cycling of dissolved organic nitrogen in estuarine sediments. *Limnol. Oceanogr.* **43**, 1796–1813.

Canfield D. E., Jorgensen B. B., Fossing H., Glud R., Gundersen J., Ramsing N. B., Thamdrup B., Hansen J. W., Nielsen L. P. and Hall P. O. (1993a) Pathways of organic carbon oxidation in three continental margin sediments. *Mar. Geol.* **113**, 27–40.

Canfield D. E., Jorgensen B. B., Fossing H., Glud R., Gundersen J., Ramsing N. B., Thamdrup B., Hansen J. W., Nielsen L. P. and Hall P. O. (1993b) Pathways of organic carbon oxidation in three continental margin sediments. *Mar. Geol.* **113**, 27–40.

Cao J., Lam K. C., Dawson R. W., Liu W. X. and Tao S. (2004) The effect of pH, ion strength and reactant content on the complexation of Cu2+ by various natural organic ligands from water and soil in Hong Kong. *Chemosphere* **54**, 507–514.

Capone D. G. and Kiene R. P. (1988) Comparison of microbial dynamics in marine and freshwater sediments: Contrasts in anaerobic carbon catabolism. *Limnol. Oceanogr.* **33**, 725–749.

Catalá T. S., Reche I., Fuentes-Lema A., Romera-Castillo C., Nieto-Cid M., Ortega-Retuerta E., Calvo E., Álvarez M., Marrasé C., Stedmon C. A. and Álvarez-Salgado X. A. (2015) Turnover time of fluorescent dissolved organic matter in the dark global ocean. *Nat. Commun.* **6**, 5986.

Cathalot C., Rabouille C., Tisnérat-Laborde N., Toussaint F., Kerhervé P., Buscail R., Loftis K., Sun M. Y., Tronczynski J., Azoury S., Lansard B., Treignier C., Pastor L. and Tesi T. (2013) The fate of river organic carbon in coastal areas: A study in the RhÔne River delta using multiple isotopic (δ13C, δ14C) and organic tracers. *Geochim. Cosmochim. Acta* **118**, 33–55.

Chefetz B., Salloum M. J., Deshmukh A. P. and Hatcher P. G. (2002) Structural Components of Humic Acids as Determined by Chemical Modifications Chromatography / Mass Spectrometry. *Soil Sci. Soc. Am. J.* **66**, 1159–1171.

Chen C.-T. A., Liu K.-K. and Macdonald R. (2003) Continental Margin Exchanges. In *Ocean Biogeochemistry: The role of the ocean carbon cycle in global change* (ed. M. Fasham). pp. 53–98.

Chen M. and Hur J. (2015) Pre-treatments, characteristics, and biogeochemical dynamics of dissolved organic matter in sediments: A review. *Water Res.* **79**, 10–25.

Chen R. F., Bada J. L. and Suzuki Y. (1993) The relationship between dissolved organic carbon (DOC) and fluorescence in anoxic marine porewaters: Implications for estimating benthic DOC fluxes. *Geochim. Cosmochim. Acta* **57**, 2149–2153.

Chen Y., Senesi N. and Schnitzer M. (1977) Information Provided on Humic Substances by E4/E6 Ratios. *Soil Sci. Soc. Am. J.* **41**, 352.

Chin Y.-P., Traina S. J., Swank C. R. and Backhus D. (1998) Abundance and properties of dissolved organic matter in pore waters of a freshwater wetland. *Limnol. Oceanogr.* **43**, 1287–1296.

Chynoweth D. P. (1996) Environmental impact of biomethanogenesis. *Environ. Monit. Assess.* **42**, 3–18.

Ciobanu M.-C., Burgaud G., Dufresne A., Breuker A., Rédou V., Ben Maamar S., Gaboyer F., Vandenabeele-Trambouze O., Lipp J. S., Schippers A., Vandenkoornhuyse P., Barbier G., Jebbar M., Godfroy A. and Alain K. (2014) Microorganisms persist at record depths in

the subseafloor of the Canterbury Basin. *ISME J.* **8**, 1370–1380.

Clark M. W., McConchie D., Lewis D. W. and Saenger P. (1998) Redox stratification and heavy metal partitioning in Avicennia-dominated mangrove sediments: a geochemical model. *Chem. Geol.* **149**, 147–171.

Coble P. G. (2008) Oceanography: Cycling coloured carbon. *Nat. Geosci.* **1**, 575–576.

Coble P. G. (1996) Characterization of marine and terrestrial DOM in seawater using excitation-emission matrix spectroscopy. *Mar. Chem.* **51**, 325–346.

Coble P. G. (2007) Marine optical biogeochemistry: the chemistry of ocean color. *Chem. Rev.* **107**, 402–418.

Coble P. G., Green S. A., Blough N. V. and Gagosian R. B. (1990) Characterization of dissolved organic matter in the Black Sea by fluorescence spectroscopy. *Nature* **348**, 432–435.

Colberg P. J. and Young L. Y. (1982) Biodegradation of lignin-derived molecules under anaerobic conditions. *Can. J. Microbiol.* **28**, 886–889.

Colussi F., Garcia W., Rosseto F. R., De Mello B. L. S., De Oliveira Neto M. and Polikarpov I. (2012) Effect of pH and temperature on the global compactness, structure, and activity of cellobiohydrolase Cel7A from Trichoderma harzianum. *Eur. Biophys. J.* **41**, 89–98.

Comisarow M. B. and Marshall A. G. (1974a) Fourier transform ion cyclotron resonance spectroscopy. *Chem. Phys. Lett.* **25**, 282–283.

Comisarow M. B. and Marshall A. G. (1974b) Frequency-sweep fourier transform ion cyclotron resonance spectroscopy. *Chem. Phys. Lett.* **26**, 489–490.

Cory R. M. and Kaplan L. A. (2012) Biological lability of streamwater fluorescent dissolved organic matter. *Limnol. Oceanogr.* **57**, 1347–1360.

Cory R. M. and McKnight D. M. (2005) Fluorescence spectroscopy reveals ubiquitous presence of oxidized and reduced quinones in dissolved organic matter. *Environ. Sci. Technol.* **39**, 8142–8149.

Cossins A. R. and Prosser C. L. (1978) Evolutionary adaptation of membranes to temperature. *Proc. Natl. Acad. Sci.* **75**, 2040–2043.

Costa M. C., Mota S., Nascimento R. F. and Santos A. B. Dos (2010) Bioresource Technology Anthraquinone-2 , 6-disulfonate (AQDS) as a catalyst to enhance the reductive decolourisation of the azo dyes Reactive Red 2 and Congo Red under anaerobic conditions. *Bioresour. Technol.* **101**, 105–110.

Creighton T. E. (1983) *Proteins: structure and molecular properties*. 2nd. ed., Freeman, New York.

Crozier T. E. and Yamamoto S. (1974) Solubility of hydrogen in water, sea water, and sodium chloride solutions. *J. Chem. Eng. Data* **19**, 242–244.

Cuss C. W. and Guéguen C. (2016) Analysis of dissolved organic matter fluorescence using self-organizing maps: mini-review and tutorial. *Anal. Methods* **8**, 716–725.

Cuss C. W. and Guéguen C. (2015) Relationships between molecular weight and fluorescence properties for size-fractionated dissolved organic matter from fresh and aged sources. *Water Res.* **68**, 487–97.

D'Hondt S., Jørgensen B. B., Miller D. J., Batzke A., Blake R., Cragg B. A., Cypionka H., Dickens G. R., Ferdelman T., Hinrichs K.-U., Holm N. G., Mitterer R., Spivack A., Wang G., Bekins B., Engelen B., Ford K., Gettemy G., Rutherford S. D., Sass H., Skilbeck C. G., Aiello I. W., Guèrin G., House C. H., Inagaki F., Meister P., Naehr T., Niitsuma S., Parkes R. J., Schippers A., Smith D. C., Teske A., Wiegel J., Padilla C. N. and Acosta J. L. S. (2004) Distributions of Microbial Activities in Deep Subseafloor Sediments. *Science.* **306**, 2216–2222.

D'Andrilli J., Chanton J. P., Glaser P. H. and Cooper W. T. (2010) Characterization of dissolved organic matter in northern peatland soil porewaters by ultra high resolution mass spectrometry. *Org. Geochem.* **41**, 791–799.

Daniel R. M. (1996) The upper limits of enzyme thermal stability. *Enzyme Microb. Technol.* **19**, 74–79.

Dauwe B. and Middelburg J. J. (1998) Amino acids and hexosamines as indicators of organic matter degradation state in North Sea sediments. *Limnol. Oceanogr.* **43**, 782–798.

Dauwe B., Middelburg J. J. and Herman P. M. J. (2001) Effect of oxygen on the degradability of organic matter in subtidal and intertidal sediments of the North Sea area. *Mar. Ecol. Ser.* **215**, 13–22.

Davidovits J. (1993) From Ancient CONCRETE TO GEOPOLYMERS. *Arts Métiers* **180**, 1–6.

Demirel B. and Scherer P. (2008) The roles of acetotrophic and hydrogenotrophic methanogens during anaerobic conversion of biomass to methane: A review. *Rev. Environ. Sci. Biotechnol.* **7**, 173–190.

Dittmar T., Koch B., Hertkorn N. and Kattner G. (2008) A simple and efficient method for the solid-phase extraction of dissolved organic matter (SPE-DOM) from seawater. *Limnol. Oceanogr. Methods* **6**, 230–235.

Dittmar T. and Lara R. J. (2001) Molecular evidence for lignin degradation in sulfate-reducing mangrove sediments (Amazõnia, Brazil). *Geochim. Cosmochim. Acta* **65**, 1417–1428.

Dittmar T., Whitehead K., Minor E. C. and Koch B. P. (2007) Tracing terrigenous dissolved

organic matter and its photochemical decay in the ocean by using liquid chromatography/mass spectrometry. *Mar. Chem.* **107**, 378–387.

Drake H. L., Küsel K. and Matthies C. (2013) *Acetogenic prokaryotes*., Springer-Verlag Berlin, Heidelberg.

Durbin A. M. and Teske A. (2011) Microbial diversity and stratification of South Pacific abyssal marine sediments. *Environ. Microbiol.* **13**, 3219–3234.

Dworkin M., Falkow S., Rosenberg E., Schleifer A.-H. and Stackebrandt E. (2006) The Prokaryotes: Symbiotic Associations, Biotechnology, Applied Microbiology. *The Prokaryotes*, 1–184.

Elling F. J., Könneke M., Mußmann M., Greve A. and Hinrichs K.-U. (2015) Influence of temperature, pH, and salinity on membrane lipid composition and TEX86 of marine planktonic thaumarchaeal isolates. *Geochim. Cosmochim. Acta* **171**, 238–255.

Emerson S. and Hedges J. I. (1988) Progresses controlling the organic carbon content of open ocean sediments. *Palaeogeogr. Palaeoclimatol. Palaeoecol.* **3**, 621–634.

Ernst R. R., Bodenhausen G. and Wokaun A. (1987) Principles of nuclear magnetic resonance in one and two dimensions. *Princ. Nucl. Magn. Reson. One Two Dimens.* **14**, 50–60.

Ertel J. R. and Hedges J. I. (1985) Sources of sedimentary humic substances: vascular plant debris. *Geochim. Cosmochim. Acta* **49**, 2097–2107.

Evans W. C. and Fuchs G. (1988) Anaerobic degradation of aromatic compounds. *Annu. Rev. Microbiol.* **42**, 289–317.

Fellman J. B., Hood E. and Spencer R. G. M. (2010) Fluorescence spectroscopy opens new windows into dissolved organic matter dynamics in freshwater ecosystems: A review. *Limnol. Oceanogr.* **55**, 2452–2462.

Ferretto N., Tedetti M., Guigue C., Mounier S., Redon R. and Goutx M. (2014) Identification and quantification of known polycyclic aromatic hydrocarbons and pesticides in complex mixtures using fluorescence excitation-emission matrices and parallel factor analysis. *Chemosphere* **107**, 344–353.

Flerus R., Lechtenfeld O. J., Koch B. P., McCallister S. L., Schmitt-Kopplin P., Benner R., Kaiser K. and Kattner G. (2012) A molecular perspective on the ageing of marine dissolved organic matter. *Biogeosciences* **9**, 1935–1955.

Frazier S. W., Kaplan L. A. and Hatcher P. G. (2005) Molecular characterization of biodegradable dissolved organic matter using bioreactors and C-12/C-13 tetramethylammonium hydroxide thermochemolysis GC-MS. *Environ. Sci. Technol.* **39**, 1479–1491.

Freund F., Dickinson J. T. and Cash M. (2002) Hydrogen in Rocks: An Energy Source for

Deep Microbial Communities. *Astrobiology* **2**, 83–92.

Fu P., Wu F., Liu C.-Q., Wei Z., Bai Y. and Liao H. (2006) Spectroscopic characterization and molecular weight distribution of dissolved organic matter in sediment porewaters from Lake Erhai, Southwest China. *Biogeochemistry* **81**, 179–189.

Gagliano M. C., Braguglia C. M., Gianico A. and Mininni G. (2014) ScienceDirect Thermophilic anaerobic digestion of thermal pretreated sludge : Role of microbial community structure and correlation with process performances. *Water Res.* **68**, 498–509.

Gan S., Wu Y. and Zhang J. (2016) Bioavailability of dissolved organic carbon linked with the regional carbon cycle in the East China Sea. *Deep Sea Res. Part II Top. Stud. Oceanogr.* **124**, 19–28.

Gauglitz G. and Vo-Dinh T. (2003) *Handbook of Spectroscopy,Volume 1*. ed. G. G. and T. Vo-Dinh, WILEY-VCH Verlag GmbH & Co. KGaA, Weinheim.

Glombitza C., Jaussi M., Røy H., Seidenkrantz M. S., Lomstein B. A. and Jørgensen B. B. (2015) Formate, acetate, and propionate as substrates for sulfate reduction in sub-arctic sediments of Southwest Greenland. *Front. Microbiol.* **6**, 1–14.

Gomez-Saez G. V., Niggemann J., Dittmar T., Pohlabeln A. M., Lang S. Q., Noowong A., Pichler T., Wörmer L. and Bühring S. I. (2016) Molecular evidence for abiotic sulfurization of dissolved organic matter in marine shallow hydrothermal systems. *Geochim. Cosmochim. Acta* **190**, 35–52.

Gonsior M., Peake B. M., Cooper W. T., Podgorski D., D'Andrilli J. and Cooper W. J. (2009) Photochemically induced changes in dissolved organic matter identified by ultrahigh resolution fourier transform ion cyclotron resonance mass spectrometry. *Environ. Sci. Technol.* **43**, 698–703.

Gray H. B. (1965) *Electrons and chemical bonding*., New York.

Green N. W., Perdue E. M., Aiken G. R., Butler K. D., Chen H., Dittmar T., Niggemann J. and Stubbins A. (2014) An intercomparison of three methods for the large-scale isolation of oceanic dissolved organic matter. *Mar. Chem.* **161**, 14–19.

Gu Q. and Kenny J. E. (2009) Improvement of Inner Filter Effect Correction Based on Determination of Effective Geometric Parameters Using a Conventional Fluorimeter Improvement of Inner Filter Effect Correction Based on Determination of Effective Geometric Parameters Using a Conventi. *Anal. Chem.* **81**, 420–426.

Guldberg L. B., Finster K., Jørgensen N. O. G., Middelboe M. and Lomstein B. A. (2002) Utilization of marine sedimentary dissolved organic nitrogen by native anaerobic bacteria. *Limnol. Oceanogr.* **47**, 1712–1722.

Guo W., Xu J., Wang J., Wen Y., Zhuo J. and Yan Y. (2010) Characterization of dissolved

organic matter in urban sewage using excitation emission matrix fluorescence spectroscopy and parallel factor analysis. *J. Environ. Sci.* **22**, 1728–1734.

Guo X., He X., Zhang H., Deng Y., Chen L. and Jiang J. (2012) Characterization of dissolved organic matter extracted from fermentation effluent of swine manure slurry using spectroscopic techniques and parallel factor analysis (PARAFAC). *Microchem. J.* **102**, 115–122.

Hackett W. F., Connors W. J., Kirk T. K. and Zeikus J. G. (1977) Microbial decomposition of synthetic 14C labeled lignins in nature: lignin biodegradation in a variety of natural materials. *Appl. Environ. Microbiol.* **33**, 43–51.

Hansen A. M., Kraus T. E. C., Pellerin B. A., Fleck J. A., Downing B. D. and Bergamaschi B. A. (2016) Optical properties of dissolved organic matter (DOM): Effects of biological and photolytic degradation. *Limnol. Oceanogr.* **61**, 1015–1032.

Hansen T. A. (1993) Carbon metabolism of sulfate-reducing bacteria. In *The Sulfate-Reducing Bacteria: Contemporary Perspectives* pp. 21–40.

Hansen T. A. (1994) Metabolism of sulfate-reducing prokaryotes. *Antonie van Leeuwenhoek, Int. J. Gen. Mol. Microbiol.* **66**, 165–185.

Hao J. and Wang H. (2015) Volatile fatty acids productions by mesophilic and thermophilic sludge fermentation: Biological responses to fermentation temperature. *Bioresour. Technol.* **175**, 367–373.

Hartnett H., Keil R., Hedges J. and Devol A. (1998) Influence of oxygen exposure time on organic carbon preservation in continental margin sediments. *Nature* **391**, 572–575.

Harwood C. S., Burchhardt G., Herrmann H. and Fuchs G. (1998) Anaerobic metabolism of aromatic compounds via the benzoyl-CoA pathway. *FEMS Microbiol. Rev.* **22**, 439–458.

Hattori S. (2008) Syntrophic Acetate-Oxidizing Microbes in Methanogenic Environments. *Microbes Environ.* **23**, 118–127.

Hawkes J. A., Hansen C. T., Goldhammer T., Bach W. and Dittmar T. (2016) Molecular alteration of marine dissolved organic matter under experimental hydrothermal conditions. *Geochim. Cosmochim. Acta* **175**, 68–85.

Hawkes J. A., Rossel P. E., Stubbins A., Butterfield D., Connelly D. P., Achterberg E. P., Koschinsky A., Chavagnac V., Hansen C. T., Bach W. and Dittmar T. (2015) Efficient removal of recalcitrant deep-ocean dissolved organic matter during hydrothermal circulation. *Nat. Geosci.* **8**, 1–6.

Hedges J. I., Baldock J. A., Gélinas Y., Lee C., Peterson M. and Wakeham S. G. (2001) Evidence for non-selective preservation of organic matter in sinking marine particles. *Nature* **409**, 801–4.

Hedges J. I., Eglinton G., Hatcher P. G., Kirchman D. L., Arnosti C., Derenne S., Evershed R. P., K.ogel-Knabner I., de Leeuw J. W., Littke R., Michaelis W. and Rullkotter J. (2000) The molecularly uncharacterized component of nonliving organic matter in natural environments. *Org. Geochem.* **31**, 945–958.

Hedges J. I. and Keil R. G. (1999) Organic geochemical perspectives on estuarine processes: Sorption reactions and consequences. *Mar. Chem.* **65**, 55–65.

Hedges J. I. and Keil R. G. (1995) Sedimentary organic matter preservation: an assessment and speculative synthesis. *Mar. Chem.* **49**, 81–115.

Hedges J. I., Keil R. and Benner R. (1997) What happens to terrestrial organic matter in the ocean? *Org. Geochem.* **27**, 195–212.

Hellevang H. (2008) On the forcing mechanism for the H2-driven deep biosphere. *Int. J. Astrobiol.* **7**, 157–167.

Henrichs S. M. (1980) Biogeochemistry of Dissolved Free Amino Acids in Marine Sediments. *Massachusetts Institute of Technology*.

Henrichs S. M. (1992) Early diagenesis of organic matter in marine sediments: progress and perplexity. *Mar. Chem.* **39**, 119–149.

Henrichs S. M. and Farrington J. W. (1979) Amino acids in interstitial waters of marine sediments [10]. *Nature* **279**, 319–322.

Henrichs S. M. and Farrington J. W. (1987) Early diagenesis of amino acids and organic matter in two coastal marine sediments. *Geochim. Cosmochim. Acta* **51**, 1–15.

Henrichs S. M. and Reeburgh W. S. (1987) Anaerobic mineralization of marine sediment organic matter: Rates and the role of anaerobic processes in the oceanic carbon economy. *Geomicrobiol. J.* **5**, 191–237.

Her N., Amy G., McKnight D., Sohn J. and Yoon Y. (2003) Characterization of DOM as a function of MW by fluorescence EEM and HPLC-SEC using UVA, DOC, and fluorescence detection. *Water Res.* **37**, 4295–4303.

Hertkorn N., Benner R., Frommberger M., Schmitt-Kopplin P., Witt M., Kaiser K., Kettrup A. and Hedges J. I. (2006) Characterization of a major refractory component of marine dissolved organic matter. *Geochim. Cosmochim. Acta* **70**, 2990–3010.

Hertkorn N., Harir M., Koch B. P., Michalke B. and Schmitt-Kopplin P. (2013) High-field NMR spectroscopy and FTICR mass spectrometry: powerful discovery tools for the molecular level characterization of marine dissolved organic matter. *Biogeosciences* **10**, 1583–1624.

Herzsprung P., Hertkorn N., von Tümpling W., Harir M., Friese K. and Schmitt-Kopplin P. (2014) Understanding molecular formula assignment of Fourier transform ion cyclotron

resonance mass spectrometry data of natural organic matter from a chemical point of view. *Anal. Bioanal. Chem.* **406**, 7977–7987.

Heuer V. B. (2014) Report and preliminary results of R/V POSEIDON cruise POS450, DARCSEAS II – Deep subseafloor Archaea in the Western Mediterranean Sea: Carbon Cycle, Life Strategies, and Role in Sedimentary Ecosystems.

Heuer V. B., Krüger M., Elvert M. and Hinrichs K.-U. (2010) Experimental studies on the stable carbon isotope biogeochemistry of acetate in lake sediments. *Org. Geochem.* **41**, 22–30.

Heuer V. B., Pohlman J. W., Torres M. E., Elvert M. and Hinrichs K.-U. (2009) The stable carbon isotope biogeochemistry of acetate and other dissolved carbon species in deep subseafloor sediments at the northern Cascadia Margin. *Geochim. Cosmochim. Acta* **73**, 3323–3336.

Heuer V., Elvert M., Tille S., Krummen M., Mollar X. P. and Hmelo L. R. (2006) Online δ 13 C analysis of volatile fatty acids in sediment / porewater systems by liquid chromatography – isotope ratio mass spectrometry. *Limnol. Oceanogr. Methods* **4**, 346–357.

Hinrichs K. -U., Hayes J. M., Sylva S. P., Brewer P. G. and DeLong E. F. (1999) Methane-consuming archaebacteria in marine sediments. *Nature* **398**, 802–805.

Horsfield B., Schenk H. J., Zink K., Ondrak R., Dieckmann V., Kallmeyer J., Mangelsdorf K., di Primio R., Wilkes H., Parkes R. J., Fry J. and Cragg B. (2006) Living microbial ecosystems within the active zone of catagenesis: Implications for feeding the deep biosphere. *Earth Planet. Sci. Lett.* **246**, 55–69.

Huang S.-B., Wang Y.-X., Ma T., Tong L., Wang Y.-Y., Liu C.-R. and Zhao L. (2015) Linking groundwater dissolved organic matter to sedimentary organic matter from a fluvio-lacustrine aquifer at Jianghan Plain, China by EEM-PARAFAC and hydrochemical analyses. *Sci. Total Environ.* **529**, 131–139.

Hubert C., Arnosti C., Brüchert V., Loy A., Vandieken V. and Jørgensen B. B. (2010) Thermophilic anaerobes in Arctic marine sediments induced to mineralize complex organic matter at high temperature. *Environ. Microbiol.* **12**, 1089–1104.

Hubert C., Loy A., Nickel M., Arnosti C., Baranyi C., Brüchert V., Ferdelman T., Finster K., Christensen F. M., Rosa de Rezende J., Vandieken V. and Jørgensen B. B. (2009) A constant flux of diverse thermophilic bacteria into the cold Arctic seabed. *Science (80).* **325**, 1541–1544.

Hudson N., Baker A. and Reynolds D. (2007) Fluorescence analysis of dissolved organic matter in natural, waste and polluted waters - A review. *River Res. Appl.* **23**, 631–649.

Huguet A., Vacher L., Relexans S., Saubusse S., Froidefond J. M. and Parlanti E. (2009)

Properties of fluorescent dissolved organic matter in the Gironde Estuary. *Org. Geochem.* **40**, 706–719.

Icenhower J. P. and Dove P. M. (2000) The dissolution kinetics of amorphous silica into sodium chloride solutions: Effects of temperature and ionic strength. *Geochim. Cosmochim. Acta* **64**, 4193–4203.

Inagaki F., Hinrichs K. -U., Kubo Y., Bihan M., Bowden S. A., Bowles M., Elvert M., Glombitza C., Gross D., Harrington G. J., Heuer V. B., Hong W. L., Hori T., Hoshino T., Ijiri A., Imachi H., Ito M., Kaneko M., Lever M. A., Li K., Limmer D., Lin Y. S., Liu C. H., Methé B. A., Morita S., Morono Y., Murayama M., Ohkouchi N., Ono S., Park Y. S., Phillips S. C., Prieto-Mollar X., Purkey M., Riedinger N., Sanada Y., Sauvage J., Snyder G., Susilawati R., Takano Y., Tanikawa W., Tasumi E., Terada T., Tomaru H., Trembath-Reichert E., Wang D. T. and Yamada Y. (2016) IODP Expedition 337: Deep Coalbed Biosphere off Shimokita - Microbial processes and hydrocarbon system associated with deeply buried coalbed in the ocean. *Sci. Drill.* **21**, 17–28.

Inagaki F., Hinrichs K. -U., Kubo Y., Bowles M. W., Heuer V. B., Ijiri A., Imachi H., Ito M., Kaneko M., Lever M. A., Morita S., Morono Y., Tanikawa W., Bihan M., Bowden S. A., Elvert M., Glombitza C., Gross D., Harrington G. J., Hori T., Li K., Limmer D., Murayama M., Ohkouchi N., Ono S., Purkey M., Sanada Y., Sauvage J., Snyder G., Takano Y., Tasumi E., Terada T., Tomaru H., Wang D. T. and Yamada Y. (2015) Exploring deep microbial life in coal-bearing sediment down to ~2.5 km below the ocean floor. *Science (80-.).* **349**, 420–424.

Inagaki F., Nunoura T., Nakagawa S., Teske A., Lever M., Lauer A., Suzuki M., Takai K., Delwiche M., Colwell F. S., Nealson K. H., Horikoshi K., D'Hondt S. and Jorgensen B. B. (2006) Biogeographical distribution and diversity of microbes in methane hydrate-bearing deep marine sediments on the Pacific Ocean Margin. *Proc. Natl. Acad. Sci.* **103**, 2815–2820.

Ishii S. K. L. and Boyer T. H. (2012) Behavior of Reoccurring PARAFAC Components in Fluorescent Dissolved Organic Matter in Natural and Engineered Systems: ACritical Review. *Environ. Sci. Technol.* **46**, 2006–2017.

Ishiwatari R., Morinaga S., Yamamoto S., Machihara T., Rubinsztain Y., Ioselis P., Aizenshtat Z. and Ikan R. (1986) A study of formation mechanism of sedimentary humic substances-I. Characterization of synthetic humic substances (melanoidins) by alkaline potassium permanganate oxidation. *Org. Geochem.* **9**, 11–23.

Jaffé R., Cawley K. M. and Yamashita Y. (2014) Applications of excitation emission matrix fluorescence with parallel factor analysis (EEM-PARAFAC) in assessing environmental dynamics of natural dissolved organic matter (DOM) in aquatic environments: A review. *ACS Symp. Ser.* **1160**, 27–73.

Jiao N., Herndl G. J., Hansell D. A., Benner R., Kattner G., Wilhelm S. W., Kirchman D. L.,

Weinbauer M. G., Luo T., Chen F. and Azam F. (2011) The microbial carbon pump and the oceanic recalcitrant dissolved organic matter pool. *Nat. Rev. Microbiol.* **9**, 555–555.

Jørgensen B. B. (1982) Mineralization of organic matter in the sea bed - the role of sulphate reduction. *Nature* **296**, 643–645.

Jørgensen B. B. and Boetius A. (2007) Feast and famine — microbial life in the deep-sea bed. *Nat. Rev. Microbiol.* **5**, 770–781.

Jørgensen B. B. and Marshall I. P. G. (2016) Slow Microbial Life in the Seabed. *Ann. Rev. Mar. Sci.* **8**, 311–332.

Jorgensen S. L., Hannisdal B., Lanzén A., Baumberger T. and Flesland K. (2012) Correlating microbial community pro fi les with geochemical data in highly strati fi ed sediments from the Arctic Mid-Ocean Ridge. **109**, 16764–16765.

Kallmeyer J., Pockalny R., Adhikari R. R., Smith D. C. and D'Hondt S. (2012) From the Cover: Global distribution of microbial abundance and biomass in subseafloor sediment. *Proc. Natl. Acad. Sci.* **109**, 16213–16216.

Kashefi K. and Lovley D. R. (2003) Extending the Upper Temperature Limit for Life. *Science (80-.).* **301**, 2003.

Kellerman A. M., Dittmar T., Kothawala D. N. and Tranvik L. J. (2014) Chemodiversity of dissolved organic matter in lakes driven by climate and hydrology. *Nat. Commun.* **5**, 3804.

Kellerman A. M., Kothawala D. N., Dittmar T. and Tranvik L. J. (2015) Persistence of dissolved organic matter in lakes related to its molecular characteristics. *Nat. Geosci.* **8**, 454–457.

Kim D., Lai H.-T., Chilingar G. V and Yen T. F. (2006) Geopolymer formation and its unique properties. *Environ. Geol.* **51**, 103–111.

Kim S., Kramer R. W. and Hatcher P. G. (2003) Graphical Method for Analysis of Ultrahigh-Resolution Braodband mass spectra of Natural Organic Matter, the Van Krevelen diagram. *Anal. Chem.* **75**, 5336–5344.

Klüpfel L., Piepenbrock A., Kappler A. and Sander M. (2014) Humic substances as fully regenerable electron acceptors in recurrently anoxic environments. *Nat. Geosci.* **7**, 195–200.

Knicker H. and Hatcher P. G. (1997) Survival of protein in an organic-rich sediment: Possible protection by encapsulation in organic matter. *Naturwissenschaften* **84**, 231–234.

Koch B. P. and Dittmar T. (2016) Erratum: From mass to structure: An aromaticity index for high-resolution mass data of natural organic matter (Rapid Communications in Mass Spectrometry (2006) 20 (926-932) DOI: 10.1002/rcm.2386). *Rapid Commun. Mass Spectrom.* **30**, 250.

Koch B. P. and Dittmar T. (2006) From mass to structure: an aromaticity index for high-resolution mass data of natural organic matter. *Rapid Commun. Mass Spectrom.* **20**, 926–932.

Koch B. P., Dittmar T., Witt M. and Kattner G. (2007) Fundamentals of molecular formula assignment to ultrahigh resolution mass data of natural organic matter. *Anal. Chem.* **79**, 1758–63.

Koch B. P., Kattner G., Witt M. and Passow U. (2014) Molecular insights into the microbial formation of marine dissolved organic matter: recalcitrant or labile? *Biogeosciences Discuss.* **11**, 3065–3111.

Koch B. P., Witt M., Engbrodt R., Dittmar T. and Kattner G. (2005) Molecular formulae of marine and terrigenous dissolved organic matter detected by electrospray ionization Fourier transform ion cyclotron resonance mass spectrometry. *Geochim. Cosmochim. Acta* **69**, 3299–3308.

Koch R., Zablowski P., Spreinat A. and Antranikian G. (1990) Extremely thermostable amylolyfic enzyme from the archaebacterium Pyrococcus furiosus. *FEMS Microbiol. Lett.* **71**, 21–26.

Koho K. A., Nierop K. G. J., Moodley L., Middelburg J. J., Pozzato L., Soetaert K., van der Plicht J. and Reichart G.-J. (2013) Microbial bioavailability regulates organic matter preservation in marine sediments. *Biogeosciences* **10**, 1131–1141.

Komada T., Schofield O. M. E. and Reimers C. E. (2002) Fluorescence characteristics of organic matter released from coastal sediments during resuspension. *Mar. Chem.* **79**, 81–97.

Kristensen E., Ahmed S. I. and Devol A. H. (1995) Aerobic and anaerobic decomposition of organic matter in marine sediment : Which is fastest ? *Limnol. Ocean.* **40**, 1430–1437.

Krom M. . and Sholkovitz E. (1977) Nature and reactions of dissolved organic matter in the interstitial waters of marine sediments. *Geochim. Cosmochim. Acta* **41**, 1565–1574.

Kubista M., Sjoeback R., Eriksson S. and Albinsson B. (1994) Experimental correction for the inner-filter effect in fluorescence spectra. *Analyst* **119**, 417.

Kujawinski E. B. and Behn M. D. (2006) Automated analysis of electrospray ionization fourier transform ion cyclotron resonance mass spectra of natural organic matter. *Anal. Chem.* **78**, 4363–4373.

Kujawinski E. B., Hatcher P. G. and Freitas M. A. (2001) High-Resolution Fourier Transform Ion Cyclotron Resonance Mass Spectrometry of Humic and Fulvic Acids: Improvements and Comparisons. *Anal. Chem.* **74,** 554–560.

Kujawinski E. B., Del Vecchio R., Blough N. V, Klein G. C. and Marshall A. G. (2004) Probing

molecular-level transformations of dissolved organic matter: Insights on photochemical degradation and protozoan modification of DOM from electrospray ionization Fourier transform ion cyclotron resonance mass spectrometry. In *Marine Chemistry* pp. 23–37.

Kvenvolden K. A. (1995) A review of the geochemistry of methane in natural gas hydrate. *Org. Geochem.* **23**, 997–1008.

Labes A. and Schönheit P. (2001) Sugar utilization in the hyperthermophilic, sulfate-reducing archaeon Archaeoglobus fulgidus strain 7324: starch degradation to acetate and CO 2 via a modified Embden-Meyerhof pathway and acetyl-CoA synthetase (ADP-forming). *Arch. Microbiol.* **176**, 329–338.

Lakemond C. M. M., De Jongh H. H. J., Hessing M., Gruppen H. and Voragen A. G. J. (2000) Soy glycinin: Influence of pH and ionic strength on solubility and molecular structure at ambient temperatures. *J. Agric. Food Chem.* **48**, 1985–1990.

Lam P. and Kuypers M. M. M. (2011) Microbial Nitrogen Cycling Processes in Oxygen Minimum Zones. *Ann. Rev. Mar. Sci.* **3**, 317–345.

Landén A. and Hall P. O. J. (2000) Benthic flux and pore water distribution of dissolved free amino acids in the open Skagerrak. *Mar. Chem.* **71**, 53–68.

Lansard B., Rabouille C., Denis L. and Grenz C. (2009) Benthic remineralization at the land-ocean interface: A case study of the Rhône River (NW Mediterranean Sea). *Estuar. Coast. Shelf Sci.* **81**, 544–554.

Lechtenfeld O. J., Kattner G., Flerus R., McCallister S. L., Schmitt-Kopplin P. and Koch B. P. (2014) Molecular transformation and degradation of refractory dissolved organic matter in the Atlantic and Southern Ocean. *Geochim. Cosmochim. Acta* **126**, 321–337.

Leenheer J. A. and Rostad C. (2004) Tannins and Terpenoids as Major Precursors of Suwannee River Fulvic Acid. *Sci. Investig. Rep. 2004-5276*.

Leloup J., Fossing H., Kohls K., Holmkvist L., Borowski C. and Jørgensen B. B. (2009) Sulfate-reducing bacteria in marine sediment (Aarhus Bay, Denmark): abundance and diversity related to geochemical zonation. *Environ. Microbiol.* **11**, 1278–1291.

Leong L. E. X., Denman S. E., Hugenholtz P. and McSweeney C. S. (2016) Amino Acid and Peptide Utilization Profiles of the Fluoroacetate-Degrading Bacterium Synergistetes Strain MFA1 Under Varying Conditions. *Microb. Ecol.* **71**, 494–504.

Leschine S. B. (1995) Cellulose degradation in anaerobic environments. *Annu. Rev. Microbiol.* **49**, 399–426.

Lever M. A. (2012) Acetogenesis in the energy-starved deep biosphere-a paradox? *Front. Microbiol.* **2**, 1–18.

Lever M. A, Rogers K. L., Lloyd K. G., Overmann J., Schink B., Thauer R. K., Hoehler T. M.

and Jørgensen B. B. (2015) Life under extreme energy limitation: a synthesis of laboratory- and field-based investigations. *FEMS Microbiol. Rev.*, 1–41.

Li X., Dai X., Dai L. and Liu Z. (2015) RSC Advances Two-dimensional FTIR correlation spectroscopy reveals chemical changes in dissolved organic matter during the biodrying process of raw sludge and anaerobically digested sludge. *RSC Adv.* **5**, 82087–82096.

Li X., Dai X., Takahashi J., Li N., Jin J., Dai L. and Dong B. (2014) Bioresource Technology New insight into chemical changes of dissolved organic matter during anaerobic digestion of dewatered sewage sludge using EEM-PARAFAC and two-dimensional FTIR correlation spectroscopy. *Bioresour. Technol.* **159**, 412–420.

Lin H.-T., Cowen J. P., Olson E. J., Amend J. P. and Lilley M. D. (2012) Inorganic chemistry, gas compositions and dissolved organic carbon in fluids from sedimented young basaltic crust on the Juan de Fuca Ridge flanks. *Geochim. Cosmochim. Acta* **85**, 213–227.

Lin H., Hsieh C., Cowen J. P. and Rappé M. S. (2015) Data report : dissolved and particulate organic carbon in the deep sediments of IODP Site U1363 near Grizzly Bare seamount 1. **327**.

Lin Q., Wang J., Taladay K., Lu H., Hu G., Sun F. and Lin R. (2016) Coupled pyrite concentration and sulfur isotopic insight into the paleo sulfate-methane transition zone (SMTZ) in the northern South China Sea. *J. Asian Earth Sci.* **115**, 547–556.

Lin Y.-S., Heuer V. B., Goldhammer T., Kellermann M. Y., Zabel M. and Hinrichs K.-U. (2012) Towards constraining H2 concentration in subseafloor sediment: A proposal for combined analysis by two distinct approaches. *Geochim. Cosmochim. Acta* **77**, 186–201.

Lin Y.-S, Koch B. P., Feseker T., Ziervogel K., Goldhammer T., Schmidt F., Witt M., Kellermann M. Y., Zabel M. and Teske A. (2017) Near-surface Heating of Young Rift Sediment Causes Mass Production and Discharge of Reactive Dissolved Organic Matter. *Nat. Publ. Gr.*, 1–10.

Lipp J. S., Morono Y., Inagaki F. and Hinrichs K.-U. (2008) Significant contribution of Archaea to extant biomass in marine subsurface sediments. *Nature* **454**, 991–994.

Liu Y. and Whitman W. B. (2008) Metabolic, Phylogenetic, and Ecological Diversity of the Methanogenic Archaea. *Ann. N. Y. Acad. Sci.* **1125**, 171–189.

Liu Z., Sleighter R. L., Zhong J. and Hatcher P. G. (2011) The chemical changes of DOM from black waters to coastal marine waters by HPLC combined with ultrahigh resolution mass spectrometry. *Estuar. Coast. Shelf Sci.* **92**, 205–216.

Ljungdahl L. G. (1986) The Autotrophic Pathway of acetate synthesis in acetogenic bacteria. *Annu. Rev. Microbiol.*, 415–450.

Ljungdahl L. G. and Eriksson K.-E. (1985) Ecology of microbial cellulose degradation. *Adv.*

Microb. Ecol. **8**, 237–299.

Lollar B. S., Lacrampe-Couloume G., Slater G. F., Ward J., Moser D. P., Gihring T. M., Lin L. H. and Onstott T. C. (2006) Unravelling abiogenic and biogenic sources of methane in the Earth's deep subsurface. *Chem. Geol.* **226**, 328–339.

Lomstein B. A., Jensen A. G. U., Hansen J. W., Andreasen J. B., Hansen L. S., Berntsen J. and Kunzendorf H. (1998) Budgets of sediment nitrogen and carbon cycling in the shallow water of Knebel Vig, Denmark. *Aquat. Microb. Ecol.* **14**, 69–80.

Lomstein B. A., Jørgensen B. B., Schubert C. J. and Niggemann J. (2006) Amino acid biogeo- and stereochemistry in coastal Chilean sediments. *Geochim. Cosmochim. Acta* **70**, 2970–2989.

Lønborg C. and Álvarez-Salgado X. A. (2012) Recycling versus export of bioavailable dissolved organic matter in the coastal ocean and efficiency of the continental shelf pump. *Global Biogeochem. Cycles* **26**, n/a-n/a.

Lønborg C., Álvarez-Salgado X. A., Davidson K., Martínez-García S. and Teira E. (2010) Assessing the microbial bioavailability and degradation rate constants of dissolved organic matter by fluorescence spectroscopy in the coastal upwelling system of the Ría de Vigo. *Mar. Chem.* **119**, 121–129.

Lønborg C., Álvarez-Salgado X. A., Davidson K. and Miller A. E. J. (2009) Production of bioavailable and refractory dissolved organic matter by coastal heterotrophic microbial populations. *Estuar. Coast. Shelf Sci.* **82**, 682–688.

Lovley D. R. and Chapelle F. H. (1995) Deep Subsurface Microbial Processes. *Rev. Geophys.* **33**, 365–381.

Lovley D. R., Coates J. D., Blunt-Harris E. L., Phillips E. J. P. and Woodward J. C. (1996) Humic substances as electron acceptors for microbial respiration. *Nature* **382**, 445–448.

Lovley D. R. and Goodwin S. (1988) Hydrogen concentrations as an indicator of the predominant terminal electron accepting reaction sin aquatic sediments. *Geochim. Cosmochim. Acta* **52**, 2993–3003.

Luciani X., Mounier S., Redon R. and Bois A. (2009) A simple correction method of inner filter effects affecting FEEM and its application to the PARAFAC decomposition. *Chemom. Intell. Lab. Syst.* **96**, 227–238.

Ludwig W., Meybeck M. and Abousamra F. (2003) Riverine transport of water, sediments, and pollutants to the Mediterranean Sea. *Medit. Action Tech. Rep. Ser.*, 1–121.

Lützow M. V., Kögel-Knabner I., Ekschmitt K., Matzner E., Guggenberger G., Marschner B. and Flessa H. (2006) Stabilization of organic matter in temperate soils: Mechanisms and their relevance under different soil conditions - A review. *Eur. J. Soil Sci.* **57**, 426–445.

Mackie R. I., White B. A and Bryant M. P. (1991) *Lipid metabolism in anaerobic ecosystems.*,

Maie N., Scully N. M., Pisani O. and Jaffé R. (2007) Composition of a protein-like fluorophore of dissolved organic matter in coastal wetland and estuarine ecosystems. *Water Res.* **41**, 563–570.

Malcolm L. R. (1990) The uniqueness of humic substances in each of soil, stream and marine environments. *Anal. Chim. Acta* **232**, 19–30.

Manciulea A., Baker A. and Lead J. R. (2009) A fluorescence quenching study of the interaction of Suwannee River fulvic acid with iron oxide nanoparticles. *Chemosphere* **76**, 1023–1027.

Marcaillou B., Henry P., Kinoshita M., Kanamatsu T., Screaton E., Daigle H., Harcouët-Menou V., Lee Y., Matsubayashi O., Kyaw Thu M., Kodaira S. and Yamano M. (2012) Seismogenic zone temperatures and heat-flow anomalies in the To-nankai margin segment based on temperature data from IODP expedition 333 and thermal model. *Earth Planet. Sci. Lett.* **349**–**350**, 171–185.

Martin W. and Müller M. (1998) The hydrogen hypothesis for the first eukaryote. *Nature* **392**, 37–41.

Martínez-Pérez A. M., Nieto-Cid M., Osterholz H., Catalá T. S., Reche I., Dittmar T. and Álvarez-Salgado X. A. (2017) Linking optical and molecular signatures of dissolved organic matter in the Mediterranean Sea. *Sci. Rep.* **7**, 3436.

Martínez C. M., Celis L. B. and Cervantes F. J. (2013) Immobilized humic substances as redox mediator for the simultaneous removal of phenol and Reactive Red 2 in a UASB reactor. *Appl. Microbiol. Biotechnol.* **97**, 9897–9905.

Matsumurat M., Becktelt W. J., Levitr M. and Matthewstl B. W. (1989) Stabilization of phage T4 Iysozyme by engineered disulfide bonds. *Proc Natl Acad Sci U S A* **86**, 6562–6566.

Mayumi D., Mochimaru H., Tamaki H., Yamamoto K., Yoshioka H., Suzuki Y., Kamagata Y. and Sakata S. (2016) Methane production from coal by a single methanogen. *Science (80).* **354**, 222–225.

McKee G. A. and Hatcher P. G. (2010) Alkyl amides in two organic-rich anoxic sediments: A possible new abiotic route for N sequestration. *Geochim. Cosmochim. Acta* **74**, 6436–6450.

Mcknight D. M., Boyer E. W., Westerhoff P. K., Doran P. T., Kulbe T. and Andersen D. T. (2001) Spectrofluorometric characterization of dissolved organic matter for indication of precursor organic material and aromaticity. *PoLAR* **46**, 38–48.

Medrano-E'Vers A., Morales-Hernández A. E., Valencia-López R. and Hernández-Salcedo D. R. (2017) Enfermedad granulomatosa crónica. *Med. Interna Mex.* **33**, 407–414.

Middelburg J. J. (1989) A simple rate model for organic matter decomposition in marine sediments. *Geochim. Cosmochim. Acta* **53**, 1577–1581.

Middelburg J. J., Vlug T. and Vandernat F. J. W. A. (1993) Organic-Matter Mineralization in Marine Systems. *Glob. Planet. Change* **8**, 47–58.

Mincks S. L., Smith C. R. and DeMaster D. J. (2005) Persistence of labile organic matter and microbial biomass in Antarctic shelf sediments: Evidence of a sediment "food bank." *Mar. Ecol. Prog. Ser.* **300**, 3–19.

Miralles J., Radakovitch O. and Aloisi J. C. (2005) 210Pb sedimentation rates from the Northwestern Mediterranean margin. *Mar. Geol.* **216**, 155–167.

Mistry B. (2009) *A handbook of Spectroscopic Data Chemistry (UV, IR, PMR, 13CNMR and Mass Spectroscopy)*., Oxford Book Company, Jaipur.

Miyatake T., MacGregor B. J. and Boschker H. T. S. (2013) Depth-Related Differences in Organic Substrate Utilization by Major Microbial Groups in Intertidal Marine Sediment. *Appl. Environ. Microbiol.* **79**, 389–392.

Mobed J. J., Hemmingsen S. L., Autry J. L. and Mcgown L. B. (1996) Fluorescence characterization of IHSS humic substances: Total luminescence spectra with absorbance correction. *Environ. Sci. Technol.* **30**, 3061–3065.

Moini M., Jones B. L., Rogers R. M. and Jiang L. (1998) Sodium trifluoroacetate as a tune/calibration compound for positive- and negative-ion electrospray ionization mass spectrometry in the mass range of 100-4000 Da. *J. Am. Soc. Mass Spectrom.* **9**, 977–980.

Mopper K., Stubbins A., Ritchie J. D., Bialk H. M. and Hatcher P. G. (2007) Advanced instrumental approaches for characterization of marine dissolved organic matter: extraction techniques, mass spectrometry, and nuclear magnetic resonance spectroscopy. *Chem. Rev.* **107**, 419–42.

Morono Y., Terada T., Nishizawa M., Ito M., Hillion F., Takahata N., Sano Y. and Inagaki F. (2011) Carbon and nitrogen assimilation in deep subseafloor microbial cells. *Proc. Natl. Acad. Sci. U. S. A.* **108**, 18295–300.

Murphy K. R., Butler K. D., Spencer R. G. M., Stedmon C. A., Boehme J. R. and Aiken G. R. (2010) Measurement of dissolved organic matter fluorescence in aquatic environments: An interlaboratory comparison. *Environ. Sci. Technol.* **44**, 9405–9412.

Murphy K. R., Stedmon C. A., Graeber D. and Bro R. (2013) Fluorescence spectroscopy and multi-way techniques. PARAFAC. *Anal. Methods* **5**, 6557.

Murphy K. R., Stedmon C. A., Waite T. D. and Ruiz G. M. (2008) Distinguishing between terrestrial and autochthonous organic matter sources in marine environments using fluorescence spectroscopy. *Mar. Chem.* **108**, 40–58.

Muyzer G. and Stams A. J. M. (2008) The ecology and biotechnology of sulphate-reducing bacteria. *Nat. Rev. Microbiol.* **6**, 441–54.

Novak J. T. and Carlson D. A. (1970) The Kinetics of Anaerobic Long Chain Fatty Acid Degradation. *J. (Water Pollut. Control Fed.* **42**, 1932–1943.

Ohno T. (2002) Fluorescence inner-filtering correction for determining the humification index of dissolved organic matter. *Environ. Sci. Technol.* **36**, 742–746.

Oni O. E., Schmidt F., Miyatake T., Kasten S., Witt M., Hinrichs K. -U. and Friedrich M. W. (2015) Microbial communities and organic matter composition in surface and subsurface sediments of the Helgoland mud area, North Sea. *Front. Microbiol.* **6**, 1–16.

Oremland R. S. and Polcin S. (1982) Methanogenesis and sulfate reduction: competitive and noncompetitive substrates in estuarine sediments. *Appl. Environ. Microbiol.* **44**, 1270–1276.

Oremland R. S. and Taylor B. F. (1978) Sulfate Reduction and Methanogenesis in Marine-Sediments. *Geochim. Cosmochim. Acta* **42**, 209–214.

Pantoja S., Lee C. and Marecek J. F. (1997) Hydrolysis of peptides in seawater and sediment. *Mar. Chem.* **57**, 25–40.

Parkes R. J., Cragg B., Roussel E., Webster G., Weightman A. and Sass H. (2014) A review of prokaryotic populations and processes in sub-seafloor sediments, including biosphere:geosphere interactions. *Mar. Geol.* **352**, 409–425.

Parkes R. J., Linnane C. D., Webster G., Sass H., Weightman A. J., Hornibrook E. R. C. and Horsfield B. (2011) Prokaryotes stimulate mineral H2 formation for the deep biosphere and subsequent thermogenic activity. *Geology* **39**, 219–222.

Parlanti E., Worz K., Geoffroy L. and Lamotte M. (2000) Dissolved organic matter ¯uorescence spectroscopy as a tool to estimate biological activity in a coastal zone submitted to anthropogenic inputs. *Org. Geochem.* **31**, 1765–1781.

Parnell J. and Mcmahon S. (2016) Physical and chemical controls on habitats for life in the deep subsurface beneath continents and ice. *Philos. Trans. R. Soc. A* **374**, 20140293.

Payne W. J. (1981) *Denitrification*., Wiley, New York.

Peleato N. M., Legge R. L. and Andrews R. C. (2017) Investigation of fluorescence methods for rapid detection of municipal wastewater impact on drinking water sources. *Spectrochim. Acta - Part A Mol. Biomol. Spectrosc.* **171**, 104–111.

Perminova I. V., Dubinenkov I. V., Kononikhin A. S., Konstantinov A. I., Zherebker A. Y., Andzhushev M. A., Lebedev V. A., Bulygina E., Holmes R. M., Kostyukevich Y. I., Popov I. A. and Nikolaev E. N. (2014) Molecular mapping of sorbent selectivities with respect to isolation of arctic dissolved organic matter as measured by fourier transform

mass spectrometry. *Environ. Sci. Technol.* **48**, 7461–7468.

Plugge C. M., Zhang W., Scholten J. C. M. and Stams A. J. M. (2011) Metabolic Flexibility of Sulfate-Reducing Bacteria. *Front. Microbiol.* **2**, 1–8.

Pollo S. M. J., Adebusuy A. A., Straub T. J., Foght J. M., Zhaxybayeva O. and Nesbo C. L. (2016) Temperature-Induced Transcriptional Responses of a Deep-Biosphere Bacterium Illuminate its Adaptation to Growth from 20°C to 79°C. *bioRxiv*, 60053.

Poncet-Legrand C., Cabane B., Bautista-Ortín A.-B., Carrillo S., Fulcrand H., Pérez J. and Vernhet A. (2010) Tannin oxidation: intra- versus intermolecular reactions. *Biomacromolecules* **11**, 2376–2386.

Poulin B. A., Ryan J. N. and Aiken G. R. (2014) The effects of iron on optical properties of dissolved organic matter. *Environ. Sci. Technol.* **48**, 10098–10106.

Rabi I. I., Zacharias J. R., Millman S. and Kusch P. (1938) A New Method of Measuring Nuclear Magnetic Moment. *Phys. Rev.* **53**, 318–318.

Ramsay I. R. and Pullammanappallil P. C. (2001) Protein degradation during anaerobic wastewater treatment: Derivation of stoichiometry. *Biodegradation* **12**, 247–257.

Riedinger N., Strasser M., Harris R. N., Klockgether G., Lyons T. W. and Screaton E. J. (2015) Deep subsurface carbon cycling in the Nankai Trough (Japan) - Evidence of tectonically induced stimulation of a deep microbial biosphere. *Geochemistry, Geophys. Geosystems* **16**, 3257–3270.

De Rosa M., Esposito E., Gambacorta A., Nicolaus B. and Bu'Lock J. D. (1980) Effects of temperature on ether lipid composition of Caldariella acidophila. *Phytochemistry* **19**, 827–831.

Rosario-Ortiz F. L. and Korak J. A. (2017) Oversimplification of Dissolved Organic Matter Fluorescence Analysis: Potential Pitfalls of Current Methods. *Environ. Sci. Technol.* **51**, 759–761.

Roussel E. G., Bonavita M.-A. C., Querellou J., Cragg B. A, Webster G., Prieur D. and Parkes R. J. (2008) Extending the sub-sea-floor biosphere. *Science* **320**, 1046.

Roussel E. G., Cragg B. A., Webster G., Sass H., Tang X., Williams A. S., Gorra R., Weightman A. J. and Parkes R. J. (2015) Complex coupled metabolic and prokaryotic community responses to increasing temperatures in anaerobic marine sediments: critical temperatures and substrate changes. *FEMS Microbiol. Ecol.* **91**, fiv084.

Rowe G. T. and Deming J. W. (2011) An alternative view of the role of heterotrophic microbes in the cycling of organic matter in deep-sea sediments. *Mar. Biol. Res.* **7**, 629–636.

Rysgaard S., Fossing H. and Jensen M. M. (2001) Organic matter degradation through oxygen respiration, denitrification, and manganese, iron, and sulfate reduction in marine

sediments (the Kattegat and the Skagerrak). *Ophelia* **55**, 77–91.

Saparpakorn P., Kim J. H. and Hannongbua S. (2007) Investigation on the binding of polycyclic aromatic hydrocarbons with soil organic matter: a theoretical approach. *Molecules* **12**, 703–715.

Schink B. (1997) Energetics of syntrophic cooperation in methanogenic degradation. *Microbiol. Mol. Biol. Rev.* **61**, 262–280.

Schippers A., Neretin L. N., Kallmeyer J., Ferdelman T. G., Cragg B. A., Parkes R. J. and Jørgensen B. B. (2005) Prokaryotic cells of the deep sub-sea oor biosphere identi ed as living bacteria. *Nature* **433**, 861–864.

Schmidt F. (2009) Molecular level studies on the distribution and fate of organic matter at continental margins. *University of Bremen.*

Schmidt F., Elvert M., Koch B. P., Witt M. and Hinrichs K.-U. (2009) Molecular characterization of dissolved organic matter in pore water of continental shelf sediments. *Geochim. Cosmochim. Acta* **73**, 3337–3358.

Schmidt F., Hinrichs K.-U. and Elvert M. (2010) Sources, transport, and partitioning of organic matter at a highly dynamic continental margin. *Mar. Chem.* **118**, 37–55.

Schmidt F., Koch B. P., Elvert M., Schmidt G., Witt M. and Hinrichs K. -U. (2011) Diagenetic transformation of dissolved organic nitrogen compounds under contrasting sedimentary redox conditions in the black sea. *Environ. Sci. Technol.* **45**, 5223–5229.

Schmidt F., Koch B. P., Goldhammer T., Elvert M., Lin Y., Wendt J., Zabel M., Heuer V. B. and Hinrichs K. -U. (2017) Unraveling signatures of biogeochemical processes and the depositional setting in the molecular composition of pore water DOM across different. *Geochim. Cosmochim. Acta*. **207**, 57–80.

Schmidt F., Koch B. P., Witt M. and Hinrichs K.-U. (2014) Extending the analytical window for water-soluble organic matter in sediments by aqueous Soxhlet extraction. *Geochim. Cosmochim. Acta* **141**, 83–96.

Schmidt O., Horn M. A., Kolb S. and Drake H. L. (2015) Temperature impacts differentially on the methanogenic food web of cellulose-supplemented peatland soil. *Environ. Microbiol.* **17**, 720–734.

Schouten S., Hopmans E. C., Schefuß E. and Sinninghe Damsté J. S. (2002) Distributional variations in marine crenarchaeotal membrane lipids: A new tool for reconstructing ancient sea water temperatures? *Earth Planet. Sci. Lett.* **204**, 265–274.

Schulten H.-R. and Leinweber P. (2000) New insights into organic-mineral particles: composition, properties and models of molecular structure. *Biol. Fertil. Soils* **30**, 399–432.

Schulten H.-R. and Schnitzer M. (1997) Chemical Model Structures for Soil Organic Matter and Soils. *Soil Sci.* **162**, 115–130.

Schulten H.-R. and Schnitzer M. (1995) Three-Dimensional Models for Humic Acids and Soil Organic Matter. *Naturwissenschaften* **82**, 487–498.

Schulz H. D., Dahmke A., Schinzel U., Wallmann K. and Zabel M. (1994) Early diagenetic processes, fluxes, and reaction rates in sediments of the South Atlantic. *Geochim. Cosmochim. Acta* **58**, 2041–2060.

Schulz H. D. and Zabel M. (2006) *Marine Geochemistry*. 2nd Editio., Springer-Verlag Berlin, Heidelberg.

Schulz S. and Conrad R. (1996) Influence of temperature on pathways to methane production in the permanently cold profundal sediment of Lake Constance. *FEMS Microbiol. Ecol.* **20**, 1–14.

Schuring J., Fischer W. R. and Duijnisveld W. H. (1999) Redox: Fundamentals, Processes and Applications. *Springer*, 273.

Scott D. T., Mcknight D. M., Blunt-Harris E. L., Kolesar S. E. and Lovley D. R. (1998) Quinone moieties act as electron acceptors in the reduction of humic substances by humics-reducing microorganisms. *Environ. Sci. Technol.* **32**, 2984–2989.

Seidel M., Beck M., Greskowiak J., Riedel T., Waska H., Suryaputra I. G. N. A., Schnetger B., Niggemann J., Simon M. and Dittmar T. (2015) Biogeochemistry of dissolved organic matter in an intertidal sandy beach. *Mar. Chem.* **176**, 150–163.

Seidel M., Beck M., Riedel T., Waska H., Suryaputra I. G. N. a, Schnetger B., Niggemann J., Simon M. and Dittmar T. (2014) Biogeochemistry of dissolved organic matter in an anoxic intertidal creek bank. *Geochim. Cosmochim. Acta* **140**, 418–434.

Senesi N. and Miano T. (1991) Characterization, differentiation, and classification of humic substances by fluorescence spectroscopy. *Soil Sci.* **152**, 259–270.

Sierra M. M., Donard O. F., Etcheber H., Soriano-Sierra E. and Ewald M. (2001) Fluorescence and DOC contents of pore waters from coastal and deep-sea sediments in the Gulf of Biscay. *Org. Geochem.* **32**, 1319–1328.

Simoneit B. R. T. and Sparrow M. A. (2002) Dissolved organic carbon in interstitial waters from sediments of Middle Valley and Escanaba Trough, Northeast Pacific, ODP Legs 139 and 169. *Appl. Geochemistry* **17**, 1495–1502.

Sleep N. H., Meibom A., Fridriksson T., Coleman R. G. and Bird D. K. (2004) H2-rich fluids from serpentinization: geochemical and biotic implications. *Proc. Natl. Acad. Sci. U. S. A.* **101**, 12818–12823.

Sleighter R. L. and Hatcher P. G. (2008) Molecular characterization of dissolved organic matter

(DOM) along a river to ocean transect of the lower Chesapeake Bay by ultrahigh resolution electrospray ionization Fourier transform ion cyclotron resonance mass spectrometry. *Mar. Chem.* **110**, 140–152.

Sleighter R. L., Liu Z., Xue J. and Hatcher P. G. (2010) Multivariate Statistical Approaches for the Characterization of Dissolved Organic Matter Analyzed by Ultrahigh Resolution Mass Spectrometry. *Environ. Sci. Technol.* **44**, 7576–7582.

Snowden M. J., Chowdhry B. Z., Vincentb B. and Morrisb G. E. (1996) Colloidal copolymer microgels of N-isopropylacrylamide and acrylic acid: pH, ionic strength and temperature effects. *J. Chem. SOC.* **92**, 5013–5016.

Soffientino B., Spivack A. J., Smith D. C. and D'Hondt S. (2009) Hydrogenase activity in deeply buried sediments of the Arctic and North Atlantic Oceans. *Geomicrobiol. J.* **26**, 537–545.

Sogin M. L. (1991) Early evolution and the origin of eukaryotes. *Curr. Opin. Genet. Dev.* **1**, 457–463.

Sokolova T. G., Jeanthon C., Kostrikina N. A., Chernyh N. A., Lebedinsky A. V., Stackebrandt E. and Bonch-Osmolovskaya E. A. (2004) The first evidence of anaerobic CO oxidation coupled with H2 production by a hyperthermophilic archaeon isolated from a deep-sea hydrothermal vent. *Extremophiles* **8**, 317–323.

Sousa D. Z., Smidt H., Alves M. M. and Stams A. J. M. (2009) Ecophysiology of syntrophic communities that degrade saturated and unsaturated long-chain fatty acids. *FEMS Microbiol. Ecol.* **68**, 257–272.

Stams A. J. M. and Plugge C. M. (2009) Electron transfer in syntrophic communities of anaerobic bacteria and archaea. *Nat. Rev. Microbiol.* **7**, 568–577.

Stedmon C. A. and Bro R. (2008) Characterizing dissolved organic matter fluorescence with parallel factor analysis: A tutorial. *Limnol. Oceanogr. Methods* **6**, 572–579.

Stedmon C. A. and Markager S. (2005a) Resolving the variability of dissolved organic matter fluorescence in a temperate estuary and its catchment using PARAFAC analysis. *Limnol. Oceanogr.* **50**, 686–697.

Stedmon C. A. and Markager S. (2005b) Tracing the production and degradation of autochthonous fractions of dissolved organic matter using fluorescence analysis. *Limnol. Oceanogr.* **50**, 1415–1426.

Stedmon C. A., Markager S., Tranvik L., Kronberg L., Slätis T. and Martinsen W. (2007) Photochemical production of ammonium and transformation of dissolved organic matter in the Baltic Sea. *Mar. Chem.* **104**, 227–240.

Stevenson F. J. (1994) *Humus Chemistry-Genesis, Composition, Reactions,*. 2nd Editio., John

Wiley & Sons, New York.

Strasser M., Dugan B., Kanagawa K., Moore G. F., Toczko S., Maeda L., Kido Y., Thu M. K., Sanada Y., Esteban L., Fabbri O., Geersen J., Hammerschmidt S., Hayashi H., Heirman K., Hüpers A., Jurado Rodriguez M. J., Kameo K., Kanamatsu T., Kitajima H., Masuda H., Milliken K., Mishra R., Motoyama I., Olcott K., Oohashi K., Pickering K. T., Ramirez S. G., Rashid H., Sawyer D., Schleicher A., Yehua S., Skarbek R., Song I., Takeshita T., Toki T., Tudge J., Webb S., Wilson D. J., Wu H.-Y. and Yamaguchi A. (2014) Site C0012. *Proc. Integr. Ocean Drill. Progr.* **338**.

Stubbins A., Lapierre J., Berggren M., Prairie Y. T., Dittmar T. and Del Giorgio P. A. (2014) What's in an EEM? Molecular Signatures Associated with Dissolved Organic Fluorescence in Boreal Canada. *Environ. Sci. Technol.* **48**, 10598–10606.

Sutton R. and Sposito G. (2005) Molecular structure in soil humic substances: The new view. *Environ. Sci. Technol.* **39**, 9009–9015.

Szatmari P. (1989) Petroleum Formation by Fischer-Tropsch Synthesis in Plate-Tectonics. *Aapg Bull. Assoc. Pet. Geol.* **73**, 989–998.

Tabatabai M. A. (1974) A Rapid Method for Determination of Sulfate in Water Samples. *Environ. Lett.* **7**, 237–243.

Tarvin D. and Buswell A. M. (1934) The Methane Fermentation of Organic Acids and Carbohydrates. *J. Am. Chem. Soc.* **56**, 1751–1755.

Tfaily M. M., Corbett J. E., Wilson R., Chanton J. P., Glaser P. H., Cawley K. M., Jaffé R. and Cooper W. T. (2015) Utilization of PARAFAC-Modeled Excitation-Emission Matrix (EEM) Fluorescence Spectroscopy to Identify Biogeochemical Processing of Dissolved Organic Matter in a Northern Peatland. *Photochem. Photobiol.* **91**, 684–95.

Tfaily M. M., Hamdan R., Corbett J. E., Chanton J. P., Glaser P. H. and Cooper W. T. (2013) Investigating dissolved organic matter decomposition in northern peatlands using complimentary analytical techniques. *Geochim. Cosmochim. Acta* **112**, 116–129.

Thauer R. K., Möller-Zinkhan D. and Spormann A. M. (1989) Biochemistry of acetate catabolism in anaerobic chemotrophic bacteria. *Annu. Rev. Microbiol.* **43**, 43–67.

Tijhuis L., van Loosdrecht M. C. M. and Heijnen J. J. (1993) A thermodynamically based correlation for maintenance Gibbs energy requirements in anaerobic and aerobic chemotrophic growth. *Biotechnol. Bioeng.* **42**, 509–519.

Tong C., She C. X., Jin Y. F., Yang P. and Huang J. F. (2013) Methane production correlates positively with methanogens, sulfate-reducing bacteria and pore water acetate at an estuarine brackish-marsh landscape scale. *Biogeosciences Discuss.* **10**, 18241–18275.

Torres M. E., Cox T., Hong W. L., Mcmanus J., Sample J. C., Destrigneville C., Gan H. M.,

Gan H. Y. and Moreau J. W. (2015) Crustal fluid and ash alteration impacts on the biosphere of Shikoku Basin sediments, Nankai Trough, Japan. *Geobiology* **13**, 562–580.

Tucker S. A., Amszi V. L. and Acree W. E. (1992) Primary and secondary inner filtering. Effect of K2Cr2O7 on fluorescence emission intensities of quinine sulfate. *J. Chem. Educ.* **69**, A8.

Tuominen L., Kairesalo T. and Hartikainen H. (1994) Comparison of methods for inhibiting bacterial activity in sediment. *Appl. Environ. Microbiol.* **60**, 3454–3457.

Valle J., Gonsior M., Harir M., Enrich-Prast A., Schmitt-Kopplin P., Bastviken D., Conrad R. and Hertkorn N. (2017) Extensive processing of sediment pore water dissolved organic matter during anoxic incubation as observed by high-field mass spectrometry (FTICR-MS). *Water Res.* doi: 10.1016/j.watres.2017.11.015

Vandecasteele J.-P. (2008) Petroleum Microbiology: Concepts, Environmental Implications, Industrial Applications. , 880.

Verhaart M. R. A., Bielen A. A. M., Oost J. van der, Stams A. J. M. and Kengen S. W. M. (2010) Hydrogen production by hyperthermophilic and extremely thermophilic bacteria and archaea: mechanisms for reductant disposal. *Environ. Technol.* **31**, 993–1003.

Vogt G., Woell S. and Argos P. (1997) Protein thermal stability, hydrogen bonds, and ion pairs. *J. Mol. Biol.* **269**, 631–643.

Waggoner D. C., Chen H., Willoughby A. S. and Hatcher P. G. (2015) Formation of black carbon-like and alicyclic aliphatic compounds by hydroxyl radical initiated degradation of lignin. *Org. Geochem.* **82**, 69–76.

Wagner S., Riedel T., Niggemann J., Vähätalo A. V., Dittmar T. and Jaffé R. (2015) Linking the Molecular Signature of Heteroatomic Dissolved Organic Matter to Watershed Characteristics in World Rivers. *Environ. Sci. Technol.* **49**, 13798–13806.

Wakeham S. G. and Canuel E. A. (2006) Degradation and preservation of organic matter in sediments. *Handb. Environ. Chem. Vol. 2 React. Process. 2* **2**, 295–321.

Wakeham S. G., Lee C., Hedges J. I., Hernes P. J. and Peterson M. L. J. (1997) Molecular indicators of diagenetic status in marine organic matter. *Geochim. Cosmochim. Acta* **61**, 5363–5369.

Walsh J. J. (1991) Importance of continental margins in the marine biogeochemical cycling of carbon and nitrogen. *Nature* **350**, 53–55.

Wang G., Spivack A. J. and D'Hondt S. (2010) Gibbs energies of reaction and microbial mutualism in anaerobic deep subseafloor sediments of ODP Site 1226. *Geochim. Cosmochim. Acta* **74**, 3938–3947.

Wang Z., Cao J. and Meng F. (2015) Interactions between protein-like and humic-like

components in dissolved organic matter revealed by fluorescence quenching. *Water Res.* **68**, 404–413.

Wellsbury P., Goodman K., Barth T., Cragg B. A., Barnes S. P. and Parkes R. J. (1997) Deep marine biosphere fuelled by increasing organic matter availability during burial and heating. *Nature* **388**, 573–576.

Weston N. B., Porubsky W. P., Samarkin V. a., Erickson M., Macavoy S. E. and Joye S. B. (2006) Porewater stoichiometry of terminal metabolic products, sulfate, and dissolved organic carbon and nitrogen in estuarine intertidal creek-bank sediments. *Biogeochemistry* **77**, 375–408.

Weston N. B., Porubsky W. P., Samarkin V. A., Erickson M., Macavoy S. E. and Joye S. B. (2006) Porewater stoichiometry of terminal metabolic products, sulfate, and dissolved organic carbon and nitrogen in estuarine intertidal creek-bank sediments. *Biogeochemistry* **77**, 375–408.

Whitman W. B., Coleman D. C. and Wiebe W. J. (1998) Prokaryotes: the unseen majority. *Proc Natl Acad Sci U S A* **95**, 6578–6583.

Widdel F. and Bak F. (1992) Gram-negative mesophilic sulfate-reducing bacteria. *Prokaryotes. 2nd ed.* **IV**, 3352–3378.

Widdel F. and Pfennig N. (1977) A new anaerobic, sporing, acetate-oxidizing, sulfate-reducing bacterium, Desulfotomaculum (emend.) acetoxidans. *Arch. Microbiol.* **112**, 119–122.

Wolin M. J. and Miller T. L. (1987) Bioconversion of organic carbon to CH4 and CO2. *Geomicrobiol J* **5**, 239–260.

Wüthrich K. (1994) NMR assignments as a basis for structural characterization of denatured states of globular proteins. *Curr. Opin. Struct. Biol.* **4**, 93–99.

Yamano M., Honda S. and Uyeda S. (1984) Nankai Trough: A hot trench? *Mar. Geophys. Res.* **6**, 187–203.

Yamashita Y., Cory R. M., Nishioka J., Kuma K., Tanoue E. and Jaffé R. (2010) Fluorescence characteristics of dissolved organic matter in the deep waters of the Okhotsk Sea and the northwestern North Pacific Ocean. *Deep Sea Res. Part II Top. Stud. Oceanogr.* **57**, 1478–1485.

Yamashita Y. and Tanoue E. (2004) Chemical characteristics of amino acid-containing dissolved organic matter in seawater. *Org. Geochem.* **35**, 679–692.

Yamashita Y. and Tanoue E. (2003) Chemical characterization of protein-like fluorophores in DOM in relation to aromatic amino acids. *Mar. Chem.* **82**, 255–271.

Yamashita Y. and Tanoue E. (2008) Production of bio-refractory fluorescent dissolved organic matter in the ocean interior. *Nat. Geosci.* **1**, 579–582.

Yang L., Hong H., Guo W., Huang J., Li Q. and Yu X. (2011) Effects of changing land use on dissolved organic matter in a subtropical river watershed, southeast China. *Reg. Environ. Chang.* **12**, 145–151.

Yang Z., Du M. and Jiang J. (2016) Reducing capacities and redox potentials of humic substances extracted from sewage sludge. *Chemosphere* **144**, 902–908.

Zang X., Van Heemst J. D. H., Dria K. J. and Hatcher P. G. (2000) Encapsulation of protein in humic acid from a histosol as an explanation for the occurrence of organic nitrogen in soil and sediment. *Org. Geochem.* **31**, 679–695.

Zellner G. and Winter J. (1987) Secondary alcohols as hydrogen donors for CO2-reduction by methanogens. *FEMS Microbiol. Lett.* **44**, 323–328.

Zhang W. Z., Chen X. Q., Zhou J. M., Liu D. H., Wang H. Y. and Du C. W. (2013) Influence of Humic Acid on Interaction of Ammonium and Potassium Ions on Clay Minerals. *Pedosphere* **23**, 493–502.

Zhou Z., Liu Z. and Guo L. (2013) Chemical evolution of Macondo crude oil during laboratory degradation as characterized by fluorescence EEMs and hydrocarbon composition. *Mar. Pollut. Bull.* **66**, 164–175.

Zhuang G. (2014) Methylotrophic methanogenesis and potential methylated substrates in marine sediment. University of Bremen.

Zhuang G. C., Lin Y. S., Elvert M., Heuer V. B. and Hinrichs K. -U. (2014) Gas chromatographic analysis of methanol and ethanol in marine sediment pore waters: Validation and implementation of three pretreatment techniques. *Mar. Chem.* **160**, 82–90.

Zinder S. (1993) Physiological ecology of methanogens. In *Methanogenesis: Ecology, Physiology, Biochemistry and Genetics* pp. 128–206.

Zinder S. H. and Koch M. (1984) Non-aceticlastic methanogenesis from acetate: acetate oxidation by a thermophilic syntrophic coculture. *Arch. Microbiol.* **138**, 263–272.

Zsolnay Á. (2003) Dissolved organic matter: artefacts, definitions, and functions. *Geoderma* **113**, 187–209.

Contributions to publications

Manuscript 1

Application of Excitation Emission Matrix Spectroscopy (EEMs) for the characterization of dissolved organic matter (DOM) in anoxic marine sediments

Shuchai Gan, Verena B. Heuer, Frauke Schmidt, Lars P. Wörmer, Kai-Uwe Hinrichs

S. Gan designed the project under supervision of V. B. Heuer and K.-U. Hinrichs. S.Gan measured the EEMs. S. Gan and L. Wörmer measured the FT-ICR MS samples. F. Schmidt contributed to the interpretation of FT-ICR MS data. S Gan wrote the paper with input from all coauthors. In preparation for *Marine Chmistry.*

Manuscript 2

Impact of redox conditions on the quality of dissolved organic matter (DOM) during incubation of sediments from the Rhône River Delta

Shuchai Gan, Frauke Schmidt, Verena B. Heuer, Tobias Goldhammer, Mathias Witt, Kai-Uwe Hinrichs

S. Gan, F. Schmidt, V. B. Heuer, K.U. Hinrichs designed the project together. S. Gan conducted the incubation, collected pore water samples. T. Goldhammer measured DOC, DIC. S. Gan measured the EEMs, sulfate, ammonia, H_2, CH_4 and acetate. FT-ICR MS samples were extracted by S. Gan and measured by F. Schmidt and M. Witt. With suggestions from F. Schmidt, S.Gan interpreted the data and wrote the paper with input from all coauthors. In preparation for *Geochimica et Cosmochimica Acta.*

Manuscript 3

Biotic and abiotic carbon cycling in geothermally heated sediments from the Nankai Trough

Shuchai Gan, Verena B. Heuer, Frauke Schmidt, Lars P. Wörmer, Rishi R. Adhikari, Kai-Uwe Hinrichs

S. Gan, V. B. Heuer, F. Schmidt, K.U. Hinrichs designed the project together. S. Gan conducted the incubation experiment. FT-ICR MS samples were extracted by S. Gan and measured with assistance of L. Wörmer. S. Gan measured the EEMs, sulfate, ammonia, H_2, CH_4 and acetate. R. R. Adhikari measured the hydrogenase enzyme activity. S. Gan interpreted the data and wrote the paper with input from all coauthors. In preparation for *Geochimica et Cosmochimica Acta.*